GIS-enabled Spatial Analysis and Modeling of Geotechnical Soil Properties for Seismic Risk Assessment of Levee Systems

by

Mustafa M. H. Saadi

A dissertation submitted in partial fulfillment
of the requirements for the degree of
Doctor of Philosophy
(Civil Engineering)
in The University of Michigan
2012

Doctoral Committee:

        Assistant Professor Adda Athanasopoulos-Zekkos, Chair
        Professor Roman D. Hryciw
        Associate Professor Joseph D. Grengs
        Assistant Professor Dimitrios Zekkos

"Unfortunately, soils are made by nature and not by man, and the products of nature are always complex . . . . As soon as we pass from steel and concrete to earth, the omnipotence of theory ceases to exist . . . . A natural soil is never homogeneous. Its properties change from point to point, while our knowledge of these properties is limited to those few spots at which the samples have been collected."

Karl von Terzaghi (Terzaghi 1936)

Presidential Address, Proceedings of the First International Conference on Soil Mechanics and Foundation Engineering

DEDICATION

To Hasan and Yusuf

ACKNOWLEDGEMENTS

First and foremost, I would like to thank my advisor, Dr. Adda Athanasopoulos-Zekkos, for her guidance, insight, and continuous support throughout the past years. Her dedication, teaching skills, and enthusiasm for the subject matter were a vital source of motivation for me to complete this research project and thesis.

I would also like to thank my committee members for their valuable suggestions and comments. Specifically, Dr. Roman Hryciw for never hesitating to help anyone who knocks on his door, and for the gratifying experience of attending his lectures, Dr. Dimitrios Zekkos for his contagious love of knowledge and passion for the geoenvironmental and geotechnical engineering discipline, and Dr. Joseph Grengs for introducing me to GIS and its endless potential applications, and for his positive encouragement whenever I was going through a difficult time.

It was a privilege to be around and attend presentations by our esteemed Professors Richard Woods and Donald Gray. I also thank Dr. Radoslaw Michalowski for inspiring me to be curious and inquisitive and look beyond what might otherwise seem obvious. I am particularly grateful to Dr. Nancy Love, not just for what she has done for the department as a chairperson, but also for her advice and backing at a particular crucial moment in my graduate studies.

iii

TABLE OF CONTENTS

LIST OF TABLES

LIST OF FIGURES

LIST OF APPENDICES

ABSTRACT

Flood protection systems are complex, interconnected engineered systems, where failure at one location means the failure of the entire system. Earthen levees, the systems' major component, are at risk from many causes of failure including seepage, erosion and instability due to seismic loading, yet there are currently no guidelines available for the seismic design of levees.

Levees stretch for long distances and are formed through various geologic processes and human activities over time, however information regarding soil properties is collected only at limited point locations and varies significantly both laterally and with depth. Levee vulnerability analyses are currently performed only at locations with known soil properties. Prediction of levee performance in locations where no soil data is available becomes a limitation for system risk assessment studies.

A simplified methodology is proposed to predict soil variability in riverine geologic environments for the seismic risk assessment of earthen levee systems. A key step in this methodology is to provide a continuous characterization of soil conditions throughout the system. The proposed model correlates soil properties to preselected regional variables and is implemented, using geostatistical kriging, in a Geographic Information Systems (GIS) environment. GIS was crucial in this research and proved to

be the appropriate platform for input, manipulation, analysis, and output presentation of spatial and non-spatial data.

Correlation relationships between soil strength parameters and geological and river geometry factors are presented for a pilot study area in California. Global observations that apply across the study area included the increasing trend of shear strength, S_u, with increasing distance from the river, and decreasing trend of S_u with increasing river Sinuosity Index levels. Only local trends were observed in the relation of friction angle, ϕ, with Sinuosity Index, as well as in the relation of S_u and ϕ with geological formations. The proposed methodology also includes steps for seismic response analysis of levee segments, and flood scenarios in protected areas. Since seismic response of earthen structures is controlled primarily by input ground motions, a methodology for selecting ground motions based on their mean period, T_m, for liquefaction triggering assessment of levees is also developed.

CHAPTER 1

Introduction

1.1 Introduction

Flood protection systems are important parts of the civil infrastructure of the United States. Recent natural disasters like Hurricane Katrina have provided warnings with regards to the need to maintain and upgrade the aging and deteriorating flood protection systems. Furthermore, the American Society of Civil Engineers (ASCE), in its most recently released Infrastructure Report Card (ASCE 2009), gave the country's infrastructure an overall average performance grade of D. The newest infrastructure category, levees, received a D- (The levee report card is included in Appendix A). The Department of Water Resources (DWR) in California is currently helping lead the efforts for improving the nation's flood protection infrastructure by re-evaluating the vulnerability of the flood protection systems in the San Joaquin and Sacramento River Valleys and in the Sacramento Delta region (URS 2008; DWR 2011a).

The vast majority of U.S. river cities, now growing at increasing rates, are protected from flooding by earthen levees. Present day earthen levees are at risk from many causes of failure (Figure 1.1) including seepage (both underseepage and through seepage), erosion and instability due to seismic loading. Seismic loading is a potentially grave hazard in many areas of the nation. Guidelines for a seismic element of levee

design have never been implemented as a national standard practice, so there are many thousands of miles of seismically vulnerable levees throughout the nation (Figures 1.2 and 1.3). California has recently allocated major state bond funds in the amount of $5 billion, and is taking a lead in beginning to address this risk, but the problem is national in scope.
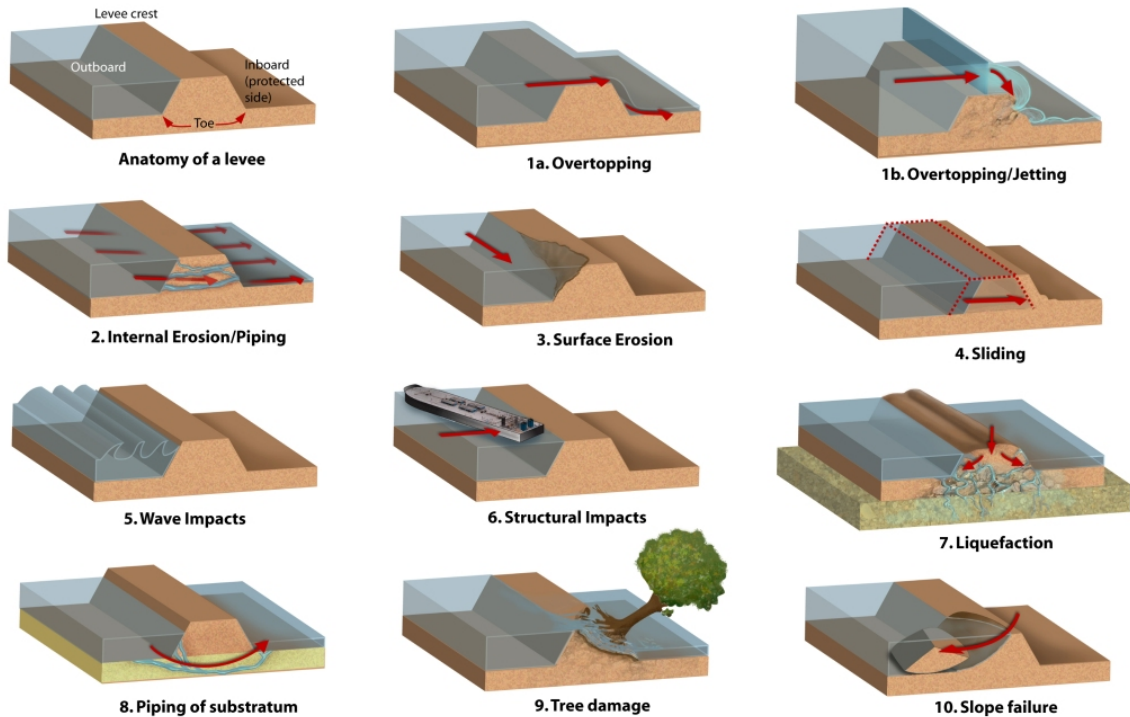
Figure 1.1 Basic levee failure mechanisms (Deretsky 2010).

Of particular interest to seismically active regions is the uncertainty in the dynamic response and performance of levees. This response is dependent on the seismic event itself, as well as the levee geometry and the properties of the levee materials and the foundation soils. Due to the large physical extent of such systems along rivers and canals, and in the absence of as-built documentation, soil investigation data is at best available at scattered intervals along the levee length, carries a high level of uncertainty,

and can be inconsistent, unreliable or incomplete depending on when and by whom the

investigation was carried out.
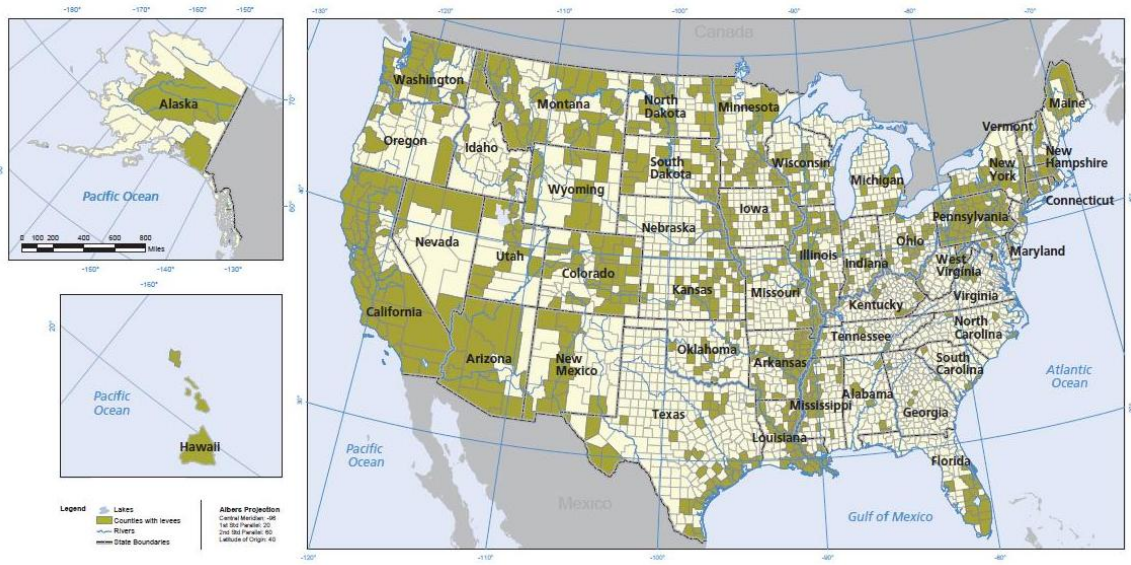
Figure 1.2 Map of United States counties that contain levees (ASCE 2010).
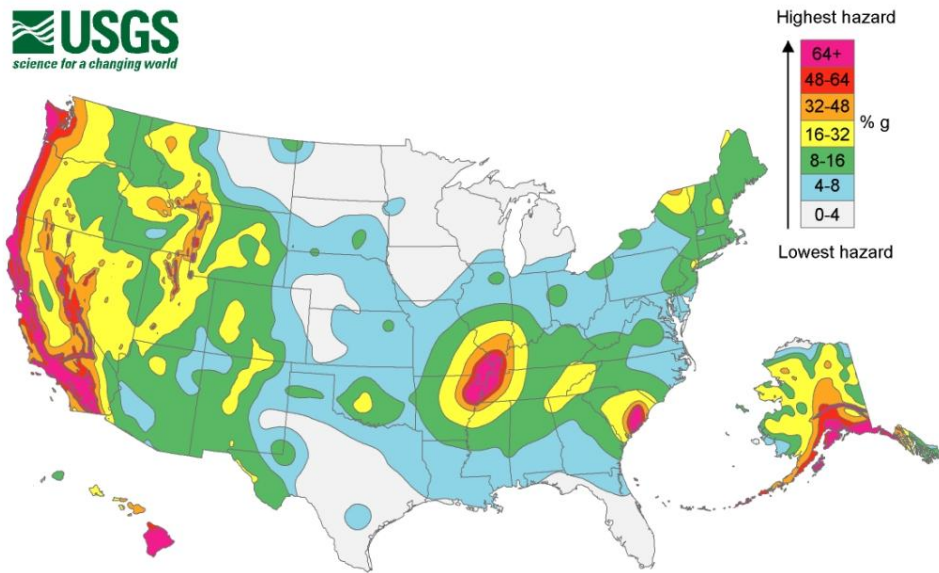
Figure 1.3 National Seismic Hazard Map across the United States showing the levels of horizontal shaking that have a 2-in-100 chance of being exceeded in a 50-year period. Shaking is expressed as a percentage of **g**, the acceleration of a falling object due to gravity (USGS 2008).

Earthen flood protection systems are complex, interconnected, adaptive engineered systems where failure at one location means failure of the system, and failure at different locations may result in flooding of different areas. The general risk assessment aspect of such engineered systems has recently become the topic of research efforts such as the Resilient and Sustainable Infrastructure Networks project (RESIN 2011). However, even though levees stretch for long distances and are in part formed through various geologic processes and human activities over time, information regarding soil properties is collected only at a limited number of point locations and can vary significantly both laterally and with depth. Hence, this becomes a limitation in prediction of the performance of levees in locations where no soil data is available.

Analyses with regard to levee vulnerability were performed to date only at locations with known soil properties (e.g. DRMS 2006a; DRMS 2006b; URS 2008). A simplified procedure for the assessment of seismic vulnerability at a particular levee location with known soil properties has been proposed (Athanasopoulos-Zekkos 2008) and is currently being adopted within the Urban Levee Project led by URS Corp. for the Department of Water Resources in California. The spatial continuity of the results however, is particularly critical in levee systems since failure of a levee at any location could result in the failure of the function of the overall flood protection system. The estimate of the earthen levee response in locations with no available soil data therefore becomes an issue of major concern. As such, it is critically important to develop an approach for assessing the risk of failure continuously along the length of levees.

1.2　Research Objectives

The scope of this thesis is the development of a Geographic Information System (GIS) based tool and methodology to analyze and model the spatial variability of geotechnical soil properties in deltaic and riverine geologic environments for assessing the seismic vulnerability of earthen levee systems.

Seismic risk of levees is typically associated with (a) seismic slope instability induced by soil liquefaction of the levee materials or the foundation materials, and (b) seismically induced permanent deviatoric-type displacements. Therefore, and as a prerequisite to any seismic evaluation of levee vulnerability, this research project aims to incorporate and analyze information at locations of known soil stratigraphy and soil properties and subsequently analytically interpolate in between these locations using geostatistical analysis methods in order to provide spatially continuous results in terms of relevant soil parameters. The spatial distribution of the results is particularly critical in levee systems since investigation and analyses are only performed at selected locations of the levees, but failure of a levee at any location could result in the failure of the overall flood protection system.

Comprehensive seismic hazard and risk analyses must include consideration of geological earthquake sources, path effects, local site and topographic effects. Thus, a large number of factors, many of which are spatially variable, will influence the estimation of soil properties needed for seismic evaluation of the levee system. This effort requires the management of large databases and the storing and updating of

information. Computer based Geographic Information Systems are ideally suited to fulfill the needs of earthquake hazard and risk analyses (Frost et al. 1992), and are uniquely suited for managing, processing and analyzing information that is spatially distributed, as is the case with levee systems. GIS is suggested as a tool for this approach for its ability to manipulate and query georeferenced data, its spatial correlation and analysis functions, integrated database, and advanced result presentation capabilities.

The approach to achieving the research project's objectives, in a study area protected from floods by levees in a typical deltaic and riverine geologic environment, included collection of soil stratigraphy and soil property information at locations where a geotechnical investigation has been performed. This data was manipulated in a GIS environment to represent the distribution of regional factors, and geometric layout and features of the levee system. Analysis was performed to determine factors that best correlate with the spatial variation of the soil properties, and a model was developed for estimating soil stratigraphy and parameters in areas where borehole data is not available.

The goal of this dissertation is also to provide a way to help develop maps of potential flooding for areas protected by earthen levees. A schematic showing the overall research project steps and a sample of resulting output of flooding scenario maps is shown in Figure 1.4.

The developed model can be used to assess the probability of seismic failure of levee segments using, for example, the seismic vulnerability criteria proposed by

6

Athanasopoulos-Zekkos (2008) and the determined soil properties distribution. Based on that, flooding scenarios can be simulated for the range of levee segments' failure probabilities, leading to a seismic risk assessment of the levee system as a whole based on a combination of flooding scenarios and socio-economic factors in the protected areas.
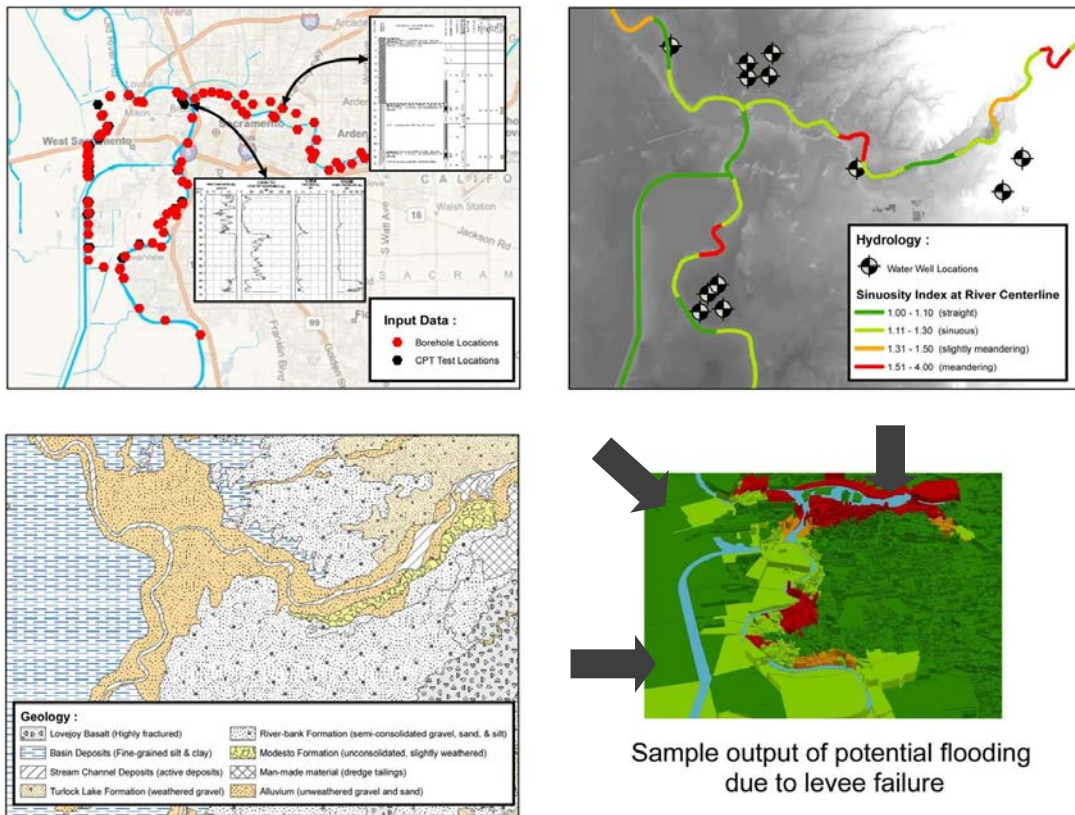
Figure 1.4 Schematic of proposed research overall steps and resulting sample output

1.3 Contribution

Hurricanes, heavy storms, or extreme rainfall conditions can be estimated and predicted days in advance, thus allowing mobilization of resources to either try to contain the flooding, or evacuate the population on time. However, in the case of seismic activity, and due to the unpredictable nature of earthquake occurrence time, location, and

7

magnitude, it is imperative to take the necessary precautions and remediation measures prior to the occurrence of the event.

In this context, the results of this project can be applied to reducing losses from earthquake induced levee failures by prioritizing levee system sections that should be strengthened or repaired. The evaluation of high-risk sections is not based simply on a binary "failure vs. not-failure" outcome, but should be a function of the expected resulting damage to the vulnerable flooded area. This damage can be measured by human deaths and injuries, economic losses, as well as disruption to civil infrastructure. As an example, in the event of a major earthquake of magnitude greater than 6.5 affecting California's San Joaquin-Sacramento delta, economic losses have been estimated at $30 to $40 billion, with the potential large-scale failure of the delta levee system resulting, also, in the backflow of saltwater and degrading the potable water supply of 23 million people in central and southern California (Hess et al. 2006; California DWR & DFG 2008).

The proposed approach enables decision-making prioritization regarding mitigation works, as well as the prediction of levee system performance for specific seismic event scenarios, using the spatial correlation models of soil stratigraphy and properties for riverine and deltaic environments. The combination of such soil material variability models and spatial correlation with seismic response at typical levee cross-sections will in turn provide a new approach to the seismic risk assessment of engineered earthen systems.

1.4   Overview of Dissertation

This dissertation is divided into seven chapters.

Chapter 2 presents an overview of Flood Protection and Control Systems, with an emphasis on the geotechnical reliability and risk assessment of these systems. It then describes the Sacramento River Flood Control System which is used as a case study for this research project.

In *Chapter* 3, the spatial variability of soil properties is discussed, with an introduction to the spatial parameter modeling and estimation process using geostatistics.

Chapter 4 presents the steps taken to analyze and model the spatial variability of geotechnical soil properties in the study areas of the Sacramento River Flood Control System. Observed correlations with regional factors in the areas of study are also presented, analyzed and discussed.

Chapter 5 describes an overall GIS-enabled approach to seismic risk assessment of levee systems. It includes a background section on the current state of knowledge of GIS and information technology applications in civil engineering in general, and geotechnical engineering in particular.

In *Chapter 6*, steps for modeling system response and flood scenarios are presented to demonstrate that the proposed methodology is feasible. This includes a

discussion of a proposed method for ground motion selection for site-specific seismic response analysis.

Finally, *Chapter 7* draws conclusions from the research study and presents recommendations for future work.

CHAPTER 2

Flood Protection and Control Systems

2.1   Introduction

Flood Protection and Control Systems are complex, interconnected engineered systems, important for handling water resources, but also for protecting urban areas, important civil infrastructure elements, and agricultural land properties that lie in or cross potential floodplains (Athanasopoulos-Zekkos 2008). An important part of these systems are earthen levees. Levees are natural or man-made structures that protect land from flooding, or help in directing the flow of water. They are typically constructed parallel to rivers or channels and prevent flooding of the adjacent land by restraining the water to one side of the levee.

An earthen levee is usually formed by the natural deposition of sediments due to the repeated overflow of a river (Figure 2.1). The coarsest sediments (sands) undergo rapid deposition immediately adjacent to the channel, while the finest sediments (silts and clays) are deposited out on the floodplain, away from the channel (Mount 1995). This natural process is sometimes followed by human addition of soil material to raise the levee to the desired level. Such levees are highly heterogeneous and the material properties are variable along the levee length as well as within the levee stratification. This is mainly due to (a) the meandering of rivers which results in crisscrossing of

previous channel deposits, and (b) the variety and nature of material hauled and deposited by human activity. These earthen levees can run from tens to thousands of miles long and are thus viewed as series systems, where failure at one location results in the whole system failing to perform what is expected of it, which is to keep water out of the floodplain.
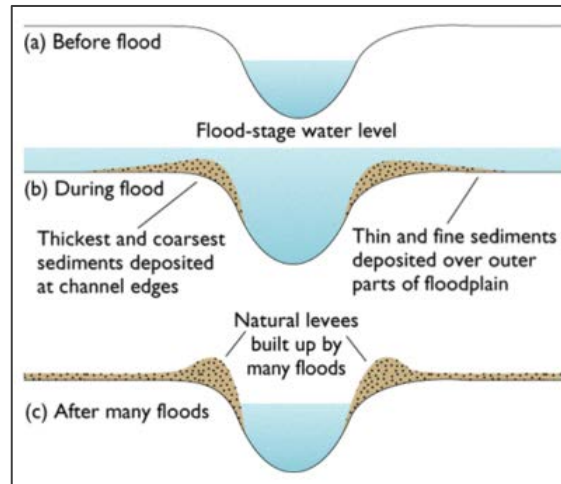
Figure 2.1 Process of levee formation due to seasonal flooding (Mount 1995).

Two of the most intricate and extensive flood protection systems in the United States are (a) the Mississippi River and (b) the Sacramento and San Joaquin Rivers systems (Figure 2.2). Some of the Mississippi River levees are near areas of moderate shaking risk (Figure 2.3).The Sacramento and San Joaquin Rivers system falls in a region of high seismicity (Figures 2.4 and 2.5) where damage to the flood protection system due to strong ground shaking can have a detrimental effect on the protected areas. In addition to the risk of failure from overtopping, erosion, slope instability, under-seepage, and through-seepage, levees in seismic regions are at risk of failure due to loss of freeboard caused by (1) liquefaction (loss of strength in material forming the levee and/or foundation layer), or (2) seismically-induced permanent displacements.
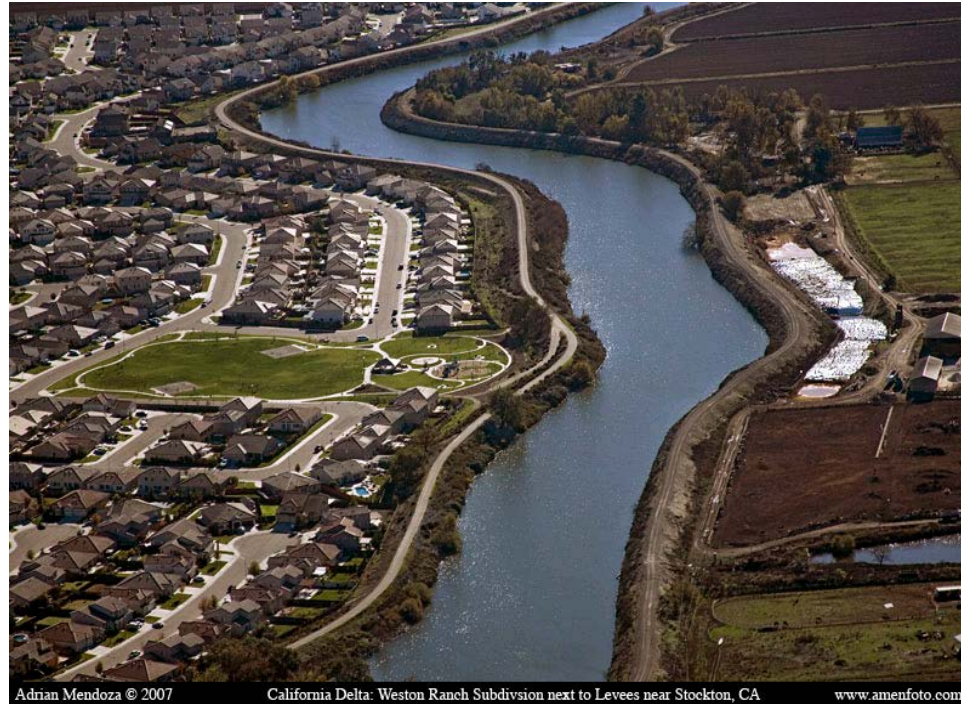
Figure 2.2 Levees protecting agricultural land and residential neighborhoods in California's Sacramento-San Joaquin Delta.

In presenting a case history on the California delta levee system, Gilbert et al. (2011) list the possible hazards and environmental factors affecting the system as: floods, earthquakes, winds/waves, "sunny-day" hazards (localized animal holes, seepage and piping), and environmental factors such as subsidence and climate change (sea level rise, or changes in precipitation).Among all the above factors, seismic events were found to be the dominant contributor to risk in the California delta levee system. The seismic hazard is spatially distributed, with a potential of failure over thousands of feet, at multiple locations at a time. The seismic failure modes for the system in the case history included (1) embankment and/or foundation liquefaction, and (2) embankment stability and inertial effects. The case history showed that the predicted seismic failures are most likely to occur as a result of liquefaction. Furthermore, in the recent Tohoku earthquake of

13

March 11, 2011 numerous levee reaches sustained moderate to major damage, and this damage was mostly ascribed to foundation liquefaction (EERI/GEER 2011).
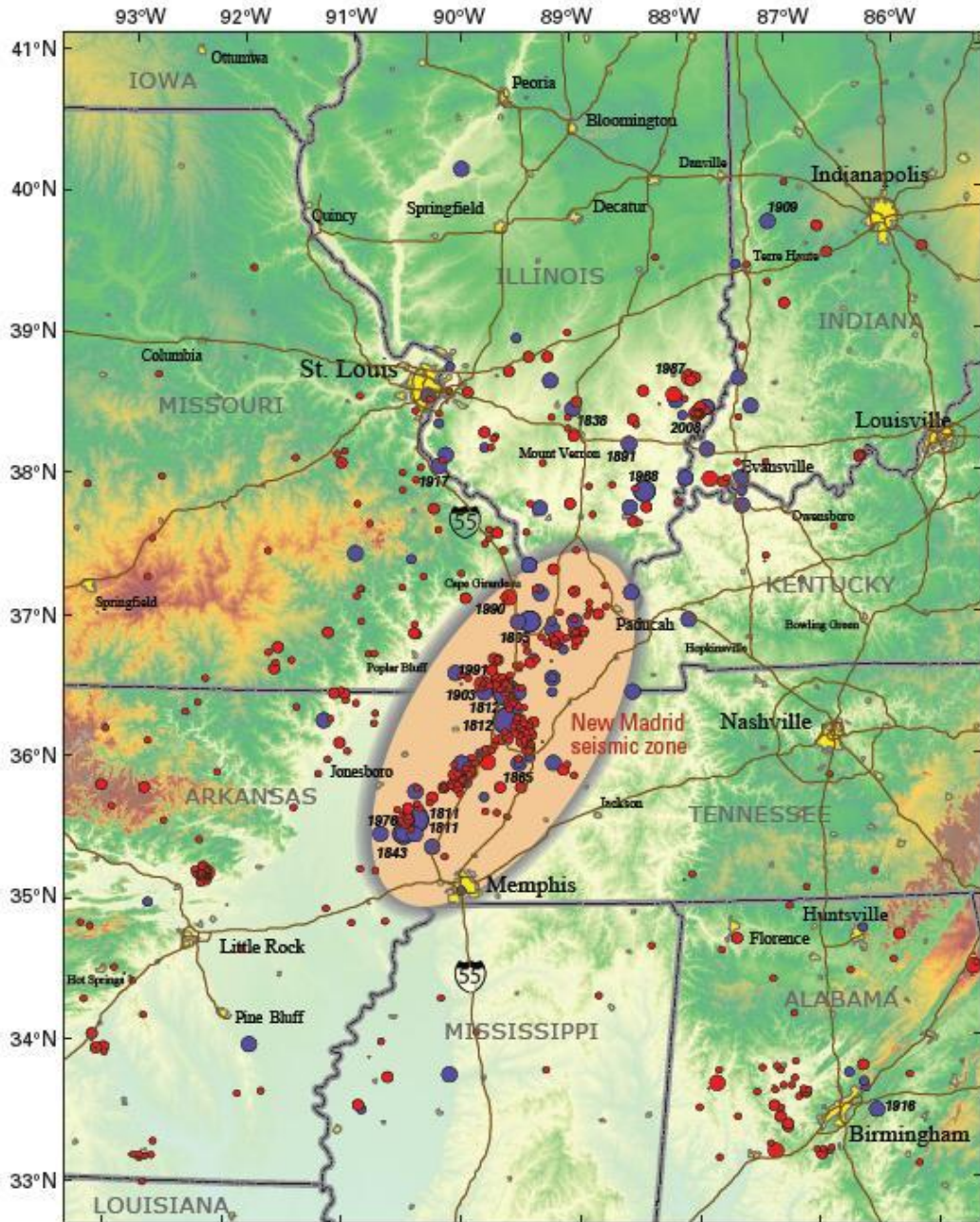
Figure 2.3 Map showing earthquakes greater than magnitude 2.5 in the central United States (USGS 2009a). Red and blue circles represent earthquakes before and after 1973 respectively, larger earthquakes are represented by larger circles.

Figure 2.4 The California levee system (Harder 2008).

Figure 2.5 Major faults of California (USGS 2009b).

The evaluation of the seismic response of earthen levee depends mainly on the dynamic properties of the soil forming both the levee and underlying foundation. In addition to the properties of unit weight, γ, friction angle, ϕ, and cohesion, c, the relevant dynamic properties of interest are: (1) small strain shear modulus, $\mathbf{G_{max}}$, or alternatively the shear wave velocity, $\mathbf{V_S}$, (2) shear modulus reduction vs. shear strain curves, and (3) damping ratio vs. shear strain curves. Recent studies by Athanasopoulos-Zekkos (2008) showed that the variability in seismic levee response due to the ground motion selection was much higher than the variability in response due to soil properties or levee geometry. Thus this research project focused on the estimation of stratigraphy and soil strength parameters to be used for the seismic risk assessment. A complete review of the seismic response of levees is beyond the scope of this thesis, and can be found in Athanasopoulos-Zekkos (2008).

2.2 Reliability and Risk Assessment of Flood Control Systems

2.2.1 Introduction

Risk assessment is usually performed with the objective of proving input for making decisions. In the case of engineered systems, such decisions have to do with the viability of a new proposed system, or the continuing viability of an existing system. Examples of engineered systems include nuclear power plants, railway systems, bridges, petrochemical installations, dams and others. For a system to be viable, it must fulfill the requirements placed on it, one of which is performing at an acceptable level of safety (Stewart and Melchers 1997).

When a system is part of a larger system, the failure assessment is usually conditional. The output from failure of a sub-system will form part of the input and assessment of the larger system. It is therefore important to understand the relationships between the overall system and its elements or components. A system representation can therefore be modeled in terms of logically interrelated constituents at various levels of detail or scale. Management of the risks is performed by selecting components with individual appropriate reliability, and then combining these so as to ensure an adequate reliable joint functionality (Faber et al. 2007).

The failure of an engineered system occurs once the system is not able to achieve an "acceptable" level of performance. Therefore a crucial step is identifying individual system elements that are prone to failure, the causes of such element failures, and the effect that those would have on the performance of the overall system.

Christian and Baecher (2011) give an overview of the historical relation between reliability studies and geotechnical engineering. In the initial years where geotechnical engineering was being established as a discipline of its own, little interaction took place between the geotechnical and the reliability study efforts. In the 1970s, pioneering efforts of researchers such as T. H. Wu, Peter Lumb, Allin Cornell, and Robert Whitman showed that the reliability and geotechnical practices did have things in common. In more recent years, there have been great advances in applying probabilistic reliability ideas to geotechnical problems which is reflected both in the increasing numbers of papers and in greater interest on the part of clients and practical engineers in expressing reliability in

quantitative terms. The geotechnical engineering discipline has learned a lot in the process, but it has also discovered that some issues remain difficult to resolve in a satisfactory manner.

2.2.2 Geotechnical Reliability of Levees

A large number of studies have focused on the probabilistic approach to the hydrological and economic aspect of levees. These studies primarily addressed issues related to determining the optimum levee heights against parameters of cost, benefit, and damage. The geotechnical reliability of the levee itself is either neglected, suggesting that the relative probability of failure due to geotechnical reasons is negligible, or it was left for others to determine a suitable probability of failure for various geotechnical failure modes (Wolff 2008).

Among the first notable research efforts on probabilistic analysis of the geotechnical reliability of levees was the work of Duncan and Houston (1983), Peter (1982), and Vrouwenvelder (1987). Later on, the U.S. Army Corps of Engineers introduced probabilistic concepts to levee evaluation (USACE 1991; 1999). Voortman (2003) summarized the history of dike design in the Netherlands, but noted that "probabilistic methods are sometimes applied, but a required failure probability is not defined in Dutch law". None of the above mentioned research and guidelines on geotechnical reliability of levees took into consideration seismically induced failure modes. Furthermore, Wolff (2008) states that additional work is needed to better model spatial variability and system reliability.

The U.S Army Corps of Engineers policy guidelines (1999) affecting the majority of earthen levee design included research done by Wolff (1994), which was later presented as a detailed framework for the analysis of levee reliability for five modes of failure: overtopping (J) , slope stability (SS), under seepage (US), through seepage (TS), and surface erosion (SE) (Wolff 2008). In this work, the probability of failure P_f was conditionally defined given a Flood Water Elevation (FWE) as:

$$Pf \mid FWE = f(FWE, X1, ..., Xn) \qquad \text{Equation 2.1}$$

where $X_1, ... X_n$ are soil parameters.

The Reliability R has been defined as:

$$R = 1 - P_f \qquad \text{Equation 2.2}$$

The reliability and the annual probability of failure of the levee system are defined as:

$$R_{system} = R_1 \times R_2 \times ... \times R_n \qquad \text{Equation 2.3}$$

and

$$P_{f\ system} = 1 - R_{system} \qquad \text{Equation 2.4}$$

where $R_1, ... R_n$ are the reliabilities of individual levee segments. The above formulas assume statistical independence of segments, which is not always true in actual conditions. To account for this, Wolff discusses the notion of a spatial segment correlation distance which is difficult to estimate as it requires a relatively large set of equally spaced data, which in turn is generally not available.

The USACE guidelines and the approach above proposed by Wolff were criticized by a National Research Council report (2000) titled "Risk Analysis and Uncertainty in Flood Damage Reduction Studies". The report's recommendations included the following:

19

"The Corps' risk analysis method should evaluate the performance of a levee as a spatially distributed system. Geotechnical evaluation should account for the potential of failure at any point along the levee…and should consider multiple modes of failure, correlation of embankment and foundation properties and the potential for multiple levee section failures. The current procedure treats a levee within each damage reach as independent and distinct from one reach to the next… This does not provide a sufficient analysis of the performance of the entire levee"

It is noted that the application of probabilistic analysis in civil engineering is a continuously developing engineering approach, more so in geotechnical engineering, and even more so in applications to levees. As such, analysis done using probabilistic approaches should be expected to provide relative reliability, as opposed to true or absolute reliability measures (Wolff 2008).

Recent work by Vanmarcke (2011) provides an example of probabilistic estimation of risk of slope failure in long earth slopes (such as dikes, dams, and levees). Even though the author's focus was on the comparison of two- and three-dimensional approaches to risk assessment of long slopes, his conclusions highlighted the importance of probabilistic analysis in identifying over-conservatism in some traditional 2D methods of analysis.

Under the general topic of "Unresolved problems in geotechnical risk and reliability", Christian and Baecher (2011) address the issue of theoretical upper- and

lower-bound probability limits of geotechnical systems failure given different possible failure modes, and raise the issue of un-resolved estimation of the degree of interdependency between these various modes. In addition, the authors also revisit previous work (Vanmarcke 1977) regarding determining system-wide probability of failure based on individual segments (using levee "reaches" as an example of system segments). Their conclusion is that such previous "theoretically elegant form equations" over-estimate the probability of failure of systems in practice, and proposes a future focus on a better understanding of correlations among the uncertainties affecting each levee reach.

2.3   Sacramento River Flood Control System

2.3.1   Introduction

California has a wide range of climatic, topographic, and geologic features, all of which result in varied and challenging floodplain issues. A report prepared by the Information Center for the Environment at the University of California, Davis has identified 172,000 miles of rivers in California with 70,000 miles of rivers downstream from dams. All areas of the State are subject to flooding and resultant losses. The Central Valley specifically is subject to large and devastating floods that would impact millions of people currently located in flood hazard areas or dependent upon support from facilities in identified or unidentified floodplain areas. In addition, California has over 13,000 miles of levees that protect residential and agricultural lands (DWR 2011a).

The study area used for this research project encompasses the levee system protecting Sacramento City as well as the Feather River, both situated at the northeastern

limit of the San Joaquin-Sacramento delta region, where the levee material and cross-sections can be considered typical of the area. A possible earthquake related levee system failure in Sacramento alone, as per one estimate, might put at risk more than 400,000 people and 170,000 structures, and have a potential economical impact of \$7 to \$15 billion (Hess et al. 2006). The study area is representative of the larger region constituting the greatest population density in Northern California and carrying more than 25% of the nation's annualized risk (FEMA 2008).

2.3.2 Historical Background

Around 150 years ago, the levees of the Sacramento-San Joaquin Delta were raised to prevent flooding of what remains some of the most fertile farmland in the nation (DWR 2011a). The native soils in the area were primarily used to create the levee system. These were mainly peat soils, excellent for agriculture, but a very poor choice as foundations for levee barriers against a constant river flow. Meanwhile, gold mining in the Sierra Nevada used environmentally destructive high-pressure water jets that washed away entire mountainsides into local streams and rivers, creating enormous amounts of silt deposited in the riverbeds, raising the channel bottom levels, which increased flood risk. To counter that effect, levees were built very close to the river channels to keep water velocity high and thereby scour away the sediment. However, the erosive forces of the constrained rivers continue to eat away at the levee system, and the flow constriction in time of floods actually causes flooding upstream and downstream of levee protected areas as shown in Figure 2.6.
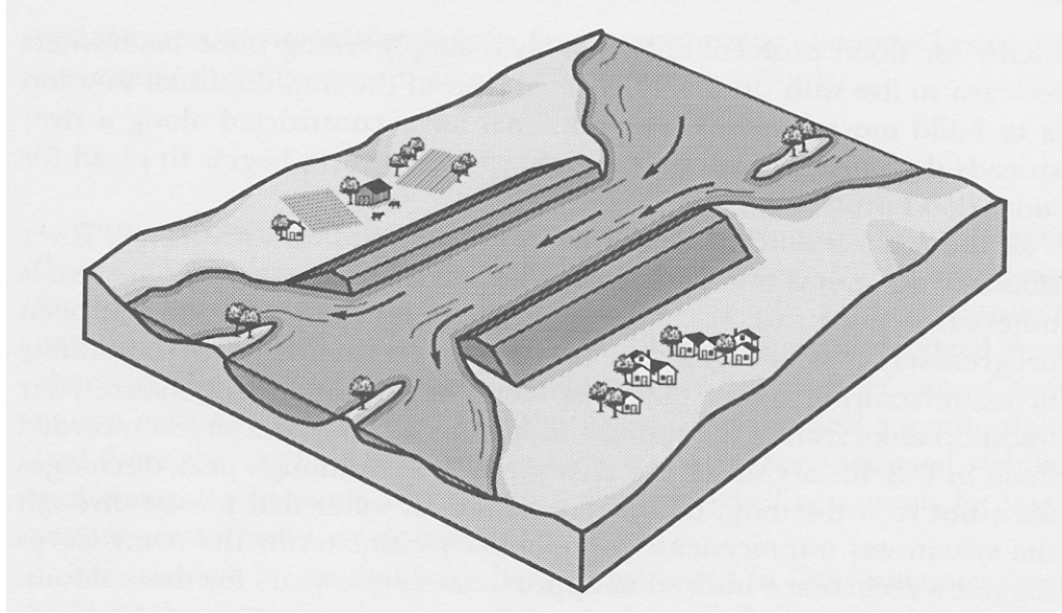
Figure 2.6 Flow constriction associated with levees (Mount 1995).

In addition, the peat soils behind the levees have subsided in many locations (Figure 2.7) with some of the protected parcels now more than 20 feet below sea level in the delta region.
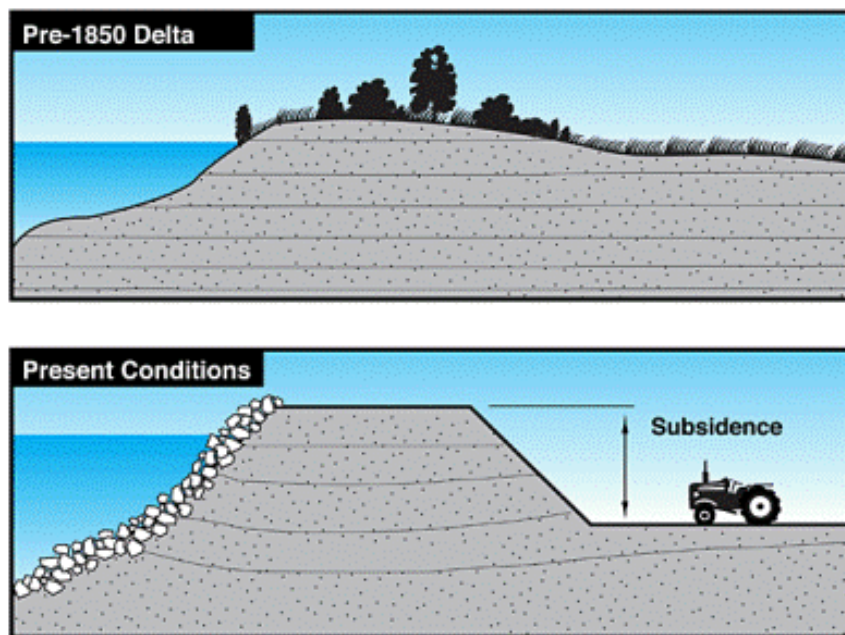
Figure 2.7 Subsidence of soil behind levees (DWR 2011a).

The efforts to control flooding in the Sacramento Valley, which began in the Gold Rush days, continue today in an ongoing project called the Sacramento River Flood Control Project (SRFCP). In 1917, a joint session of Congress passed the Flood Control Act Public Law 64-367 (Appendix B), which initiated what was to become the SRFCP (U.S. Congress 1917). Section 2 of the related Senate Bill provides for the "control of the floods, removal of debris, and the general improvement of the Sacramento River" (Figure 2.8).

Mr. VARDAMAN (for Mr. RANSDELL), from the Committee on Commerce, submitted the following

REPORT.

[To accompany H. R. 14777.]

The Senate Committee on Commerce, having had under consideration H. R. 14777, "An act to provide for the control of the floods of the Mississippi River, and for other purposes," which passed the House of Representatives May 17, 1916, reports the same back to the Senate without amendment and with the recommendation that the bill do pass.

Very able reports accompanying this bill (H. Doc. 616, 64th Cong., 1st sess.) were presented to the House of Representatives on April 29, 1916, by Representative Humphreys, of Mississippi, chairman of the Committee on Flood Control, and by Representative Curry, of California, a member of the committee. These two reports cover the subject matter of the bill so thoroughly that the Senate Committee on Commerce feels that it can add nothing thereto, and therefore adopts same as its report, which it attaches hereto and makes a part hereof.

[House Report No. 616, Sixty-fourth Congress, first session.]

The bill contains three sections.

The first provides for the control of the floods and the general improvement of the Mississippi River and authorizes the Secretary of War to carry on continuously for that purpose the plans of the Mississippi River Commission, the expenditure not to exceed in the aggregate $45,000,000.

Section 2 provides for the control of the floods, removal of débris, and the general improvement of the Sacramento River, Cal. The Secretary of War for this purpose is authorized to carry on continuously the plans of the California Débris Commission, the expenditure not to exceed in the aggregate $5,600,000.

Section 3 provides machinery under the Secretary of War by which any flood problem, other than the Mississippi and Sacramento, may be examined and reported upon by the Engineers of the Army when authorized hereafter by Congress.

Figure 2.8 Excerpt from the Senate Committee on Commerce's report recommending the passing of the bill that will become known as the Flood Act of 1917 (U.S. Congress 1917).

Construction of the SRFCP began in 1918 and the project's main components were completed in 1968 after the closure of Oroville Dam. From the 1940s through the 1970s, the SRFCP was augmented with several large, multipurpose dams, which are now an integral part of the system (James and Singer 2008).

Currently, the Sacramento River Flood Control Project includes approximately 1,100 miles of levees, in addition to overflow weirs, pumping plants, and a series of bypass channels that are designed to protect the communities and agricultural lands of the Sacramento Valley and the Delta. Figure 2.9 reflects the effect that the bypasses can have on the actual Sacramento River levels during flooding. Figure 2.10 shows the water flow in the Yolo Bypass is considerably larger than in the Sacramento River, which gives an idea of the potential flooding that would have occurred along the river if the bypass wasn't there.
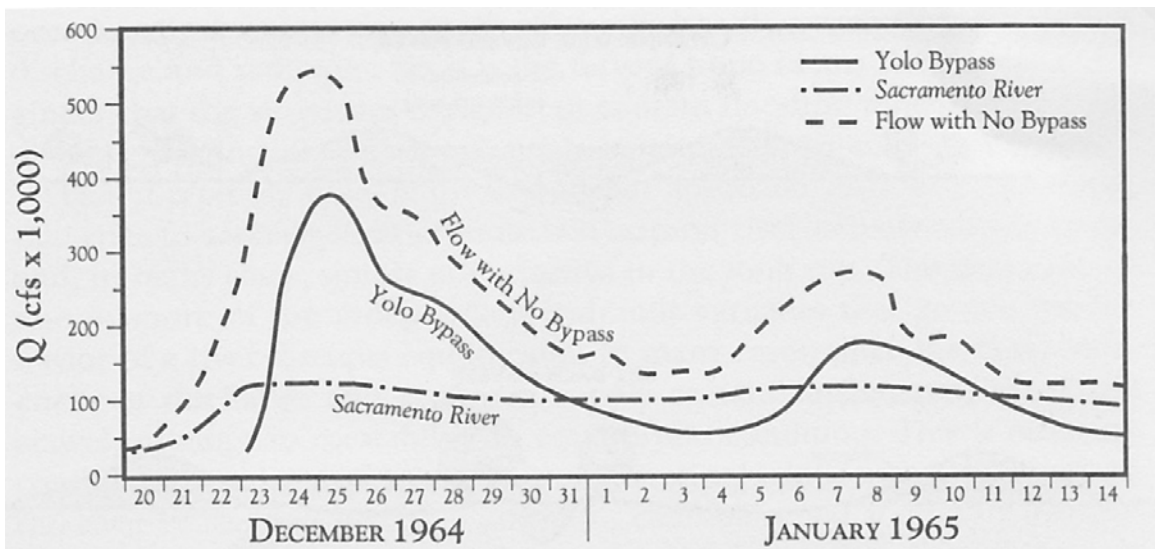
Figure 2.9 Impact of the Yolo Bypass on flood flows within the Sacramento River (Mount 1995).

25

Figure 2.10 Sacramento River, foreground, and Yolo Bypass, in the distance (Austin 2011).

Nowadays, the SRFCP levees protect not only farms, but also hundreds of thousands of people who live and work in Central Valley communities. State highways, railroad lines, water supply pipelines that serve much of the San Francisco Bay area, energy transmission lines, and petroleum pipelines also now cross the delta and rely on the continued stability of delta levees. Altogether, more than $47 billion in infrastructure is protected by Central Valley levees (DWR 2011a).

2.3.3   Components and Extent of Sacramento River Flood Control Project

The majority of the components of the Sacramento River Flood Control Project lie in the region extending from the Sacramento-San Joaquin River Delta in the south, to Chico city and Butte Basin in the north (Figure 2.11).
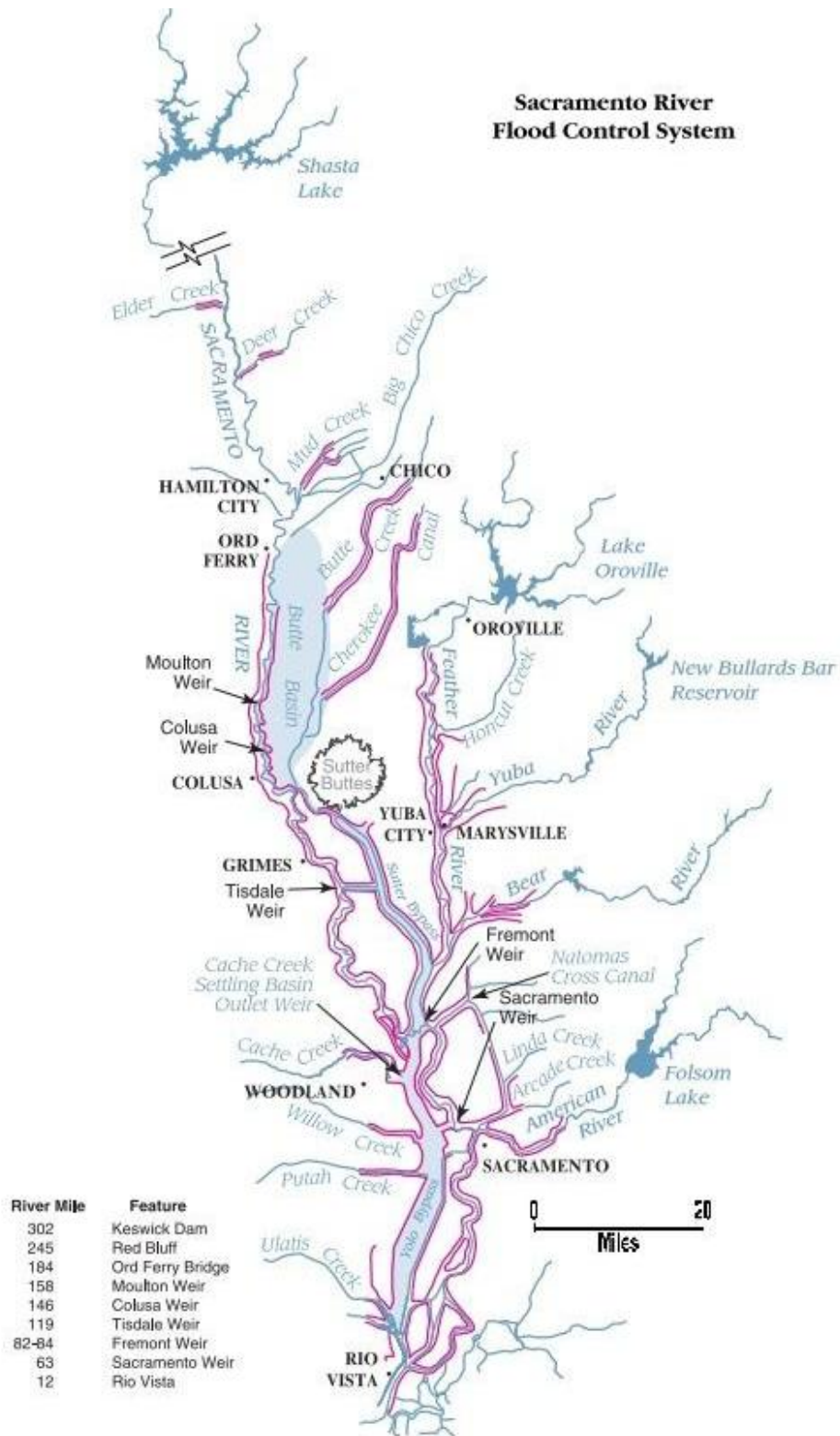
Figure 2.11 Sacramento River Flood Control Project general features (DWR 2011b).

The specific areas used for data analysis and model development in this study were sub-sections of the larger SRFCP, namely:

- **Feather River**, comprising data collected from the Feather River South (between Yuba and Bear Rivers), levees around the City of Marysville, and Feather River North (Between Yuba River and the City of Oroville), and

- **City of Sacramento**, comprising data from the regions of West Sacramento and the American River.

Sacramento City is referred to by some as "The most flood prone city not named New Orleans" (Bailey 2008) . The Sacramento Area Flood Control Agency states that the city has a low estimated flood protection level as compared to other major river cities in the U.S. (Figure 2.12) with a 85-year flood protection, meaning that in any given year there is a one-in-85 chance that a storm might occur that is beyond the containment capacity of levees and reservoirs in the area (DWR 2011a).
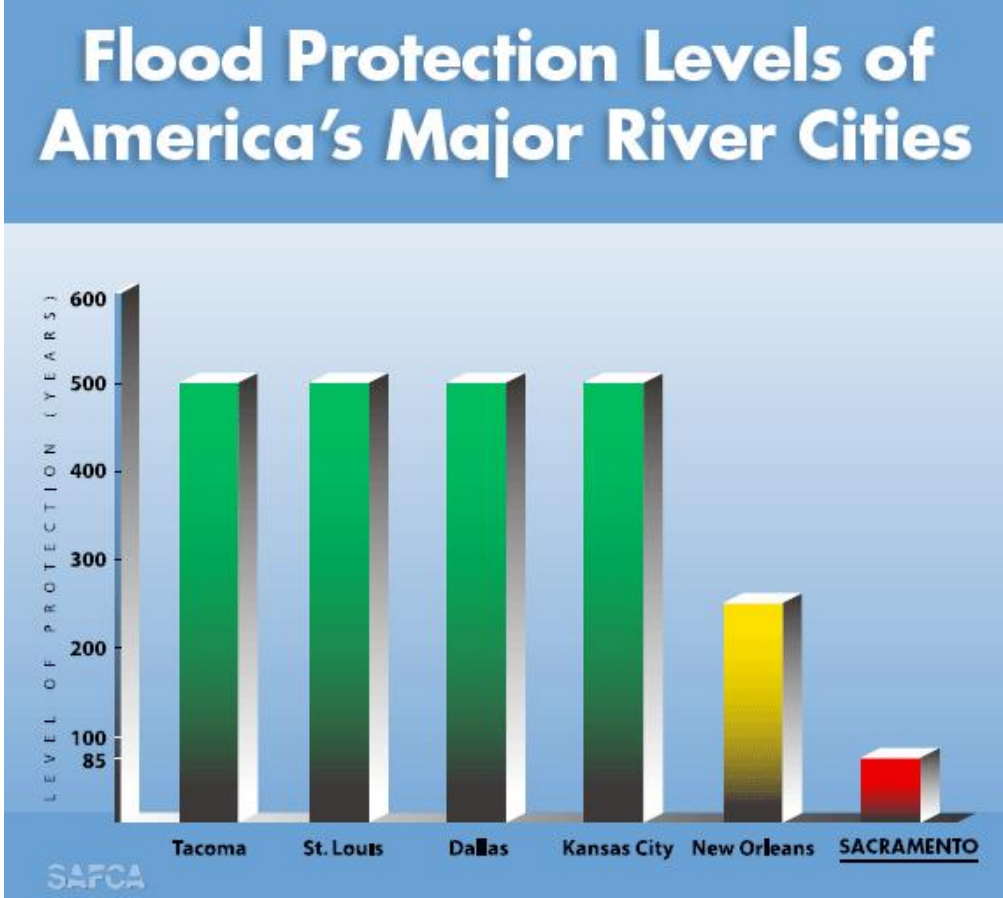
Figure 2.12 Flood protection level of major river cities in the United States (DWR 2011a).

CHAPTER 3

Modeling Spatial Variability of Soil Parameters

3.1   Introduction

Soils and rocks in their natural state are among the most variable of all engineering materials. Quantitative measurements of soil properties in the early 1900's differentiated the new discipline of soil mechanics from the engineering of earth works in the previous periods. However, these measurements revealed a great amount of variability in properties, not only from site to site and layer to layer, but even within what seemed to be a homogenous material (Baecher and Christian 2008). The variation in these parameters, due to inherent variations in composition and consistency during formation, is thus a three dimensional problem that involves the vertical stratification at any given point, as well as the planar deviations within a specific layer.

Ranges of data variation for soil property parameters have been reported by many researchers, especially starting in the 1960's (Lumb 1966; Lumb 1974; Lee et al. 1983; Lacasse and Nadim 1996). Despite the work that has been done on this issue, it is not a closed matter, and more needs to be done, particularly on quantifying the level of additional effort required to improve existing characterization of a particular site (Christian and Baecher 2011).

One way to measure the variability of soil properties is similar to the work by Phoon and Kulhawy (1996). The extent, to which soil data might vary, is measured by the coefficients of variation (COV) for a variety of soil properties (Table 3.1). The COV is defined as the standard deviation divided by the mean. The range of values of the COV is large and is only reflective of conditions at a particular site. As such, there is a need for extending such measures of variability beyond site specific conditions, and applying them to more general conditions of geological or geographical environments such as riverine or deltaic regions, in the case of this project.

Table 3.1 Coefficient of variation for common field measurements (Phoon and Kulhawy 1996)

Test type	Property	Soil type	Mean	Units	Cov(%)
	q_T	Clay	0.5–2.5	MN/m^2	< 20
CPT	q_c	Clay	0.5–2	MN/m^2	20–40
	q_c	Sand	0.5–30	MN/m^2	20–60
VST	s_u	Clay	5–400	kN/m^2	10–40
SPT	N	Clay and Sand	10–70	blows/ft	25–50
	A reading	Clay	100–450	kN/m^2	10–35
	A reading	Sand	60–1300	kN/m^2	20–50
	B reading	Clay	500–880	kN/m^2	10–35
DMT	B Reading	Sand	350–2400	kN/m^2	20–50
	I_D	Sand	1–8		20–60
	K_D	Sand	2–30		20–60
	E_D	Sand	10–50	MN/m^2	15–65
	p_L	Clay	400–2800	kN/m^2	10–35
PMT	p_L	Sand	1600–3500	kN/m^2	20–50
	E_{PMT}	Sand	5–15	MN/m^2	15–65
	w_n	Clay and silt	13–100	%	8–30
	W_L	Clay and silt	30–90	%	6–30
	W_P	Clay and silt	15–15	%	6–30
Lab Index	PI	Clay and silt	10–40	%	—[a]
	LI	Clay and silt	10	%	—[a]
	γ, γ_d	Clay and silt	13–20	KN/m^3	< 10
	D_r	Sand	30–70	%	10–40; 50–70[b]

Notes

[a] COV = (3–12%)/mean.

[b] The first range of variables gives the total variability for the direct method of determination, and the second range of values gives the total variability for the indirect determination using SPT values.

Furthermore, although some of the general trends of variability in soil and rock can be anticipated, the uncertainty in practice can be larger than expected, with significant implications to geotechnical design and analysis (Christian and Baecher 2011). For example, while the unit weight of soil in a fill might be expected to have a relatively low coefficient of variation, actual experience shows that field measurements of density yields surprising ranges of values, and the variance in the unit weight can have a large effect on the uncertainty in the factor of safety in slope stability calculations.

Figure 3.1 shows how the uncertainty in soil property estimates is divided into what is caused by the data scatter and what is caused by systematic errors (Baecher and Christian 2008; Christian and Baecher 2011; Gilbert et al. 2011). Variations in soil parameters (data scatter) involves (a) actual spatial variability from one point to another, and (b) noise introduced by methods of measurement. The systematic errors on the other hand include (c) statistical analysis errors due to limited numbers of observations, and (d) model bias errors due to the approximate nature of our mathematical modeling of the physics of soil behavior.

Basic questions need to be asked about the design of the data collection or sampling process, the conceptualization and measurement of the recorded variables, and sources of non-sampling error (e.g. testing apparatus imprecision, subjective recording of observed results). A critical perspective on spatial data is required in order to recognize the various levels of data uncertainty and bias, compare multiple data sources whenever possible, and report the uncertainties and biases in the resulting work.

(a)	**(b)**	**(c)**	**(d)**
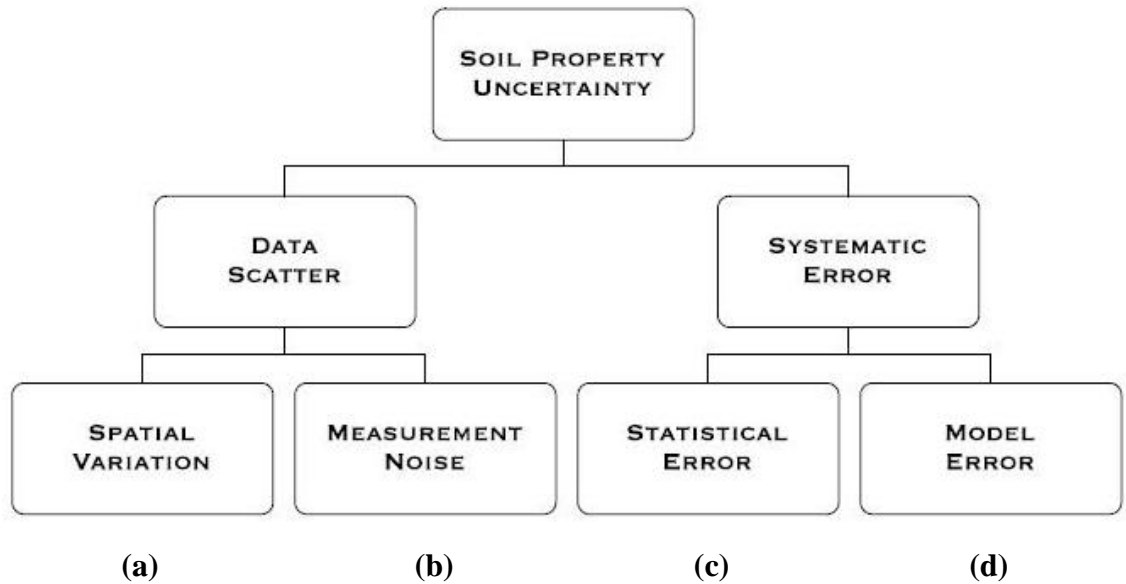
Figure 3.1 Contributions to soil engineering property uncertainty (Christian and Baecher 2011).

In the absence of unlimited resources that would permit as many boreholes and tests as needed, geotechnical engineers find themselves most of the time having to deal with limited site investigation data. The traditional approach in dealing with limitation in design has been to use characteristic values of the soil properties combined with a factor of safety. However, for a particular soil layer, soil parameter data sampled at multiple locations on a site would likely plot in a bell-shaped curve. This variability, even in the smallest of sites, suggests that geotechnical engineering systems are amenable to a statistical approach, and most soil properties can be regarded as randorn variables conforming to the "normal" or "Gaussian" theoretical distribution, thus established statistical methods based on the normal distribution may safely be applied in estimating design parameters (Lumb 1966; Fenton and Griffiths 2008).

The precision of soil parameters values depends on (a) the reliability of the sampled results, and (b) the estimation of values at unsampled locations. The reliability of measured soil specimen properties depends on the number of samples obtained as well as the testing methods and equipment used.

Soil properties are deterministic, and can be assessed on site by running an infinite number of tests; however, in addition to the cost, that would basically destroy the material of interest on site. A full analysis of the reliability of a geotechnical problem over the whole of the site thus requires a realistic random soils model. Existing research on the nature of soil spatial variability needs development and further study, and establishing the variability of a property requires different approaches for different properties, different materials, and different methods of testing (Fenton and Griffiths 2008; Christian and Baecher 2011).

3.2   Overview of Geostatistics

Geostatistics provides a methodology to quantify spatial uncertainty. The "Geo" prefix, from Greek for "earth" or "land" or "Ground", emphasizes the spatial aspect of the problem. "Statistics" comes into play because probability distributions are the meaningful way to represent the range of possible values of a variable of interest, and it is suited to the randomness of spatial variations (Chiles and Delfiner 1999).

Geostatistics is a relatively specialized subject matter that was initially defined by Georges Matheron in 1962 for his own developed methodology of ore reserve evaluation (Matheron 1962). Nowadays the application of geostatistics extends to many fields in the

earth sciences including not only the subsurface, but the land, atmosphere and oceans as well (Chiles and Delfiner 1999; Haining et al. 2010). Until the late 1980s, geostatistics was essentially viewed as a means to describe the spatial patterns and predict the values of soil properties at a number of locations where those properties have not been measured (Vieira et al. 1983; Trangmar et al. 1986; Warrick et al. 1986). New tools were also later developed to tackle advanced problems such as simulation of the continuous spatial distribution of attribute values, assessment of uncertainty about soil quality, and modeling of space-time processes (Goovaerts 1999). Statistical methods can even be applied to quantify estimation errors as a function of spatial variability of a measured parameter and the spatial distribution of the measurement locations, without the actual knowledge of the parameter's true distribution within the study area (Alkhaled et al. 2008).

It is generally accepted that descriptions of spatial phenomena are subject to uncertainty. The growing interest of soil scientists and geotechnical engineers in the field of geostatistics arises from the realization that quantitative spatial estimation must incorporate the spatial correlation among known observations or samples. However, Christian et al. (2011) state that while there has been some success in describing spatial correlations for soil materials, using auto-correlation and geostatistics, the techniques for dealing with spatial correlation remain difficult to implement, are sometimes poorly understood by the practice, and their consequences often ignored. A further concern stated by the authors is that determining correlation patterns is not easy because it requires large amounts of data taken over a broad range of distances, which in practice

may be hard to achieve because of (1) cost of data collection and (2) project area/size limitations.

Developments of data acquisition and computational resources have provided the geostatisticians with large amounts of information, both continuous and categorical, that can be stored, managed and processed rapidly in databases (such as Geographic Information Systems). Furthermore, geostatistics was originally developed to solve practical problems in evaluating recoverable reserves in mining, and the growth of the geostatistics field is witness to its utility and success. Engineers should keep this trademark of practicality in the soil sciences, and foster the increasing and successful application of geostatistics to soil-related issues (Goovaerts 1999).

Geostatistics aims at providing quantitative descriptions of natural variables distributed in space or in both time and space. These variables can include, for geotechnical engineering practical purposes, the depths and thickness of geological layers as well as the soil properties in a region. Such variables can have a detailed complexity that it would not be possible to describe them using simplistic models or standard mathematical functions. In addition, what makes the task more complex is that these variables are often sampled very sparsely for economic reasons. The challenge is to address, prior to getting the data, the question of whether information acquired from having more samples justifies the extra cost and time.

Spatial variables are not completely random but usually exhibit some form or structure, in an average sense, reflecting the fact that points close in space tend to have similar values. Matheron (1962) coined the term "regionalized variable" to designate a numerical function $z(u)$ that depends on a continuous space index u (representing a unique location in that space), and thus defined geostatistics as "the application of probabilistic methods to regionalized variables". The main objective in geostatistics is to estimate the value of a regionalized variable at locations where it has not been measured. Typically, a regular grid is established in the area of study. Once the grid is established, with estimated values at all points, it is often used as the representation of the reality, from which one derives contour maps for instance, without any reference back to the original observed and measured values at the known locations. This is why the computation of grids requires a lot of care and cannot simply rely on simplistic interpolation techniques. One should evaluate both the accuracy and the precision of the resulting variable values in the grid.

Accuracy is defined as the degree of conformity of a calculated variable to its actual true value. Precision on the other hand is the degree to which further calculations show the same or closely similar results (Figures 3.2 and 3.3). In all cases, the estimates need to be accurate, meaning that on average they are correct (not too high or too low), which is captured by the notion of bias error. The other objective should be to achieve precision, which is quantified by the notion of error variance or standard deviation.
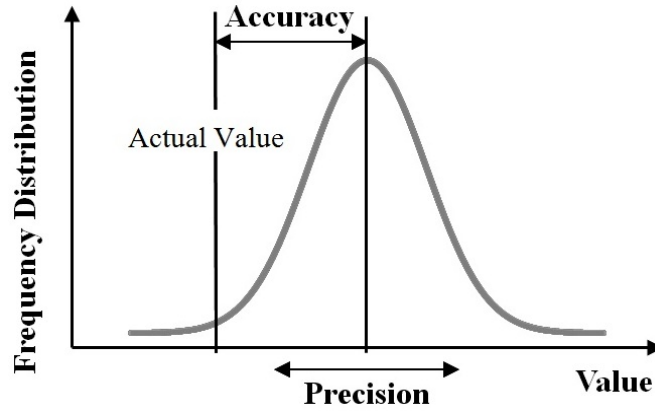
Figure 3.2 Accuracy and precision.

Figure 3.3 Combinations of high and low levels of accuracy and precision**.**

3.3   Modeling Spatial Parameters

The quantification of spatial uncertainty requires a model that specifies the mechanism by which spatial randomness occurs. Geostatistics associates the randomness with the regionalized variable itself, where the variable is regarded as one among many possible realizations of a random function. However, the value of the variable in the real world is deterministic. Thus it is important to note that probabilities do not exist in nature but only in the models. Therefore the approach to use a stochastic model is not because of

38

a belief that nature is random but because of the analytical usefulness of such models. Furthermore, one should always keep in mind that models have their limits and represent reality only to a certain point, and that there is always a possibility that the predictions made, and the assessments of uncertainty, turn out to be completely wrong, because for no foreseeable reason the phenomenon at unknown places is simply radically different from anything observed at the locations with known properties (Chiles and Delfiner 1999).

Since spatial variability is a source of spatial uncertainty, one needs to quantify and model the spatial variability. A number of questions should be raised when developing a model such as: what does an observation at one point say about values at adjacent or neighboring points? Is there continuity or no continuity at all? Are variations similar in all directions i.e. isotropic? Does the data actually exhibit a spatial trend? One key method to start addressing these questions is to look at the "variogram", which describes statistically how the values of a variable at two points in space become different as the separation distance between these two points increases. It is the simplest way to relate uncertainty with distance from a known observation value. The "semi-variogram" notation, which is literally equal to half the variogram values, is also commonly used. This is discussed in more detail in section 3.5.

Spatial modeling and geostatistical methods are goal-oriented, where the final purpose is to build an explanatory model of the world but not to solve specific problems. The models under consideration provide a description rather than an interpretation. An

example of the possibility of mis-interpretations of results of a spatial modeling approach is presented in Figure 3.4. The figure shows that it is important to combine the analytical outcome of the models with the knowledge and expertise of the analyst or engineer prior to coming up with conclusions and interpretations.

Building a geostatistical spatial model of any parameter is an iterative process that requires the designer to:

(1) determine what is to be modeled or estimated, i.e. the dependent variable.

(2) find the independent variables that might explain the process being modeled. The selection of these variables is based on theory and professional expert opinion.

(3) run regression analysis to determine which variables are effective predictors of the dependent variable. This step helps define relationships between the independent variables and the dependent variable, and removes redundant variables.

(4) remove and add independent variables, and try different combinations, until the best model possible is obtained; the one "most properly specified".
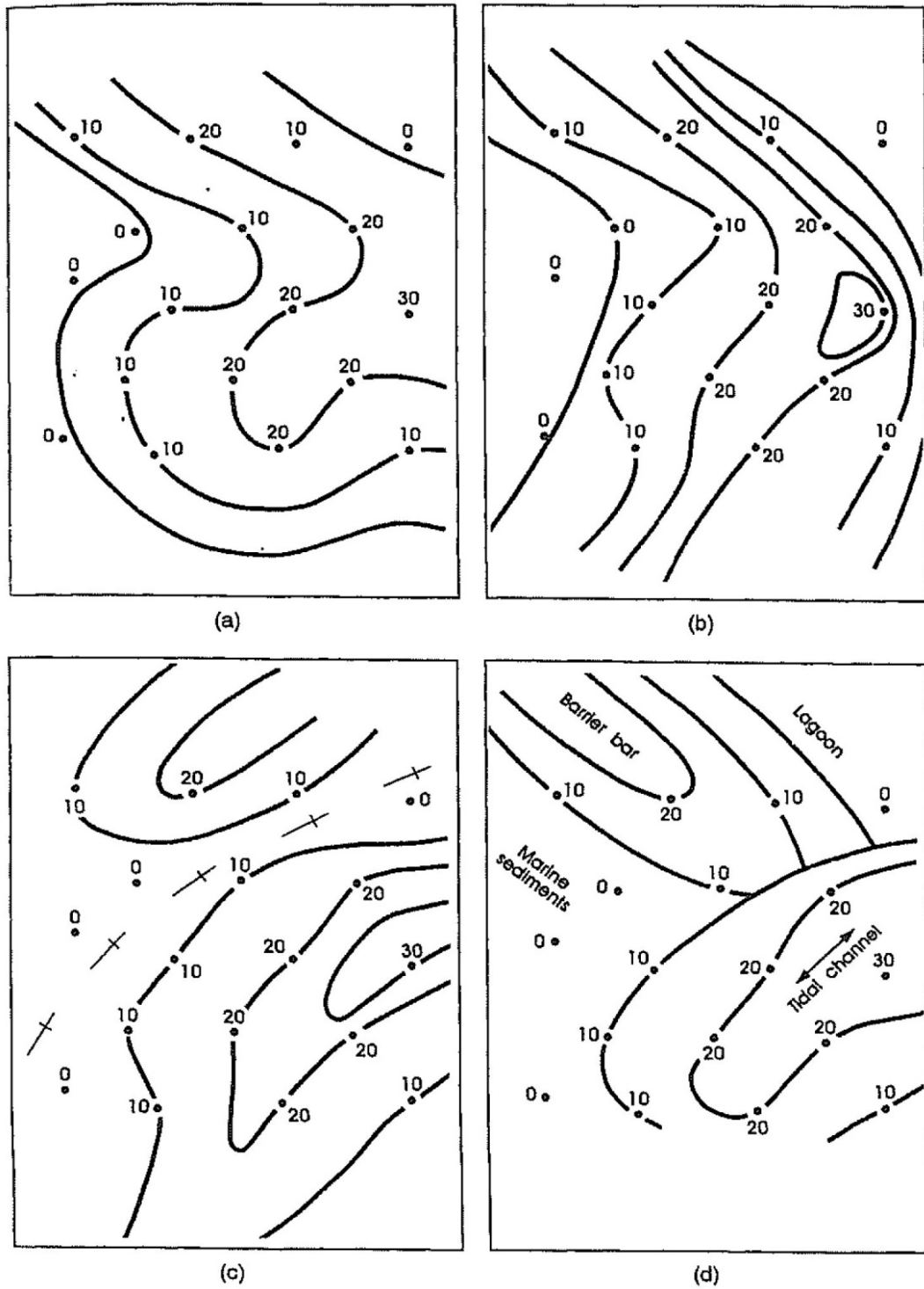
Figure 3.4 Four contour line interpretations of the same set of elevation point values(a) meandering channel, (b) in-fill channel, (c) transgressive filling paleo-valleys, and (d) barrier bar eroded by tidal channel (Chiles and Delfiner 1999).

3.4   Overview of Regression Analysis

Regression Analysis (RA) is a set of statistical techniques and methods that allow the examination, modeling, and exploration of data relationships. Ordinary Least-Squares regression is the best known of all regression techniques, and it is also the starting point for more complex spatial regression methods. RA attempts to show the degree to which one or more variables (independent) potentially promote positive or negative change in another variable (dependent).

There are three broad main reason for the use of RA based techniques (ESRI 2009a):

a. To model a phenomenon in order to better understand it and to use that understanding for decision making (e.g. codes, policy or legislation, etc)

b. To test a hypothesis about what is thought to be the causes/effects of variables on others

c. To model a phenomenon in order to predict values of that phenomenon at other locations or times i.e. to build a consistent and accurate prediction model

Regression analysis creates an equation that relates what is being modeled or estimated (dependent variable) to a set of explanatory or independent (also called auxiliary) variables that are believed to cause or influence the dependent variable values. The general form of a regression equation is:

$$Y = f(X, \beta) \hspace{3cm} \text{Equation 3.1}$$

where Y is the dependent variable, X are the independent variables, and β are the unknown coefficients.

A set of known dependent values, referred to as observed values, are needed as a start at the known locations of interest. The values of the independent variables should be known at both known locations of interest (observed) and at locations where the dependent variable is to be estimated (predicted).

Regression analysis returns a value for the coefficients (**β** symbols), one for each independent variable. The regression coefficients represent the strength and type of relationship that the explanatory independent variables have to the dependent variable of interest. When the relation is positive (i.e. an increase in one independent variable causes an increase in the dependent variable) then the sign of the associated coefficient is also positive. Similarly, coefficients for negative relationships have a negative sign. Furthermore, when the relationship is a strong one, the coefficient is large. The first regression coefficient **β_0** is called the intercept, and represents the expected value of the dependent variable if all the independent variables are set to zero.

The difference between the observed values at the known locations and what the resulting model predicts at these same locations is called the "residual". Residuals are the "unexplained" part of the dependent variable equation represented by the error term **ε**. Using known values of the dependent and the independent variables, regression based models try to predict the dependent variable. The predicted values will rarely match the observed values, and the difference is the residuals. The magnitude, as well as the distribution of the residuals, is one form of looking at the model fit.

Regression analysis performs a null-hypothesis statistical test that calculates a probability, called **p-value**, for the coefficients associated with the independent variables. The null hypothesis, corresponding to a p-value of 100%, states that the coefficient is zero, and thus the associated independent variable is not helping to define the model (i.e. the relation between the independent and dependent variable is one of complete randomness). On the other hand, if the p-value is for example 1%, that means that the coefficient is significantly different than zero, and is statistically significant at the 99% confidence level. That also means that the independent variable is an "effective predictor" for the dependent variable. Associated with p-values are what are called **z-scores**. These are measures of standard deviation. Very low or very high z-scores, associated with very small p-values, are found in the tails of the normal distribution. A numerical example reflecting the above concepts is presented (ESRI 2009b): for a standard normal distribution, the critical z-score when using a 95% confidence level are -1.96 and +1.96 std deviations. The p-value for a 95% confidence level is 5%. Thus if the z score is between -1.96 and +1.96, the p-value will be larger than 5%, and the null-hypothesis cannot be rejected, i.e. the exhibited relationship is very likely to be a random one . However, if the z-score is outside this range, the relationship is then probably too unusual for it to be just another version of random chance, and the p-values will be small i.e. the spatial relationship or pattern deviates significantly from a hypothetical random pattern. In summary, the idea is that the values in the middle of the normal distribution represent the expected outcome in the absence of any strong relation between the variables at hand. The acceptance of confidence levels is what determines what threshold of p-values will be accepted.

3.5 Basics of Spatial Statistics and Regression

General terms used in spatial statistics nomenclature include:

○ Aspatial data: contains only attribute (i.e. feature) information

○ spatial data: contains both attribute and location (coordinates, elevation) information

○ Spatial autocorrelation: correlation/relationship between spatial random variables depends on the distance and/or direction between locations.

○ Stationarity: a relationship that is uniform across space i.e. it is 'global' and applies in the same manner over all the study area. Differences in values may depend on the relative location of the measurements (i.e. distance and direction between two points of measurement) but not on the absolute location of the measurements.

○ Non-stationarity: the relationship varies by absolute location across space (i.e. has 'local' characteristics in different regions of the study area).   Local statistics models are valid for non-stationary relationships because the values of the observations are spatially dependent on each other

○ Directional patterns of relationships:

  • Isotropic: the relationship varies only with distance between points

  • Anisotropic: the relationship varies by distance and direction between points.

All spatial regression analysis starts with simple ordinary least square regression analysis, which will help start building the ultimate model by finding the important independent variables.

Data of a spatial nature has two main characteristics that make it difficult to meet the requirements and assumptions of ordinary non-spatial statistical regression methods:

(1) geographic features are most of the time spatially autocorrelated, which means that features close to each other tend to be more similar than features farther away. In traditional regression methods this creates an over-count type of bias (Figure 3.5) which can be accounted for using methods such as "kriging", discussed in section 3.6. A traditional statistician sees Spatial Autocorrelation as a bad thing that needs to be removed from the data, through for example resampling, or corrected in the modeling (because it undermines or violates underlying assumptions of many traditional non-spatial regression models). The geographer or GIS user sees it as information bearing evidence and reflection of underlying spatial associations among the geographic entities, and thus is crucial in the understanding of the process being studied (Miller 2004).

(2) In many instances, the process under study behaves differently in different regions of the study area. This is referred to as regional variation, and the process is in that case referred to as non-stationary. Ordinary Least-square regression, and other models that work on the overall global scale of the data, create equations that attempt to describe the overall relationships in an area. When relationships actually behave differently in different parts of the study area, these models will be representing the average of these different local relationships.
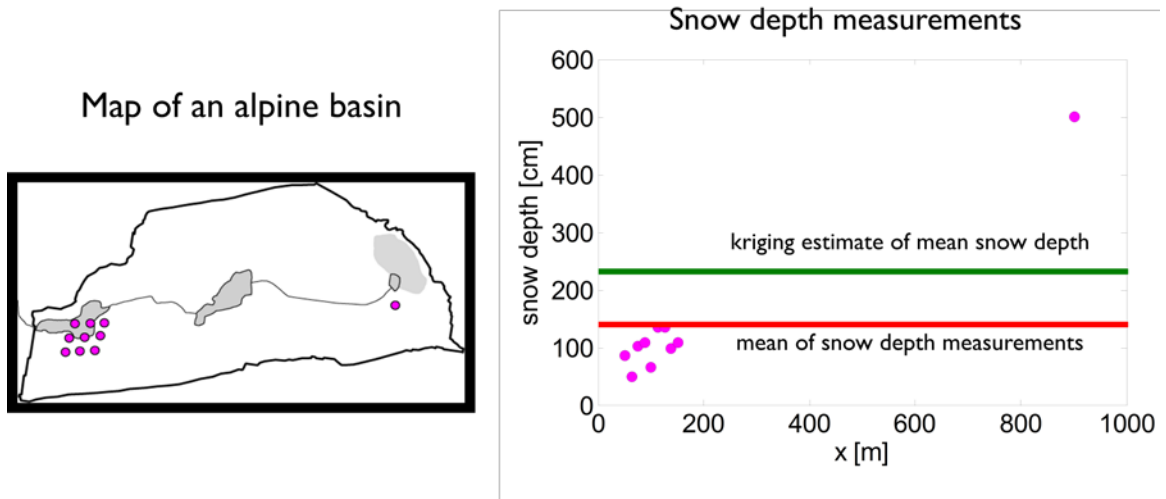
Figure 3.5 Comparison of values from a spatially independent mean with an over-count type of bias (lower line), and a spatially correlated kriging estimate average (upper line) (Zhou 2009).

When least-square regression models are used, there are a number of options that can be applied to address the problem of regional variation:

(1) Include a variable that would explain the regional variation. The variable may take different values depending on the feature locations.

(2) Use methods that incorporate regional variation into the regression models, such as geographically weighted regression.

(3) Redefine or reduce the size of the study area until there are no regional variations. Of course this would result in more areas of study, and thus more models.

Spatial data analysis starts with the presentation of measured or known data, of continuous or categorical nature, at a number of sampled locations. The spatial distribution of continuous or categorical variables is not random; observations close to

47

one another tend to be more alike than those apart. Tobler's First Law of Geography (1970) states that: "everything is related to everything else, but near things are more related than distant things". The law remains enduring today, as the concepts of "near" and "related" are at the core of spatial analysis and modeling, and the rise of geographic information science and technology allows greater sophistication when measuring and analyzing these concepts (Miller 2004). The concept of "related" refers to at least a positive or negative correlation of some degree between two entities. The concept of "near" on the other hand is typically defined based on Euclidean straight-line distance connecting two locations. Nearness should not be limited to an empty space concept because other attributes such as terrain and land cover will affect the realistic shortest path, and as such a least-cost distance concept can also be used as needed in specific cases.

A basic crucial element in geostatistical analysis is the Semivariogram (or Variogram, which is double the semivariogram) which reflects the variance of the difference between a variable's values at two locations. The x-axis represents the distance between any two paired locations, and the y-axis represents the squared difference of the values at the linked pairs of locations. A typical variogram is presented in Figure 3.6 showing the following basic elements:

Nugget : the magnitude of a variogram's discontinuity (i.e. random error) at the origin. It reflects the relationship between variable values at locations that are "very" close together; such discontinuity (the existence of a nugget between nearby

locations) is based on measurement error and/or spatial discontinuity; it is the y-intercept of the variogram.

Correlation Range: the approximate cut-off distance at which the variogram begins to flatten out. It implies that no spatial relationship exists between the variable values at locations separated by this, or a larger, distance.

Sill variance: the value on the y-axis that the variogram attains at the range limit. The higher the sill of a variogram, the higher the prediction variances between different locations.
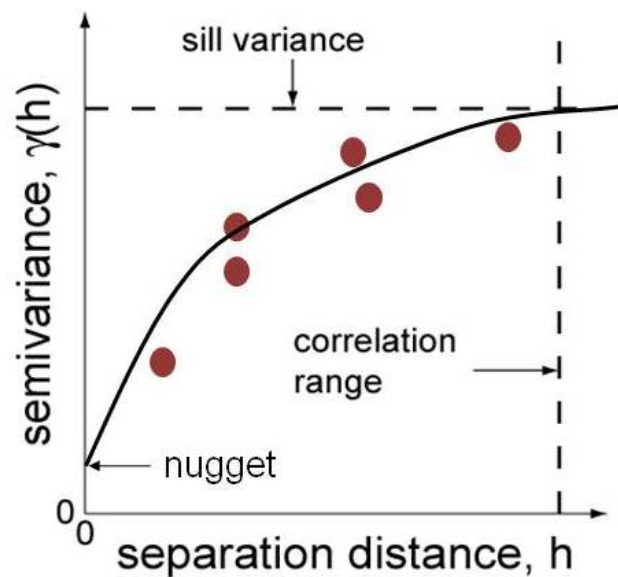
Figure 3.6 Sample semivariogram and basic components (Zhou 2009).

Ideally, reliable estimation of semivariogram values requires at least 150 data pairs (which corresponds to ~19 input data locations in the geographic region), and larger samples are needed to describe anisotropic (direction-dependent) variation (Webster and

49

Oliver 1993). This does not mean, however, that geostatistics cannot be applied to smaller data sets. It is noteworthy that geostatistics has become the reference approach for characterization of petroleum reservoirs where the information available typically reduces to a few wells. Sparse data are often supplemented by expert knowledge or ancillary information originating from a better sampled area deemed similar to the study area (Goovaerts 1999).

When the problem at hand consists of describing the spatial pattern of a *continuous* attribute, **z**, for example a soil property such as cohesion or the angle of internal, the information available would be in the form of values $z(u_\alpha)$ of the variable **z** at **n** number of locations u_α, where $\alpha=1,2,\ldots,n$.

The spatial pattern of the variable, based on the known values, is usually described using what is called the "experimental semivariogram", $\gamma(\mathbf{h})$, which measures the average dissimilarity between known data separated by a distance vector **h**. It is computed as the average squared difference between the components of data pairs:

$$\gamma(h)= \frac{1}{2*N(h)} * \sum_{\alpha=1}^{N(h)} \left[z(u_\alpha)- z(u_\alpha+h)\right]^2 \qquad \text{Equation 3.2}$$

where the sum is from $\alpha =1$ to $N(h)$, and $N(h)$ is the number of data pairs that fall within a given (user-specified) class of distance and direction.

The spatial pattern of *categorical* data, which is the case of many soil variables that take only a finite number of states or classification, can be described in a similar matter as above, by the introduction of an indicator function that reflects the absence or

presence of a certain variable class or category. In this case, let **s** be a categorical attribute with **K** possible states s_k, where k=1,2, . . . ,K such that the K states are exhaustive and mutually exclusive in the sense that one and only one state s_k occurs at each location **u** . The pattern of variation of a category s_k can therefore be characterized by the semivariogram:

$$\gamma(h\;;s_k) = \frac{1}{2*N\,(h)} * \sum_{\alpha=1}^{N(h)} \left[\, i(u_\alpha\;;s_k) - i(u_\alpha + h\;;s_k) \right]^2 \qquad \text{Equation 3.3}$$

defined with the indicator function :

$$i(u_\alpha;\; s_k) = \begin{cases} 1, & s(u_\alpha) = s_k \\ 0, & \text{otherwise} \end{cases} \qquad \text{Equation 3.4}$$

In this case, the indicator semivariogram value measures how often two locations a vector **h** apart belong to different categories (i.e. $s_{k'} \neq s_k$), and the smaller the variogram values, the more spatially connected is the category s_k.

3.6   Introduction to Kriging

"Kriging" is a generic name adopted by geostatisticians for a family of generalized least-square regression algorithms (Goovaerts 1999). Although fundamental features of geostatistics (including concepts of spatial dependence, correlation range, and ideas preceding the variaogram) have been studied since the beginning of the 20$^{\text{th}}$ century (Haining et al. 2010), the theory of Kriging was formally developed by the French mathematician Georges Matheron based on the Master's thesis of Daniel Krige (1951). Kriging is a geostatistical estimation technique that uses a linear combination of surrounding sampled values to minimize errors in making predictions in unsampled areas (Figure 3.7).
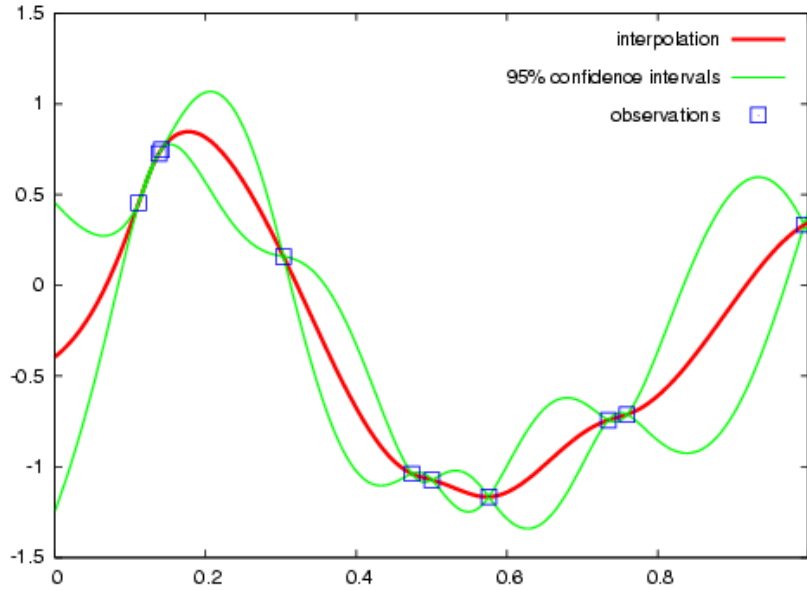
Figure 3.7 Example of one-dimensional data interpolation by kriging, with confidence intervals. Squares indicate the location of the data. The kriging interpolation is in red and the confidence intervals in green (Vazquez 2005).

The simplest case is estimating the value of a continuous attribute **z** at any unsampled location **u** using sampled known data, $z(u_\alpha)$, at **n** locations u_α,, where $\alpha=1,2,\ldots,n.$. In fact, all kriging estimators are actually but variations of the linear regression estimator $Z^*(u)$ defined as:

$$Z^*(u)- m(u)= \sum_{\alpha=1}^{n(u)} \lambda_\alpha(u)^*[\, Z(u_\alpha)- m(u_\alpha)] \qquad \text{Equation 3.5}$$

where $\lambda_\alpha(u)$ are weights, $m(u)$ is the assumed mean at location u, and $n(u)$ is the number of sampled data points within the neighborhood (user-defined) of u, chosen so as to minimize the error variance:

$$\sigma_{Error}^2 (u) = \text{Variance } [Z^*(u) - Z(u)] \qquad \text{Equation 3.6}$$

These weights are obtained by solving a system of linear equations which is known as the 'kriging system.'

Kriging is then qualified by different adjectives depending on the underlying models: simple kriging, ordinary kriging, universal kriging, etc. and practitioners can get confused in the face of the number of kriging methods available. Differences between kriging methods reside in the model considered for the trend m(u) in the above equation. The various kriging methods include, but are not limited to:

Simple Kriging (SK) assumes the local means are constant and equal to the mean across the study area, which is assumed to be known.

m(u) = m, constant and known for all u in the study area

Ordinary Kriging (OK) assumes that the local means aren't necessarily closely related to the population mean and so only uses the samples in the local neighborhood of the estimate. This approach accounts for local fluctuations of the mean by limiting the domain of stationarity of the mean to the local neighborhood level (determined by the user).

m (u') = constant, but unknown, for all u' in a single neighborhood area

Universal Kriging (Also called Kriging with a trend, KT) is appropriate if there is a gradual trend in the data so that the mean is no longer spatially constant and the variogram is no longer appropriate to model the spatial autocorrelation structure. The approach considers that the unknown local mean m(u') varies in each neighborhood. The trend by which the mean varies in the neighborhood is modelled as a linear combination of functions of the location (u) as follows:

$$m(u') = \Sigma\, a_k(u')\,.\,f_k(u')$$

where in this case of linearity of the trend $a_k(u')$ are unknown but deemed to be constant $(a_k(u') = a_k)$ within each local neighborhood of the study area.

Cokriging: in this approach, the variable of interest (less abundantly sampled) is combined with a secondary variable (that is more abundantly sampled) to make the estimations of the primary dependent variable. In this case the cross-relationships of the two sampled variables must be assessed via a cross-semivariogram.

Note that Wackernagel (1994) stated that the additional modeling and computational effort implied by cokriging is not worth doing when primary and secondary variables are recorded at the same locations and the direct semivariogram of the primary variable is proportional to the cross semivariograms with the secondary variables. Furthermore, practice has shown that cokriging improves over kriging only when the primary variable is substantially undersampled with regard to the secondary variables and those secondary data are well correlated with the primary value to be estimated (Journel and Huijbregts 1978; Goovaerts 1998).

An example is presented (Goovaerts 1999) comparing simple kriging (SK), ordinary kriging (OK), and universal kriging (or kriging with a trend KT), as shown in Figure 3.8 for estimation of Cadmium level values in soil along a road transect. The figure shows that in this case Simple Kriging is inappropriate because it does not account for the increase in Cd concentration along the transect.
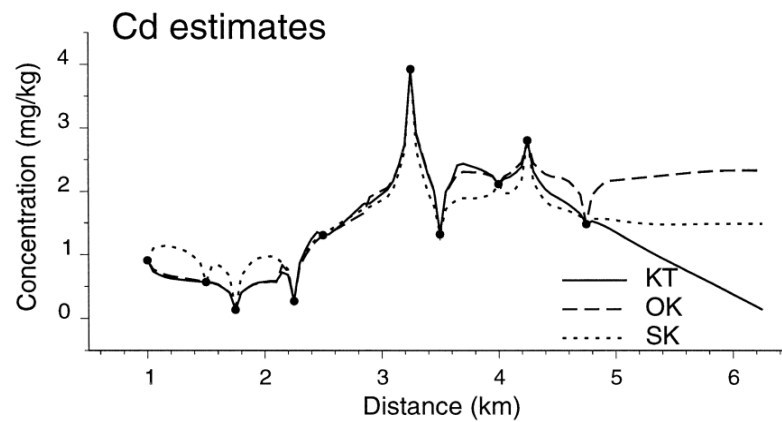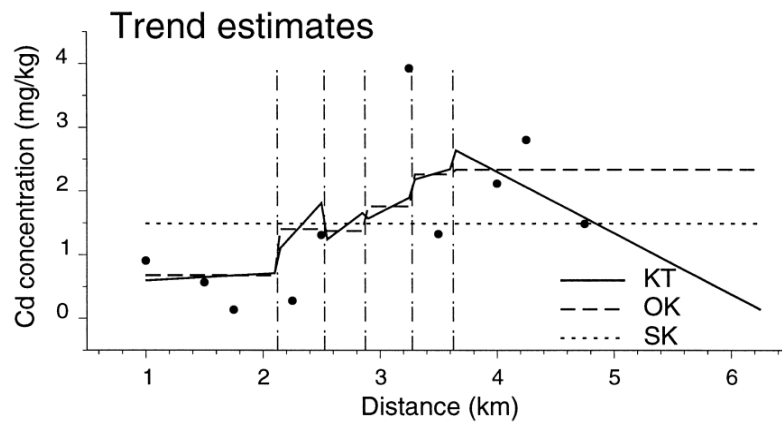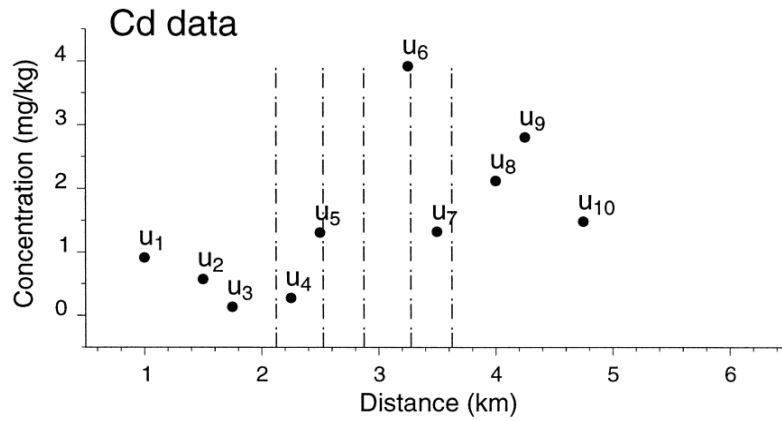
Figure 3.8 Impact of the kriging algorithm on the estimation of the trend (middle graph) and of cadmium (Cd) concentration in the soil (bottom graph) along a transect. The vertical dashed lines delineate the segments that are estimated using the same five Cd concentrations. For example, the first segment, 1–2.1 km, includes all estimates that are based on the data at locations u_1 to u_5 (Goovaerts 1999).

Ordinary Kriging with local search neighborhoods provides results similar to Universal Kriging while being easier to implement. Large differences between the two estimators (OK and KT) arise only beyond the last location u_{10} and are due to the arbitrary extrapolation of the trend model evaluated from the last five data (in this example, calculations in each neighborhood are made using the five closest measurement points).

As such, Ordinary Kriging is shown to be a satisfactory and efficient approach to estimating the dependent variable in this case. Note also that in this example the linear trend (Universal Kriging) model yields negative estimates of concentration around 7 km. Such abnormal results show that the blind use of complex trend models is risky and may yield worse estimates than straightforward ordinary kriging.

CHAPTER 4

Spatial Analysis and Modeling of Geotechnical Soil Properties in the Sacramento River Flood Control System

4.1   Introduction

To achieve the main objective of this thesis, it was important to understand and investigate the spatial distribution of soil properties and levee characteristics in the geographical area under consideration. In this research project the dependent variables are the soil type (e.g. sand, clay, silt) and its associated properties (e.g. shear strength and unit weight). This is done by selecting independent variables to correlate with the dependent variables and then applying a geostatistical kriging approach to estimate the dependent variable spatial distribution. The selection of the independent variables is based on theory and engineering judgment. The underlying geology and river geomorphology in the study area have played an important role in identifying these variables in this research project.

4.2   Study Area

The area of study used in this project as defined in section 2.3.3 of this dissertation is centered on the City of Sacramento, and the Feather River north and south of the City of Marysville in California (Figures 4.1 and 4.2).
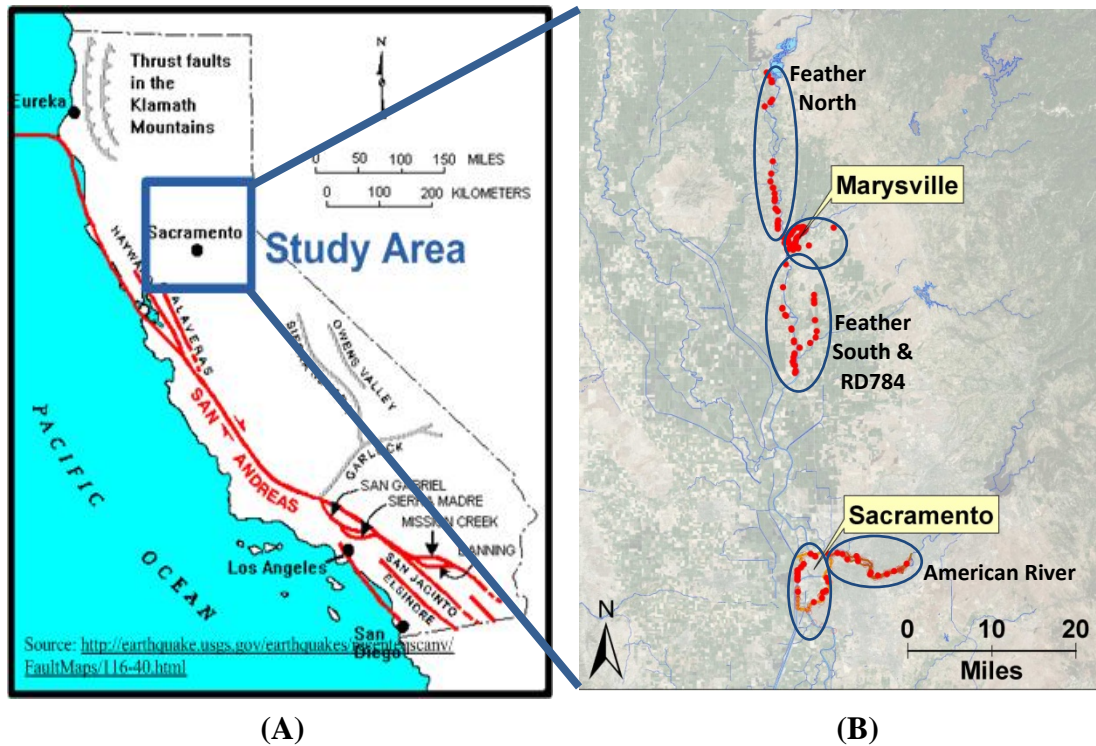
Figure 4.1 (A) Location of the study area in the state of California, with (B) close up view and details of the locations of available geotechnical investigation boreholes around Cities of Sacramento and Marysville.

To be consistent with the Sacramento River Flood Control system and the California Department of Water Resources maps, the areas studied are grouped as:

1. **City of Sacramento,** comprising of:

    • West Sacramento region

    • American River

2. **Feather River,** comprising of:

    • Feather River South and Reclamation District 784

    • City of Marysville

    • Feather River North
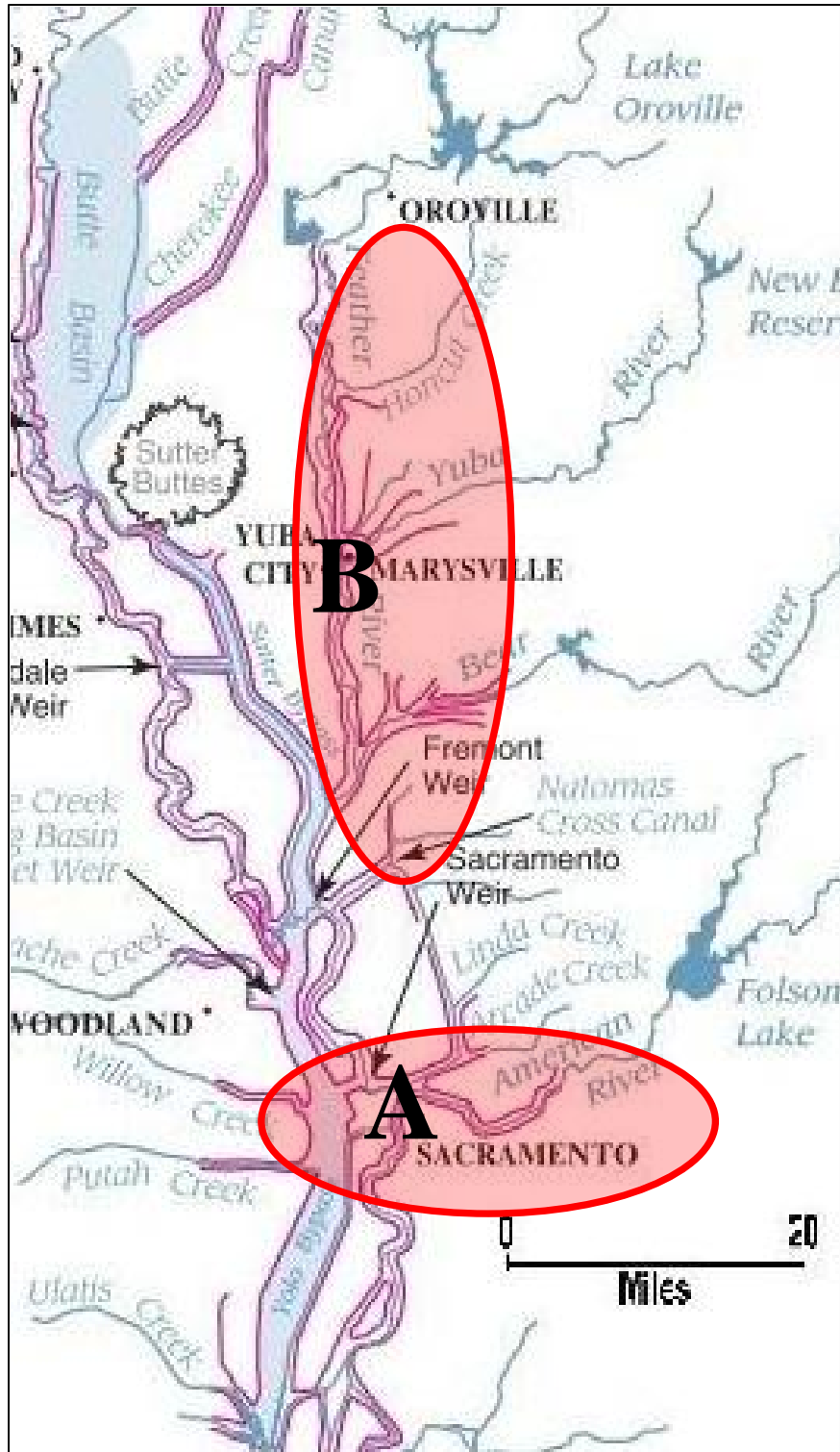
Figure 4.2 Areas of study within the Sacramento River Flood Control Project: (A) Sacramento City and (B) Feather River (DWR 2011b).

4.3   Data Collection and Characterization of Study Area

4.3.1   Data Types and Definition of Levee Components

The data needed to analyze the soil variability in deltaic and riverine environments consist of:

(1) Soil Properties at Select Locations: unit weight, γ, friction angle, ϕ, cohesion, c, small strain shear modulus, G_{max}, or shear wave velocity, V_s, shear modulus reduction vs. shear strain curves, and damping ratio vs. shear strain curves.

(2) Area Attributes: Underlying geology, digital elevation models, river or channel geometry, and water level.

Data used for this study has been collected from a number of sources. Some of the spatial data was available from online databases such as the United States Geological Survey's Natural Map Viewer (USGS 2010). Other data was not available in GIS format, especially data relating to geotechnical investigation and levee layouts, and had to be manually digitized. Collected data, with their respective source in parenthesis, are:

• **Surface soil data** (Soil Survey Geographic Database – SSURGO)

• **Underlying geology features** (United States Geological Survey – USGS)

• **Hydrological features and characteristics** (National Hydrography Dataset – NHD)

• **Ground water table** (Source: National Water Information System –USGS)

• **Terrain elevation data** (National Elevation Dataset – NED)

- **County limit, cities, and road networks** (state, county, and city authorities)

- **Population** (US Census Bureau)

- **Land cover** (Multi-Resolution Land Characterization-MRLC)

- **Aerial maps** (Bing maps, through the ArcGIS online Server)

- **Levee geometry and soil properties** (Soil report prepared for the US Army Corps of Engineers (1987) for Sacramento city area, as well as maps and borehole logs provided by URS Corporation (2010) which are part of the URS Corporation and the California Department of Water Resources Urban Levee Evaluation Program)

The <u>Levee System</u> is defined as the collection of earthen embankments with a corresponding delineated protected area. All parts of the levee system need not be physically connected. There may exist areas of discontinuity where no levee exists. The Levee System has a number of Nodes, or points, that define its geometry and have specific characteristics (Figure 4.3). Nodes can be classified as:

- **End Nodes**: The point at the physical end of a stretch of levee

- **Intersection Node**: The point where two (or more) parts of the levee system meet

- **Intermediate Node:** A point along a levee stretch, which is neither an end node, nor an intersection node, and might represent a change in the levee geometry

- **Data Node**: A point on, or near, the levee that has defined soil parameter data obtained by in-situ or laboratory testing.

61
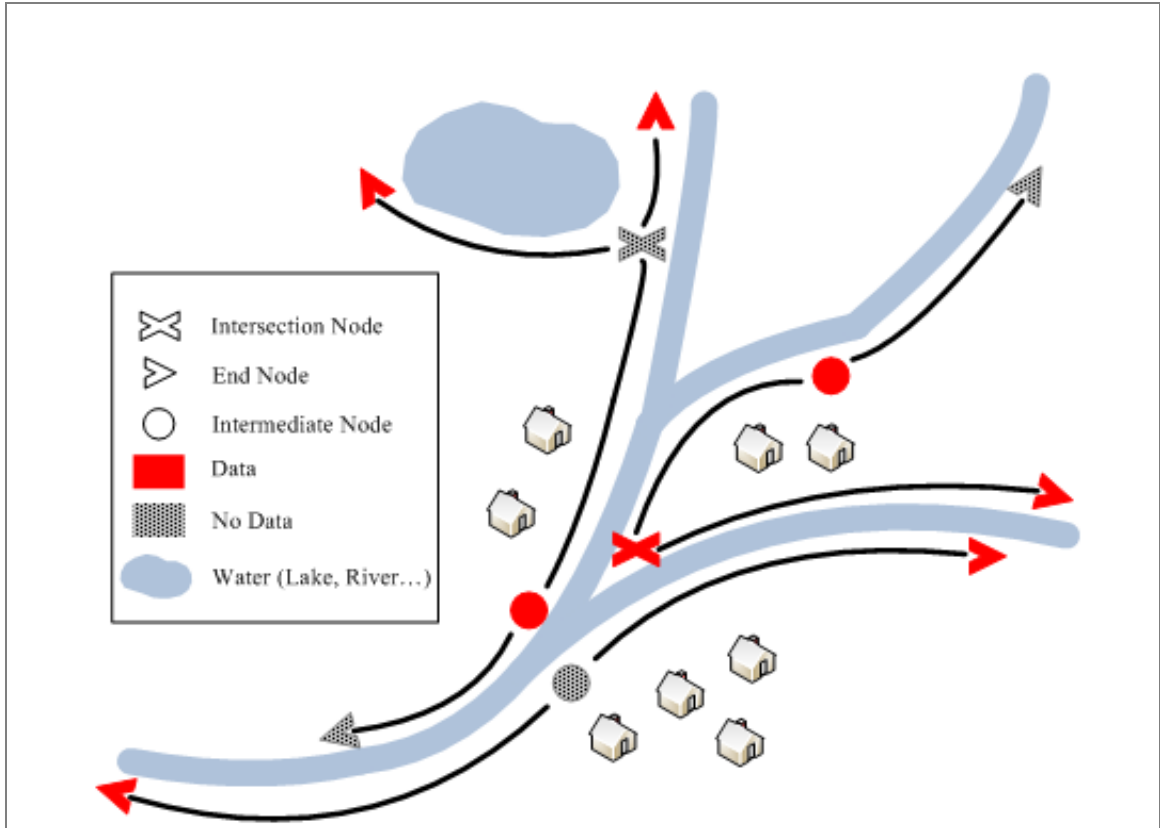
Figure 4.3 Typical node classification and levee segmentation diagram.

Rules for Node Identification are: (a) End Nodes, Intersection Nodes, and Intermediate Nodes are *mutually exclusive*, i.e. a node cannot be identified as more than one of those three cases, and (b) End Node, Intersection Node, and Intermediate Nodes have to be also defined as *either* a Data Node, *or* a No-Data Node. The Levee System is divided for analysis purposes into <u>Segments</u> called levee reaches. Levee reaches can be modeled based on the distribution of levee sections of similar embankment and foundation characteristics. As an example, reach lengths in a case history on the California delta levee system (Gilbert et al. 2011) varied from couple of thousand feet to over 10 thousand feet.

4.3.2 Levee Layout and Geometry

The California Department of Water Resources (DWR 2011c), partnering with FEMA, is assembling critically needed levee information on geometry, landmarks, test locations, history, etc. for all the levees in the state. However, this is an ongoing project and information was not available at the time of this study in soft-copy GIS format, and therefore the analysis relied on the manual digitization of levee layout (Figures 4.4 and 4.5).
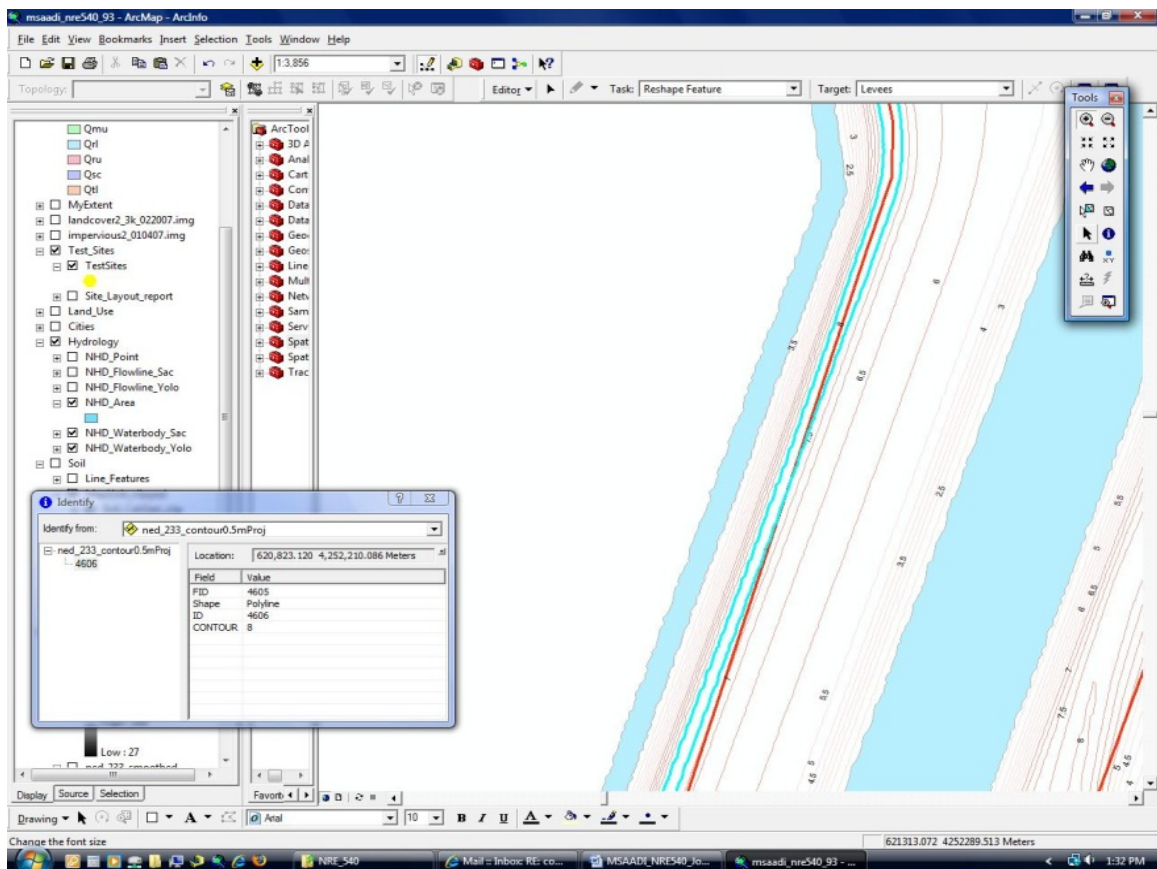
Figure 4.4 Determination of the geometric layout of the levee features (centerline at levee top in red) by tracing the highest contour lines (blue) and matching with aerial imagery and other information.
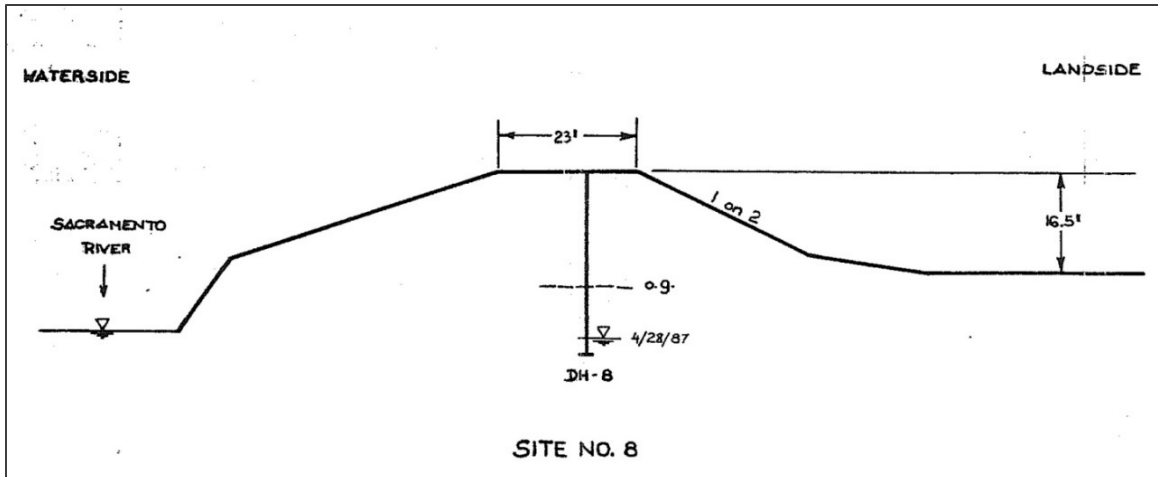
Figure 4.5 Location and extent of borehole BH-8 with respect to levee geometry
(USACE 1987).

4.3.3   River Geomorphology and Regional Underlying Geology

The study of landforms, such as naturally formed levees, and the history of
formation and dynamic processes that shape them are referred to as Geomorphology.
Rivers and streams not only carry water, but also sediment. The water mobilizes
sediments and transports it downstream where it is deposited in the form of river
embankments (natural earthen levees), deltas, or flows to the sea. An interesting example
of how river geomorphology processes can evolve on land and continue when submerged
under the ocean is presented by Posamentier (2003). Depositional elements formed by
the Mississippi river system during the mid to late Pleistocene, and currently lying at
water depths in excess of 2,500m in the Gulf of Mexico, include channels, levees, a
channel belt, and frontal splays (Figure 4.6). These deposits are presumed to be
associated with repeated deep marine turbidity flows and other mass transport processes.
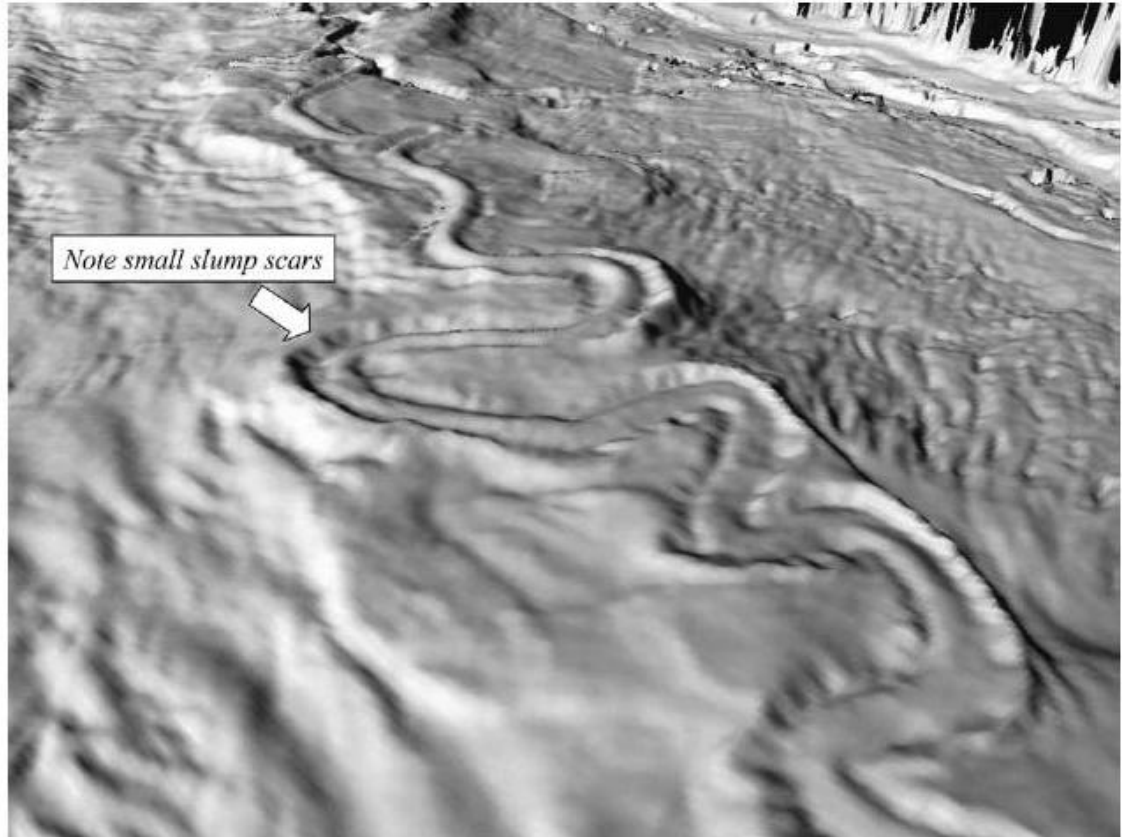
Figure 4.6 3D-perspective view of the Joshua channel belt, probably formed by the Mississippi river system during the mid to late Pleistocene and currently lying at water depths in excess of 2,500m in the Gulf of Mexico (Posamentier 2003).

In addition, natural levee development and dynamics has received relatively little fluvial geomorphic study (Kondolf and Piegay 2003). As such, the study of the complexity of a river's geomorphology, as illustrated in Figure 4.7, is important in determining the type of sediments and where they were deposited, and thus will affect the response of the adjoining levee system.
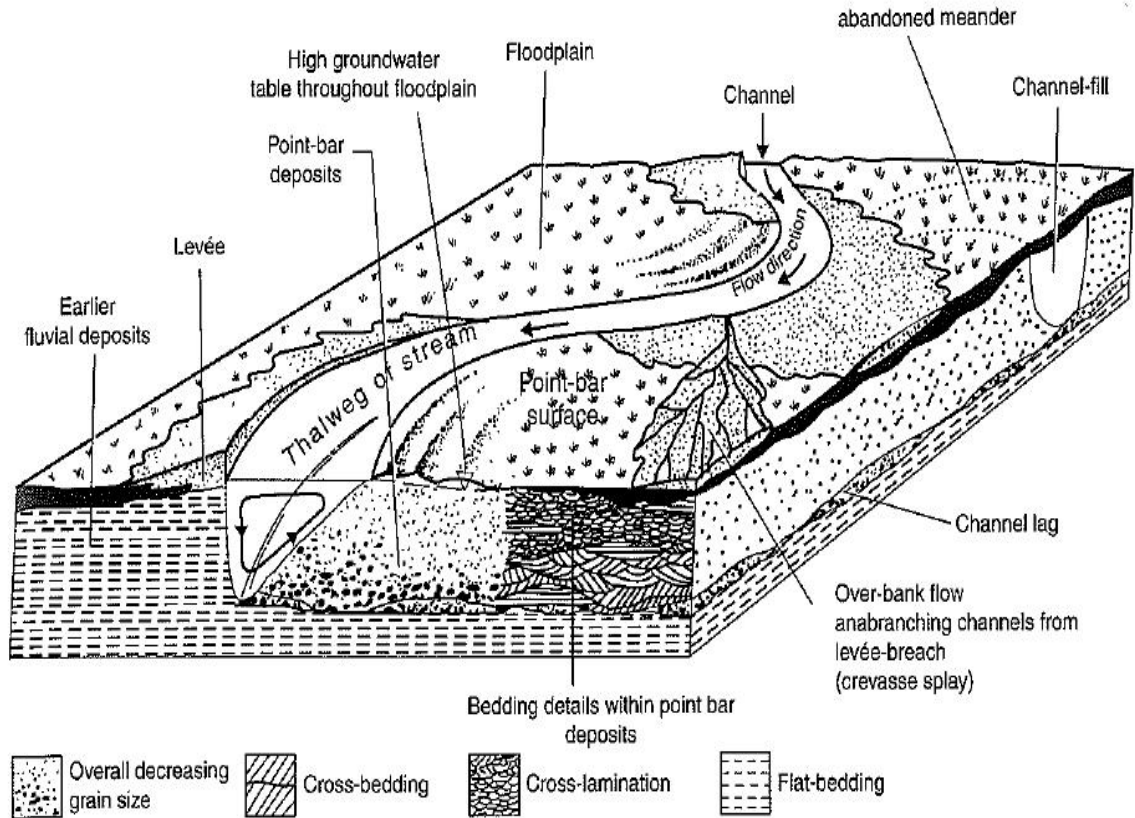
Figure 4.7 Schematic representation of a possible river geomorphology (Fookes et al. 2007).

The underlying foundation geology below the river bed of the Sacramento River in California, according to Helley and Harwood (1985), is detailed in Table 4.1. Maps were not available in soft copy GIS format, and manual tracing of the area limits was done using scanned hand-drawn USGS maps and GIS geo-referencing and editing tools (Figures 4.8 and 4.9).

Table 4.1 Underlying geology classification for the Sacramento River basin

Deposit Classification	Code	Short Description	Geological Epoch	Maximum Thickness (m)
Alluvial Deposits	**Qa**	Alluvium - Unweathered gravel, sand, & silt	Holocene	10
Basin Deposits	**Qb**	Basin Deposits, Undivided – Fine grained silt & clay	Holocene	60
Alluvial Deposits	**Qsc**	Stream Channel Deposits of open, active stream channels (morphology constantly changing)	Holocene	25
Alluvial Deposits	**Qmu**	Modesto Formation - Upper Member – Unconsolidated, unweathered mix of gravel, sand, silt and clay	Pleistocene	120
Alluvial Deposits	**Qml**	Modesto Formation - Lower Member – Unconsolidated, slightly weathered gravel, sand, silt, & clay	Pleistocene	120
Alluvial Deposits	**Qru**	Riverbank Formation - Upper Member – Unconsolidated alluvium composed of gravel, sand and silt	Pleistocene	120
Alluvial Deposits	**Qrl**	Riverbank Formation - Lower Member – Semiconsolidated gravel, sand, & silt	Pleistocene	120
Alluvial Deposits	**Qsc**	Stream Channel Deposits of open, active stream channels (morphology constantly changing)	Holocene	250
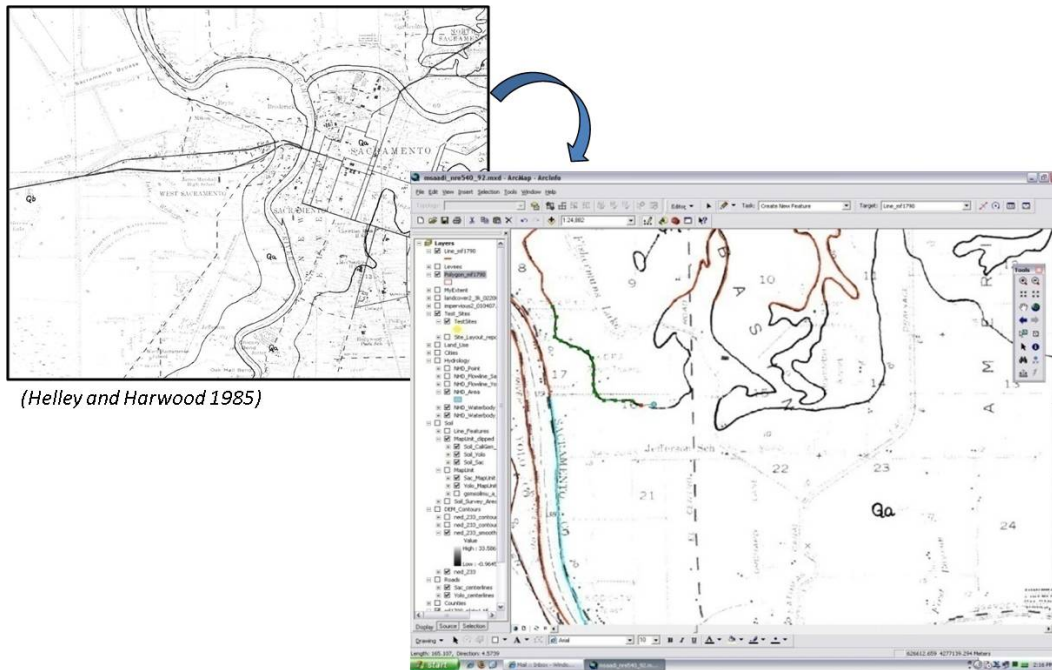
Figure 4.8 Delineation of the underlying foundation geology regions by tracing a digitized copy of the maps prepared by Helley and Harwood (1985).
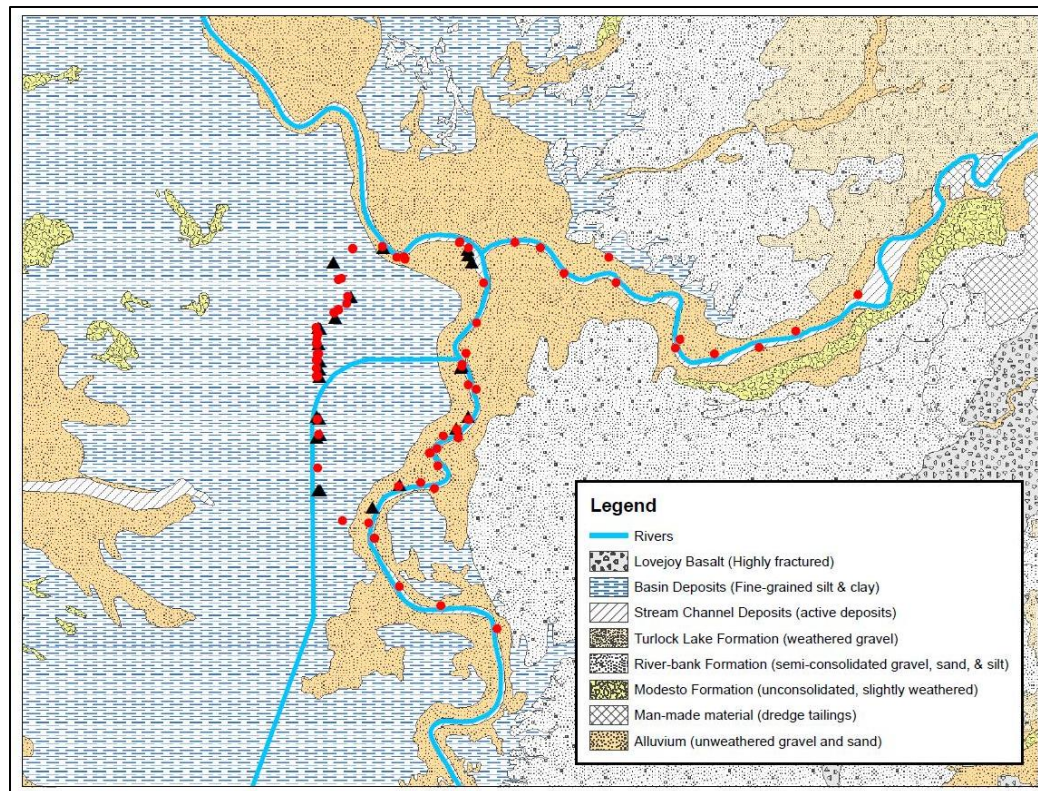
Figure 4.9 Underlying foundation geology regions drawn in ArcGIS reflecting the hand-drawn maps prepared by Helley and Harwood (1985).

4.3.4   River Characteristics and Sinuosity Index Calculations

River Meandering: A river's sinuosity is its tendency to meander back and forth across the floodplain over time, in what looks like an S-shaped pattern (Figure 4.10).
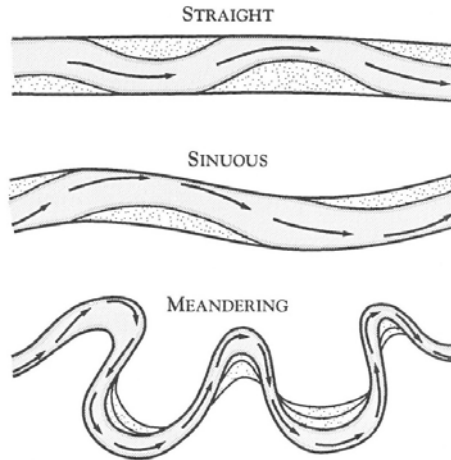
Figure 4.10 Different levels of river meandering, with arrows indicating location of highest velocity flows (Mount 1995).

Mount (1995) states that the scarcity of "perfectly straight" rivers in nature is widely believed to indicate that meandering is the more preferred state of single channel rivers. The author goes on to explain that the development of sinuosity in a river takes place due to secondary flow (flow that moves downstream in a cylindrical spiral motion within the channel). The longitudinal bed profile of most rivers is divided into series of alternating high and low gradient segments. This results in the formation of riffles (high points on bed profile) and pools (deep water areas between riffles) as illustrated in Figure 4.11. In a low-sinuosity low-gradient channel, the overall stream power is usually low, the secondary flow minimal, and thus there is little erosion of the banks and the channel remains relatively static. However, when stream power is great enough, bank erosion will

increase initiating the formation of meander bends. Increased meandering and outer bank erosion is matched by increased deposition of material on the opposite bank resulting in alternating point bars along the river length (Figure 4.12). A result of the above described process a "relatively straight" river section is expected to have less variability in the properties of the material deposited at its banks than a section that is "meandered".
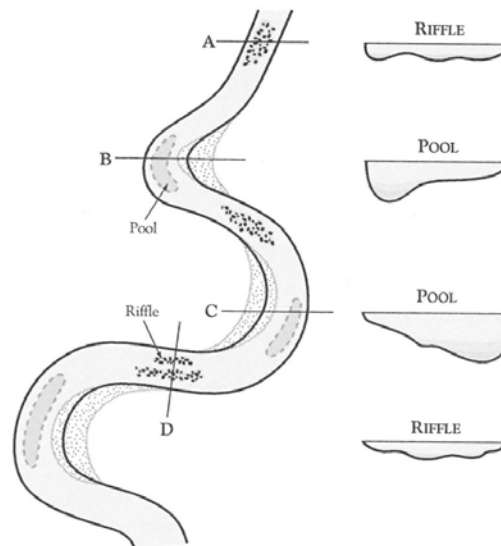
Figure 4.11 Cross-section profiles of riffles and pools (Mount 1995).
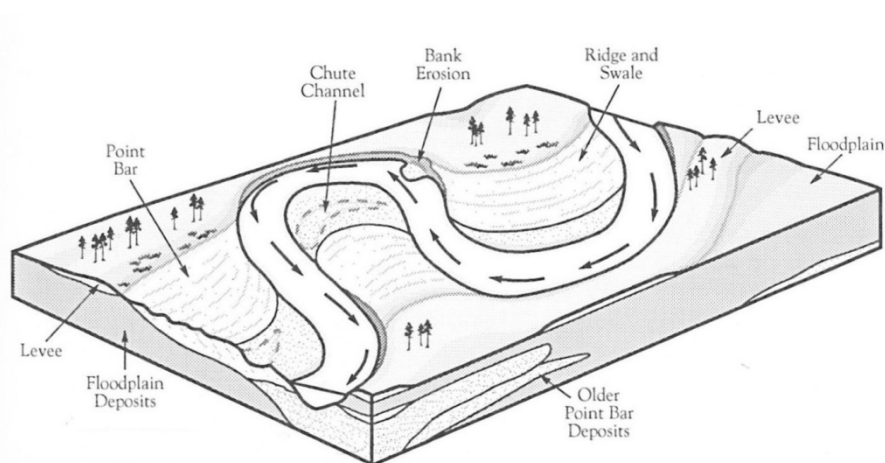
Figure 4.12 Major sedimentary features of a meandering single channel river, showing erosion and deposition process leading to formation of point bars (Mount 1995).

The meander ratio, or Sinuosity Index, SI, is a means of quantifying how much a river or stream meanders i.e. it measures the deviation of a river center path length from the shortest possible path. It is a reflection of the channel length required to cover a given point-to-point straight line distance. SI is calculated as the length of the river channel center path divided by the length of the valley containing the river. In straight streams, SI=1.0, whereas a value of 4.0 is considered to be highly intricate meandering. Researchers have used a classification of the index range of just above unity to just below 1.3 for sinuous streams, with meandering streams above 1.3 (Mueller 1968). As a general rule, meandering streams are arbitrarily defined as those with an SI value greater or equal to 1.5 (Gordon et al. 2004). For this study, the following scale was adopted:

SI value 1.0 to 1.1   Straight

SI value 1.1 to 1.3   Sinuous

SI value 1.3 to 1.5   Slightly meandering

S I value > 1.5 Meandering

Other slight variations on the above definition of Sinuosity Index exist. For example the thalweg, or line of maximum depth, can replace the river center path length in the formula. The values derived are generally higher due to the wandering of the thalweg within the channel (Figure 4.13). However, this index for instance has little geographic application, as the thalweg cannot be held as a stream channel aspect seen from the air, but rather, it is a subsurface phenomenon (Mount 1995).
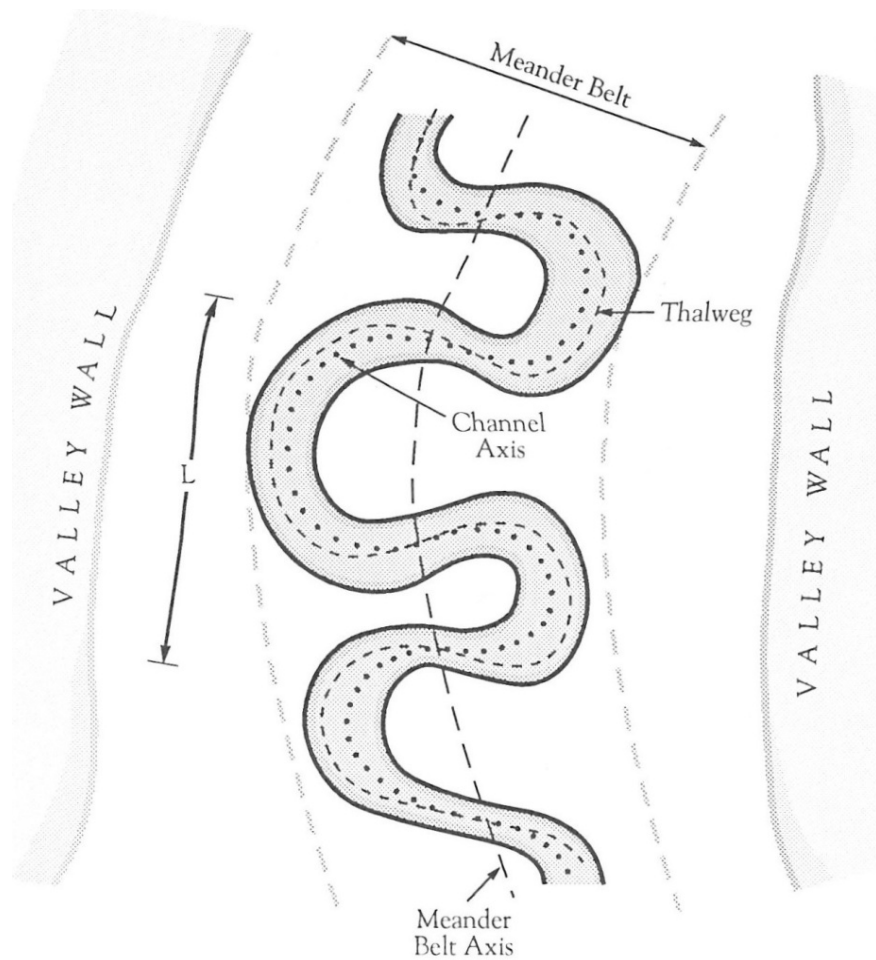
Figure 4.13 Main features used to describe sinuosity in single channel rivers. L refers to the meander wavelength (Mount 1995).

River Migration: The issue of sinuosity is further complicated by having single vs. multiple parallel river channels as can be seen in Figure 4.14 .Because of lateral migration of meandering streams, levees should be placed at a fair distance from migrating channels (Julien 2002). However, this is not always the case, especially in urban areas where insufficient space forces the building of levees at the edge of the stream. Thus it becomes important to determine the levee parts located in the highly meandered river sections in order to give them special attention in the analyses.
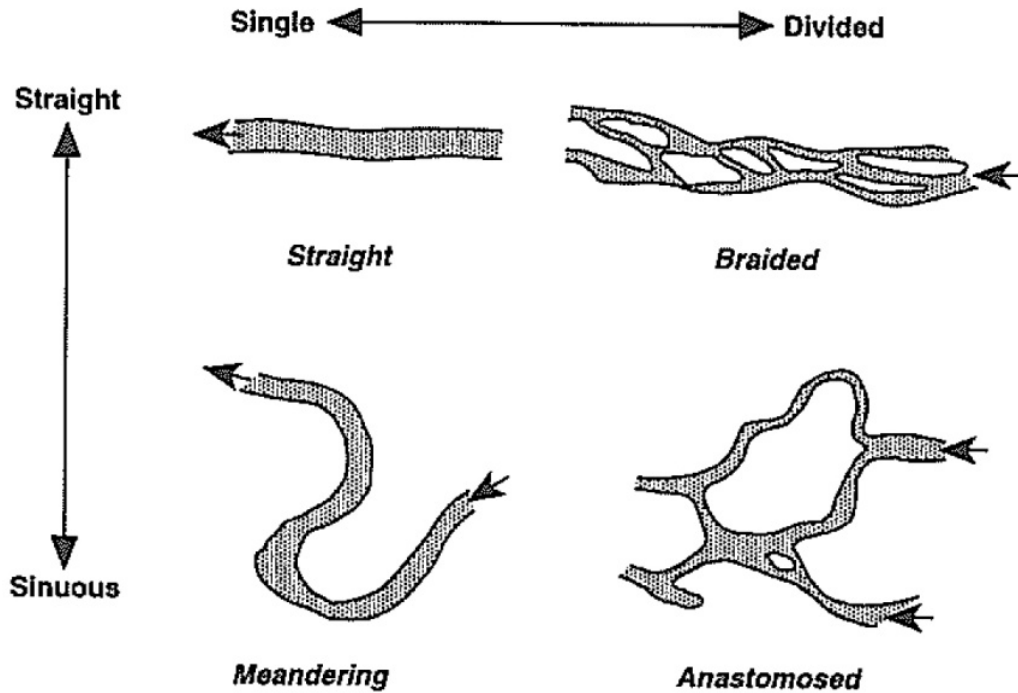
Figure 4.14 Classification of rivers based on sinuosity and degree of channel division (Thorne et al. 1997).

Sacramento River is a meandering single-channel river that occupies one relatively stable main channel surrounded by an extensive floodplain. It is a prime example of meandering river, although channeling by public works projects has greatly altered the original pattern of such rivers (Mount 1995).

Aerial photography can prove to be critical when studying river meandering and river migration. A detailed study prepared for USGS by Brice (1977) provides further information on the migration of the middle section of the Sacramento River. In the study, river migration was indirectly quantified by studying the surficial soil deposits at a certain distance from the river banks, thus establishing a river migration zone. If the levee crosses the migration zone, it was assigned a higher soil variability index. The above

73

mentioned study however has two disadvantages in that (1) the oldest mapped river layout goes back to 1896, just a few years before the Sacramento River Flood Control Project was initiated, and (2) it covers the stretch from River Mile 191 to 143, which is far from the urban area of Sacramento where geotechnical investigation data used in this study were available (River Mile 80 to 30). No similar detailed historical studies of the migration of the Sacramento River around City of Sacramento have been located, probably because of the urban nature of this region forcing the levees to constrict the migration of the river.

Sinuosity Index Calculations: It is worth noting that no streams existing in nature owe all of their sinuosity to hydraulic factors. Rather, almost all streams have some degree of both hydraulic and topographic sinuosity (Mueller 1968). However, for simplicity, it is common to derive the SI based on concepts of hydraulics.

In order to calculate SI, it is necessary first to define the length of "one meander wave" Similar to the concept of the frequency of a sinusoid wave function. This is the length of the stream in the numerator of the SI equation. Figure 4.15 shows in detail the characterization of a meandering river, with definition of inner bank (convex) and outer bank (concave).

A number of authors (Thorne et al. 1997; Julien 2002) refer back to the work by Leopold et al. (1964) who found that Meander wave length (L) varies from $L = 7.32w^{1.1}$ to $12.13 w^{1.09}$ with the average roughly equal to 10 times the River Channel Width "w" (Figure 4.16).

74
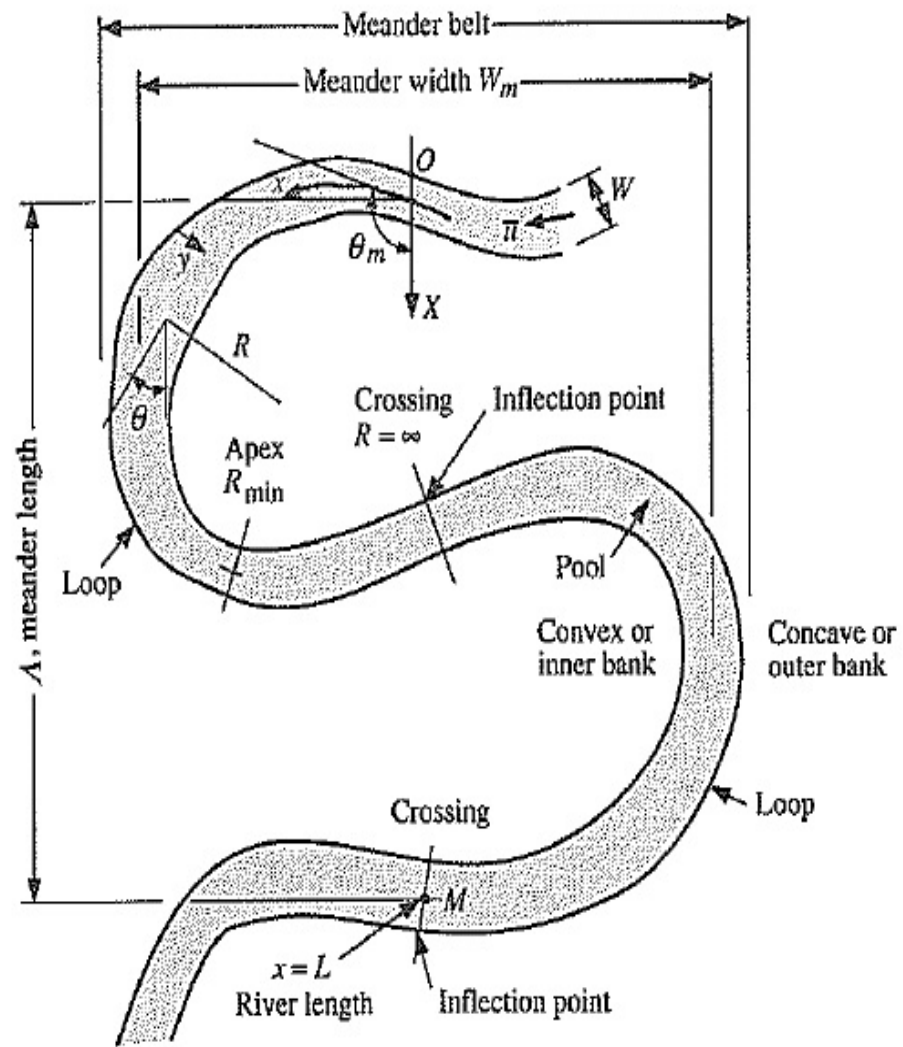
Figure 4.15 Characterization of a meandering river (Julien 2002).
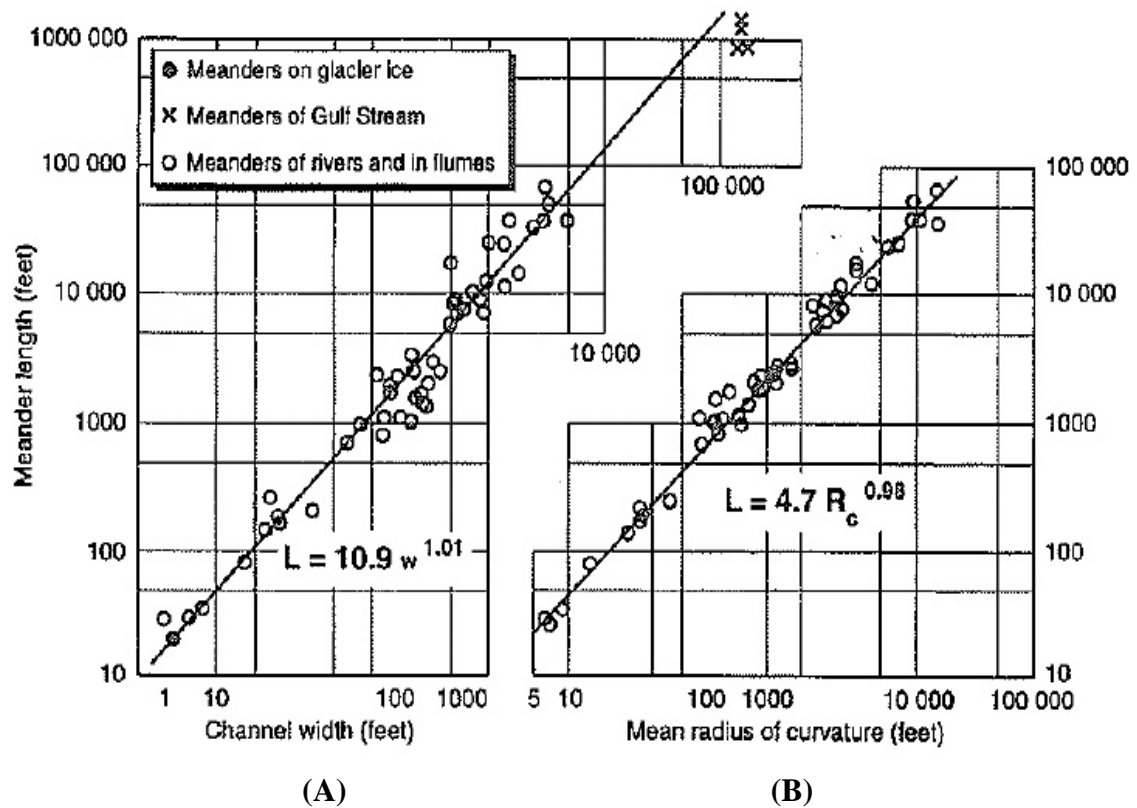
Figure 4.16 Relation of meander length to (A) width, and to (B) radius of curvature in channels (Leopold et al. 1964).

A number of meander wave lengths, referred to as **River Segmentation Levels**, were applied at the study areas in order to come up with values of Sinuosity Index. The river features are divided into segments, each equal to the Segmentation Levee of interest, and the calculated value of the Sinuosity Index is assigned to the individual segments (Figure 4.17). For the Sacramento City area, the river width varied from ~70 to ~210m, with most river segments widths around the value of 150m, giving a rough estimate of the expected Meander Length of 1,500m. Using the above mentioned equations by Leopold et al. (1964) the segmentation levels tried for Sacramento were 500m, 1500m, 1750m, 2500m, 3500m. For Feather River, the width varied from ~60 to ~150m, with most river segments widths around the value of 100m, giving a rough

estimate of the expected Meander Length of 1,000m. Similarly, using the above mentioned equations by Leopold et al. (1964) the segmentation levels tried for Sacramento were 500m, 1000m, 1500m, 2500m.
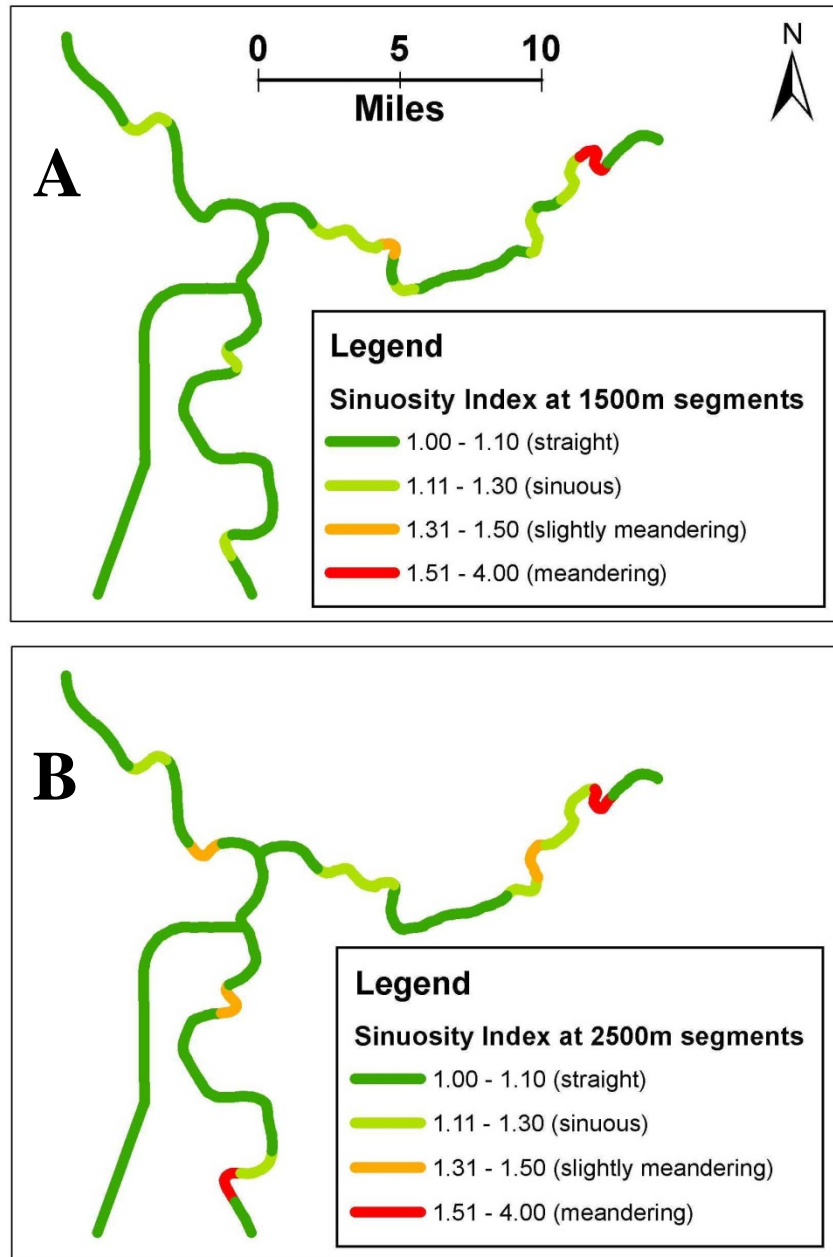
Figure 4.17 Comparison of Sinuosity Index output for different river segmentation levels at Sacramento City: (A) segmentation level of 1,500m and (B) segmentation level of 2,500m.

4.3.5 Ground Water Table Levels

The ground water table level in the study areas needs to be determined because of its direct effect on the calculation of effective stress values in soil.

The possible sources of ground water level measurements available are:

(1) **The USACE   Report** (USACE 1987): The borehole logs of the USACE investigation report show water level in City of Sacramento anywhere from -27 to -37ft from top of levee, or -10 to -17ft roughly from toe. The measurements were taken in April 1987.

(2) **URS data** (URS 2010): Cone Penetration Test (CPT) logs include plots of Dynamic Pore Water Pressure (u_2). However, the u_2 can be significantly different than the static pore water pressure, u, in cohesive layers of low permeability. As such, the u_2 values cannot be used as given to determine the ground water table in the absence of data from observation wells or piezometers.

(3) **United States Geologic Survey** (USGS 2011): The USGS maintains a distributed water database that is locally managed. Surface water, groundwater, and water quality data are compiled from these local, distributed databases into a national information system. The groundwater database contains records from about 850,000 wells that have been compiled during the course of groundwater hydrology studies over the past 100 years all over the U.S.

A subset of the USGS groundwater watch project database, is the "Active Ground Water Level Network", which contains water levels and well information from more than 20,000 wells across the nation that have been measured by the USGS or USGS cooperators at least once within the past 13 months. This network includes all of these wells, regardless of measurement frequency, aquifer monitored, or the monitoring objective.

In the above database, Sacramento County has 34 wells, all providing periodic measurement data. The number of wells reported in and around the area of study in Sacramento City is 13 wells. With the exception of one of the wells that is on the hills at the east side of Sacramento (elevation 271 ft), all the wells lie in the central valley plain with surface elevation varying between 4ft and 82ft. The 13 wells had 103 recorded water level readings dating from 1983 to 2010. Three of the records were discarded because it was noted that there had been recent pumping in the area. The remaining 100 readings were used to determine an average and a standard deviation value for each well location. Measurements were converted to reflect Absolute Elevations (Mean Sea Level = 0ft).

On average, in Sacramento City, levee crest boreholes are at 39ft, levee toe boreholes at 20ft, and water table at -1ft. This means that the ground water table level is about 40 ft below the top of levee crest boreholes, and 21 ft below the top of levee toe boreholes. This matches well with the 1987 USACE Report, where the ground water level was (25 to 37 ft) under crest boreholes, and (15 to 27 ft) under toe boreholes

Similar calculations were carried out for the Feather River area of study (Feather River South & RD784, Marysville, and Feather River North). The results of all calculated groundwater levels are summarized in Table 4.2.

Table 4.2 Calculated ground water table (GWT) levels (ft) in the study area, Mean Sea Level=0ft

Area	Crest Elevation	Toe Elevation	GWT	GWT below Crest	GWT below Toe
Feather River North	100	81	50	**50**	**31**
Marysville	88	68	40	**48**	**28**
Feather River South & RD784	73	51	30	**43**	**21**
Sacramento City	39	20	-1	**40**	**21**

As for the historical water lever change over the years in the Sacramento Basin region, a review of 18 long-term hydrographs dating back into the 1960s shows a consistent pattern of water level trends through much of the basin (DWR 2004):

- Groundwater elevations generally declined consistently from the mid-1960s to about 1980 on the order of 20 feet.
- From 1980 through 1983 water levels recovered by about 10 feet and remained stable until the beginning of the 1987 through 1992 drought.
- From 1987 until 1995, water levels declined by about 15 feet.
- From 1995 to 2000 most water levels recovered by up to 20 feet leaving them generally higher than levels prior to the 1987 through 1992 drought.

Using observations from the USGS database (2011) to complete the trend from 2000 to 2010, the average overall change in ground water table level in the Sacramento basin was a drop of 10ft over a 50 year period as detailed in Table 4.3.

Table 4.3 Changes in ground water table levels in the Sacramento River basin from 1960-2010 (DWR 2004; USGS 2011)

Period	Change (ft)
1960 - 1980	-20
1980-1983	+10
1983-1987	0
1987-1995	-15
1995-2000	+20
2000-2010	-5 ft
Over past 50 yrs	**-10 ft**

4.3.6   Geotechnical Investigation Data

As previously mentioned, geotechnical soil investigation data for the study area was collected from (1) URS corporation data from the California Urban Levee Evaluation Project (URS 2010) and (2) the USACE investigation report for Sacramento City (1987). Data from both sources included levee layout, levee geometry, boreholes logs and field tests. The total number of available logs, CPTs, and reported tests are summarized in Tables 4.4 and 4.5.

Note that a large number of historical boreholes were reported in the URS dataset. No test results were available for these, and they were short-listed and only used in the

process of identifying regional stratigraphy (section 4.4). Furthermore, duplicate stratigraphy information from piezometers that existed at close proximity to other boreholes was not included in the analysis. All remaining boreholes (Figure 4.18) were digitized into a GIS format, and available test information extracted for further analysis.

(A)   **(B)**
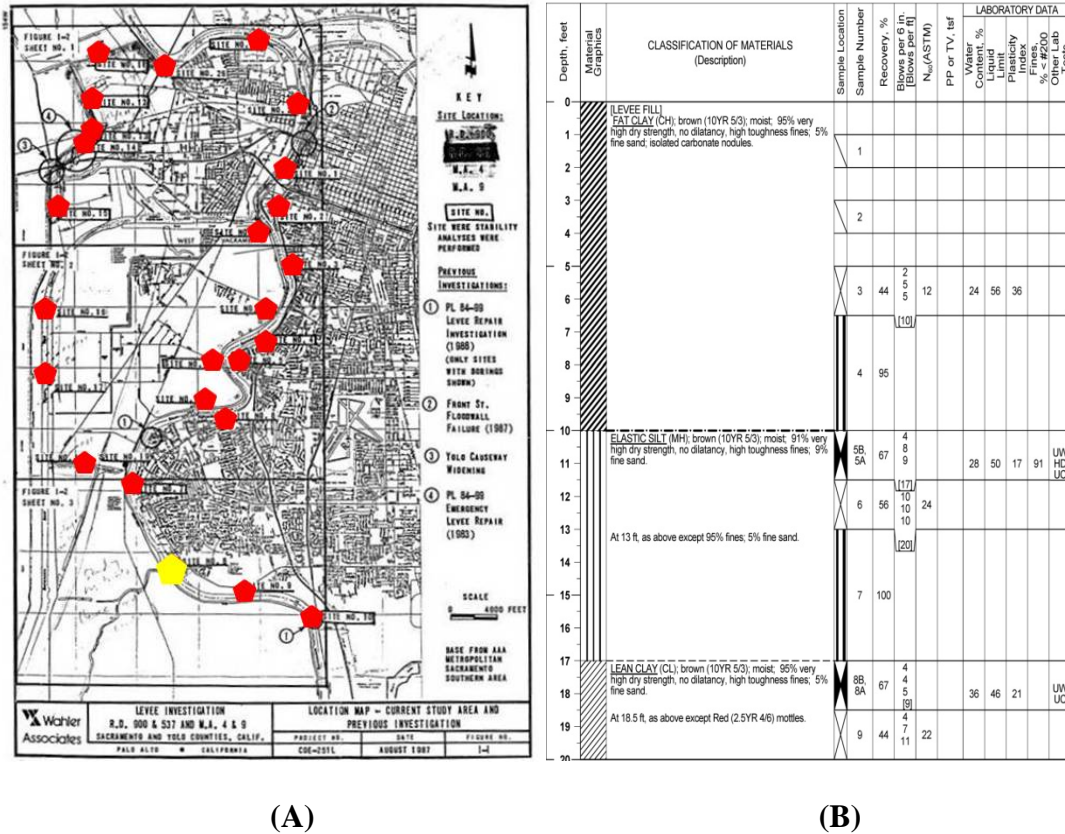
Figure 4.18 (A) Layout of borehole investigation locations in Sacramento (USACE 1987) with (B) a sample borehole log (URS 2010).

Table 4.4 Summary of available geotechnical investigation borehole logs and cone penetration tests (CPTs) in the study areas

| Area | URS Boreholes | | | | | URS Historical | USACE | URS CPTs |
	Borehole (B)	Hollow Stem Auger (A)	Hand Auger (H)	Sonic Core (S)	Piezometer (M)	Historical Log	Borehole	CPT
West Sacramento	26	-	-	-	4	9 [a]	34	25
American River	10	-	-	-	6	27 [a]	-	-
Marysville	49	-	-	4	16	-	-	-
RD784	21	-	-	2	-	-	-	-
Feather North	10	14	5	-	-	-	-	19
Feather South	14	10 [b]	6	-	-	-	-	74
Total	**267**							**118**

[a] Many more available. These are a short list of historical boreholes used for this study.

[b] One borehole was "Solid" and not "Hollow" Stem Auger

Table 4.5 Reported field and lab tests within the available geotechnical investigation boreholes and cone penetration tests (CPTs) in the study areas

Area	URS boreholes and USACE									URS CPTs			
	SPT	MC[a]	CU [b]	VS [b]	WC	LL	PI	Fines	UU[c]	Rf[d]	qt[d]	fs[d]	u₂[d]
West Sacramento	648	46	11	2	173	166	166	298	30	25			
American River	133	4	-	-	35	13	12	56	-	-			
Marysville	651	19	15	-	39	35	35	90	-	-			
RD784	217	25	19	-	111	96	96	158	-	-			
Feather North	211	2	7	-	27	25	25	81	-	19			
Feather South	233	-	22	-	93	84	84	123	-	74			
Total	**2093**				**478**	**419**	**418**	**806**	**30**				

[a] Modified California test numbers to be converted to SPT equivalent

[b] Numerical results for Consolidated Undrained (CU) triaxial tests and Vane Shear (VS) tests were not provided

[c] Unconsolidated Undrained (UU) triaxial tests were only available from the USACE (1987) data

[d] CPT logs represent continuous measurement of parameters.

Laboratory test data reported in the URS database included Consolidated Undrained Strength (CU) and Vane Shear (VS) testing. However, the numerical values of these tests were not provided. Other lab test results included Water Content (WC), Liquid Limit (LL), Plasticity Index (PI), and Fines Content (%). A plot of collected Atterberg limits (LL and PI) confirming the soil classification reported in the borehole logs is shown in Figure 4.19.
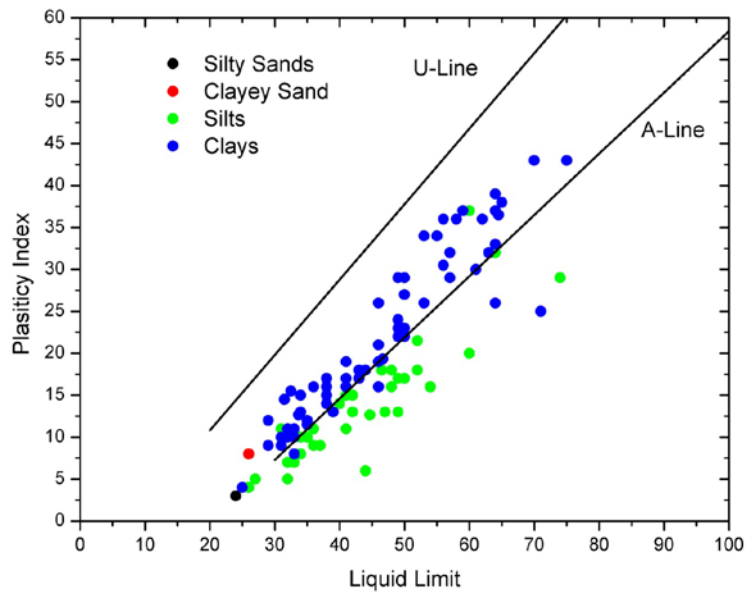
Figure 4.19 Plot of collected Atterberg limits confirming the corresponding soil classification reported in the borehole logs.

CPT data was validated through close comparison to nearby borehole logs for soil layer delineation and soil classification per Figures 4.20 and 4.21. Subsequently, resulting common site specific CPT "signatures" were developed for areas with no boreholes. No correction for thin layer effect was applied to CPT value as thin layers were hard to identify visually from the provided CPT logs.
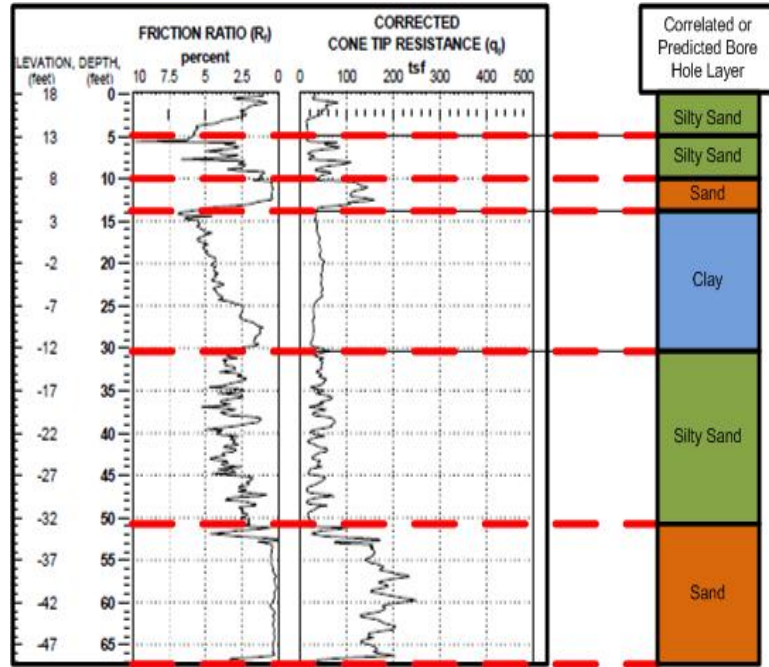
Figure 4.20 Example of delineation of soil layers in CPT logs using nearby borehole data.
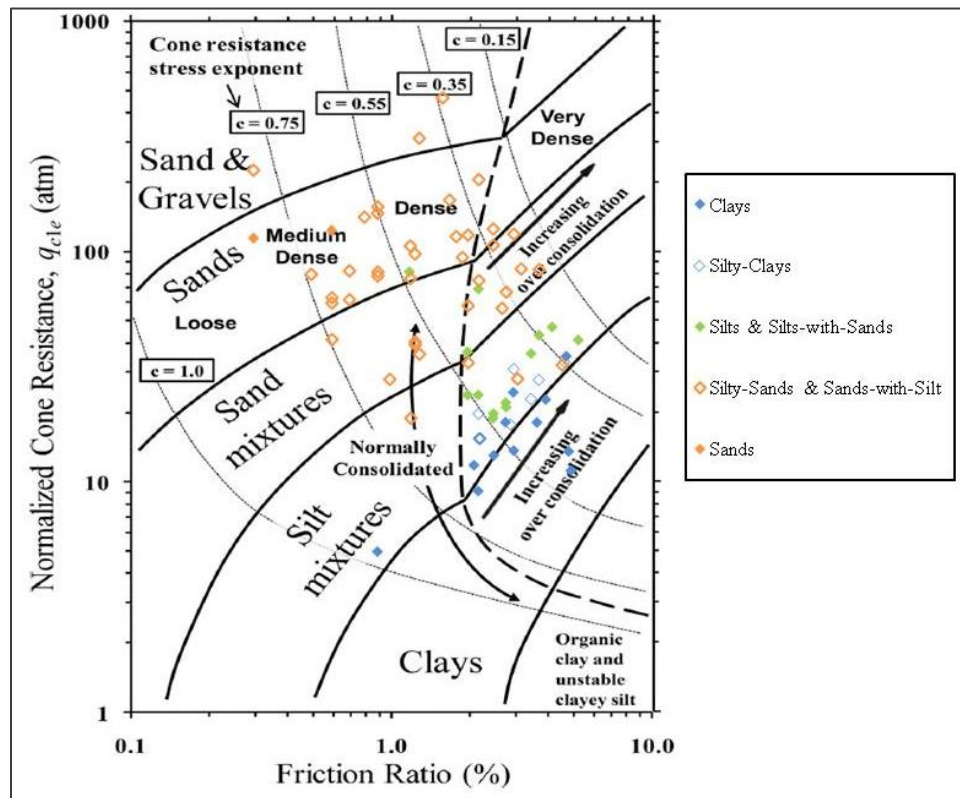
Figure 4.21 Example of collected CPT data from Sacramento City area plotted on the Olsen and Mitchell (1995) soil classification chart.

CPT cone tip resistance was used to determine Undrained Shear Strength (S_u) of cohesive soils. The following empirical correlation (Lunne et al. 1997) was used:

$$Su = \frac{(q_c - \sigma_{vo})}{N_k}$$
Equation 4.1

where q_c is the cone resistance, N_k is an empirical cone factor, and σ_{vo} is the total in-situ vertical stress.

The provided CPT logs (URS 2010) show the "corrected" tip resistance q_t. The correction was applied to account for the pore water pressure acting on the shoulder area behind the cone tip (Lunne et al. 1997):

$$q_t = q_c + u_2\,(1\text{-}a)$$
Equation 4.2

where $\mathbf{q_c}$ is the directly measured cone tip resistance, $\mathbf{u_2}$ is the pore pressure acting behind the cone, and $\mathbf{a}$ is the cone area ratio, approximately equal to the ratio of the cross-sectional area of the shaft divided by the projected area of the cone. Typical values of $\mathbf{a}$ used in the industry range between 0.8 and 0.9, and in the absence of further information, a value of 0.85 was used in the analysis. The pore water pressure correction becomes especially important in soft fine-grained saturated soils, where the pore pressures can be large relative to the cone resistance.

Alternatively, the Undrained Shear Strength (S_u) can also be derived (Lunne et al. 1997) using the equation:

$$S_u = \frac{(q_t - \sigma_{vo})}{N_{kt}}$$
Equation 4.3

where q_t is in this case the corrected cone resistance, N_{kt} is an empirical cone factor, and σ_{vo} is the total in-situ vertical stress.

The empirical parameter N_{kt} is site specific, and can be back-calculated using available triaxial compression test results (USACE 1987). It is worth noting that for the same site, the value of N_{kt} varies depending on the type of laboratory test used to determine S_u (Lunne et al. 1997).

Laboratory measured S_u values from USACE boreholes in West Sacramento were paired with corresponding nearby clay layers (at similar depth) from the URS CPTs. The maximum distance between pairs of data points was 1,500ft. In some cases there were two USACE boreholes (one at levee crest and one at levee toe) for each URS CPT log. Where appropriate, the S_u values from those two USACE boreholes were averaged for use in the comparison. As shown in Figure 4.22, the back-calculated N_{kt} values had an average of 20.8 which is at the high end of ranges of N_{kt} values reported in the literature (Lunne et al. 1997). As such, applying a value of $N_{kt} = 20$ to the available CPT cone tip resistance values in clay layers resulted in Figure 4.23 which shows compatible actual S_u lab test results of USACE in light blue vs. the S_u values derived from CPT in black.
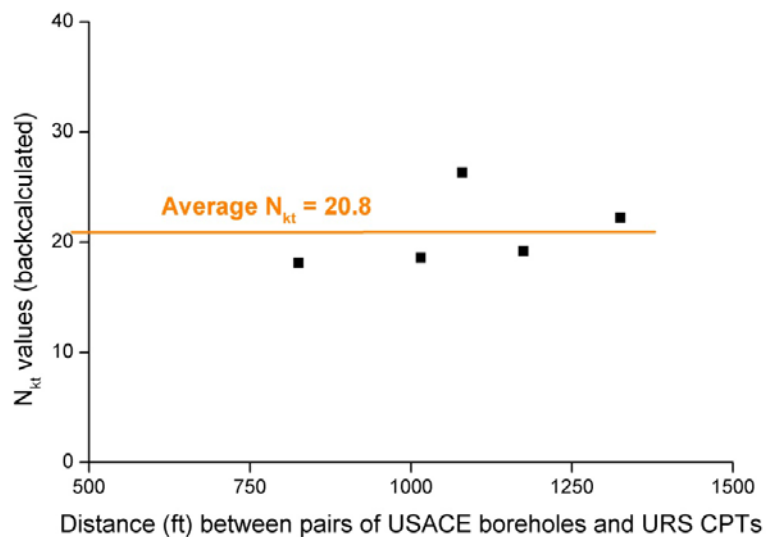
Figure 4.22 Back-calculation of N_{kt} value using laboratory triaxial test results.
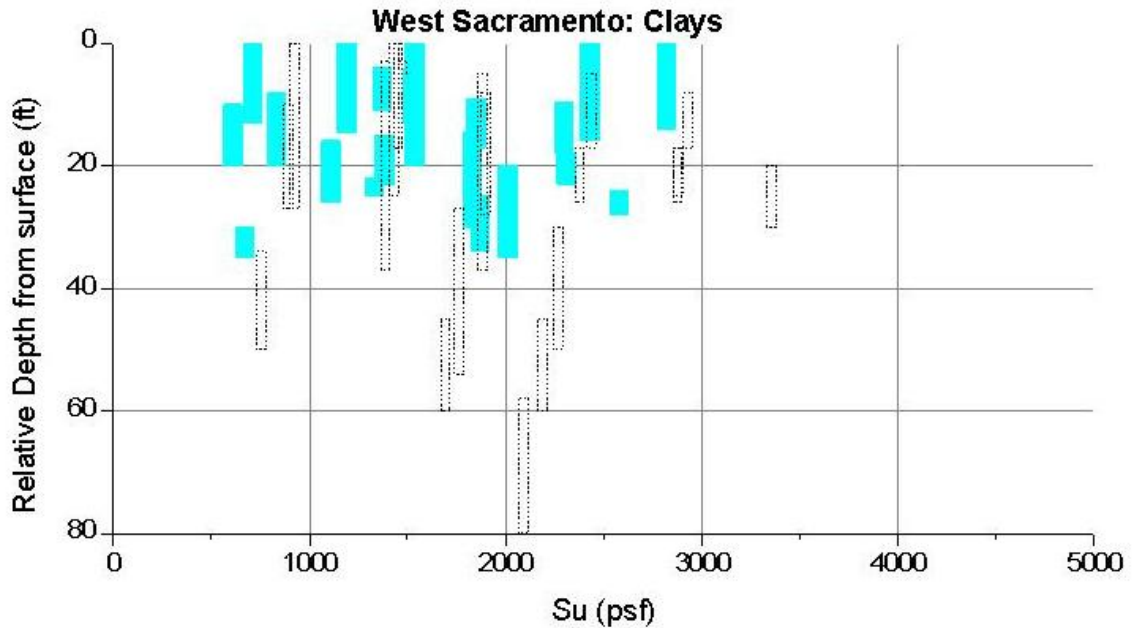
Figure 4.23 Comparison of actual S_u lab test results of USACE <u>in light blue</u> vs. the S_u values derived using an $N_{kt}=20$ from CPT <u>in black</u> for West Sacramento (depth relative to a borehole/CPT surface elevation reference = 0ft)

In order to derive friction angle, ϕ, values for cohesionless soils, Standard Penetration Test (SPT) values had to first be adjusted from N_{60} in the URS database, and **N** in the USACE data into $N_{1,60}$ using required correction factors and effective stress calculations made possible by the determined ground water table levels (section 4.3.5).

In the absence of data and related test results, the average unit weight used for dry conditions was 115pcf, and the average unit weight used for saturated conditions was 120pcf. A number of approaches were used for estimating friction angle, ϕ, values and are compared in Table 4.6.

In addition, friction angle values were also derived from Cone Penetration Test (CPT) results using Olsen and Farr (1986) as well as Robertson and Campanella (1983).

A comparison between those friction angle values and values derived from SPT using

Seed (2005) in West Sacramento is shown in Figure 4.24.

Table 4.6 Relationship between $N_{1,60}$, density and friction angle of sands using Seed (2005), Peck et al. (1974), Schmertmann (1975), and Hatanaka and Uchida (1996)

$N_{1,60}$	Density	Friction Angle, $\phi°$			
		Seed (2005)	Peck et al. (1974)	Schmertmann (1975)	Hatanaka & Uchida (1996)
<5	very loose	<31	<29	<28	<30
5-15	loose	30-36	29-31	28-38	30-37
15-30	medium	35-41	31-35	38-44	37-44
30-50	dense	40-46	35-41	44-49	44-52
>50	very dense	>42	>41	>49	>50
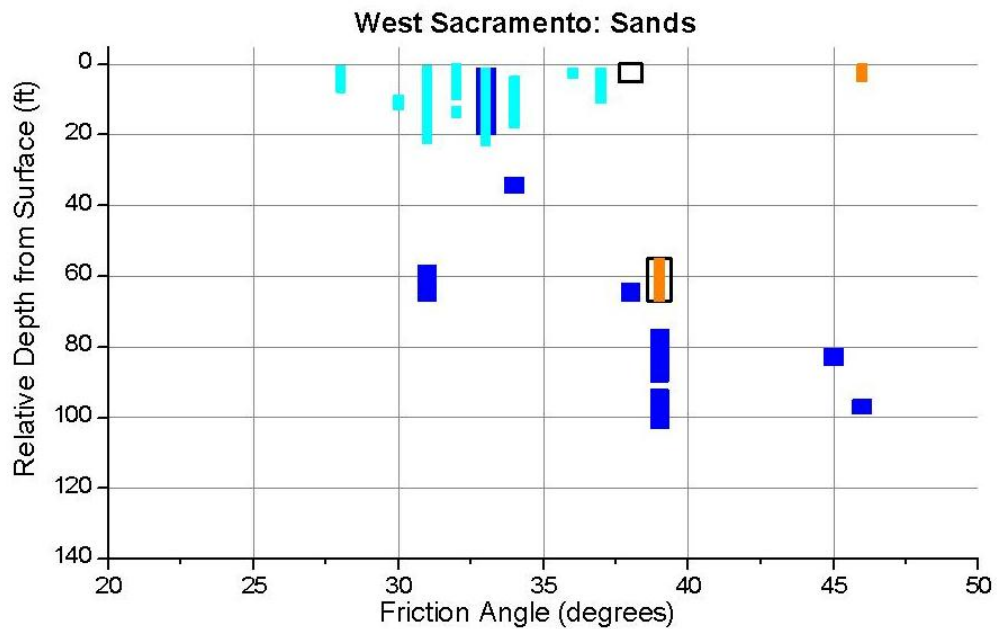
Figure 4.24 Comparison of derived friction angle, ϕ, values in West Sacramento obtained from the USACE SPT values in light blue using Seed (2005), from the URS SPT values in dark blue using Seed (2005), from URS CPT using Olsen and Farr (1986) in black, and from URS CPT using Robertson and Campanella (1983) in orange (depth relative to a borehole/CPT surface elevation reference = 0ft).

The Robertson and Campanella method (1983) applies for values exceeding 25 kPa in effective stress, corresponding roughly to 5ft depth. This explains the high values of ϕ close to the surface obtained using this method as compared to the other methods. Thus all values of friction angle derived using the Robertson and Campanella method in the top 5ft of soil from CPT data was not used in the analysis.

Based on Figure 4.24 the friction angle was derived from SPT using Seed (2005) as per Table 4.6, and from CPT using Robertson and Campanella (1983) as per Figure 4.25 , with the limitation of depth mentioned above.

FIG. 7. Proposed correlations between cone bearing and peak friction angle for uncemented, quartz sands.
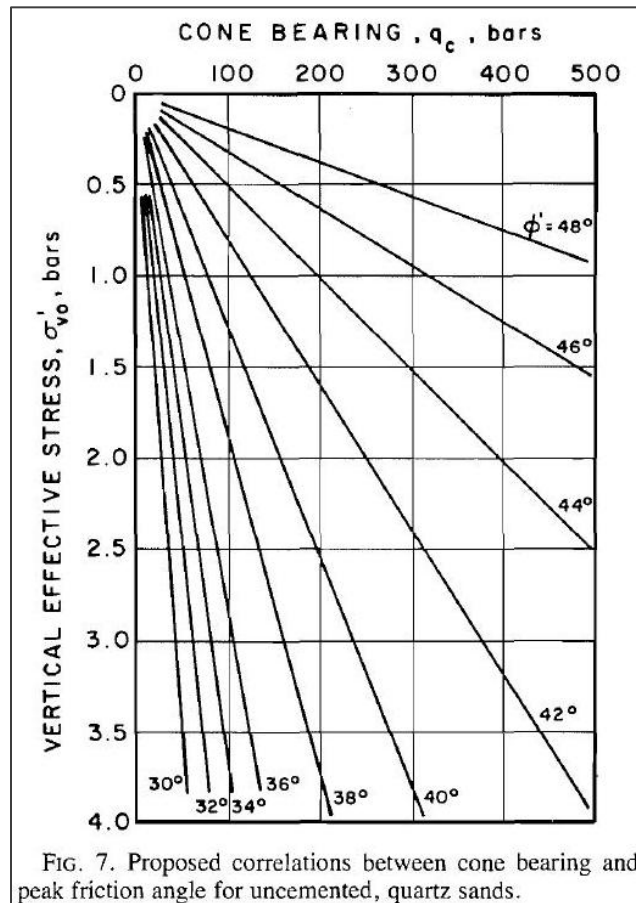
Figure 4.25 Derivation of friction angle of sands from CPT (Robertson and Campanella 1983).

91

4.3.7 Data Processing

In order to combine and use the multiple sources of data in a single ArcGIS software environment, it needs to be processed in several ways. The following is a list of steps taken in this regard:

- Hard-copy data was digitized, geo-referenced, and traced in order to create corresponding soft-copy feature classes.

- Georeferencing of borehole locations was done using coordinate values provided on the borehole logs. Coordinates were provided in "US survey ft" and needed conversion to "meters" to be consistent with the map units and the National Elevation Dataset values. The conversion was done by multiplying the U.S. survey feet by the fraction $\left(\frac{1200}{3937} \right)$.

- Feature classes (points, polylines, and polygons) as well as raster datasets were projected into a common projection system. The projection chosen was the State Plane Coordinate System, California Zone 2, using the NAD 1983 (North American Datum 1983, using the GRS 1980 spheroid).

- National Hydrology Dataset files representing rivers and water bodies are polygon shapes. These had to be converted to a multipart polyline feature representing the geometric centerline of the river.

- Feature classes and rasters were combined and stored in a single "File Geodatabase" structure. The geodatabase offers the ability, among other things, to store a rich collection of spatial data in a centralized location, maintain integrity of spatial data with a consistent, accurate database, work within a multiuser access and editing environment, integrate spatial data with other IT databases, and support custom features and behavior.

- For computing time efficiency, the data was trimmed to the geographical extent of the study areas: A large trim area representing the overall extent of the data, and two smaller trim areas for Sacramento and Feather River each.

- A number of Spatial Joins were performed as needed to relate boreholes and levees to the nearest river segment, sinuosity index value, and underlying geology classification.

4.4 Prediction of Regional Soil Stratigraphy

Prior to estimating the spatial variability of soil parameters, there is a need to estimate the soil stratigraphy in the area of study. Because of the increased uncertainties in derivation of strength parameters from in-situ tests for silts, the focus was to determine the stratigraphy of sands and clays, since the derivation of strength parameters for those two categories of soils was possible given the available data. Therefore, a general category of "**Sand**" was adopted for soils classified, according to the Unified Soil Classification System USCS (ASTM Standard D2487-11 2011), as Poorly graded Sand (SP), Well-graded sand (SW), Poorly-graded Sand with Silt i.e. 5%<%Fines<12% (SP-

SM) and Well-graded Sand with Silt i.e. 5%<%Fines<12% (SW-SM). Similarly, a general category of "**Clay**" was adopted for soils classified as Fat Clay (CH), Lean Clay (CL) and Silty Clay (CL-ML), according to USCS.

Furthermore, because of the geostatistical complexity of combining both the estimation of thickness variation of different layer types (qualitative parameter), with the estimation of the soil parameter variability within each layer (quantitative parameter), and because the focus of this research was the study of soil properties variability, soil layers were assumed to exist at a constant thickness throughout the study areas. For each of the two study areas (Sacramento and Feather River), and based on the available borehole log classifications, plots were developed to help identify the stratigraphy of the region. These plots do not include material identified as engineering fill within the levee, as the intent of the research is to study the spatial variation of naturally occurring soils. The plots also confirm that, within the area of study, the regional stratigraphy can be assumed to be uniform for the scope of this research.

The layer delineation is determined based on the number of data points occurring with depth, in combination with the layer thickness for each data point in the respective borehole log. The "**layer range**" value for each identified layer represents the thickness of the band of soil where the identified layer was observed. The delineation of clay layers takes into account the corresponding delineation of the sand layers, and vice versa. As an example, Figure 4.26 shows the approach used for the delineation of layers in the Sacramento area based on available boreholes from USACE and URS datasets.
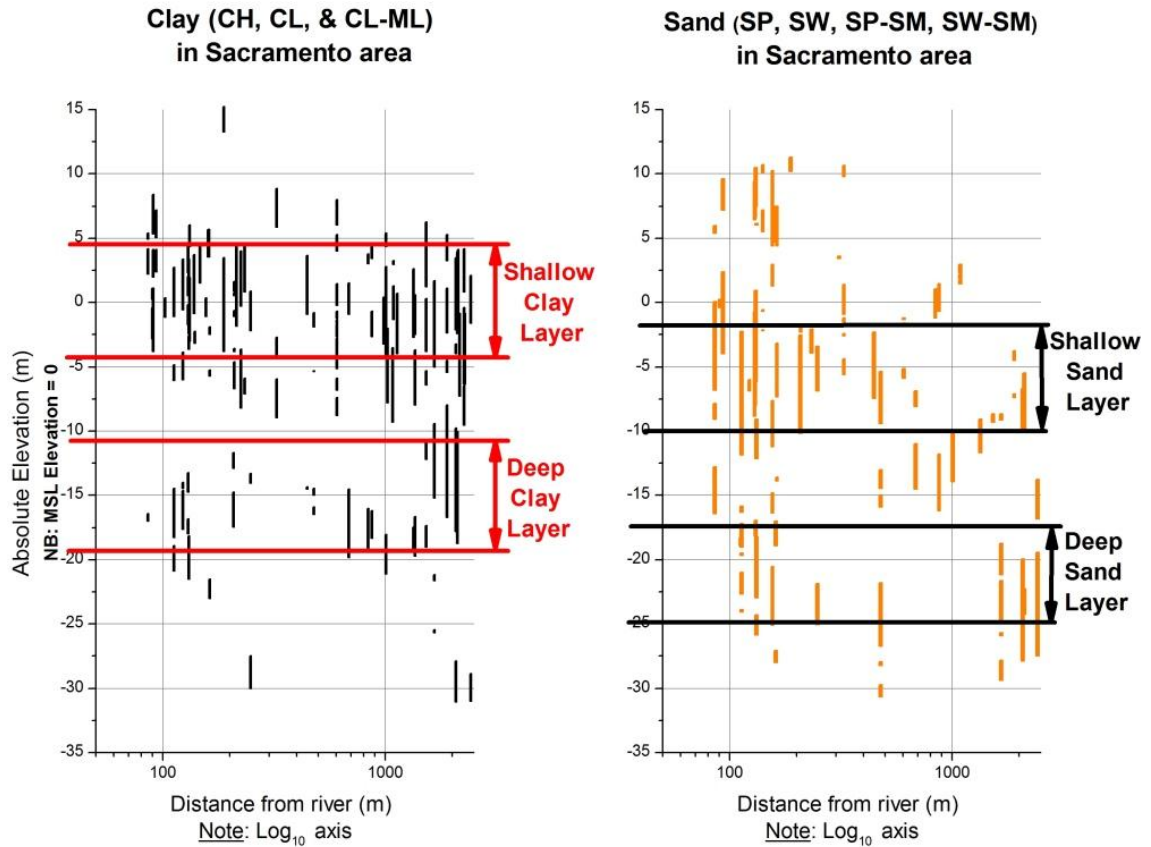
Figure 4.26 Process of layers delineation for clay and sand in Sacramento based on borehole log information.

The layers identified in Sacramento from Figure 4.26 are listed in Table 4.7. Similarly the resulting layer delineation for Feather River was performed using the URS boreholes, and the results are presented in Table 4.8 and Figures 4.27 and 4.28. Note that due to a gradual increase in surface soil elevation in the Feather River study area going from south to north, different elevations were noted in the sub-sections of "Feather River South & RD 784", Marysville, and "Feather River North".

Table 4.7 Delineation of Clay and Sand layers in Sacramento area

Location	Material	Depth	Depth order	Layer ref.	Absolute Elevation (m) MSL=0		
					From	To	Layer Range
Sacramento City	Clay	shallow	1	1st Clay	4	-4	8
	Sand	shallow	2	1st Sand	-2	-10	8
	Clay	deep*	3	2nd Clay	-11	-19	8
	Sand	deep*	4	2nd Sand	-18	-25	7

* data available only from West Sacramento URS dataset

Table 4.8 Delineation of Clay and Sand layers in Feather River area

Location	Material	Depth	Depth order	Layer ref.	Absolute Elevation (m) MSL=0		
					From	To	Layer Range
Feather South & RD784	Clay	shallow	1	1st Clay	17	10	7
Marysville					22	13	9
Feather North					25	17	8
Feather South & RD784	Sand	shallow	2	1st Sand	11	6	5
Marysville					15	8	7
Feather North					20	12	8
Feather South & RD784	Clay	deep	3	2nd Clay	7	0	7
Marysville					7	0	7
Feather North					12	6	6

Clay (CH, CL, & CL-ML)
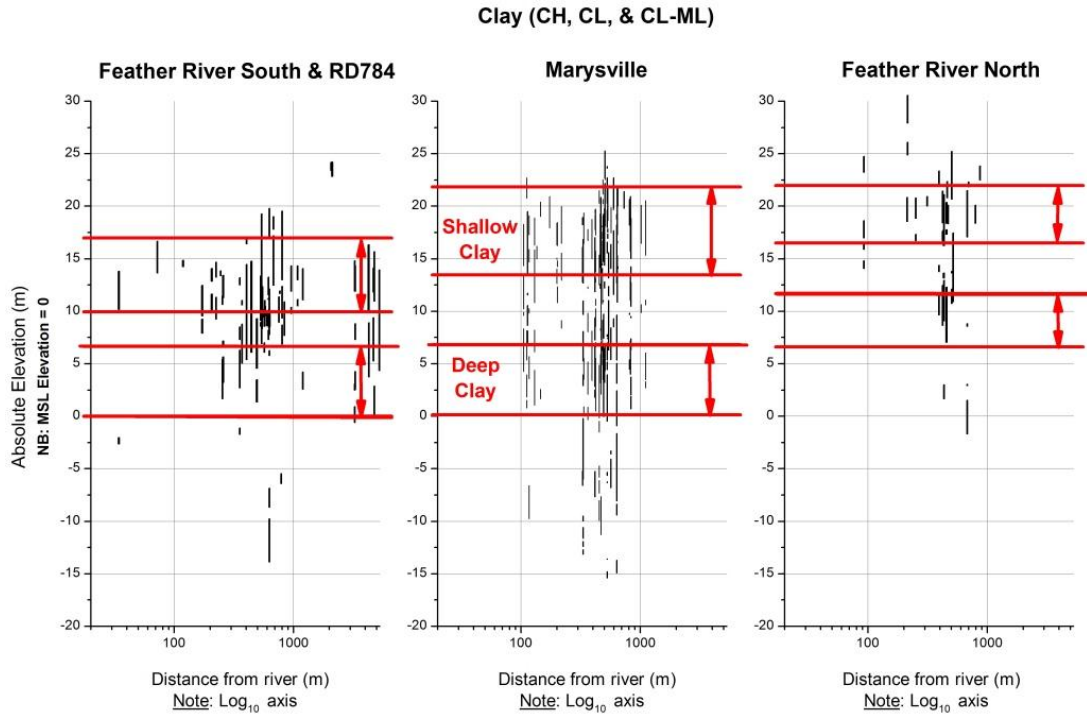
Figure 4.27 Identified clay layers in Feather River.

Sand (SP, SW, SP-SM, SW-SM)
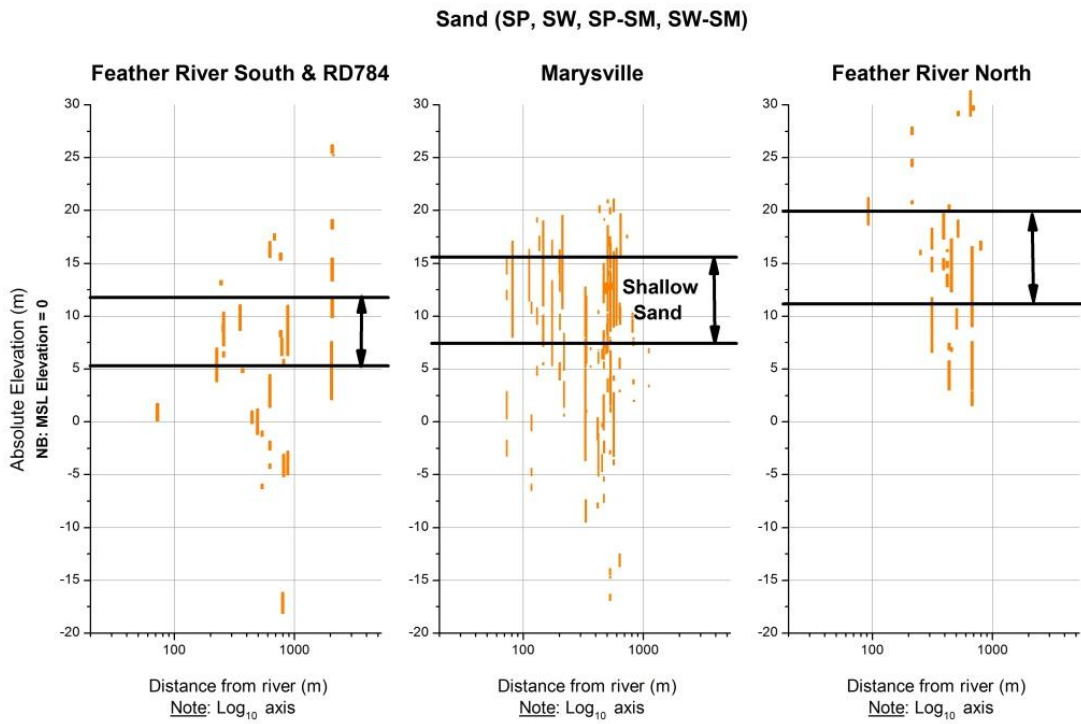
Figure 4.28 Identified sand layers in Feather River.

It is important to note that the number of layers observed depends on the available depth of the boreholes:

- Sacramento area boreholes lengths: varied from about 20 up to 30m.

- Marysville boreholes lengths: on average 20m

- Feather North and South boreholes lengths: on average 12m

As an implication of the above limiting factor, data for the "Deep Sand" and "Deep Clay" layers in Sacramento could only be obtained from the URS set of boreholes (Table 4.4). This resulted, for example, in only three data points for the Su parameter in the Sacramento "Deep Clay" layer and thus no further analysis could be done in that case. Similarly, data for the "Deep Clay" layer in Feather River was only available from the Feather River South set of boreholes.

The steps discussed in the remaining part of the dissertation have been applied to all layers of both study areas. Figures for all the layers are included in Appendices Appendix C through Appendix F. However, only figures relating to the identified "Shallow Clay layer in Sacramento" (the top layer in Figure 4.26) will be used as examples in the coming sections.

4.5   Prediction of Spatial Variability of Soil Parameters

4.5.1   Introduction

Once a soil layer's depth and thickness was identified in a region, it was possible to address the subject of estimating the spatial variability of that layer's geotechnical

parameters, particularly the shear strength parameters. A number of regional, area-specific factors were investigated for possible correlation with the spatial variability of the underlying foundation soil material properties, in order to develop the geostatistical models.

4.5.2   Correlation of Soil Parameters to Regional Factors

For the seven delineated layers of clay and sand (Tables 4.7 and 4.8) in the two study regions, the soil parameters that were studied were:

- Clays: Undrained Shear Strength (Su), Liquid Limit (LL), Plasticity Index (PI), Ratio of Water Content to Liquid Limit (WC/LL)
- Sands: Friction Angle (ϕ), Fines Content (%)

The parameters were analyzed and correlations established, where existing, with regional factors including distance to closest river, sinuosity of closest river segment, and underlying geology classification. As mentioned in the previous section, in some instances there were not enough data points to allow for regression analysis.

To study the spatial variability of the soil parameters, the concept of "**Effective Correlation Distance**" between the soil parameters and the factors was introduced. This is a physical representation of the distance beyond which no trend/correlation was observed or deemed physically significant. For **clay** parameters this distance came out to be 600m from the river centerline (Figure 4.29 is shown, as an example, for the shear strength parameter S_u of the Sacramento area shallow clay layer). In Sacramento, the average river width is 150m, and levees are typically around 100m from the river

centerline. Thus the limit of this correlation is still 500m away from the levees, which can be approximated as free-field conditions. For **sand** parameters the distance was 450m, still leaving around 350m between the levee centerline and the edge of the correlation area. A possible explanation of why sand distance is less than clay distance is the fact that sands settle closer to the levee in times of overtopping flooding.
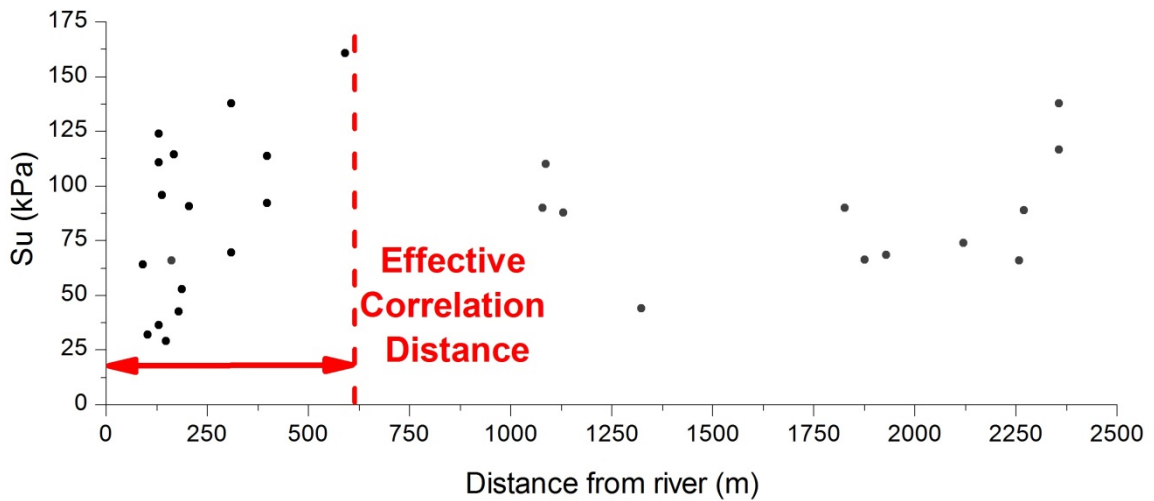
Figure 4.29 Example of determination of the "Effective Correlation Distance" for the shear strength parameter, S_u, for the Sacramento area shallow clay layer.

Tables 4.9 and 4.10 show the established "**Effective Correlation Distance**" and the "**Sinuosity Index Segmentation Level**" for all seven layers. The latter is a reflection of the river meander length period. Values imply that the Feather River (1,000m segmentation) has a shorter meander wavelength than the Sacramento River (1,750m segmentation).

100

Table 4.9 "Effective Correlation Distance" and "Sinuosity Index Segmentation Level" for soil layers in Sacramento area

Location	Material	Depth	SI segmentation level (m)	Effective correlation distance (m)					
				ϕ	Fines	S_u	LL	PI	WC/ LL
Sacramento City	Clay	shallow	1750	-	-	600	600	600	1500
	Sand	shallow	1750	450	450	-	-	-	-
	Clay	deep	1750	-	-	n/a*	1500	1500	1500
	Sand	deep	1750	450	450	-	-	-	-

* only three data points, and all are at large distance from river

Table 4.10 "Effective Correlation Distance" and "Sinuosity Index Segmentation Level" for soil layers in Feather River area

Location	Material	Depth	SI segmentation level (m)	Effective correlation distance (m)					
				ϕ	Fines	Su	LL	PI	WC/ LL
Feather River	Clay	shallow	1000	-	-	600	600	600	600
	Sand	shallow	1000	450	450	-	-	-	-
	Clay	deep	1000	-	-	600*	600*	600*	600*

* data available only from Feather River South

Figure 4.30 summarizes the plots of the shallow Clay layer parameters (S_u, LL, PI, WC/LL) in Sacramento in relation to the distance from the centerline of closest river segment. Analyzing the plot of S_u and categorizing the data points by both geology and

Sinuosity Index regional factors results in Figure 4.31, including establishing a trend of S_u variation with distance to river.

A further analysis of the particular relation between S_u with geology (Figure 4.32) and Sinuosity Index (Figure 4.33) helps to establish preliminary relationships. For example, the latter figure implies that the value of S_u decreases with increased river sinuosity.

Note that the X-axis values in Figure 4.32, representing geology, are categorical values, thus no trend or fit can be deduced, but rather establish variability of S_u parameter with each particular geology type (Table 4.1).
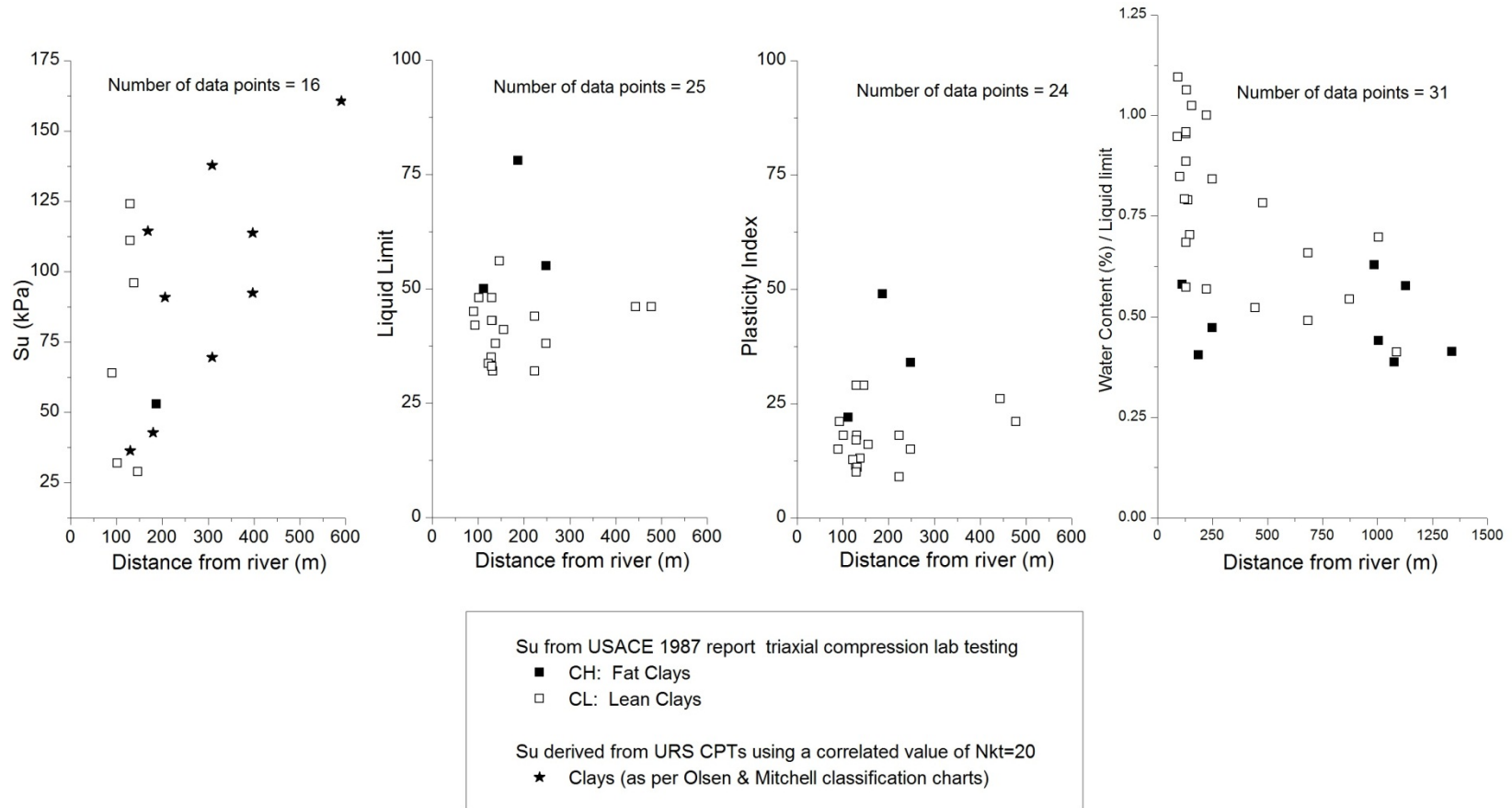
Figure 4.30 Relation of shallow clay soil parameters to distance from centerline of closest river segment in Sacramento.
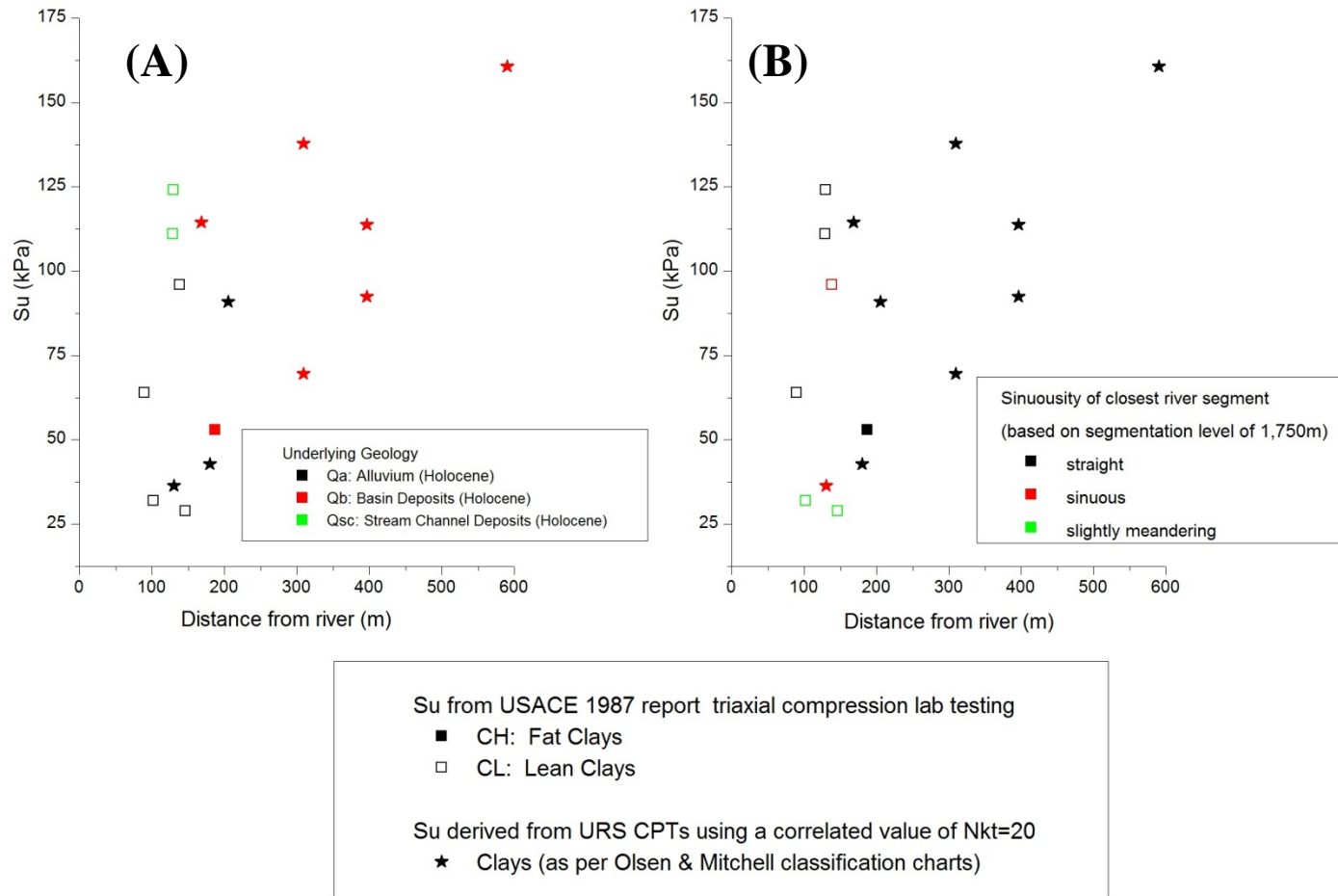
Figure 4.31 Relation of S_u (kPa) shallow clay soil parameter in Sacramento, to distance from centerline of closest river segment, categorized as per (A) Geology and (B) Sinuosity Index.
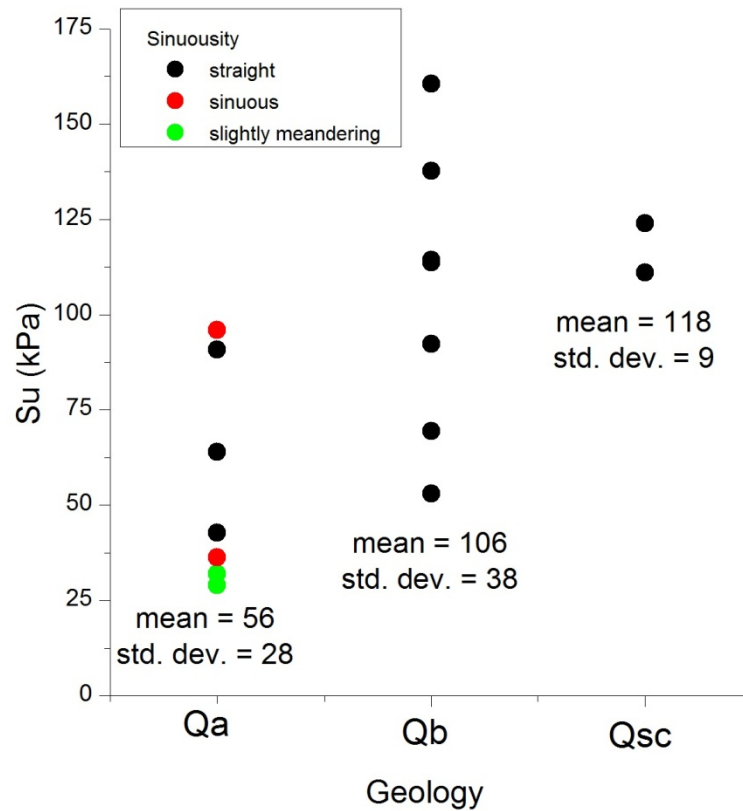
Figure 4.32 Relation of S_u (kPa) shallow clay soil parameter in Sacramento, to geology, categorized as per Sinuosity Index.
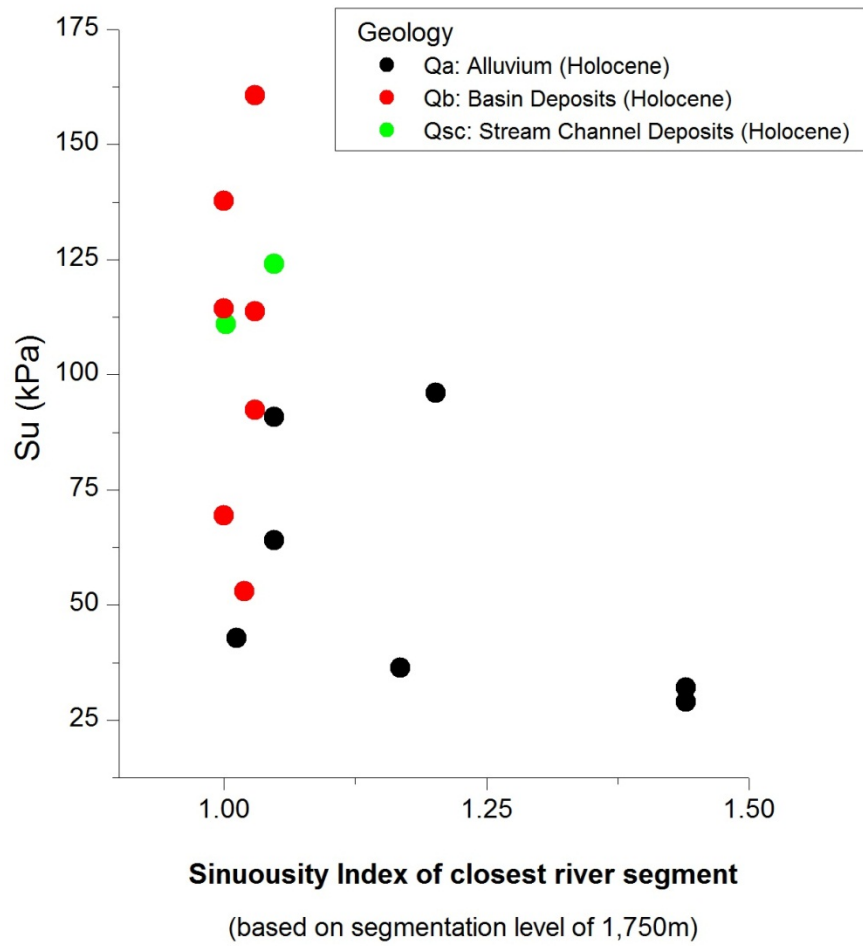
Figure 4.33 Relation of S_u (kPa) shallow clay soil parameter in Sacramento, to Sinuosity Index, categorized as per regional geology.

4.5.3 Observations of Local vs. Regional Effects

This section presents a comparison, and discussion of similarities or difference, in the soil strength parameter trends of different layers (deep and shallow) and different study areas (Sacramento and Feather River). The main objective is to define what might be regional (i.e. inside an area) vs. global effects (applicable to both areas of study).

Clay in both shallow and deep, and in both areas of study, showed increasing trend of S_u with increasing distance from river (Figure 4.34). S_u values also increased with depth, which may be attributed to consolidation of the deeper layers over time.
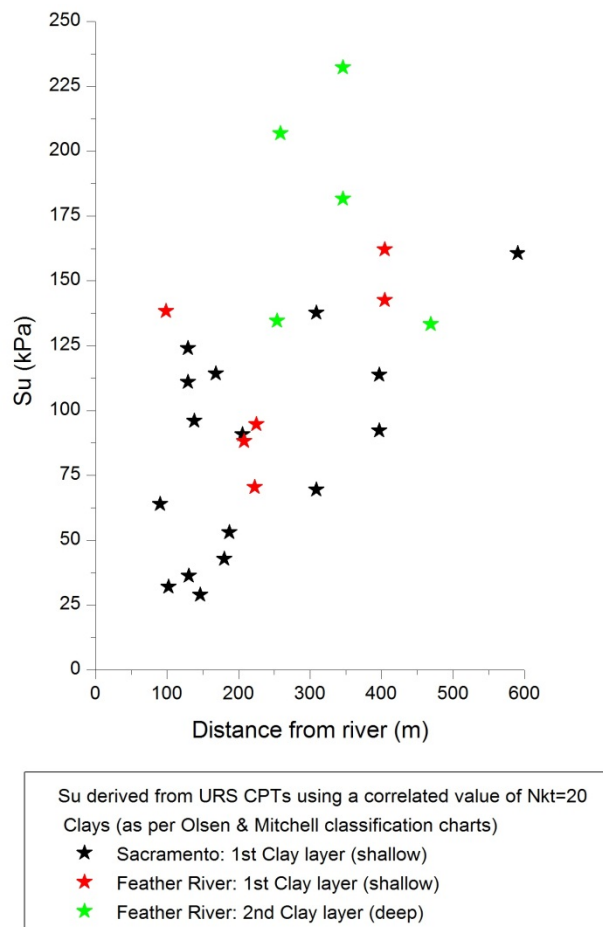
Figure 4.34 Relation of S_u (kPa) soil parameter to distance from centerline of closest river segment, in Sacramento and Feather River for both shallow and deep layers of clay.

As for <u>relation of S_u to the different geological formations</u> in the two study areas (Figure 4.35), a general observation is that clay S_u values in the areas of the **Qa** formation tend to have lower values than other areas. The **Qa** formation is defined as Alluvium - Unweathered gravel, sand, & silt, as such clay is not the main component, which might provide an explanation for the lower values of S_u for clay in these areas, as compared to other formations.
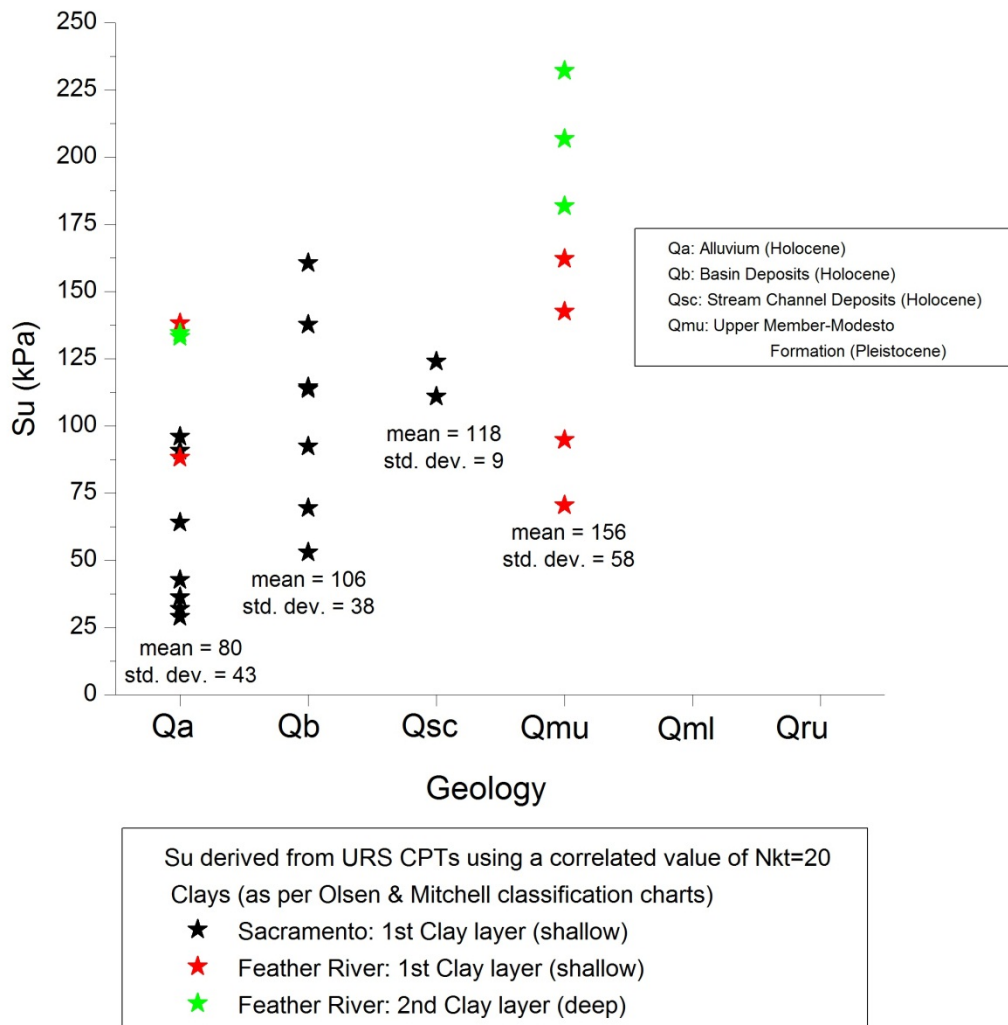
Figure 4.35 Relation of S_u (kPa) soil parameter to geology, in Sacramento and Feather River for both shallow and deep layers of clay.

For S_u relation to Sinuosity Index, (Figure 4.36) there is a large scatter, at lower sinuosity levels. The higher number of data points at this low sinuosity level is due to the smaller number of river segments that are highly sinuous.
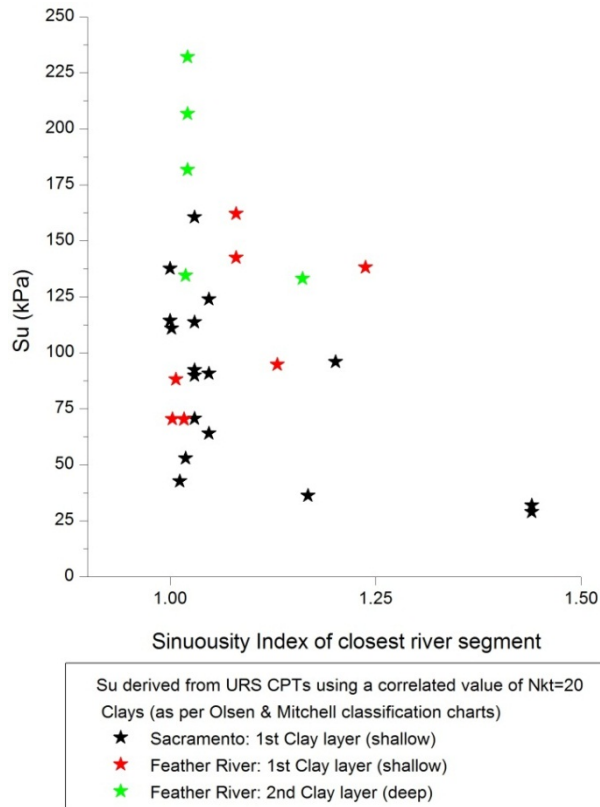
Figure 4.36 Relation of S_u (kPa) soil parameter to Sinuosity Index, in Sacramento and Feather River for both shallow and deep layers of clay.

An important observation across all areas of study, and at shallow and deep clay layers, is that S_u tends to decrease with increasing sinuosity of the closest river segment. A possible explanation of this phenomenon is that deposition of fine particles tends to be more uniform (leading to higher S_u values) if the river is less sinuous. Given the limited available data however, it should be noted that more data points are needed to draw any truly meaningful correlations between SI and shear strength or soil type. Furthermore, due to the specific case study area that was used, the limited data was primarily available

109

for SI values close to 1 (i.e. straight river sections). Note that the Sinuosity is based on segmentation level of 1,750m for Sacramento and 1,000m for Feather River as discussed in section 4.3.4.

Sand layers in both shallow and deep, as well as in both areas of study, did not show a global trend of friction angle, ϕ, with increasing distance from river (Figure 4.37). The friction angle values do not seem to be affected by the depth at which the sand layer is present.
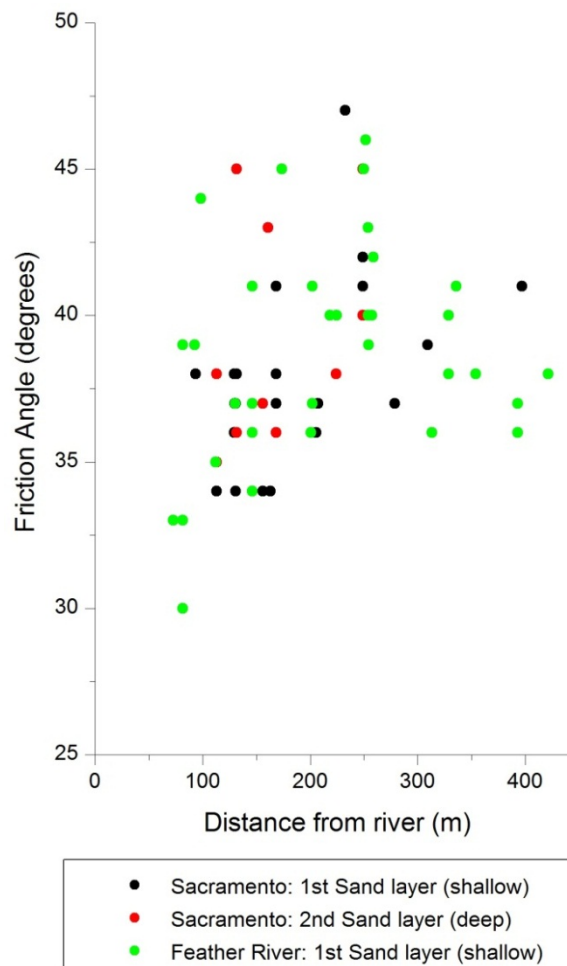
Figure 4.37 Relation of friction angle, ϕ, soil parameter to distance from centerline of closest river segment, in Sacramento and Feather River areas for both shallow and deep layers of sand.

110

No clear conclusion could be drawn (Figure 4.38) from the plot of friction angle, ϕ, with respect to different geological formations in the two study areas. Thus it is possible to draw a relation between ϕ and individual geological formation (i.e. typical value and distribution of ϕ within each geological formation). Furthermore, the sand layers in both areas of studies are present in a different range of geological formations; specifically, the Sand layers in Sacramento are present in the Qa, Qb, and Qsc formations, while the Sand layer in Feather River extends over those same three formations in addition to Qmu, Qml, and Qru (refer to Table 4.1 for detailed description of each formation).
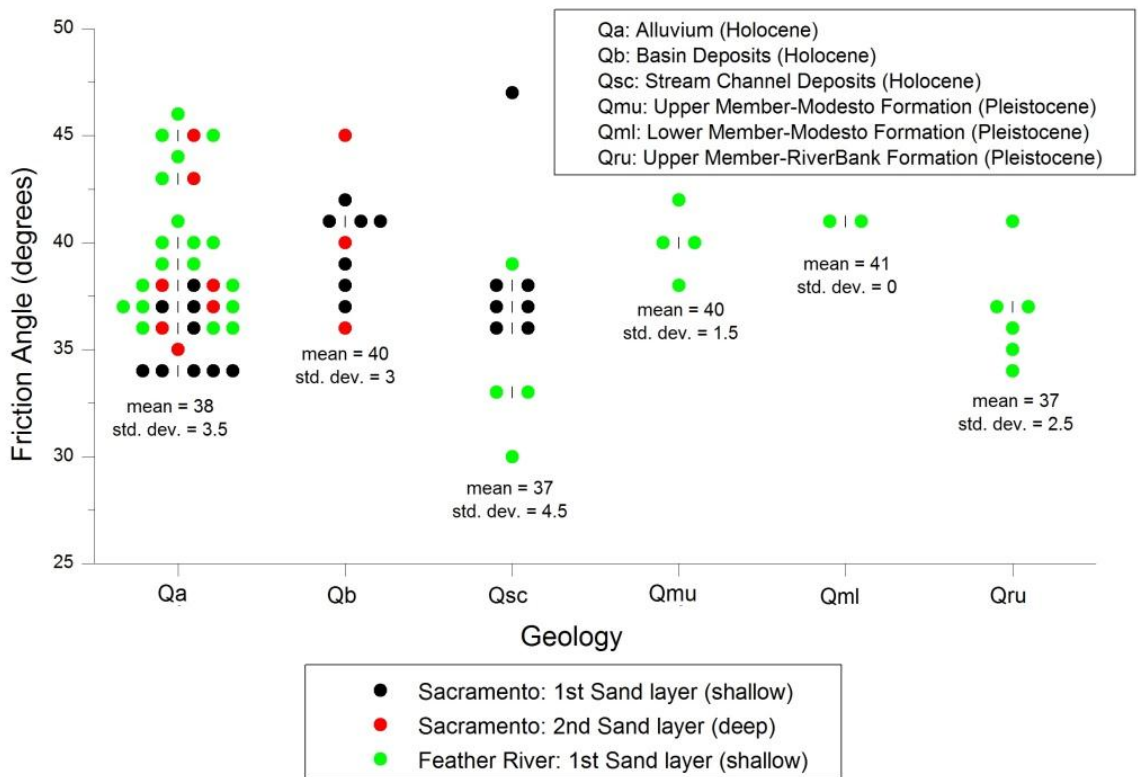
Figure 4.38 Relation of friction angle, **ϕ**, soil parameter to geology, in Sacramento and Feather River for both shallow and deep layers of sand.

For <u>friction angle, φ, vs. Sinuosity Index</u> (Figure 4.39) there is no global effect observed. Furthermore, the small number of data points at high sinuosity levels (3 points for each of the "slightly meandering" and "meandering") does not allow for statistically stable analysis. Once more, the data points in this figure come from Sinuosity Index values obtained based on different segmentation levels within the two areas of study (1,750m for Sacramento and 1,000m for Feather River).
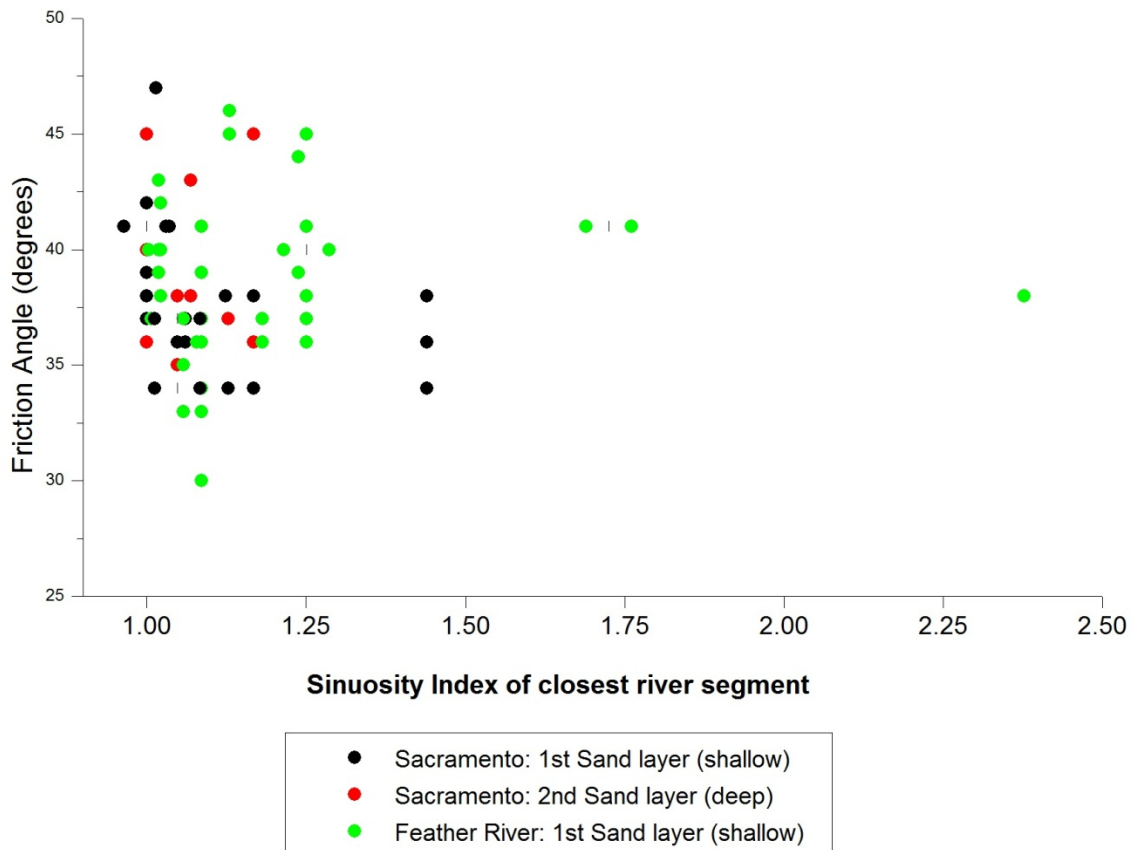
Figure 4.39 Relation of friction angle, φ, soil parameter to Sinuosity Index, in Sacramento and Feather River for both shallow and deep layers of sand.

112

4.5.4   Curve Fitting of Correlations of Soil Parameter to Regional Factors

A number of functions were tested for the best fit of the data points. The criteria for the function that best fitted the data included comparison of "Reduced Chi-Square" and "Adjusted R-square" values resulting from different fit functions.

"Adjusted R-square" measures the proportion of the variation in the dependent variable (in this case soil parameters) accounted for by the independent variables (regional factors). Adjusted R-square is a modification of the R-square measure, taking into account degrees of freedom associated with the sums of the squares of errors, and as such adjusted R-square is generally considered to be a more accurate goodness-of-fit measure. As opposed to R-square, the Adjusted R-square increases only if a new added term improves the model more than would be expected by pure chance. The adjusted R-square will always be less than or equal to R-square, and can be negative in cases when the model contains terms that do not help to predict the response. The definitions used are:

$$R - \text{Square} = 1 - \frac{\text{SSE}}{\text{SST}} \qquad \text{Equation 4.4}$$

$$\text{Adjusted R} - \text{Square} = 1 - \frac{\frac{\text{SSE}}{(n-p-1)}}{\frac{\text{SST}}{(n-1)}} \qquad \text{Equation 4.5}$$

where **n** is the number of known data points, **p** is the number of parameters of the fit function. The additional deduction of **1** is to account for the mean value of the known data points.

SSE is the Sum of Square of Errors (or residuals) from fitting the data, and SST is the

Total Sum of Squares with respect to the sample data mean:

$$SSE = \sum_{i=1}^{n}(y_i - m_i)^2 \qquad\qquad \text{Equation 4.6}$$

$$SST = \sum_{i=1}^{n}(y_i - \mu)^2 \qquad\qquad \text{Equation 4.7}$$

where **n** is the number of known data points, y_i is the ith known value, m_i is the value of

the fit model corresponding to the ith position, and **μ** is the known sample data mean.

The **"Reduced Chi-square"** is a modification of the Chi-square measure, taking

into account the degrees of freedom of the fitting model (the number of known data

points **n**, and the number of parameters **p**, as shown above for Adjusted R-square).

Higher values of Reduced Chi-square imply a poor fit. The definitions of both measures

are:

$$Chi - Square = \frac{SSE}{\sigma^2} = \frac{\sum_{i=1}^{n}(y_i - m_i)^2}{\sigma^2} \qquad\qquad \text{Equation 4.8}$$

$$Reduced\ Chi - Square = \frac{Chi-Square}{(n-p-1)} = \frac{\frac{\sum_{i=1}^{n}(y_i - m_i)^2}{\sigma^2}}{(n-p-1)} \qquad\qquad \text{Equation 4.9}$$

where σ^2 is the variance of the known data points, and other items are as previously

defined.

Power functions provided the best fit for plots of parameters vs. regional factors

and are summarized in Tables 4.11, 4.12, and 4.13 for Clay layers, and Tables 4.14, 4.15,

and 4.16 for Sand layers. The fit curves for all layers are shown on plots included in

Appendix C, and the plots of Fit Curve Residuals are shown in Appendix D. A sample of

the fit curves and residuals is shown in Figures 4.40 and 4.41 for the plot of shear strength S_u to Sinuosity Index for the shallow clay layer in Sacramento.
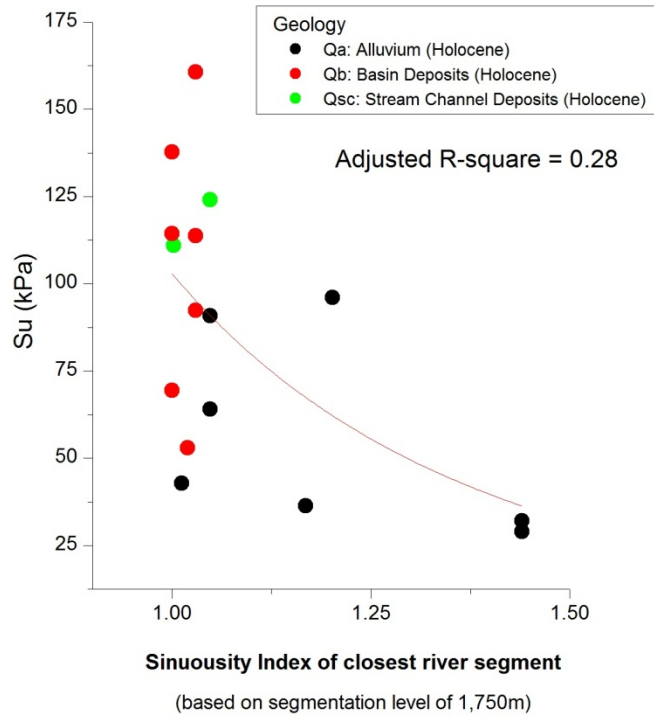
Figure 4.40 Curve fitting of shear strength S_u (kPa) to Sinuosity Index for shallow clay layer in Sacramento area.
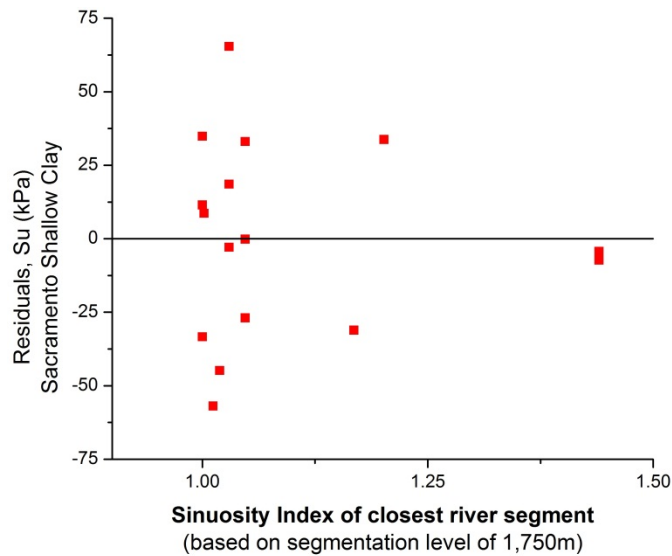
Figure 4.41 Residuals from curve fitting of shear strength S_u (kPa) to Sinuosity Index for shallow clay layer in Sacramento area.

Table 4.11 Curve fitting plots of shear strength S_u (kPa) to distance from river (m)

Location	Depth	Material	y - axis	x - axis	Fit equation	a		b		Statistics	
						Value	Standard Error	Value	Standard Error	Reduced Chi-Sqr	Adjusted R-Square
Sacramento City	shallow	Clay	S_u (kPa)	Distance to river (m)	$y = a*(1 + x)^b$	6.37	6.18	0.49	0.17	1163	0.28
Feather River	shallow	Clay			no data fit						
Feather River	deep	Clay			no data fit						
Overall	**all**	**Clay**	**S_u (kPa)**	**Distance to river (m)**	**$y = a*(1 + x)^b$**	**6.87**	**6.29**	**0.51**	**0.16**	**2006**	**0.27**

Table 4.12 Curve fitting plots of shear strength S_u (kPa) to geology

Location	Depth	Material	y -axis	x - axis	Fit type
Sacramento City	shallow	Clay	S_u (kPa)	Geology	no fit was applied as Geology is a categorical factor
Feather River	shallow	Clay			
Feather River	deep	Clay			
Overall	**all**	**Clay**	**S_u (kPa)**	**Geology**	**no fit was applied as Geology is a categorical factor**

Table 4.13 Curve Fitting Plots of Shear Strength S_u (kPa) to Sinuosity Index

Location	Depth	Material	y-axis	x - axis	Fit equation	a		b		Statistics	
						Value	Standard Error	Value	Standard Error	Reduced Chi-Sqr	Adjusted R-Square
Sacramento City	shallow	Clay	S_u (kPa)	Sinuosity Index	$y = a*(1 + x)^b$	3879	7898	-5.23	2.85	1172	0.28
Feather River	shallow	Clay			no data fit						
Feather River	deep	Clay			no data fit						
Overall	**all**	**Clay**	**S_u (kPa)**	**Sinuosity Index**	**$y = a*(1 + x)^b$**	1399	2182	-3.58	2.18	2168	0.10

Table 4.14 Curve fitting plots of friction angle φ (degrees) to distance from river (m)

Location	Depth	Material	y-axis	x - axis	Fit equation	a		b		Statistics	
						Value	Standard Error	Value	Standard Error	Reduced Chi-Sqr	Adjusted R-Square
Sacramento City	shallow	Sand				20.24	4.51	0.12	0.04	8	0.23
Sacramento City	deep	Sand	φ	Distance to river (m)	y = a*(1 + x)^b	21.57	11.49	0.12	0.10	14	0.03
Feather River	shallow	Sand				27.81	4.56	0.06	0.03	12	0.09
Overall	**all**	**Sand**	**φ**	**Distance to river (m)**	**y = a*(1 + x)^b**	**24.88**	**3.13**	**0.08**	**0.02**	**11**	**0.13**

Table 4.15 Curve fitting plots of friction angle φ (degrees) to geology

Location	Depth	Material	y -axis	x - axis	Fit type
Sacramento City	shallow	Sand			
Sacramento City	deep	Sand	φ	Geology	**no fit was applied as Geology is a categorical factor**
Feather River	shallow	Sand			
Overall	**all**	**Sand**	**φ**	**Geology**	**no fit was applied as Geology is a categorical factor**

Table 4.16 Curve Fitting Plots of friction angle ϕ (degrees) to Sinuosity Index

Location	Depth	Material	y-axis	x - axis	Fit equation	a		b		Statistics	
						Value	Standard Error	Value	Standard Error	Reduced Chi-Sqr	Adjusted R-Square
Sacramento City	shallow	Sand			y = a*(1 + x)^b	52.62	10.81	-0.45	0.28	9	0.08
Sacramento City	deep	Sand	ϕ	Sinuosity Index	no data fit						
Feather River	shallow	Sand			no data fit						
Overall	**all**	**Sand**	ϕ	**Sinuosity Index**	**no data fit**						

4.5.5 Kriging Estimation Using Measured Parameter Values

The spatial variation of the soil strength parameters in the vicinity of levees was estimated by the "Ordinary Kriging" approach (refer to discussion about types of available kriging in section 3.6). For a certain parameter, the estimated values Z^* at a location u are calculated as:

$$Z^*(u) - m(u) = \sum_{\alpha=1}^{n(u)} \lambda_\alpha(u)^* [Z(u_\alpha) - m(u_\alpha)] \qquad \text{Equation 4.10}$$

where $\lambda_\alpha(u)$ are weights, $m(u)$ is the assumed mean at location u, and $n(u)$ is the number of sampled (known) data points within the user-defined neighborhood of u, chosen so as to minimize the error variance:

$$\sigma_{\text{Error}}^2(u) = \text{Variance} [Z^*(u) - Z(u)] \qquad \text{Equation 4.11}$$

The choice for ordinary kriging (compared to other types shown in the example given in Figure 3.8) assumes that the local mean $m(u)$ isn't necessarily closely related to the population(overall) mean and so only uses the samples (known values) in the local neighborhood of the estimate. This approach accounts for local fluctuations of the mean by limiting the domain of stationarity of the mean to the local neighborhood level determined by the user. The mean $m(u')$ of the parameter is thus considered "constant, but unknown" for all locations in a single neighborhood area.

The remainder of this chapter will use the "shallow clay layer in Sacramento", with the S_u strength parameter, as an example. The same approach can be applied to any of the parameters in the other defined layers of the study areas. The following steps will demonstrate how to revise a spatially-based kriging (solely based on distance between

known points) into a revised kriged map that reflects correlation of soil parameters with regional factors in the riverine environment of the Sacramento river basin.

Geostatistical analysis was performed using the "ArcGIS Geostatistical Analyst" software extension. Figure 4.42 shows the empirical (or experimental) semi-variogram of known S_u values in the shallow clay layer of Sacramento with other Geostatistical model parameters.
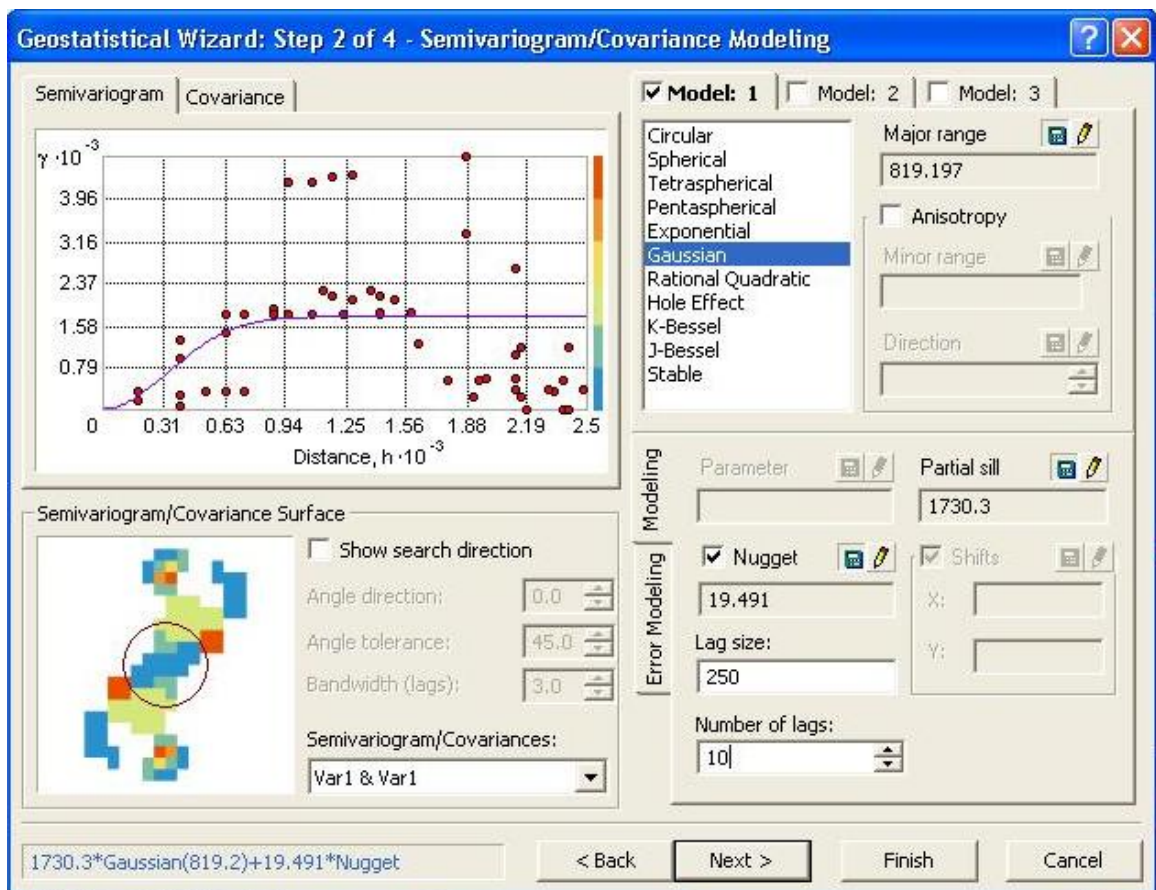
Figure 4.42 Screen shot of ArcGIS Geostatistical Analyst extension showing the ordinary kriging elements and experimental semi-variogram of known S_u values in shallow clay layer of Sacramento.

Outputs of the geostatistical analysis of the known sampled data points include cross-validation and error plots, as well as information pertaining to the main variables of interest at this stage: Nugget, range, and sill. Figure 4.43 summarizes the parameters of the kriging of the sample layer. The "**correlation range**" value in this case is roughly 819 meters, beyond which no spatial relation exists between points, i.e. a known sampled points do not affect measurements at another point situated at this, or a larger, distance.
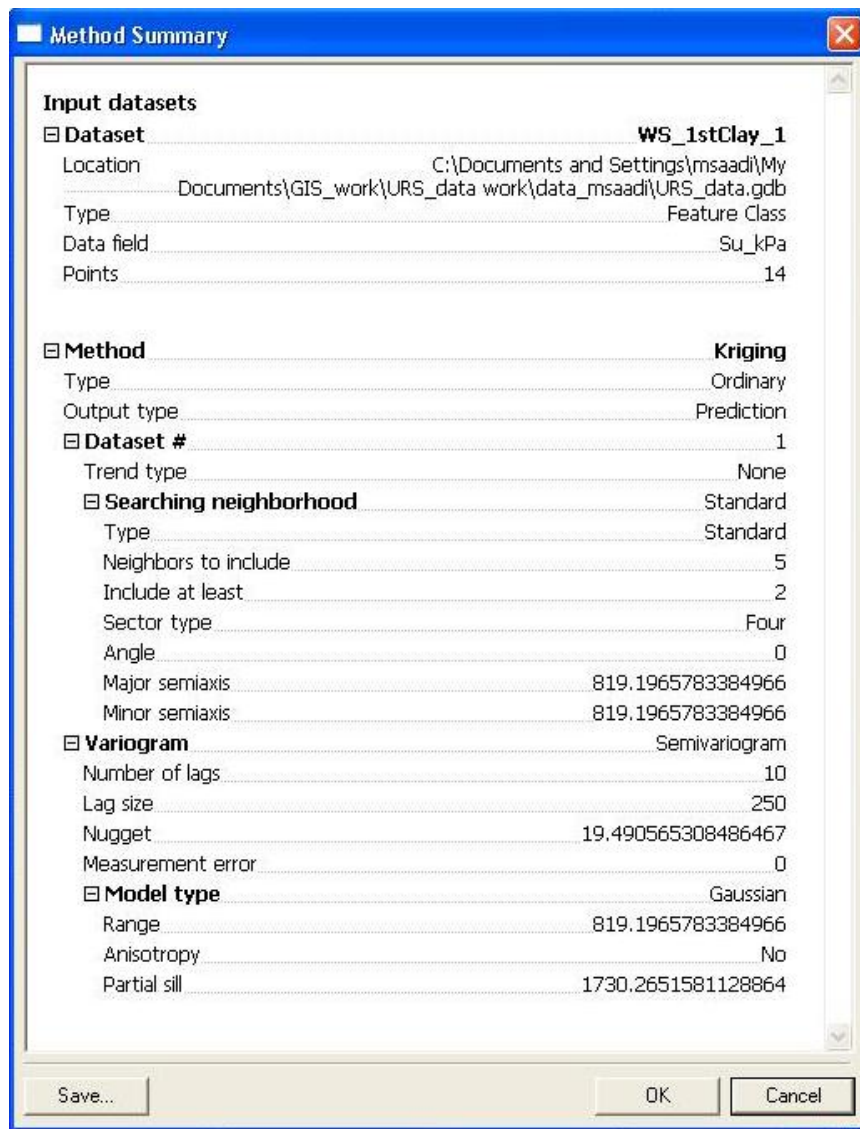
Figure 4.43 Screen shot of ArcGIS Geostatistical Analyst extension sample output/summary of the ordinary kriging method applied to the known S_u values in shallow clay layer of Sacramento.

A sample map output of the kriging approach for the estimation of the shear strength S_u of the shallow foundation clay layer in Sacramento is shown in Figure 4.44, with shaded color symbology representing variation of the estimated S_u values, classified as: Soft to Medium Clay ($S_u<50kPa$), Stiff Clay ($50kPa<S_u<100kPa$), Very Stiff Clay ($100kPa<S_u<150kPa$), and Hard Clay ($S_u>150kPa$).
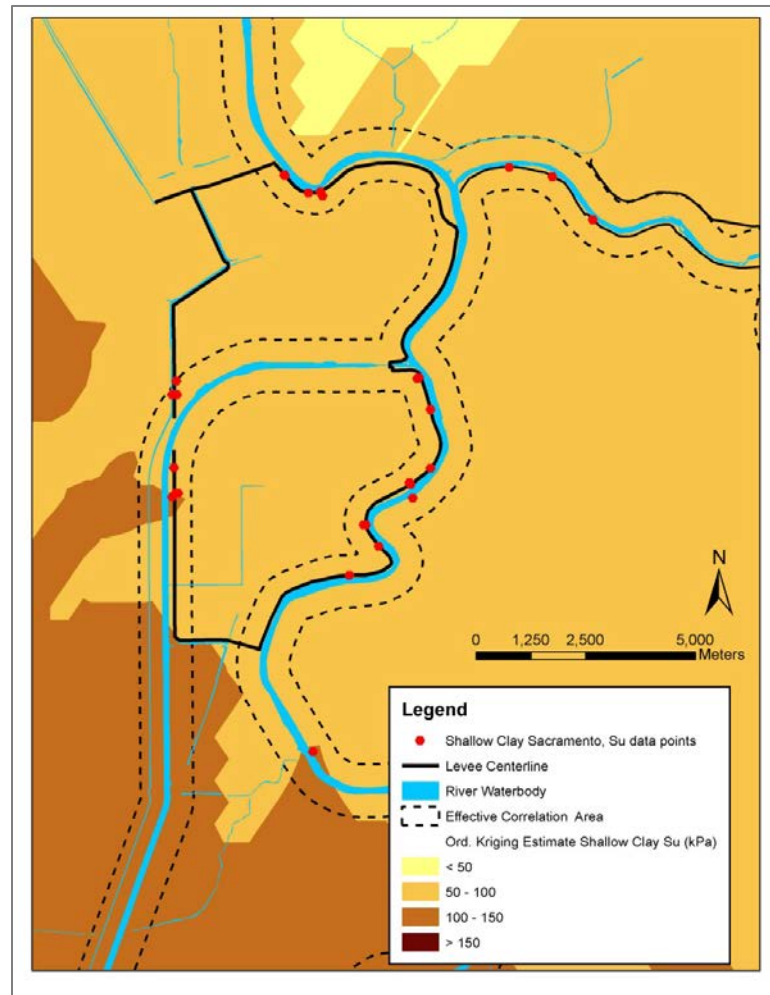
Figure 4.44 Sample output map of the ordinary kriging method applied for the S_u values in shallow clay layer of Sacramento.

The area between the dashed lines running parallel on both sides of the river represents the "Effective Correlation Distance" between the soil parameter and the

factors (refer to section 4.5.2 for definition). The focus/interest is to estimate the soil variability in within this distance from the river because (1) correlation of soil strength parameters with regional factors has been established with this limitation, and (2) this distance is far enough from the levee in a way that the soil parameter values beyond that will not affect the response levee fill.

Similar kriging estimate maps for all identified layers in the study areas are included in Appendix E, and corresponding semi-variograms for all identified layers are included in Appendix F. A summary of the range, nugget, and partial sill values from the semi-variograms is presented in Table 4.17. The "range" value for clay is almost twice as large as the value for most sands. This is consistent with the observation that the effective correlation distance for clays was also larger than that of sand by a similar margin

Table 4.17 Parameters from the ordinary kriging semi-variograms of identified soil layers in the study areas

Location	Depth	Material	Parameter	Unit	Correlation Range (m)	Nugget[a]	Partial Sill[a]
Sacramento City	shallow	Clay	S_u	kPa	819	19.5	1730
	shallow	Sand	ϕ	degrees	400	0.3	3
	deep	Clay	S_u	kPa	(see note b)		
	deep	Sand	ϕ	degrees	177[c]	1	17
Feather River	shallow	Clay	S_u	kPa	(see note b)		
	shallow	Sand	ϕ	degrees	407	1	11
	deep	Clay	S_u	kPa	(see note b)		

a: units of these elements is the "square of the corresponding parameter unit"

b: No Kriging estimate could be done due to limited number of data points available for the S_u (kPa) parameter of this layer

c: The low value of the range for the deep Sacramento river as compared to the other sand layers is due limited number of data points at large distances for this particular layer

4.5.6　Adjustment of Kriging Estimate using Regional Correlations

Within the effective correlation area, discussed in the previous section, a uniform grid of points is created. These are the locations at which the estimated kriging S_u values will be read, and adjusted as needed to reflect the correlations with regional factors. In the example shown in Figure 4.45 a sample 500mx500m grid size was chosen. The grid size has to be smaller than the "effective correlation distances" observed in section 4.5.2. In addition the grid has to be smaller or equal to the "range" values from the semi-variograms in the previous section.

The grid size can be adjusted as needed to be larger or smaller, depending on the estimate improvements that are reflected by doing that, and depending on the available computing resources. A larger grid size would not capture the correlations with the regional factors, nor will it capture the effect of spatial auto-correlation of individual soil parameters. One argument is that decreasing the grid size will give more "precise" estimations. However, it is not the intention to claim that 500m is the ideal distance between points, and a confirmation of the most effective grid size requires field validation of the estimated parameters.

Figure 4.46 represents a legend of the items mentioned in the model steps, namely the concept of "effective correlation area" and the grid of points used in the analysis.
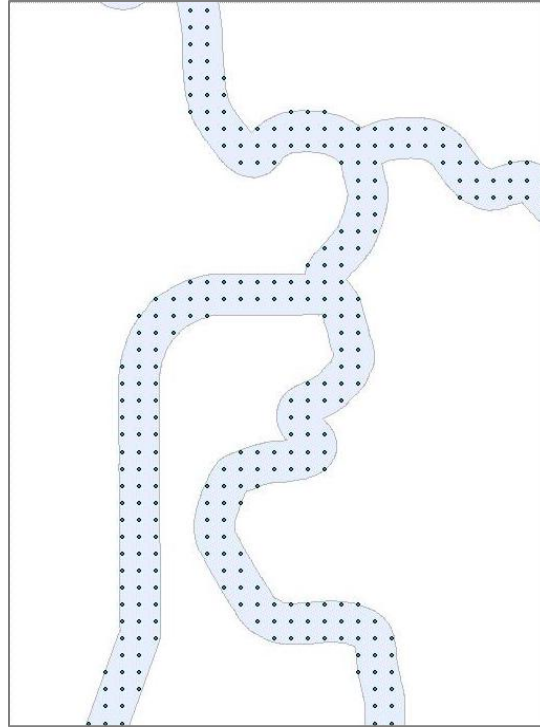
Figure 4.45 A sample 500mx500m grid of points within the effective correlation area around the river in Sacramento.
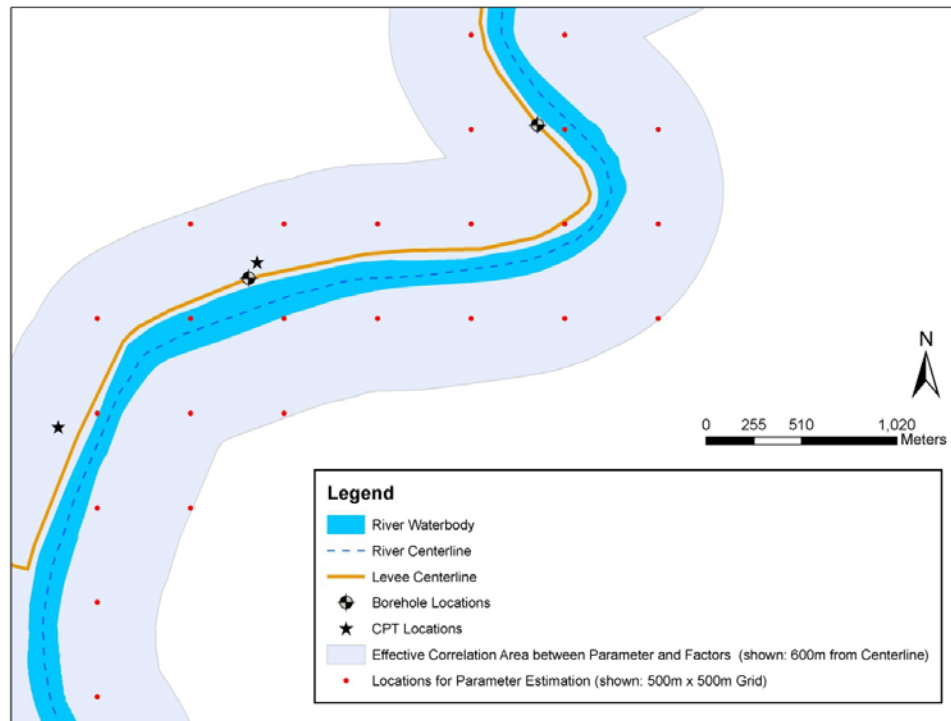
Figure 4.46 Legend of items mentioned in the proposed model steps.

Each location on the grid is assigned the attributes of:

- Experimental Kriging estimate value (Figure 4.44)

- Distance to closest segment of river (Figure 4.47)

- Geology layer (Figure 4.48)

- Sinuosity of closest segment of river (Figure 4.49)
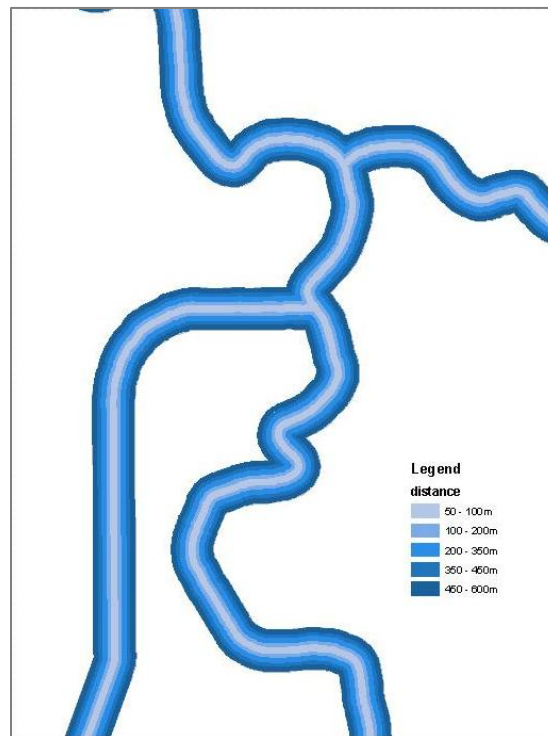
Figure 4.47 Map of the distance from river regional factor in the Sacramento Area.
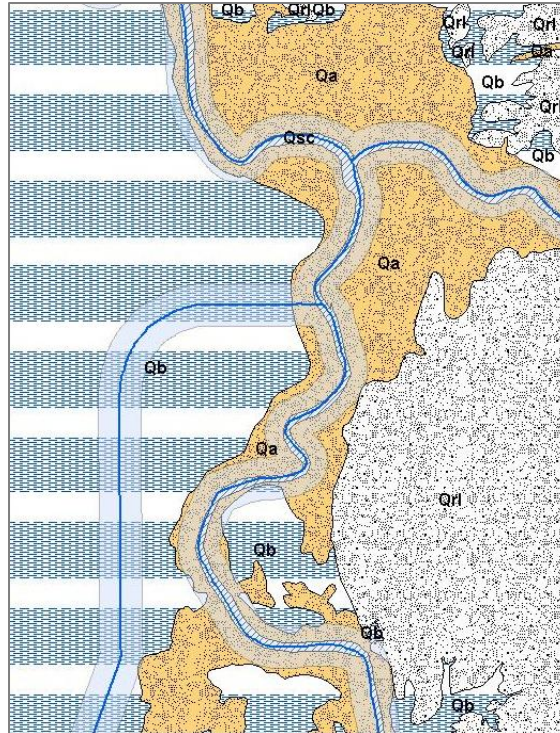
Figure 4.48 Map of the underlying geology regional factor in the Sacramento Area.
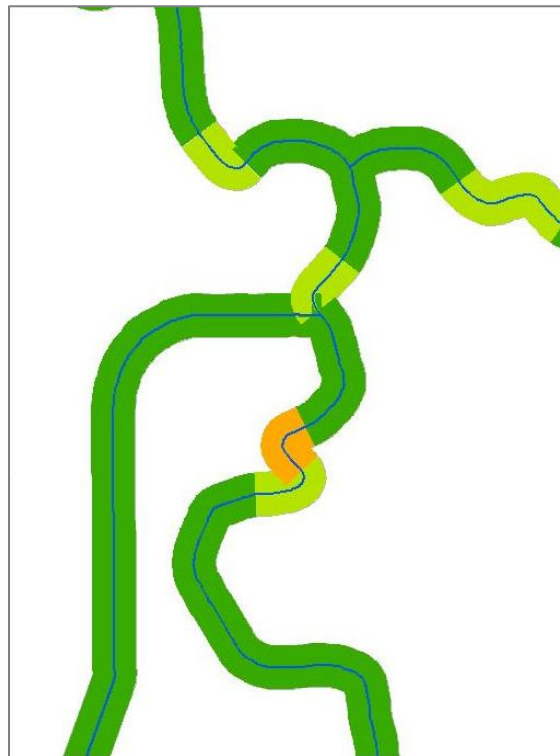
Figure 4.49 Map of the Sinuosity Index of closest river segment regional factor in the Sacramento Area.

To demonstrate the process of adjusting the kriging maps to reflect established correlations between soil strength parameters and any regional factor, a limited number of locations from the 500mx500m are used for simplicity (highlighted in blue in Figure 4.50). For example the corresponding values for location "A" highlighted in red are:

- S_u-kriging-estimate   =   72 kPa

- Distance from river   =   141 meters

- Geology   =   Qa

- Sinuosity Index   =   1.11   i.e. "sinuous"
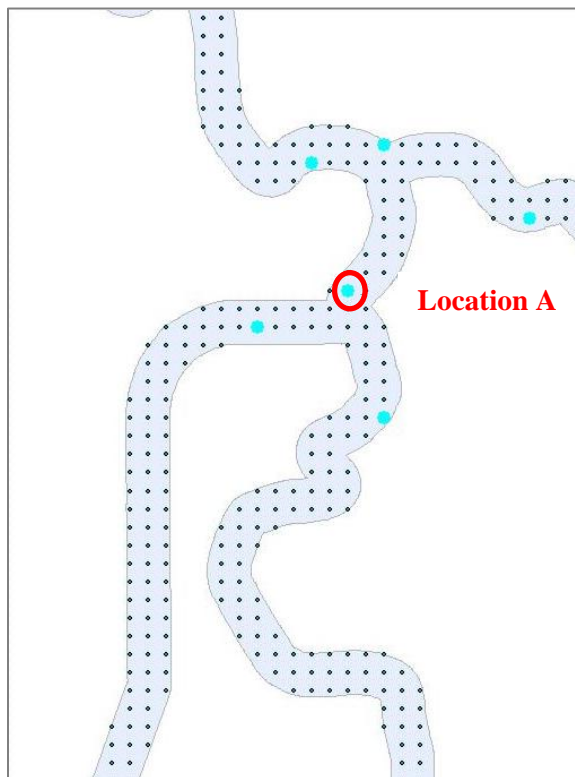
Figure 4.50 Selected number of locations, in blue, from the 500mx500m grid of points within the effective correlation area around the river in Sacramento.

The values read off the maps of both regional factor maps and experimental kriging estimate are reflected on the plots of shear strength parameter S_u vs. the corresponding factors (Figures 4.51, 4.52 and 4.53). The values for Location "A", shown in red in the said graphs fall very close to the median values expected through the best fit curves. Numerically, and for the regional factors associated with Location "A", the S_u values from the fit curve equation would be (compare to **S_u-kriging-estimate= 72kPa**):

- S_u vs. Distance curve → **mean S_u-dist = 71 kPa**

- S_u vs. Geology curve → **mean S_u-geo = 60 kPa**

- S_u vs. Sinuosity curve → **mean S_u-SI   = 65 kPa**
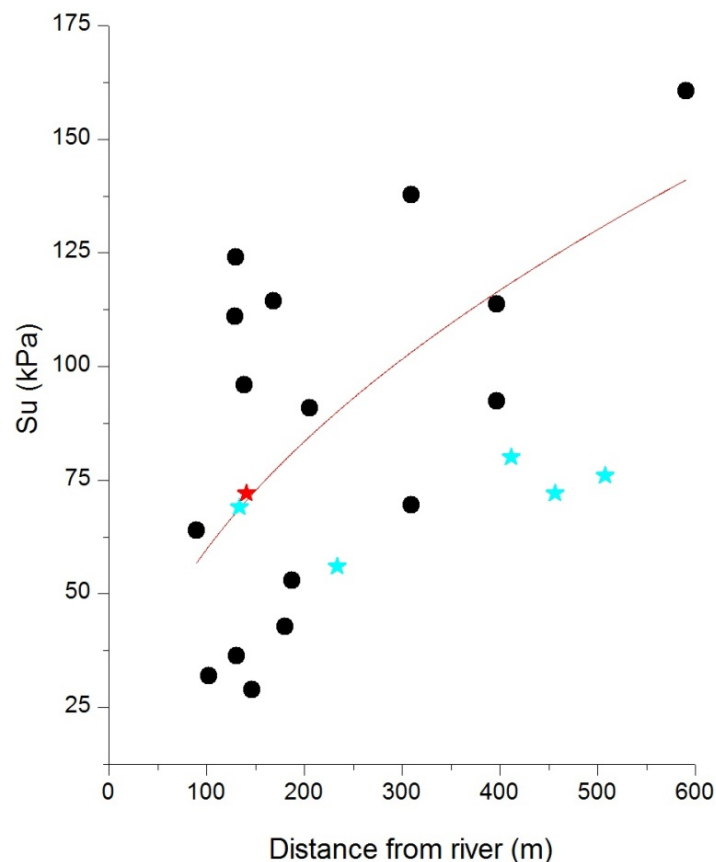
Figure 4.51 Values of the selected locations, shown with star symbols, from the 500mx500m grid, compared to the plot of S_u vs. distance from centerline of closest river segment (shallow clay layer in Sacramento).

130
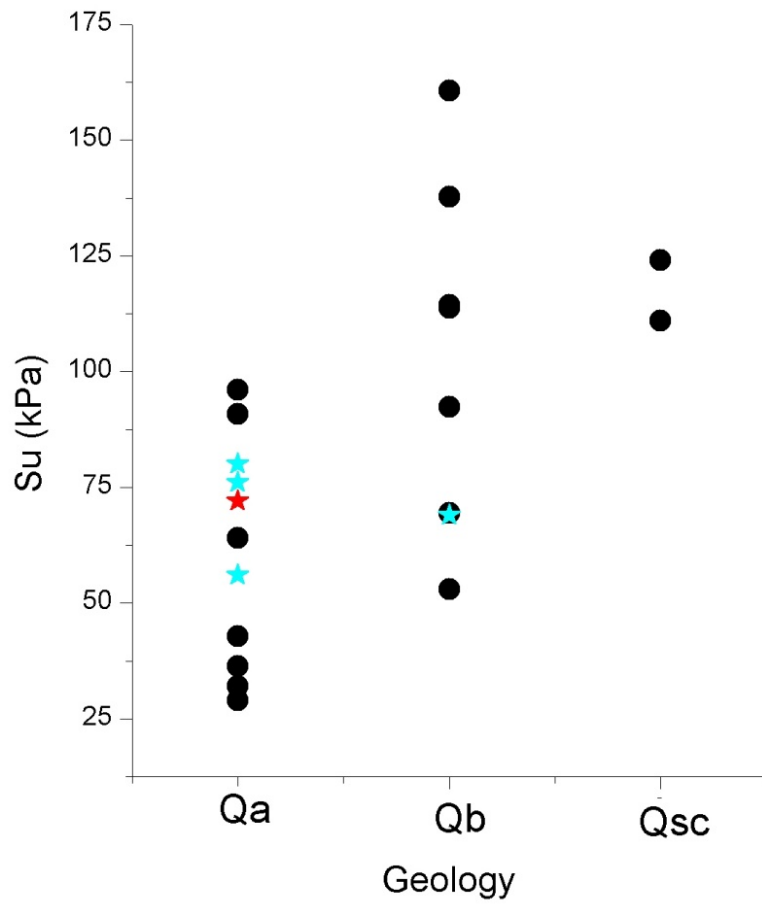
Figure 4.52 Values of the selected locations, shown with star symbols, from the 500mx500m grid, compared to the plot of S_u vs. geology (shallow clay layer in Sacramento).
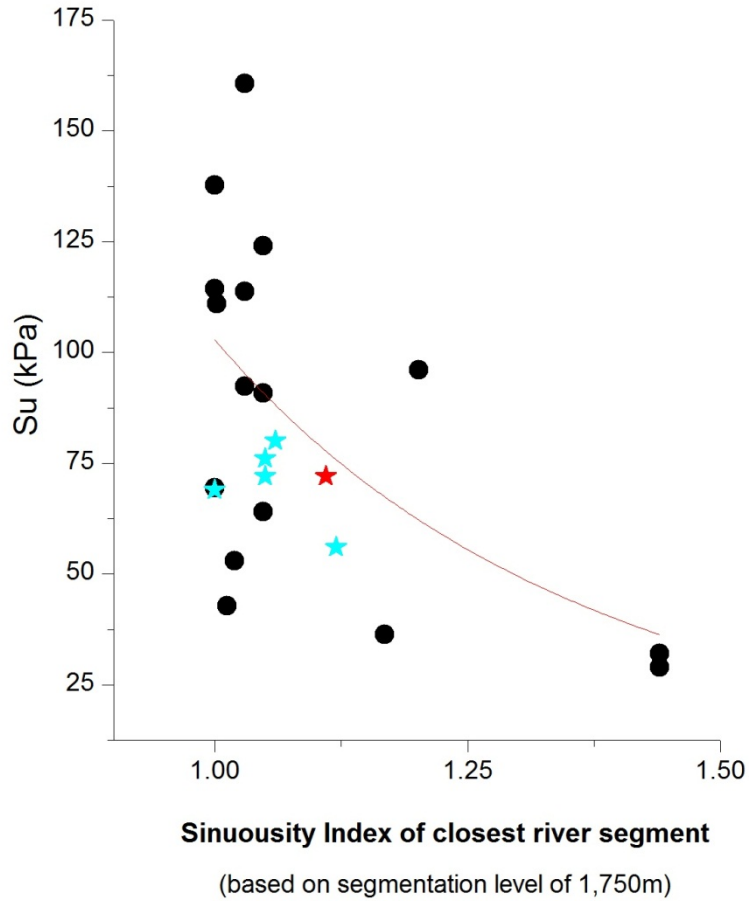
Figure 4.53 Values of the selected locations, shown with star symbols, from the 500mx500m grid, compared to the plot of S_u vs. Sinuosity Index (shallow clay layer in Sacramento).

The randomly selected locations for the above demonstration were a close match to the established correlation fit functions based on regional factors, in particular for Location "A", the differences with the fit curve <u>mean</u> values were minimal. Largest difference was in case of geology curve (72 kPa – 60 kPa = 12 kPa, i.e. 16% lower value than the kriged estimate), but even then the kriged value of 72kPa was within the range of plotted points that had a geology classification of **Qa**.

As a conclusion, the curve fits established between the soil strength parameters and the regional factors (section 4.5.2) serve as a check to the Ordinary Kriging estimation method. Any location from the grid of points that exhibits values falling away from these established trends, will have its S_u-kriging-estimate value revised in order to fall within an acceptable confidence level, i.e. a defined number of standard deviations, from the value at the best fit curve. Standard error /deviation can be defined for any distribution with finite first two moments, but it is most common to assume that the underlying distribution is normal. For example, to be within the 95% confidence interval, the kriging estimate value would need to be revised to fall within approximately "plus or minus 2 standard errors", i.e. plus or minus 2 times the root-mean-squared error, from the point of forecast (fit curve value).

Once updates are made to all values that need adjustment, the kriging estimation map is recalculated, taking into account those updated values at the relevant grid point locations. The revised kriged map at the end of the modeling process is itself a continuous spatial distribution of the soil parameter estimates, i.e. it is not a grid, and as such the value of the adjusted estimated parameter is read from any location within the effective correlation area on the map.

CHAPTER 5

A GIS-enabled Approach to Seismic Risk Assessment of Levees

5.1   Introduction

A key factor for risk assessment is the complex and efficient management of various types of information that affect the assessment. In addition, the best method for natural hazard risk management of geographically spatially distributed systems, such as the seismic response of levee systems, is probably the use of Geographic Information Systems (Frost et al. 1992). Recent advancement in GIS software tools, computing speed, and hardware capabilities allow the undertaking of such an approach. In addition to their basic and interactive mapping features, GIS tools are useful in their capability of referencing information to geographic locations, performing various spatial analysis and correlation functions, providing a user-friendly customizable interface and an integrated database management system.

5.2   The Use of Geographic Information Systems

5.2.1   Introduction

The development and use of information technology (IT) in civil engineering has had both successes and failures in the past; however, recent efforts have focused on improving the adapting of ideas and technologies across the profession as well as in the engineering education curriculum (Garrett et al. 2004; Arciszewski 2006; ASCE 2006).

Respondents to a survey report prepared for the Construction Industry Institute (Vorster and Lucko 2002) indicated that the industry is seriously lagging behind others for a variety of reasons, and that barriers frequently prevent the use, implementation, and adoption of new and existing technologies. Examples of such barriers include the wish to "do it the tried and tested way" and a lack of "technology savvy" workforce (Vorster and Lucko 2002). The report also indicated that the most important attribute for success of a new technology are demonstrable and positive benefit to cost ratio. Additional barriers to Information Technology (IT) adoption in civil engineering include low level of perceived benefits from IT investments among decision makers, and the lack of examples demonstrating its successful use by others (Anumba 1998; Andresen et al. 2000).

A research project to develop and adapt an information technology tool should have a goal of helping the ultimate user in making informed decisions. The actual challenge is not only being able to acquire or provide the needed information in an efficient manner, but most importantly to make sure it is being properly used for the above mentioned goal, and in a manner that takes into consideration the end-user needs and expectations.

Geographic Information Systems (GIS) are a computer based system and set of tools that allow the user to work with spatial data. More than merely simple mapping tool, GIS are an integrated spatial and a-spatial information database, with specific capabilities for spatially referenced data, as well as commands designed to work with multiple map layers and advanced data querying and presentation capabilities. GIS

135

software is capable of assembling, storing, manipulating, and displaying geographically referenced information efficiently. It can also be used to create integrated databases on complex indicators (e.g. hydrologic, geologic, socio-economic, etc) to use for example in modeling disaster related indices reflecting vulnerability of certain areas. Benefits of GIS thus include providing an excellent method of receiving and storing large amounts of data, allowing the retrieval and manipulation of data for further analysis, and delivering the results as maps, overlays, tables, or graphs. Additional GIS definitions and description of capabilities are available in the literature (e.g. Player 2004; Capilleri and Maugeri 2008), however a complete list is beyond the scope of this report.

The key components of a GIS are:

- Relational Database (link, query, add, delete, etc)

- Graphic Interface (represent data in either raster of vector format, or a combination)

- Data Manipulation and Analysis Environment (interpolation, querying, etc)

Current GIS software provides, as a minimum, the following capabilities:

- Data entry from a variety of sources

- Data management and attribute/feature editing

- Coordinate system manipulations

- Symbolizing features and map layer controls

- Display capabilities and layering

- Data analysis functions for identifying and checking spatial relationships

- Export capabilities and layout functions for creating maps

Available GIS software has the following benefits in particular for civil engineering information technology applications:

- High-quality maps

- Advanced specialized tools (e.g. geostatistical analysis for soil properties)

- Read/write with other format file (e.g. AutoCAD)

- Numerous third party applications available (e.g. ArcHydro for water resources)

- Internet enabled capabilities to share and allow access to data

- Customizable with programming languages such as Visual Basic, C++, or C#

The most widely used GIS software in the market is ArcGIS Desktop application by ESRI (2011). It contains specific useful tools and extensions for functions related for example to hydrology and terrain modelling. ArcGIS can be customized and extended with VBA programming macros, as well as an embedded Model Builder. In addition, the software developer, ESRI, provides many resources, codes and examples (mainly in C# and VB.net programming languages), and a number of online courses (Introduction to Programming ArcObjects with VBA, Extending the ArcGIS Desktop Application, ArcGIS Desktop Developer Guide, etc). The ArcGIS software application is built on ArcObjects which are a set of 2,700+ COM compliant (interface) object-oriented classes with a detailed hierarchy. A set of .dll library files (dynamic link libraries) and detailed ArcObjects model diagrams are also provided with the software for programming purposes. Furthermore, ArcGIS Engine is an available program that allows users to build

their own ArcGIS –based "standalone" application that can be made available for distribution.

5.2.2   GIS and Geotechnical Engineering

A key factor in the success in civil engineering endeavors is the efficient management of various type of information. As previously mentioned, GIS can help in this aspect because of its capability of referencing information to geographic locations. However, the full potential of GIS applications in Civil Engineering has not yet been realized and an ample need exists to develop innovative GIS solutions to more-complex engineering problems (Venigalla and Casey 2006).

Transportation projects particularly need effective geotechnical site investigations because of the significant investments of private and public funds, their long design lives, and impacts on the public. Player (2004) presented case study applications where GIS was used to manage geotechnical site investigation data contributing to the design of transportation projects. The result was an early identification of geotechnical barriers that could cause cost and time consuming changes to a design (excessively weak soils, compressible soils, unstable slopes, etc).

Several studies focused on modeling geospatial and time-related data. One example is an approach for slope-inclinometer displacement data and stability analysis by Lan & Martin (2007) by integrating ArcGIS and numerical modeling of a shallow subsurface slide. The GIS tools had limitations in representing time series data such as the displacement data from inclinometer or pore pressures from piezometers, and thus

additional functional tools were required and implemented. Results were exported to a modeling package to develop a comprehensive ground model for the site.

The use of GIS in slope stability monitoring and analysis was presented by Hutchinson et al. (2007). The work identified progressive zonation of movement within a slope and simulated variable movement across and within the slope mass. The work presents an integrated approach to landslide hazard monitoring, prediction, and simulation. The data interpretation process necessitated a combination of a geotechnical sensor data network, a numerical process simulation related to probable failure modes, a digital library of case histories, and a GIS-based Geotechnical Decision Support System.

Finally, the implementation of GIS applications in the actual geotechnical engineering practice has been also investigated. Hellawell (2001) presented such cases in small-scale actual projects of consultancy firms in the United Kingdom. The study showed that GIS-based analysis of geotechnical problems is a powerful and competitive approach for companies, and is easily learned by engineers and technicians, since engineers are familiar with CAD drawings, databases, spreadsheets, and data interpolation and extrapolation. However, heavy investment needed in data collection was not considered in the studied cases.

Studies about implementation of GIS in the industry show that it is mainly used for data capture and visualization, but its data analysis capability is under-utilized. A list of Pros and Cons for the use of GIS in geotechnical projects can be deduced as follows:

Pros:

- Introduction of new analysis techniques increases Client satisfaction

- Storing and accessibility to large amount of data

- Automation of manual task helps save man-hours

- Multi-disciplinary interaction and improved collaboration among parties involved

Cons:

- Data quality, format, and accuracy (e.g. geo-referencing data with design maps, compatibility of data with GIS format, etc)

- Quality control is challenging: data checking and tracking, what changes were made? by who? when? etc

- Need to create log files to track assumptions and decisions

- Confusing intermediate files and outputs

- Cost of development, training, and Quality control

- Expectations keep getting higher and increased demands as people see the benefits

5.2.3 GIS and Disaster Management

A disaster is defined as an event, occurring with or without warning, that causes serious disruption to the functioning of a community or a society; it is able to cause death, injury or disease, damage to property, economic or environmental losses which exceed the ability of the affected community or society to cope using its own resources (DKKV 2002). As such, almost all of the research in disaster analysis, mitigation, and

management defines it in terms of human sensitivity towards natural or man-made hazards. The vulnerability of people to a disaster is closely related to the extent that their life might be disrupted by it.

One of the earliest instances of utilizing a basic manual form of modern computerized GIS in an instance of disaster management/response was by John Snow (1855). In his book, Snow describes the *grand experiment of 1854*, which was a natural study of the association between water exposure and cholera. Snow recognized that allocation and near-randomization had taken place in a natural setting, and took advantage of this historical occurrence to analyze the data and derive important conclusions for the eventual control of cholera by locating the water companies that provided the exposure (Figure 5.1).
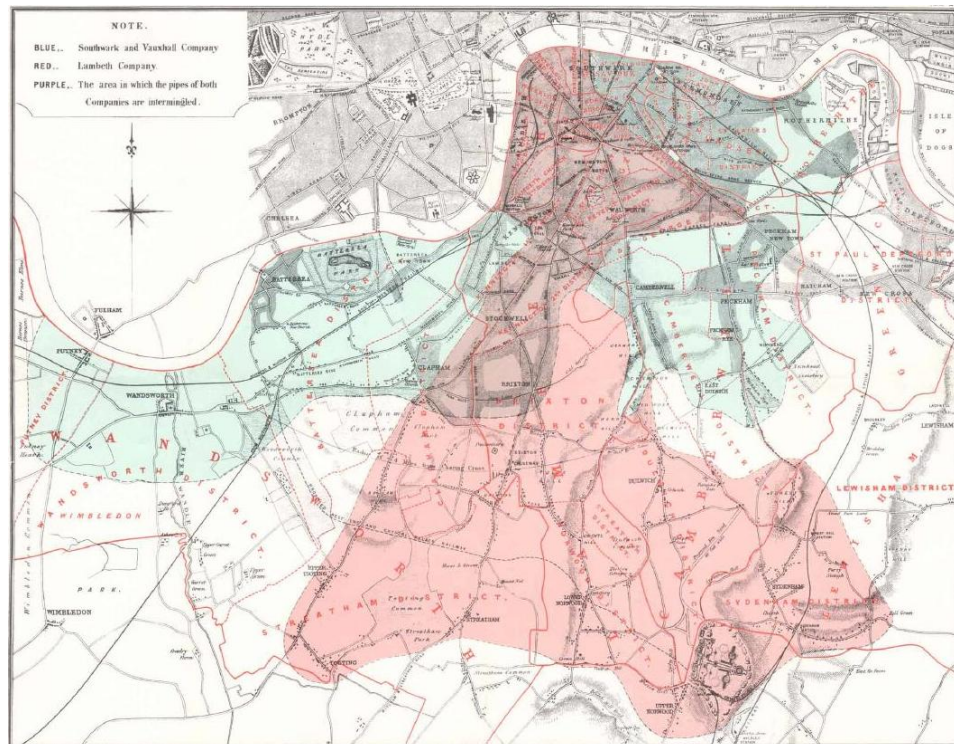
Figure 5.1 The "Grand Experiment" map of cholera outbreak analysis (Snow 1855).

Disasters can be classified into three categories: natural, man-made, and hybrid disasters. The latter is a mix of physical factors (e.g. intense rainfall over a short period) and socio-economic factors (e.g. population growth, poor living conditions, absence of green space in cities). And although each event has different impact and characteristics, all disasters share one aspect: their severity. In addition, Rudolf Enz, one of the authors of a recent study on natural catastrophes and man-made disasters (Swiss Re 2008), states that in countries with less financial resources, a catastrophic event can result in higher deficits and debt for the public sector, which not only shoulders the cost of relief efforts, but is also responsible for rebuilding public infrastructure. In Turkey, for example, an earthquake in 1999 caused an economic loss of 11 per cent of GDP. In 1986, an earthquake in El Salvador cost as much as 37 per cent of GDP.

Research on combining the use of GIS with the risk and uncertainty management of disasters started received significant attention in the 1990s (Newkirk 1993; Rejeski 1993; Coppock 1995; Davis and Keller 1997) and continues till today. Examples of applications of GIS in disaster management abound. An example is work by Abbas et al. (2009) which presents an overview of disasters and the vulnerability of human society to such events. The study contains a number of statistics about disaster costs worldwide and includes a case study for GIS-Based Disaster Management in a sub-district of India.

5.2.4   GIS and Seismic Risk Assessment

GIS has been used in a number of research projects and case studies related to earthquake engineering risk assessment. Researchers are able to plot fairly accurate

figures of the likely impact and losses due to any given seismic event. Other GIS analysis capabilities are then used to best understand this information.

Combining probabilistic risk assessment with GIS software provides new opportunities and strategies to civilian agencies for improve risk management and thus protect national assets and interests. Building models to do such an assessment involves a sequence of interrelated steps as follows (Roy 2008):

1. Hazard Module: Defines frequency and severity of a peril at a location using hazard parameters, attenuation/degradation to site, and amplification/reduction at site.

2. Exposure Module: Generates an inventory of assets at risk in the study area.

3. Vulnerability Module: Quantifies potential damage caused to each asset due to an event.

4. Damage Module: Translates the potential damage from individual assets into overall cost amounts.

5. Loss Module: Quantifies potential losses as a result of adverse events in terms of Average Annual Loss, Loss-Exceedence Probabilities, Probable Maximum Loss, etc.

McGaughey et al. (2007) presented an integrated, real-time, 3D GIS-based geotechnical hazard assessment approach applicable to underground and open-pit mines, tunnels, dams, slopes, and general seismic risk evaluation. The application accepts a wide

range of real-time data inputs to compute and display a user-defined hazard index on a geotechnical model of a mine, using observations, micro-seismicity, excavation geometry, stress, geological structure, and rock type.

The extent and type of damage caused by earthquake can also be mapped and analyzed using GIS. King (1997) talked about the integration of earthquake hazards to built structures using a comparison of damage measures between three regional earthquake damage and loss estimation methodologies. The use of GIS was mainly as a mapping tool to compare three methods' outputs, which facilitated drawing the conclusion that estimated building damage due to ground shaking is nearly the same using all methodologies, but that there is a significant impact on the estimation of total damage depending on choice of each of the three methodologies.

A research project by Wilding (2008) developed a GIS methodology to be used as a "screening tool" to evaluate geotechnical earthquake engineering hazards from a database of borehole data. The methodology was customized within the GIS environment to calculate both the liquefaction potential and a ground motion magnification factor from borehole data and ground motion time histories. The project only provides output at select point locations, and does not provide an assessment at areas with no borehole information. Furthermore, the analysis is performed for the site surface in a 1D manner, with no regard to surface structures such as levees.

An example of an actual case study and evaluation of the seismic hazard using a GIS approach was done for the city of Sellano-Italy by Capilleri & Maugeri (2008). The aim was to create micro-zonation maps of seismic hazard, which was achieved by combined geological maps, borehole location map (including field and lab test results), and actual recorded seismic event ground motions. The case study analysis used 1-D & 2-D numerical analysis to investigate role of stratigraphy on the amplification of seismic motion. The resulting output included identification and demarcation of areas of homogenous response, as well as mapping of recorded actual damage resulting from historic seismic activity.

More recently, work done by Chung and Rogers (2011) on the spatial prediction of groundwater depth to trigger liquefaction in St. Louis has used ordinary kriging and produced GIS based prediction maps estimating the threshold depths-to-groundwater contour. These contour maps were in turn used in an attempt to overcome the data uncertainty associated with estimation of saturation levels of different stratigraphic units for liquefaction potential assessment.

5.2.5   GIS and Levees

The direct application of GIS in studies and projects involving levees has mainly been limited to mapping and simulating the flooded areas, as well as using GIS as a database for soil investigation locations, data, and maintenance records.

GIS as a tool can assist floodplain managers in identifying flood prone areas in their community, and implementing mitigation or management practices. An example of flood simulation application is work by Yamaguchi et al. (2007) who developed a GIS-based flood-simulation software, due to failures at river levees, that can be applied to risk assessment in adjacent floodplains. The software provides an easy-to-use user interface, assesses flooding risk based on flow from failed levee sections on rivers surrounding a specific area or facility, and rapidly and accurately simulates flood scenarios (e.g. a particular failed levee section will flood the protected area with 15cms of water in 10 minutes, up to 50cms in 1 hour, etc). However, the cause of flooding in this study is because water overtops the river due to tide levels at the river mouths, or extensive rainfall. No analysis is performed to address structural failure.

A "Spatial Decision Support System to Optimize Inspection, Maintenance, and Reparation Operations of River Levees" was developed by Serre et al. (2006) and was applied on a limited section of levees in France. The work involved developing a GIS/MsAccess software with integrated models set up to assess levee performances. The input was from field observation cards filled by levee guards who were the main data providers. Dynamic segmentation capabilities of ArcGIS were used to manage, analyze, and represent punctual and linear levee information.

The above mentioned software deals more with "observable" problems in levees, such as for example hydraulic structure defective behavior. An observer notices the defect, notes the position using GPS, characterizes the defect using a pre-established list,

and photographs the disorder. In addition, the software has a performance multi-criteria assessment model which consists of a set of indicators/criteria combined in a function to give a Performance Indicator for each type of failure mechanism. Examples of types of criteria are: roots in impervious shoulder, scour, pipe going through levee, roots in body of levee, potential seepage, etc. The software only maps levee weak points in order to optimize maintenance work and enhance safety. However, it does not take into consideration the seismic hazard response of levees and is dependent on field observation of indicators of problems.

Finally, the Department of Homeland Security's Federal Emergency Management Agency (FEMA) has developed HAZUS-MH (acronym for Hazards U.S.-Multi-hazard); a powerful risk assessment methodology for analyzing potential losses from floods, hurricane winds and earthquakes. In HAZUS-MH, current scientific and engineering knowledge is coupled with the latest geographic information systems (GIS) technology to produce estimates of hazard-related damage before, or after, a disaster occurs. The GIS-based environment allows users to create graphics to help communities visualize and understand their hazard risks and possible solutions (FEMA 2009). However, the flooding scenarios in HAZUS-MH are a result of river water level variation and river bank and levee overtopping. Furthermore, earthquake losses do not include failure of levees, and thus do not reflect potential flooding due to such types of seismically-induced failures.

5.3   Proposed Approach to Risk Assessment of Levees

A GIS-enabled approach for the seismic risk assessment of levees systems is proposed. The approach uses as input available levee geometry and soil parameter data at finite locations, correlates the soil parameters to other factors in the area, provides an estimation of the parameters in unsampled locations, analyzes the response of the levee structure in all the segments, and generates as output an overall flooding risk measure that can be weighted by socio-economic factors in the protected areas. Saadi and Athanasopoulos-Zekkos (2010) presented a simplified version of the proposed approach offering a first-order estimate of the spatial vulnerability of a levee system, with efficient visualization of the results enabling decision makers to quickly identify critical regions.

The five main components of the framework, shown in Figure 5.2 and schematically reflected in Figure 5.3, can be summarized as follows:

Step 1 Geostatistical Model for Soil Variability: Collect and process available soil data and levee geometry and perform a geostatistical analysis to determine correlations of soil properties to other attributes in the region.

Step 2 Response of Levee Segments: Evaluate the response of levee segments between finite locations using spatial soil properties correlation models, and identify potential failure areas

Step 3 Flood Scenarios: Simulate the flood scenarios for each identified failure potential based on digital elevation models, terrain analysis, and surface hydrology

Step 4 Damage Forecasting in Protected Areas: Forecast damage from the flood

scenario including socio-economical attributes of the region of interest (i.e.

population density, land use zoning, etc)

Step 5 Risk Assessment: Assess individual segment and overall levee system risk

measure as a function of response analysis and resulting damage estimation

by developing fragility curves for a range of ground motion intensities

A GIS software application is the platform for data manipulation and processing,

as well as output representation for the above steps.
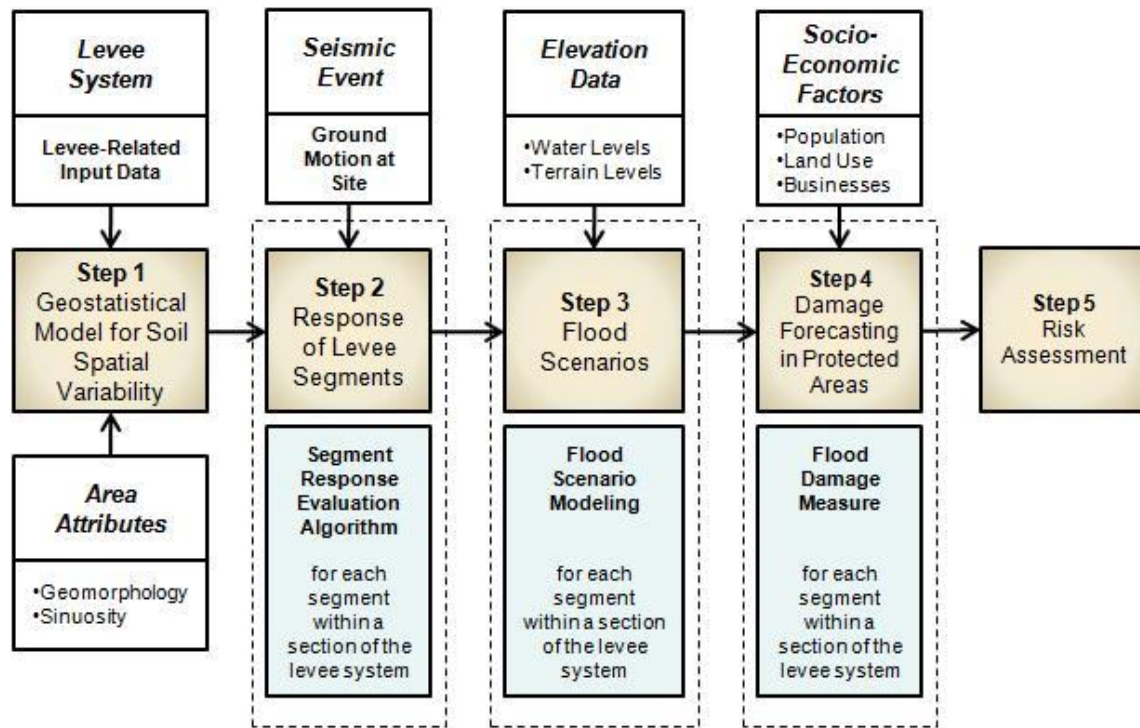
Figure 5.2 Steps in the process of seismic risk assessment of levee systems.
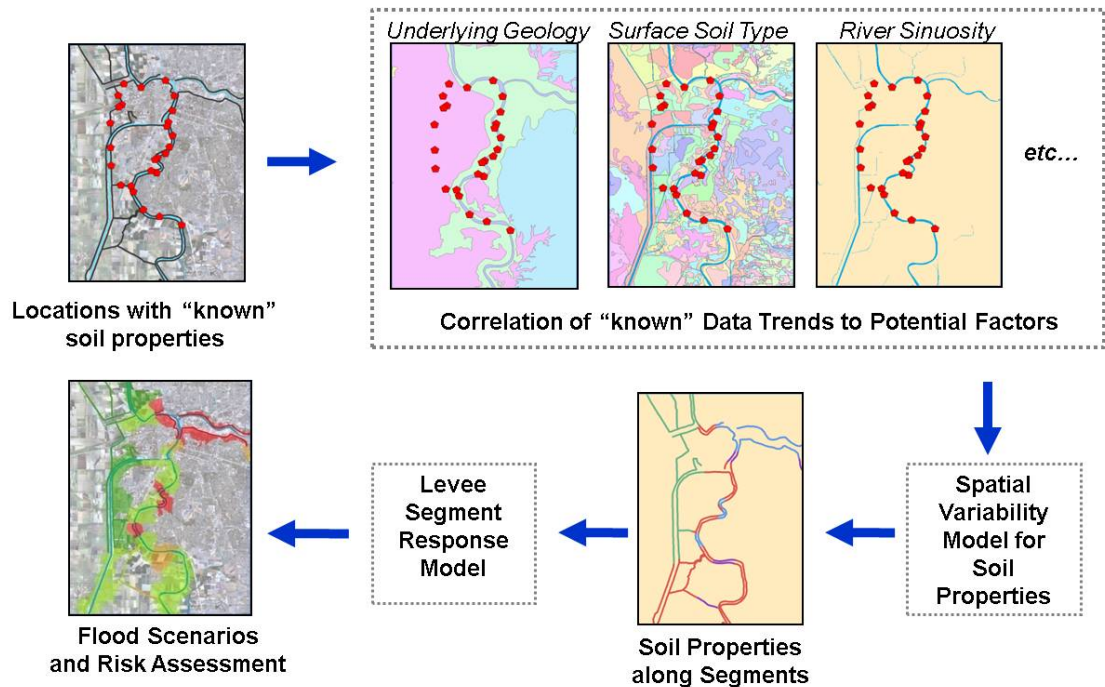
Figure 5.3 A Schematic of the proposed GIS-enabled framework leading to the seismic risk assessment of the levee system.

As previously mentioned, and as a prerequisite step to evaluating seismic response of levee systems, a characterization of the spatial variability of soil parameters throughout the study area is needed. Since soil stratigraphy and properties are only available at limited locations, a geostatistical model (detailed in Chapter 4) is developed for predicting spatial variability of soil properties in the area of interest, with specific data regarding soil stratigraphy, underlying geology, soil properties and geographic coordinates collected from a characteristic levee system (Sacramento River Flood Control System). An analysis of this data was performed to find the correlation between the measured data trends and relevant factors (i.e. river sinuosity, elevation, geology etc), and using the best suitable kriging method, the result is a spatial pattern estimation method that can be replicated over other large areas in riverine and deltaic geologic

environments. Step 1, which reflects the main objective of this dissertation project, was developed and presented in chapter 4.

Although the detailed analysis of the seismic response of levees and the resulting risk assessment is beyond the scope of this research project, simplified steps for modeling system response and flood scenarios (steps 2 to 5) are presented in chapter 6 to demonstrate that the proposed methodology is a feasible application. The last part of the proposed framework involves assigning a seismic risk measure along the levee reach of interest. More specifically, the main seismic modes of failure of levees that can be potentially considered in the response analysis of Step 2 are loss of freeboard due to (a) - soil liquefaction or (b) seismically induced permanent displacements. As detailed in Chapter 6, existing pre-established typical levee cross-section analysis (Athanasopoulos-Zekkos 2008) can be used to (1) characterize the levee at each location as one of many typical levee cross-section profiles, (2) input the specific geometric characteristics and soil parameter values specific to the levee and foundation layers at that location, and (3) evaluate the distribution of the Cyclic Stress Ratio (CSR) - a measure for probability of triggering of liquefaction- for the levee cross-sections, and (4) estimate seismically induced displacements for prescribed sliding surfaces.

CHAPTER 6

Modelling System Response and Flood Scenarios

6.1   Introduction

This chapter presents Steps 2 and 3 of the approach proposed in Chapter 5 (Figure 5.2). These steps relate to modeling levee system response and flood scenarios as a demonstration that the proposed methodology is a feasible application in practical purposes. A proposed method for ground motion selection for site-specific seismic response analysis is also included. Finally, an overview of Steps 4 and 5 regarding damage forecasting and risk assessment is presented to show how these steps can be implemented in future research work.

6.2   Response of Levee Segments

To assess the seismic vulnerability of earthen levee systems, the uncertainty in the dynamic response and performance of levees needs to be addressed. This response is heavily dependent on the uncertainty of the levee geometry, the properties of the levee materials and the foundation soils, as well as the seismic event itself (Athanasopoulos-Zekkos 2010). The assessment of the uncertainty of the seismic events can be performed by both deterministic as well as probabilistic methods (Abrahamson and Shedlock 1997). One way to approach the uncertainty in seismic events (rate of occurrence, location, magnitude, site conditions, etc) is through the use of the USGS's United States National

Seismic Hazard Maps, providing horizontal acceleration values with probabilities of exceedance. Another approach is the use of a site-specific Probabilistic Seismic Hazard Assessment (PSHA). PSHA is a standard practice in the earthquake engineering community (McGuire 2004), and allows for explicit considerations of uncertainties emanating from the interpretation of components of the hazard model (source characterization, ground motion estimation, etc)

Taking all the uncertainties of ground motions, soil properties, and levee geometry into consideration, the main modes of failure of levees in dynamic response analysis are loss of freeboard due to (a) soil liquefaction or (b) seismically induced permanent displacements. Triggering of soil liquefaction is defined based on the induced Cyclic Stress Ratio (CSR) compared to the Cyclic Resistance Ratio (CRR) of the soil materials; while permanent, deviatoric-type seismic displacements can be computed using a Newmark-type approach for prescribed sliding surfaces (Athanasopoulos-Zekkos 2008).

In this thesis, the dynamic response analysis for levee loss of freeboard due to soil liquefaction relies on pre-established typical levee cross-section analysis (Athanasopoulos-Zekkos 2008) that used a 2D finite element (QUAD4M) equivalent linear program (Hudson et al. 1994) with a wide range of ground motions to determine the median and standard deviations of Cyclic Stress Ratio (CSR) and seismically induced displacements. The above mentioned analysis relies on:

1) Characterizing the levee at each location as one of three typical levee cross-section profiles (Figure 6.1)

2) Inputting the specific geometric characteristics and soil parameter values specific to the levee and foundation layers at that location

3) Evaluating:

   a. the distribution of the CSR - a measure for probability of triggering of liquefaction- for the levee cross-sections (Figures 6.2 and 6.3), or

   b. the seismically induced displacements for prescribed sliding surfaces (Figure 6.4)
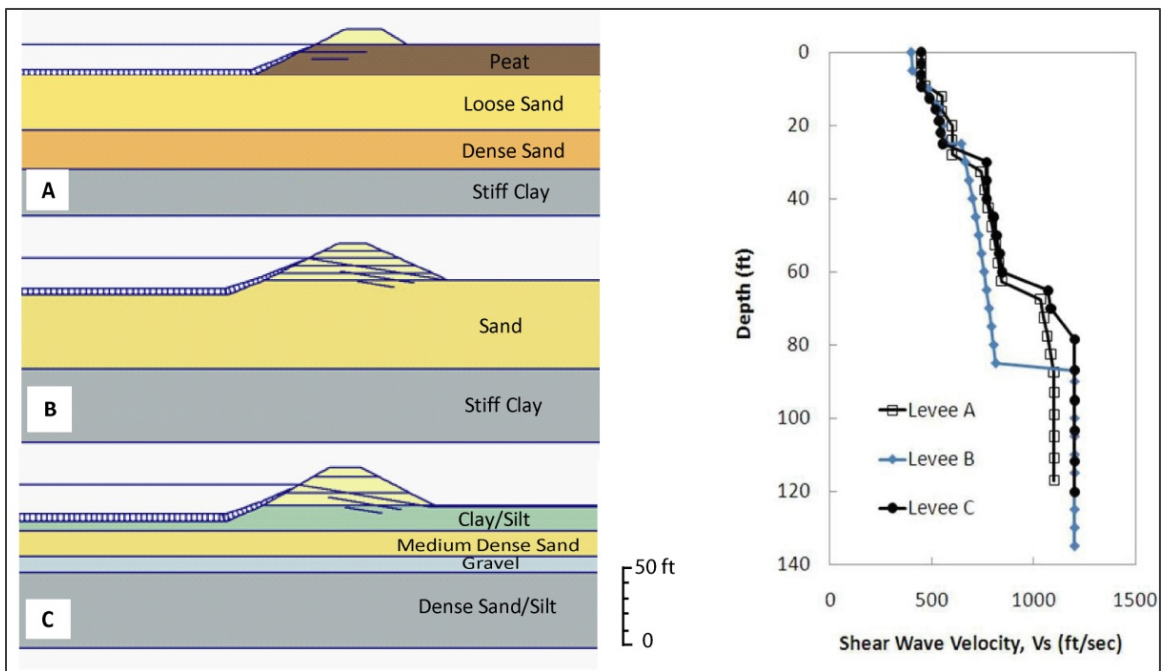
Figure 6.1 Pre-established typical levee cross-sections (Athanasopoulos-Zekkos 2008).
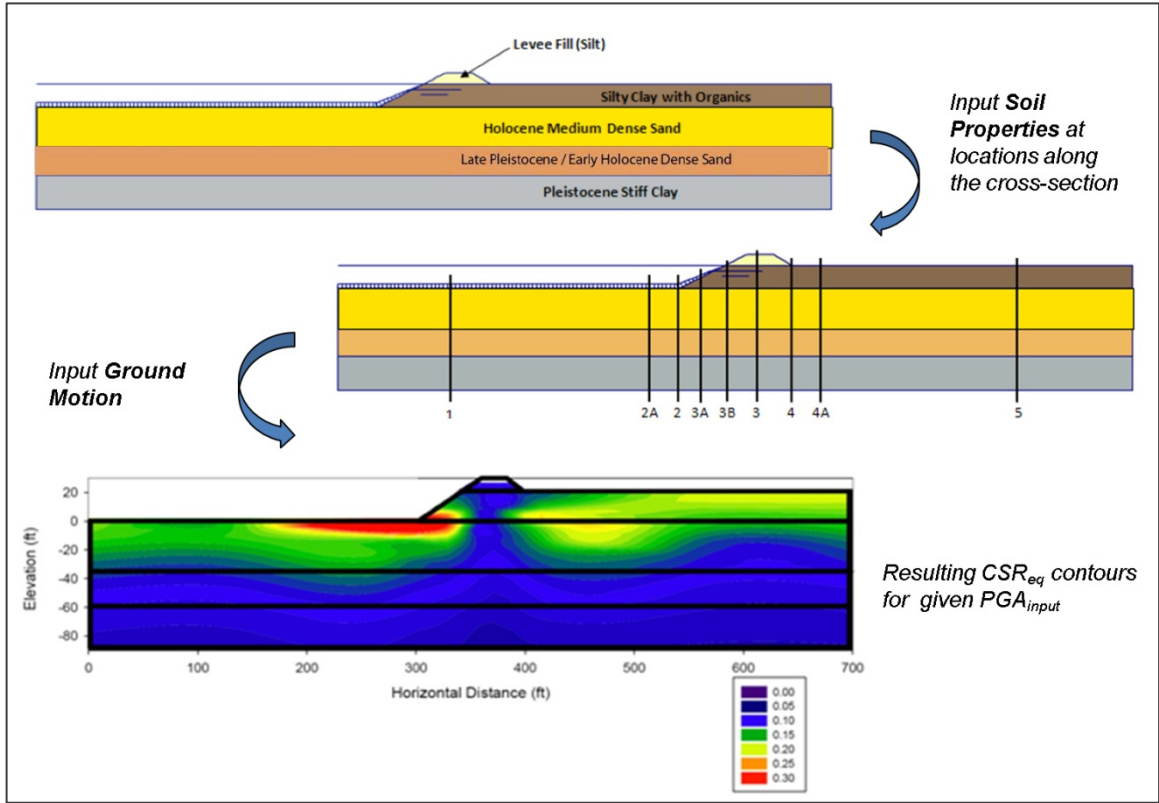
Figure 6.2 Evaluation of Median CSR_{eq} contours for cross-section Levee A for ground motions with Peak Ground Acceleration, PGA_{input} = 0.2g (Athanasopoulos-Zekkos 2008).
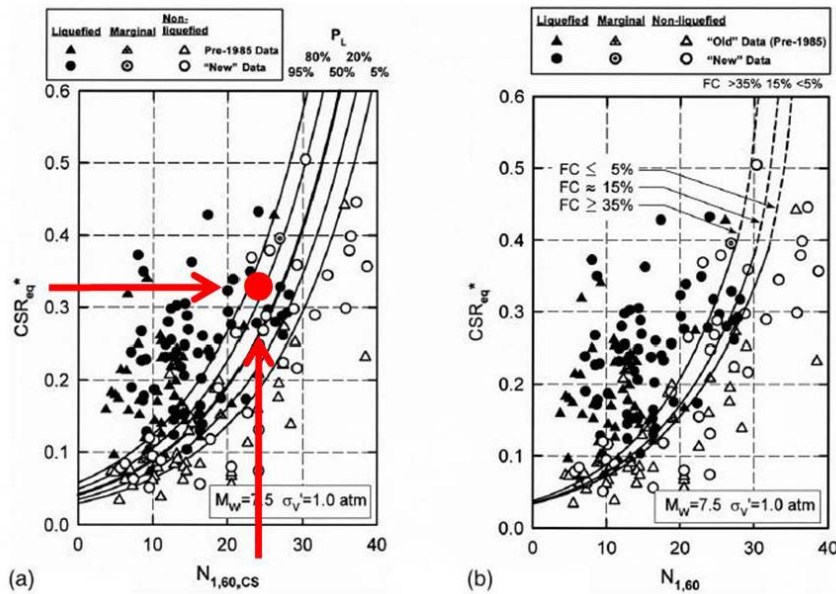
(a) Recommended probabilistic standard penetration test-based liquefaction triggering correlation for M_w=7.5 and σ'_v=1.0 atm and (b) recommended "deterministic" standard penetration test-based liquefaction triggering correlation for M_w=7.5 and σ'_v=1.0 atm, with adjustments for fines content shown

Figure 6.3 Assessment of liquefaction probability measure given site measured $N_{1,60,CS}$ values and calculated CSR_{eq} (Cetin et al. 2004).

155
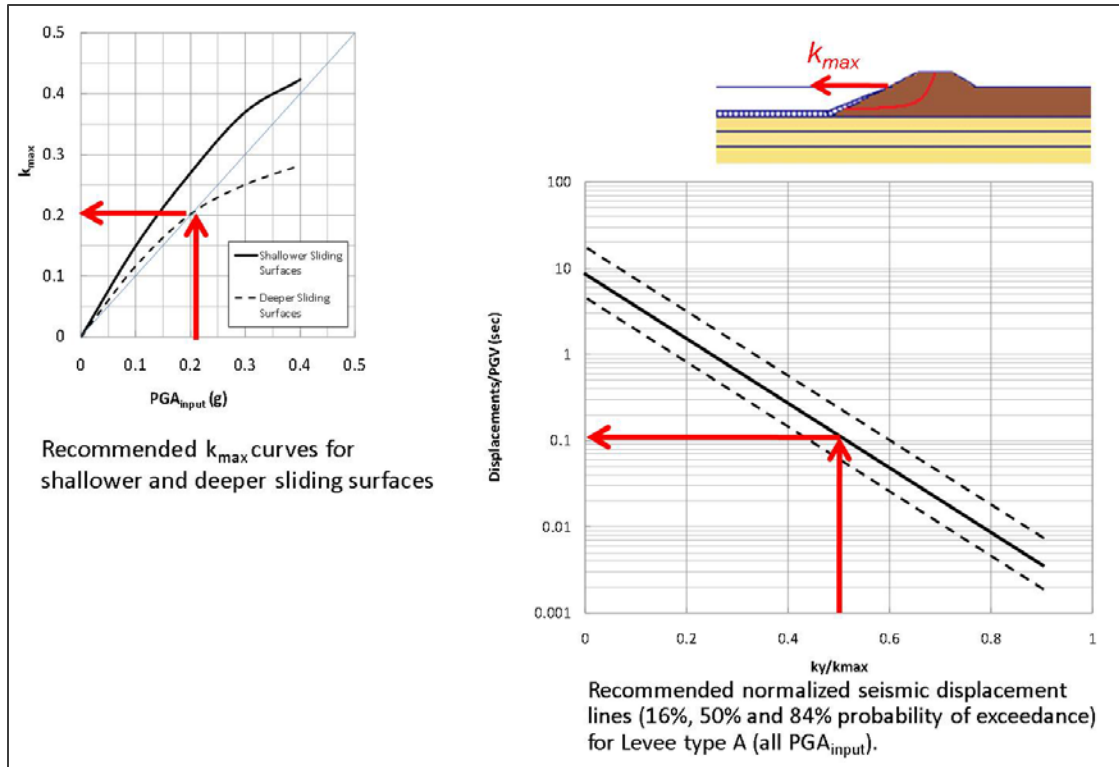
Figure 6.4 Calculation of displacement values given PGA_{input} and levee geometry information using recommended normalized seismic displacement lines (16%, 50% and 84% probability of exceedance) for Levee A (Athanasopoulos-Zekkos 2008).

Once seismic vulnerability is evaluated at one location, the simplest approach would be to linearly interpolate the risk values (e.g. as function of CSR for liquefaction, or Newmark-type displacements of prescribed sliding planes) within a segment from the known data nodes at the two ends of the segment to get the overall system vulnerability.

EXAMPLE: As a demonstration of system wide response output results, a simplistic failure probability estimation criterion is used for a first order analysis. This example, applied to the City of Sacramento, focuses only on soil liquefaction as a seismic failure mode.

Spatial joins are used to combine the levee and foundation material attributes (Figure 6.5). For this example, this is basically the step where the "segmentation" of the levees takes place in order to study the response of segments of various lengths. In the general case, the segmentation of levees depends on which foundation layer is being studied, and the variability of the soil strength parameter in that layer. For example, if liquefaction risk of the shallow sand foundation layer was being considered, the segmentation would depend on the variability of the angle of friction (and the derived $N_{1,60}$) based on predefined choice of "ranges" of the friction angle. For simplicity in this example, levee material is classified as a single layer (sand or clay) based on the major overall impression from soil investigation borehole data through the levee. The underlying geology map is used as the foundation layer, and similarly classified in a rudimentary manner (sand or clay).
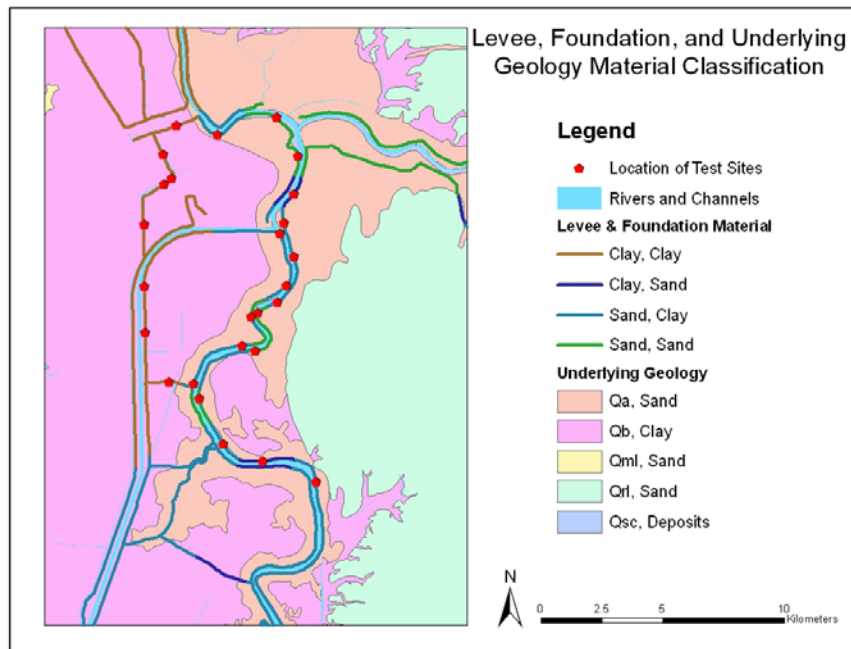
Figure 6.5 Classification of levee and foundation material, as per Table 6.1, overlaid with the underlying geology of the area.

157

Each soil layer combination, in this case the levee material and the foundation soil, is given a qualitative measure of failure potential due to liquefaction. Results from the analyses and segmentation of levees into reaches are shown in Figure 6.6, and the criteria used in the initial analysis maps are summarized in Table 6.1. This approach is very qualitative, yet helps illustrate the steps that followed the Geostatistical modelling of spatial parameters in the proposed methodology (Chapter 5). The segmentation of levees into reaches was based on the levee and foundation layer soil variability only, since the levee geometry/height is uniform across the area of study (Table 4.2).

Table 6.1 Simplistic failure criteria used for liquefaction

Levee Material	Clay	Sand	Clay	Sand
Foundation Material	Clay	Clay	Sand	Sand
Liquefaction	of no concern	of some concern	of some concern	of concern
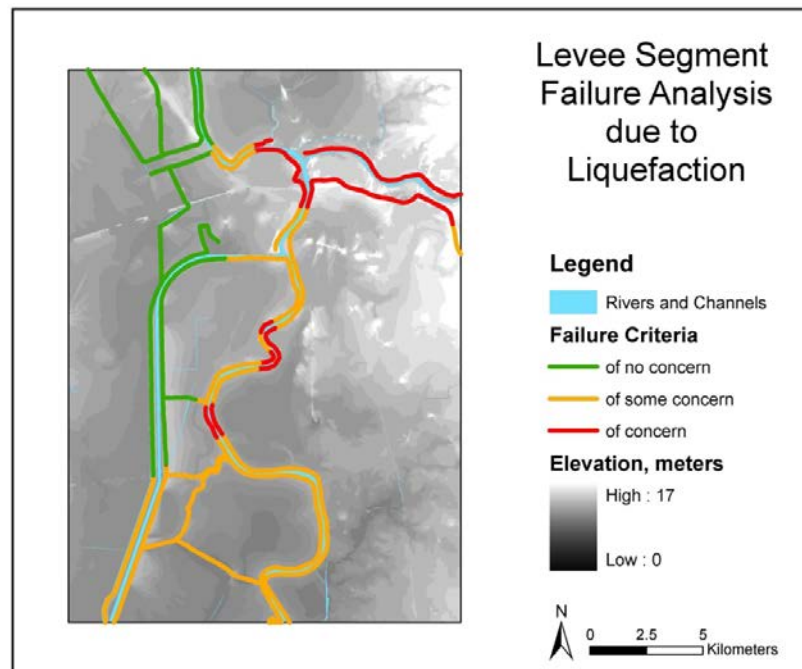
Figure 6.6 Results for failure analysis due to liquefaction.

158

6.3   Ground Motion Selection for Site-Specific Analysis

Once seismic vulnerability is evaluated, site-specific analyses can be performed for locations that appear to have increased vulnerability. In order to do that, the following method (Athanasopoulos-Zekkos and Saadi 2011) is suggested for the selection of ground-motions needed for the specific analysis.

For the liquefaction triggering evaluation, the mean period of the ground motion, T_m, is best correlated to the cyclic stress ratio, CSR (Athanasopoulos-Zekkos 2010). Regression relationships between CSR and T_m have been proposed for a series of the levee types shown in Figure 6.1, and for a number of shaking intensity levels. These relationships were developed (Athanasopoulos-Zekkos 2008) based on results from dynamic analyses of characteristic earthen levee cross-sections using a wide range of ground motions (~1,500), and it was found that, with respect to soil liquefaction, the variability in the CSR values results from the variability in the ground motions rather than soil stratigraphy.

For each levee type, the cross-section profile locations to be analyzed (Figure 6.7) were chosen to reflect conditions (1) at the free-field (i.e. far from the levee, Location G1), (2) at the levee toe (Location G2), and (3) at the levee crest (Location G3). In addition, Levee A has an asymmetric geometry where the waterside toe and the landside toe have different elevations; therefore for Levee A the analysis was also performed at the landside toe (Location G4).
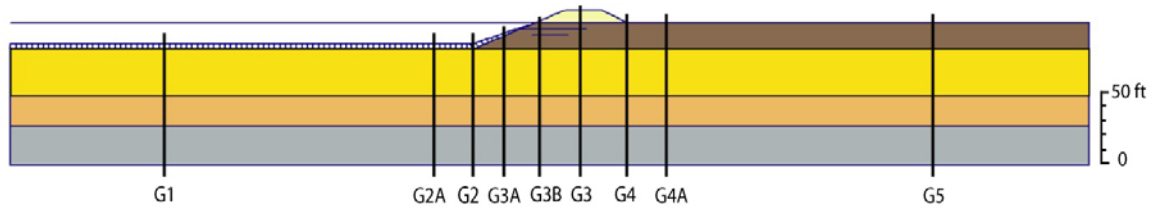
Figure 6.7 Locations of computed Cyclic Stress Ratio (CSR_{eq}) profiles for Levee A.

The analysis was carried out for four sets of ground motions representing input peak ground accelerations (PGA_{input}) of 0.1g (549 ground motions), 0.2g (459 ground motions), 0.3g (284 ground motions), and 0.4g (262 ground motions). For each set of PGA_{input} values, levee type, and location, the CSR_{eq} data points were plotted vs. T_m for all elevations. The following first observations can be made:

1) The CSR_{eq} values increase as the mean period increases, regardless of the site's natural period (Figures 6.8 and 6.9).

2) The correlation between CSR_{eq} and T_m becomes less pronounced as PGA increases (Figure 6.8). This may be due to non-linearity effects (e.g. higher shear strains, non-linear relationship between stress and strain) that are more pronounced at high accelerations, but are not captured by the equivalent-linear analyses performed herein.

3) The correlation between CSR_{eq} and the ground motion mean period becomes less pronounced with decreasing depth, as reflected in Figure 6.9. This is expected since the ground motion characteristics (e.g. T_m) change as the ground motion propagates through the soil layers and reaches the surface. Therefore T_m of the input ground motion no longer correlates well with the shear stresses produced near shallower soil layers.

4) For the case of the asymmetric geometry at Levee A where the waterside toe (location G2) and the landside toe (location G4) have different elevations, the analyses (e.g. Figure 6.2) showed that the critical (high) values of CSR_{eq} occurred at location G2, and therefore location G4 at Levee A as not be included in the analyses.
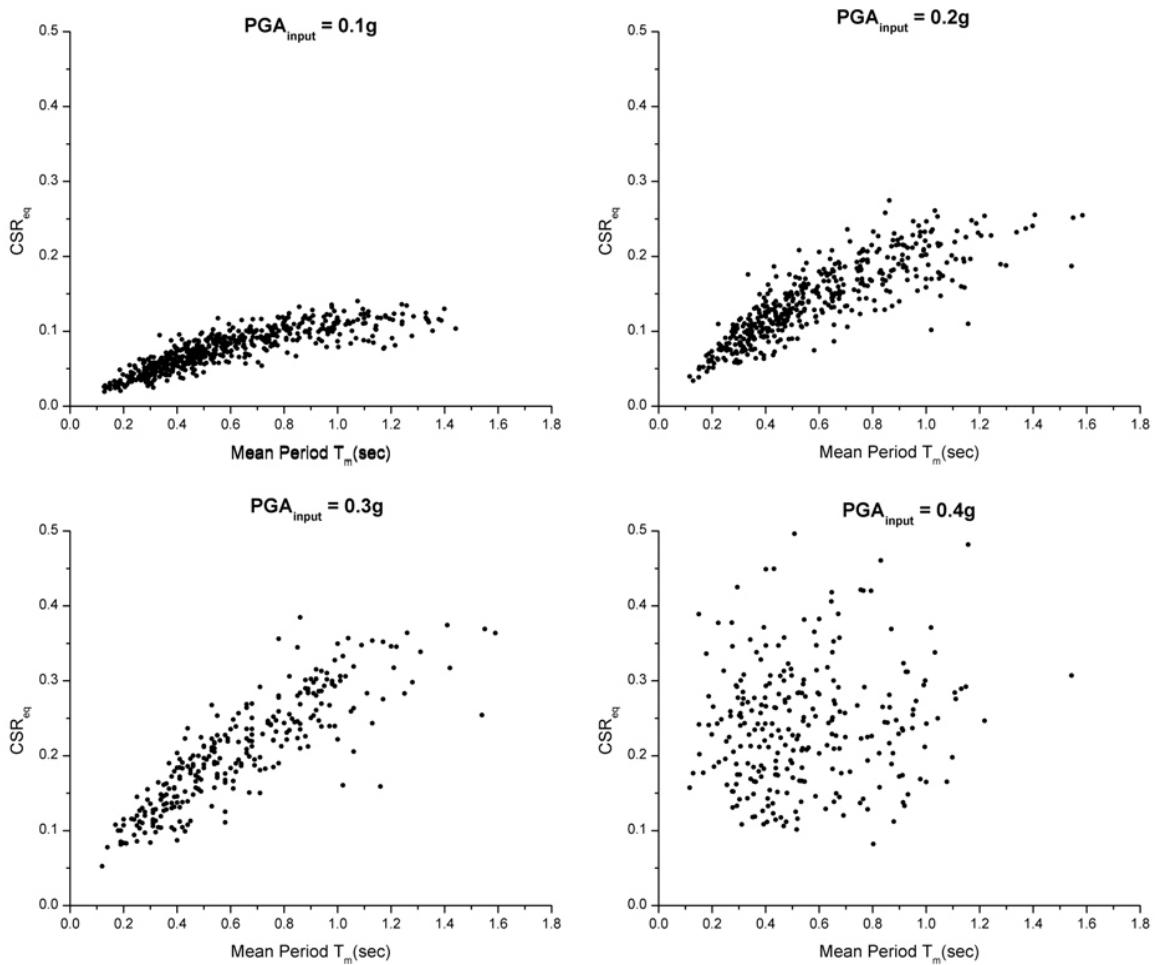
Figure 6.8 CSR_{eq} values vs. Mean Period (T_m) for Levee A, at location G1, with data shown only for 87ft from the channel bottom.
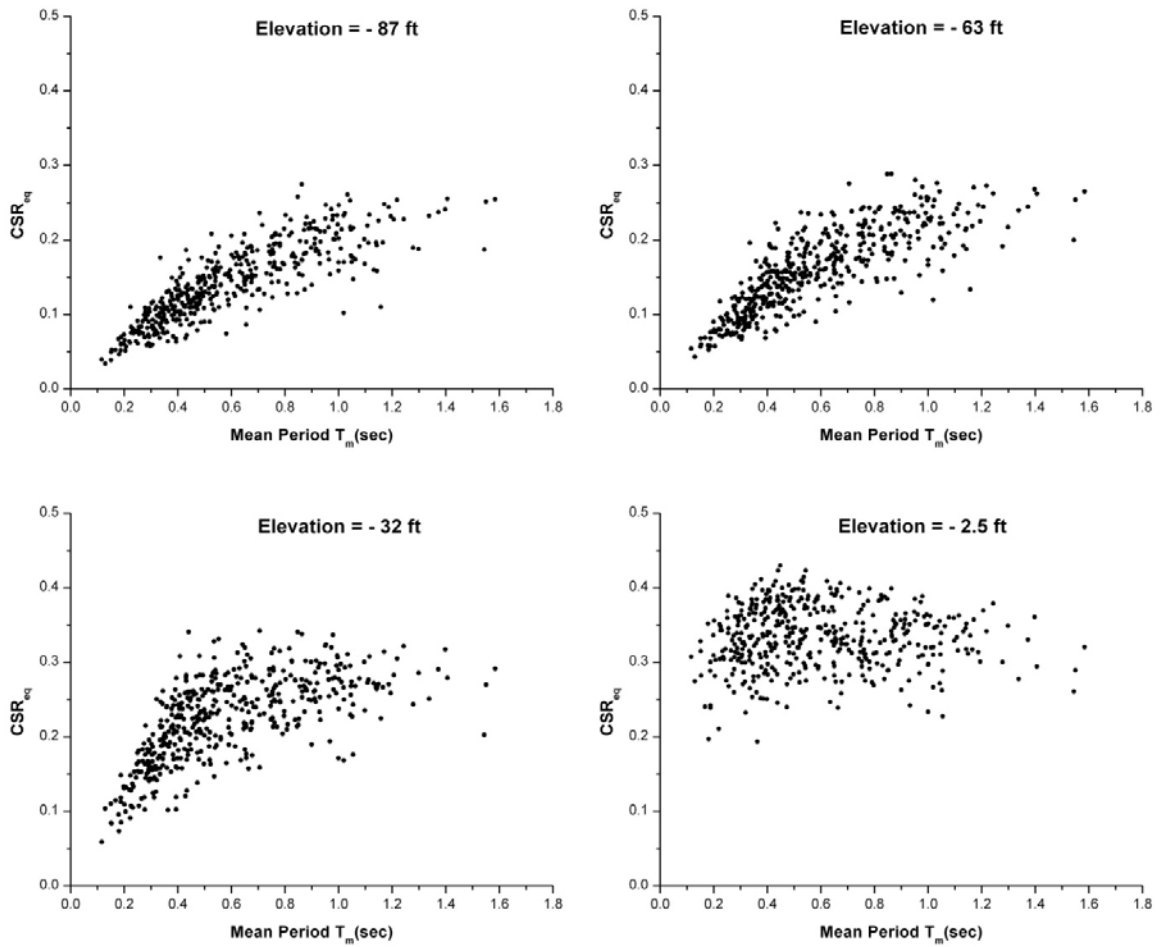
Figure 6.9 CSR_{eq} values vs. Mean Period (T_m) for Levee A, PGA_{input} of 0.2g, location G1, with data shown for representative elevations of -2.5ft, -32ft, -63ft, and -87ft from the channel bottom.

A number of functions were tested for the best fit of the scatter points. The criteria for the function that best fitted the data included comparison of residuals (defined as the percentage difference between the fitted and actual values, as compared to the actual values) and Root Mean Square Error (RMSE) values resulting from different fit functions.

The function that provided the best fit was the power function. Two forms of this function were analyzed, as shown in Equations 6.1 and 6.2 representing Form #1 and Form #2 respectively:

$$CSR_{eq} = a \cdot T_m^b + c \qquad \qquad \text{Equation 6.1}$$

$$CSR_{eq} = a \cdot T_m^b \qquad \qquad \text{Equation 6.2}$$

where a, b and c are the regression coefficients to be determined.

Form #2 reflects an intercept of zero on the CSR axis corresponding to a mean period of zero. However, applying the equation of form #1, which implies an intercept value, resulted in slightly lower RMSE values (1% to 8 % better than Form#2). Lower values of RMSE reflect a smaller difference between the actual observed values and the estimated fit values. R-square by definition theoretically ranges from 0 to 1. A higher R-square value implies a better fit. Values of R-square are very low at shallow depths, irrespective of the fit form used, which reflects the weaker correlation between CSR and T_m, as the ground motion propagates through more soil layers on its way to the surface.

Figure 6.10 shows the difference in the RMSE and R-square values based on the use of the two different power equation forms at Levee A, PGA_{input} of 0.2g, Location G1. The range and variation with elevation of the R-square values (Figure 6.10-b) is also similar for all three levee cross-sections, locations and PGA_{input} values. The RMSE values (Figure 6.10-a), however, increase with higher PGA_{input} values.
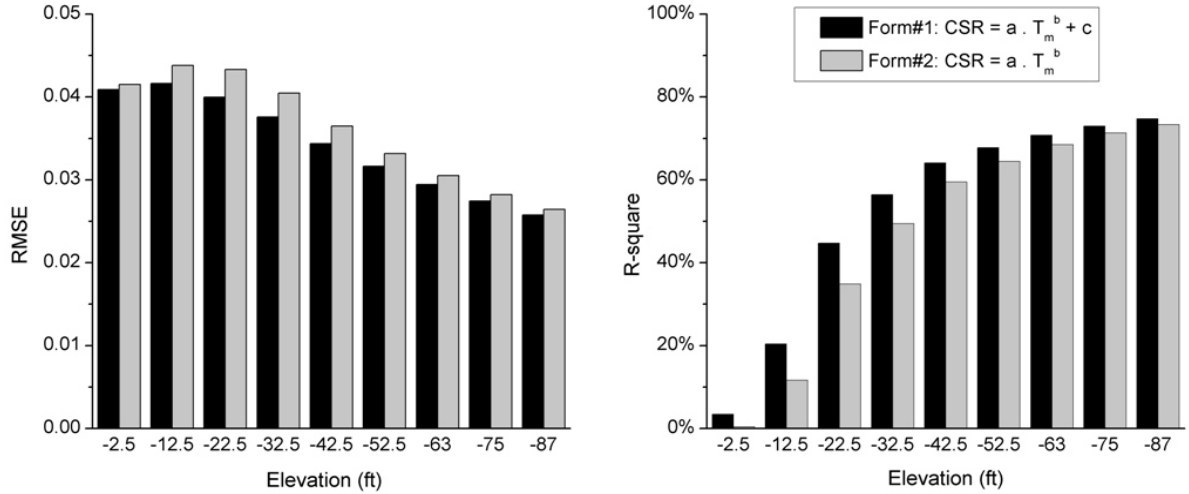
Figure 6.10 (a) RMSE and (b) R-square values for both Forms #1 and #2 at Levee A, PGA_{input} of 0.2g, Location G1.

Figure 6.11 shows the percentage residuals of CSR for both forms #1 and #2 at three elevations in Levee A, PGA_{input} of 0.2g, Location G1, calculated as shown in Equation 6.3:

$$\text{Residual}\,(\%) = \frac{(CSR_{computed} - CSR_{fit})}{CSR_{computed}} \cdot 100 \qquad \text{Equation 6.3}$$

where $CSR_{computed}$ are the computed cyclic stress ratio values and CSR_{fit} are the values obtained from the fit equations.

Figure 6.12 shows a comparison of the power function fit using both equation forms #1 and #2 at Levee A, PGA_{input} of 0.2g, Location G1, at representative elevations of -63 ft and -87 ft. The results shown in these figures are representative of all three levee types and locations.
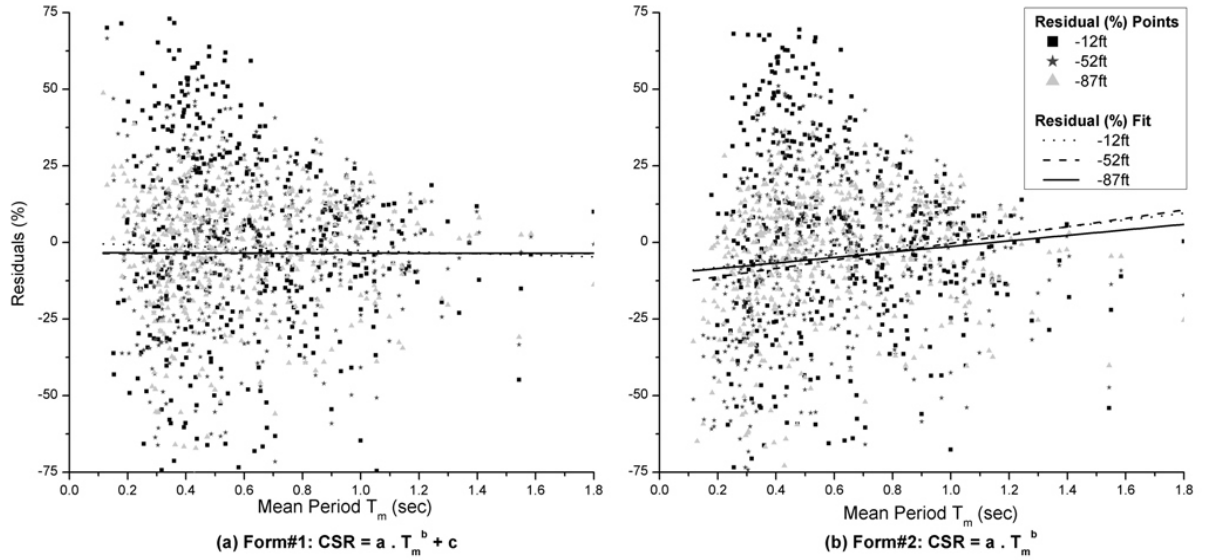
Figure 6.11. Comparison of the Percentage Residuals for both (a) form #1 and (b) form#2 at three representative elevations in Levee A, PGA$_{input}$ of 0.2g, Location G1.
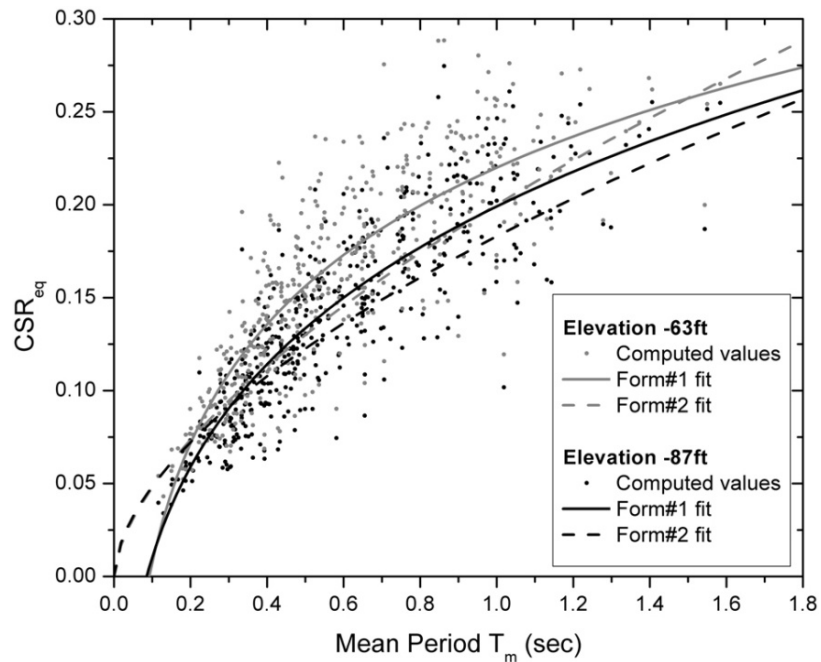
Figure 6.12. Comparison of the fit for both forms #1 and #2 at elevation -63ft and -87 ft, Levee A, PGA$_{input}$ of 0.2g, Location G1.

The majority of T_m values are in the range where equation form #1 and form #2 seem to overlap (e.g. in Figure 6.12, more than 95% of T_m values corresponding to $PGA_{input}=0.2g$ are between 0.2 and 1.2 sec). Based on the above, it can be noted that although equation form #1 has a slightly better fit to the data than equation form#2, it requires setting a minimum limit on the T_m values that can be used, since form#1 fit does not pass through the origin of the plot. Because of this constraint, and since the R-square and RMSE indicators of form#2 do not differ substantially, the analysis of the data was carried out based on the form #2 which represents a relationship between CSR_{eq} values, and the mean period T_m of the ground motions used in the form $CSReq = a*T_m^b$ as previously shown in Equation 6.2. It is also worth noting that the results from the analyses with $PGA_{input}=0.4g$ were not used in the regression because it was observed that due to non-linearity effects the correlation between CSR and T_m was very weak.

The terms "a" and "b" are coefficients that vary with each levee type, location, and elevation. In order to highlight the effect of levee geometry on the results, the variation of the coefficients "a" and "b" with elevation at each of the levees A, B, and C, and for various locations and PGA levels is shown in Figures 6.13 through 6.15.

The effect of the different stratigraphy in the three levee types is shown in Figures 6.16 through 6.18 where the variation of the coefficients "a" and "b" with elevation is plotted at each of the locations G1, G2, and G3, for all levee types, and PGA levels.

166
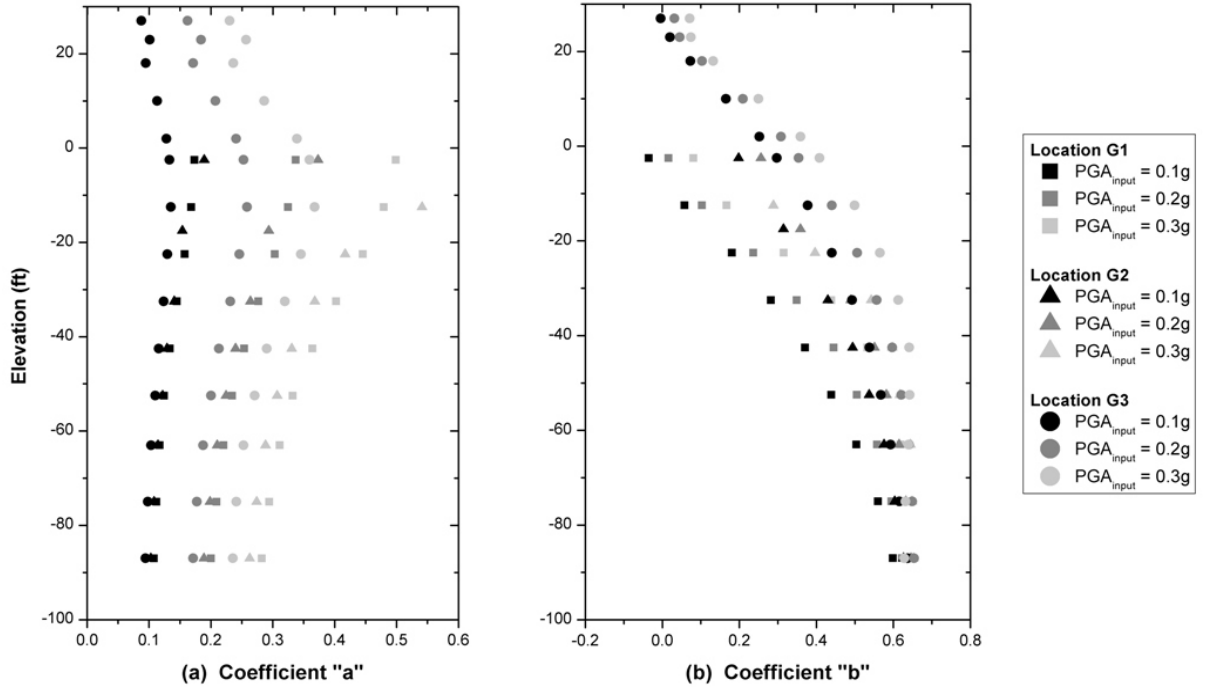
Figure 6.13 Variation of equation form#2 coefficient "a" and "b" with elevation, in levee A, for all locations and PGA$_{input}$ levels.
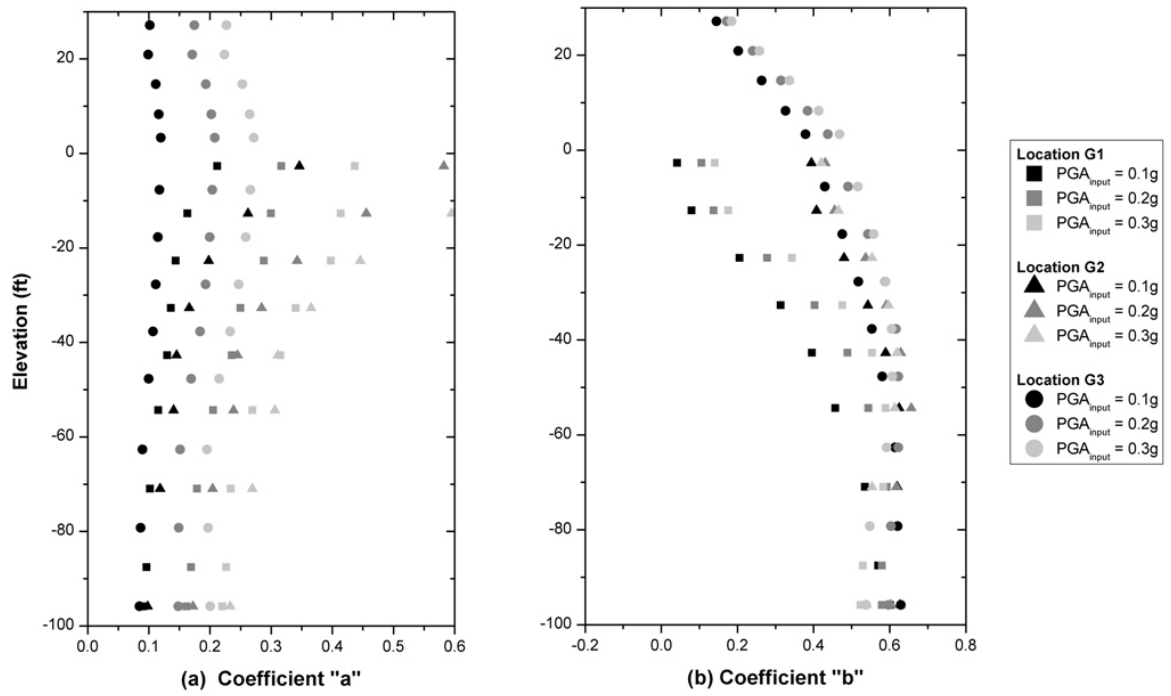
Figure 6.14. Variation of equation form#2 coefficient "a" and "b" with elevation, in levee B, for all locations and PGA$_{input}$ levels.

167
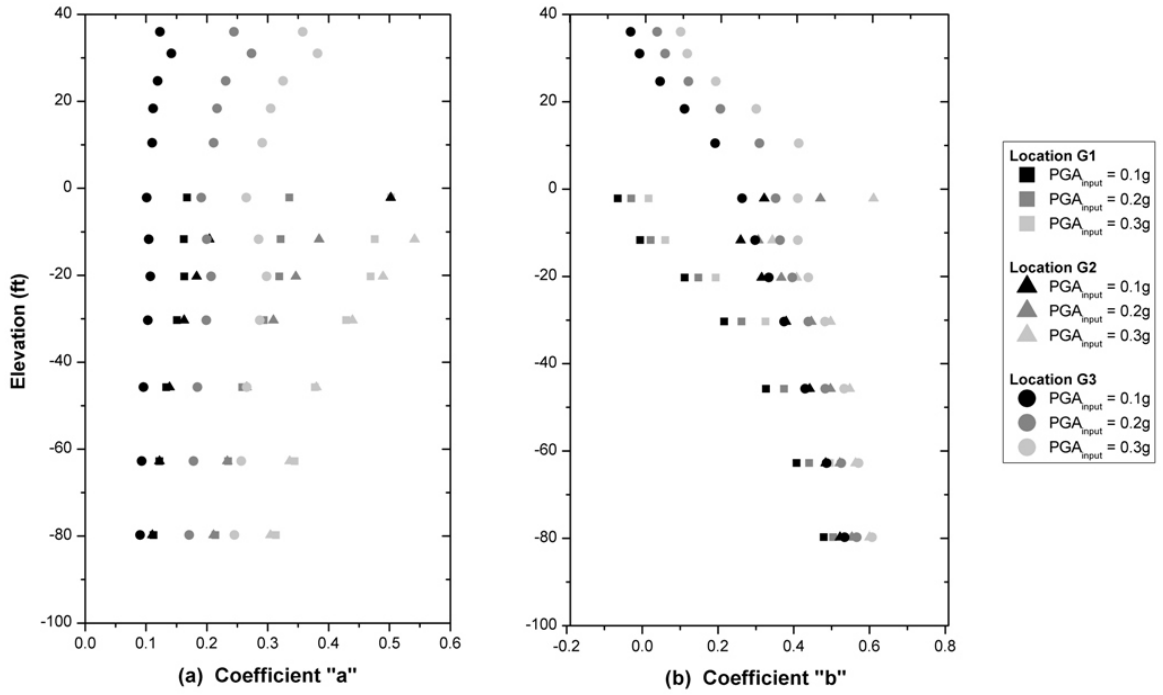
Figure 6.15. Variation of equation form#2 coefficient "a" and "b" with elevation in levee C, for all locations and PGA$_{input}$ levels.
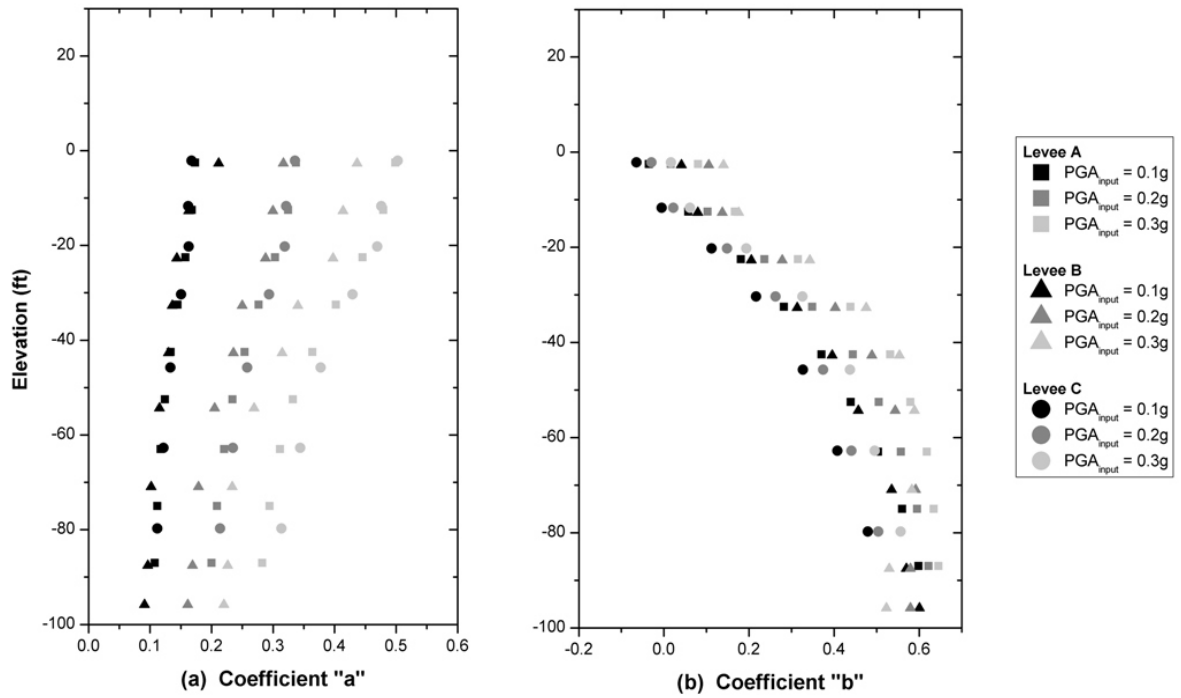
Figure 6.16. Variation of equation form#2 coefficient "a" and "b" with elevation at Location G1, for all levees and PGA$_{input}$ levels.

168
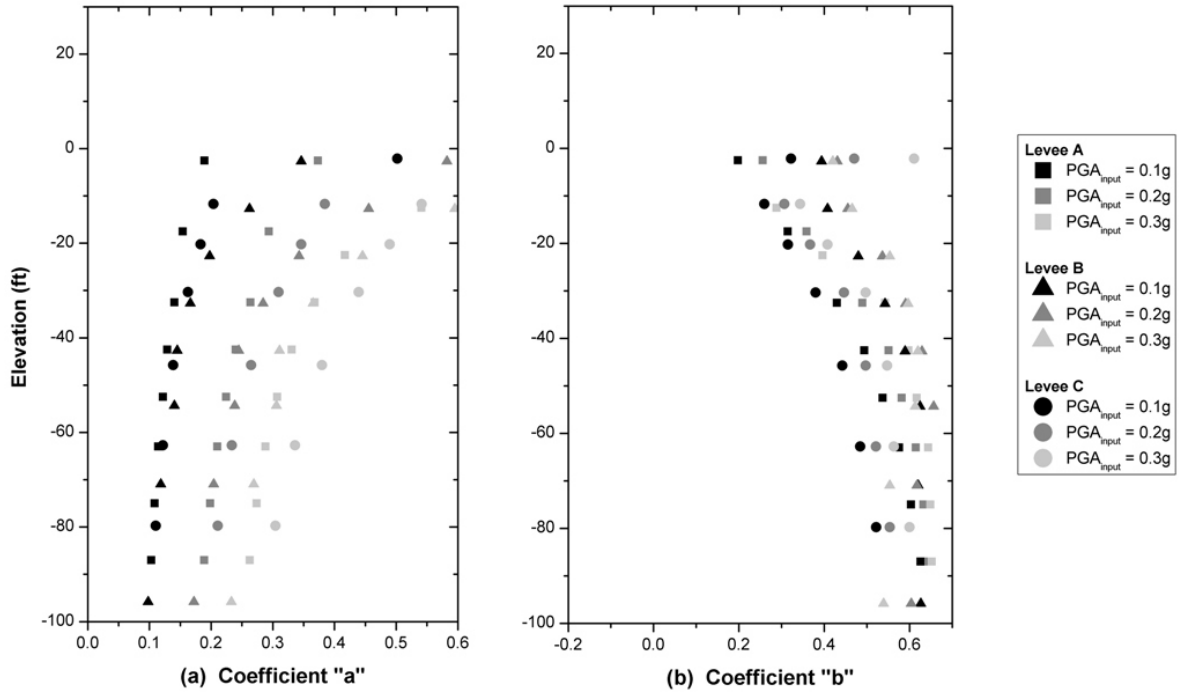
Figure 6.17. Variation of equation form#2 coefficient "a" and "b" with elevation at Location G2, for all levees and PGA_{input} levels.
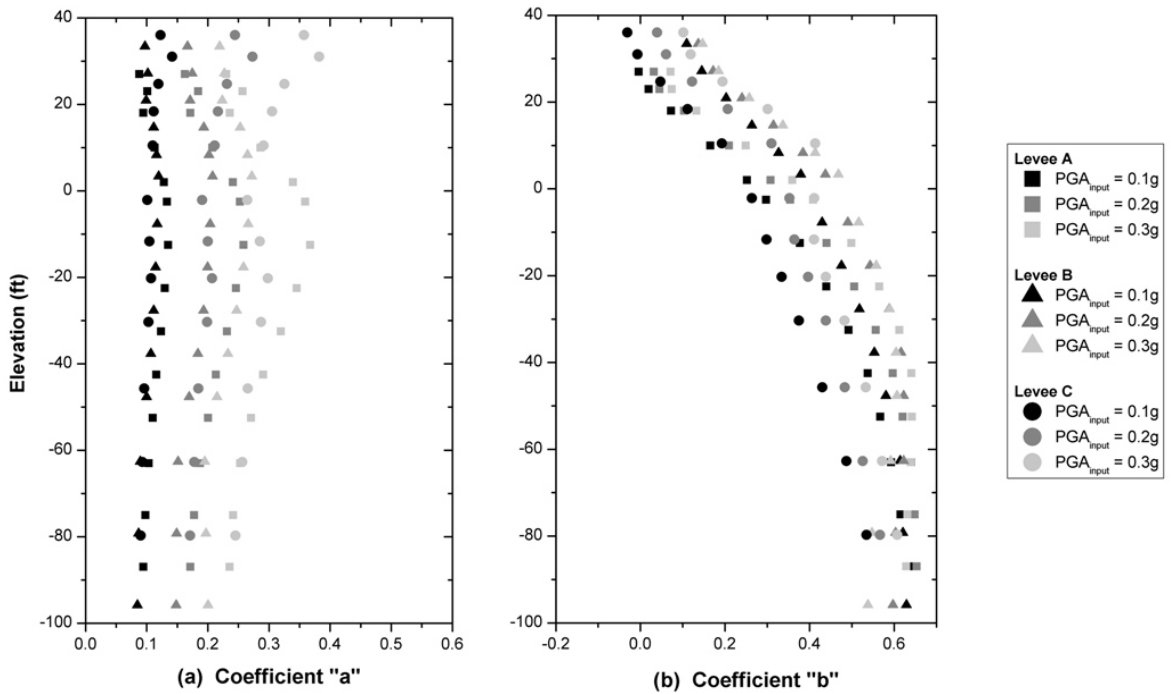
Figure 6.18. Variation of Form#2 coefficient "a" and "b" with elevation at Location G3, for all levees and PGA_{input} levels.

In looking at the parameters that affect the value of coefficient "a", Figures 6.13-a, 6.14-a, and 6.15-a show a strong correlation of this coefficient to PGA_{input} irrespective of the levee type. In addition, as PGA_{input} increases, the scatter in the range of "a" values increases as well when comparing the three different locations G1, G2, and G3. Coefficient "a" values are also clearly affected by the different locations G1, G2, and G3 in the levee cross-sections. Figures 6.16-a, 6.17-a, and 6.18-a indicate that coefficient "a" is not affected by the levee type, and thus the parameters that are considered to affect coefficient "a" and that will be included in the development of the regression will be limited to elevation, PGA_{input}, and locations.

As for coefficient "b", Figures 6.13-b, 6.14-b, and 6.15-b show that the location (i.e. free-field, levee toe, levee crest) has a more pronounced effect than PGA_{input}. Furthermore, Figures 6.16-b, 6.17-b, and 6.18-b illustrate that the coefficient "b" values are even less dependent on the levee type.

The best regression fit between the coefficients "a" and "b" in the equation of form #2 and elevation was found to have the general polynomial form, shown in Equations 6.4 and 6.5, respectively:

$$a = f(x) = p_1 . z^2 + p_2 . z + p_3 \qquad \text{Equation 6.4}$$

$$b = f(x) = q_1 . z^2 + q_2 . z + q_3 \qquad \text{Equation 6.5}$$

and thus the equation describing the relationship between CSR_{eq} and T_m has the form:

$$CSR_{eq} = (p_1. z^2 + p_2. z + p_3). T_m^{(q_1.z^2+q_2.z+q_3)} \pm \sigma_{CSR} \qquad \text{Equation 6.6}$$

where z is the depth in feet, and p_1, p_2, p_3, q_1, q_2, and q_3 are given in Tables 6.2 and 6.3, for all three locations (G1, G2, and G3), and all three shaking intensity levels (0.1g, 0.2g, and 0.3g), irrespective of the levee type. σ_{CSR} is the standard deviation Root Mean Square Error (RMSE) of CSR_{eq}.

Table 6.2 Values of p1, p2, and p3 for the fit equation between CSR_{eq} and T_m, for all locations and PGA_{input} levels

Location	PGA_{input}	p_1 x 10^{-6}	p_2 x 10^{-4}	p_3 x 10^{-1}
Free Field	0.1g	5.9	14.7	1.8
	0.2g	5.2	22.7	3.4
	0.3g	9.9	36.7	5.0
Levee Toe	0.1g	46.6	65.1	3.3
	0.2g	19.4	41.7	4.0
	0.3g	172.7	226.3	9.6
Levee Crest	0.1g	-4.2	-0.5	1.1
	0.2g	-7.9	-0.5	2.1
	0.3g	-10.2	-0.1	2.9

Table 6.3 Values of q1, q2, and q3 for the fit equation for between CSR_{eq} and T_m, for all locations and PGA_{input} levels

Location	q_1 x 10^{-5}	q_2 x 10^{-3}	q_3 x 10^{-2}
Free Field	-8.2	-14.2	-3.5
Levee Toe	-3.5	-6.3	33.2
Levee Crest	-5.0	-7.2	35

For elevations -12.5 ft, -42.5 ft, and -87 ft from the channel bottom, the proposed CSR_{eq} model fit curves are shown in Figure 6.19, and the RMSE distribution with elevation for all PGA levels and all locations is shown in Figure 6.20.
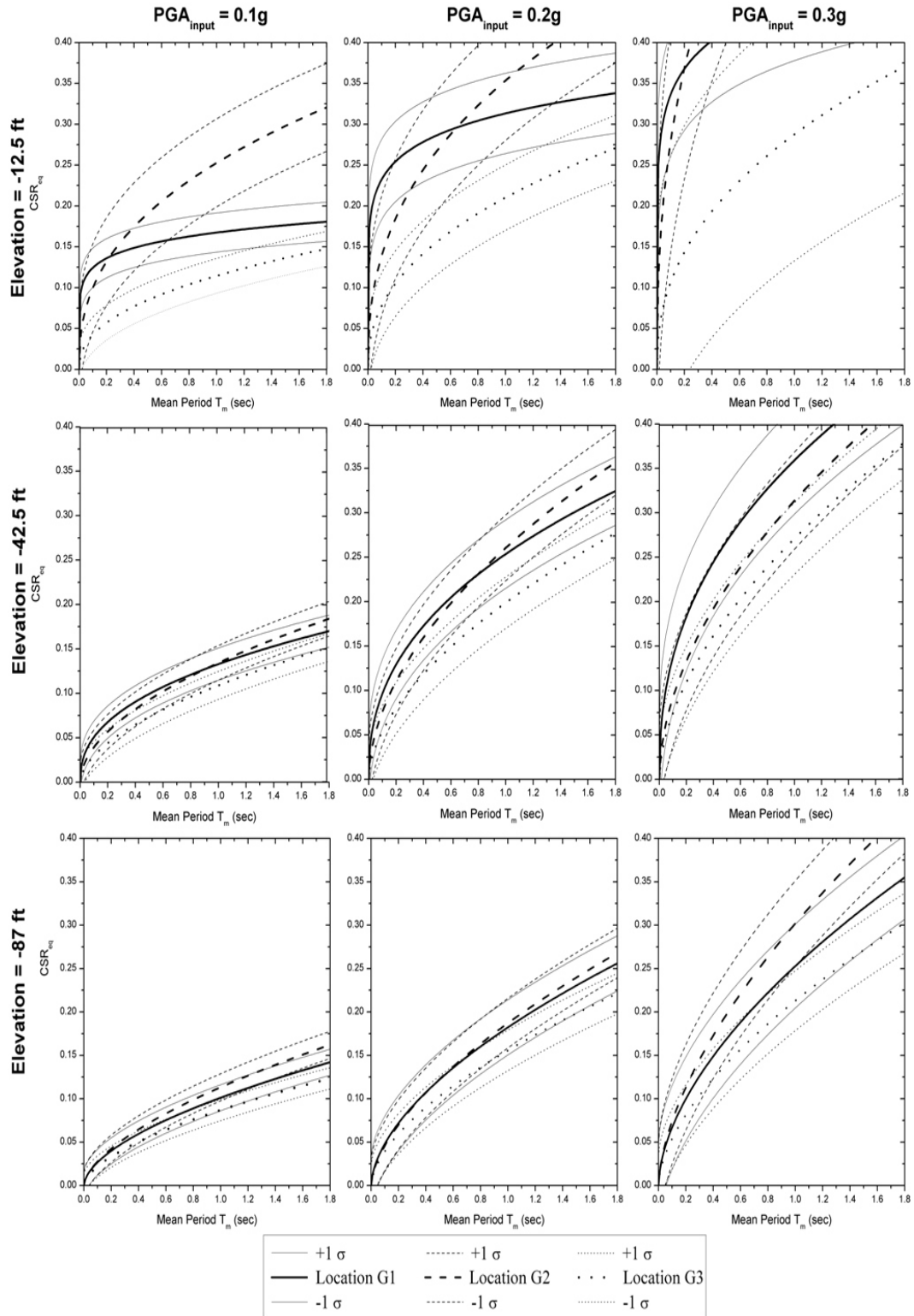
Figure 6.19 Proposed fit curves for CSR_{eq} as a function of Mean Period T_m for PGA_{input} of 0.1g, 0.2g and 0.3g, and for elevations -12.5ft, -42.5ft and -87ft. CSR_{eq} is shown at the median value ± one standard deviation Root Mean Square Error.
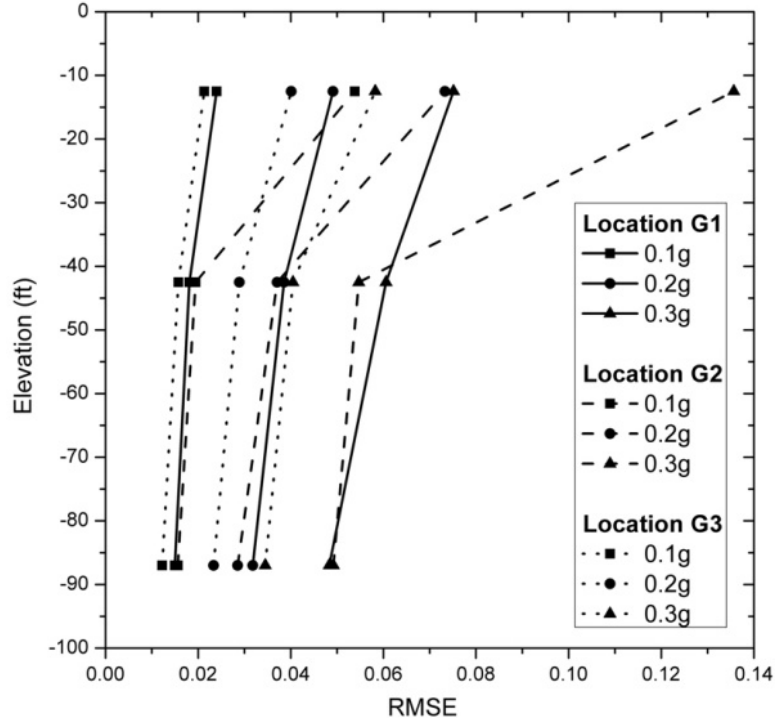
Figure 6.20. CSR_{eq} model Root Mean Square Error (RMSE) variation with elevation for all PGA_{input} levels and all locations.

The proposed model and graphs can be used as a ground motion selection criterion for dynamic analyses of earthen levees with regard to liquefaction triggering evaluations. The proposed methodology follows a similar process to the one proposed by Watson-Lamprey and Abrahamson (2006). If the time-series, after scaling, are selected such that the time series parameters (i.e. T_m) lead to a median CSR_{eq} similar to that expected for the design event, then the time series can be expected to give a near average response for a higher order liquefaction triggering evaluation using a non-linear soil model. The CSR_{eq} therefore is used as a proxy for the non-linear behavior of a more complicated yielding system in guiding the selection of time series. This approach, of defining a proxy for the behavior of a complicated yielding system has been adopted by other researchers as well (e.g. Haselton 2009). In a typical case, the design ground motion

173

is specified by a response spectrum and an earthquake scenario (M_w, EpiD). The use of the liquefaction model requires an additional parameter: the mean period of the ground motion, T_m. T_m can be estimated using the empirical models and predictive equations proposed by Rathje et al. (1998):

$$\ln(T_m) = \ln[C_1 + C_2{*}(Mw - 6) + C_3{*} R] + \sigma, \quad \text{for } M_w =< 7.25 \qquad \text{Equation 6.7}$$

$$\ln(T_m) = \ln(C_1 + 1.25{*}C_2 + C_3{*} R) + \sigma, \qquad \text{for } 7.25 < M_w < 8.0 \quad \text{Equation 6.8}$$

where for rock: C_1, C_2, C_3 and σ are 0.411, 0.0837, 0.00208, and 0.437 respectively, and for soil: C_1, C_2, C_3 and σ are 0.519, 0.0837, 0.00190, and 0.350 respectively. R in these relationships is the closest distance to the rupture plane in km.

Figure 6.21 shows a comparison of the original best fit form#2 at levee A, with the developed CSR_{eq} model equations, that is independent of levee type, for location G1, PGA_{input} 0.2g, for the representative elevations of -87ft, -42.5 ft, and -12.5ft from the channel bottom. As can be seen from the figure, there is very good agreement between the two curves and this is also true for all three levee cross-sections, for all cross-section locations and all PGA_{input} values. The proposed model was also used to compute an equivalent r_d vs. elevation distribution. The results are shown in Figure 6.22 and are in good agreement with typical r_d curves mean values proposed by Cetin et al. (2004), and Idriss and Boulanger (2006) which implies that the proposed model captures the basic characteristics of site response for the three levee profiles.
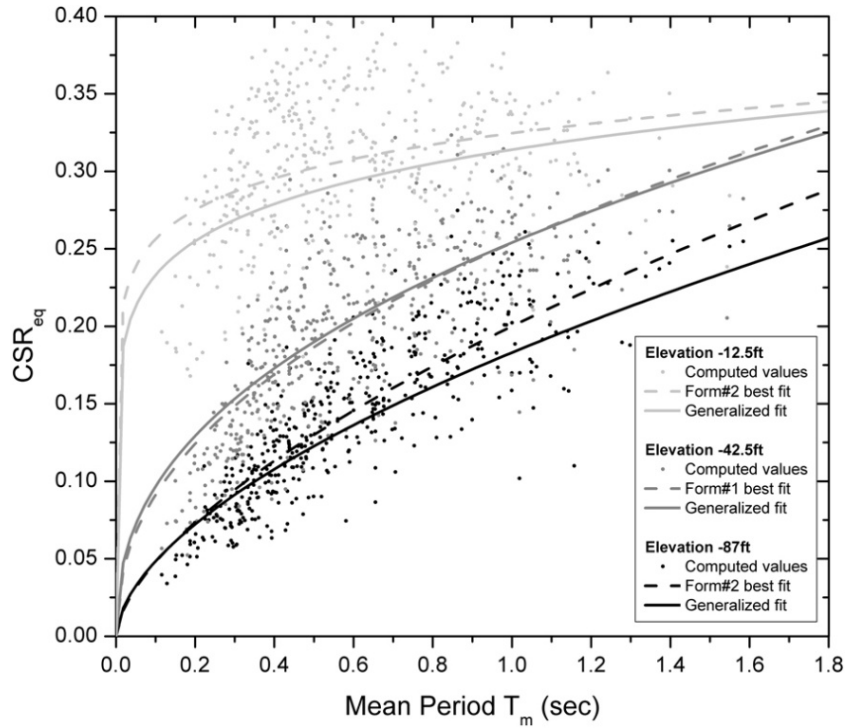
Figure 6.21. Comparison of *form#2 best fit* of CSR_{eq} vs. T_m at levee A with the *proposed model equation* for location G1, PGA_{input} of 0.2g, at representative elevations of -87ft, -42.5 ft, and -12.5ft.
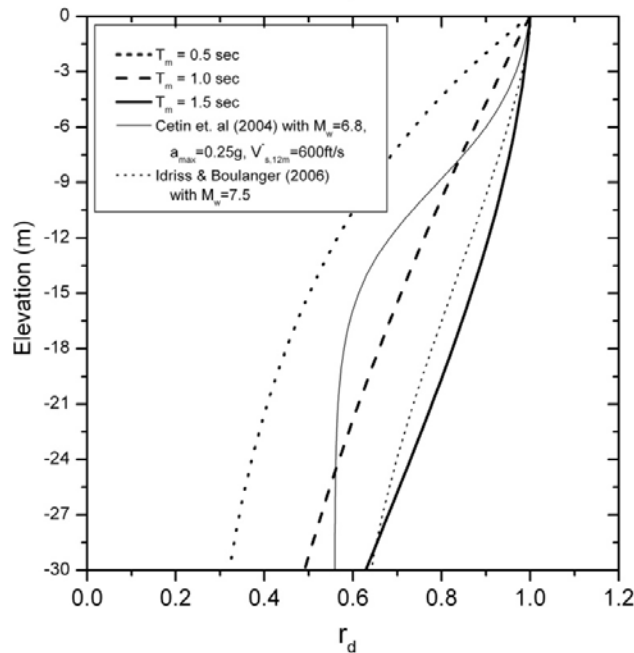
Figure 6.22. Equivalent r_d results from proposed model for free-field conditions for PGA_{input}=0.2g, superimposed with lines from recommendations by Cetin et al. (2004), and Idriss and Boulanger (2006).

Finally, the following procedure can be used to select time series:

1. Compute the median T_m given the design event parameters using Equations 6.7 and 6.8 by Rathje et al.(1998).

2. Compute the median CSR_{eq} for the design event given T_m, using Equation 6.6.

3. Select candidate ground motion recordings for scaling. This can be based on the traditional magnitude and distance bins approach. However, the bins used can be wider than typical.

4. Scale the PGA of all acceleration time series to match the PGA of the design event ground motion. Scaling factors should be between 0.5 to 2.

5. Reject records where T_m is not within a half of a standard deviation of its median value as computed in step 1.

6. Calculate the difference between the estimated CSR_{eq} for the design event (from step 2) and the median CSR_{eq} expected for each scaled ground motion (Equation 6.6) and then square the result.

7. Repeat steps 1-6 for at least three depth values. This will generate a total of three lists of scaled candidate records, one list for each depth.

8. For records that appear on all lists, calculate the root mean square of the differences for the three depths from step 7. If both horizontal components of a record appear on the list, then the component with the lower root mean square is rejected.

9. Select the record(s) which have the smallest root mean square of differences.

The proposed model can be used as a ground motion selection criterion for dynamic analyses of earthen levees with regard to liquefaction triggering evaluations. It is limited to a maximum PGA_{input} of 0.3g and for levee cross-sections that have a similar soil stratigraphy profiles to levees A, B or C (Figure 6.1).

6.4   Flood Scenarios

The next step consists of modelling the possible flood scenarios for all levee segments and then using a color code for flooding of segments of either no, little, or more concern for failing due to liquefaction. This was done using terrain slope and flow patterns obtained by analyzing the 10x10m digital elevation model data.

The ArcGIS watershed tool calculates all the area contributing flow to a particular point at a lower level. Since levees are at a higher level than the adjacent land, and the objective is to get the area where water would flood (as opposed to water collecting downstream an area to a point), a digital elevation model was inverted (positive values changed to negative values, and vice versa), and the watershed tool was applied to the inverted elevation model, with water flowing "towards" the levee locations where failure would occur. The developed "LeveeToFloodedArea" model shown in Figure 6.23 was developed in the the ArcGIS model builder environment, and included the Watershed, FlowDirection, and other raster manipulation tools.

177
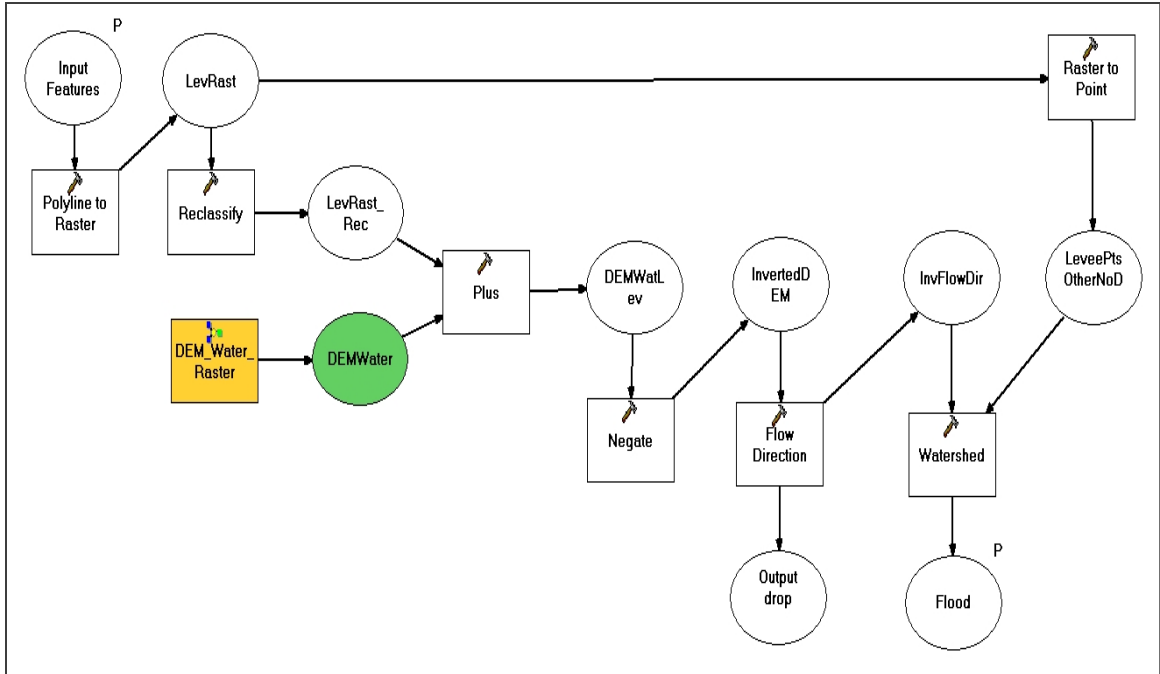
Figure 6.23 "LeveeToFloodedArea" model constructed in ArcGIS model builder.

The resulting flood scenarios for all levee segments, using the considered liquefaction method of failure, were consistent with the landscape and terrain properties and are shown in Figure 6.24 for the City of Sacramento.

The flood model above does not simulate the effect of water *accumulation* in the flooded areas, nor does it indicate where the water would ultimately go after a steady flow for a period of time. The model assumes that all the levee sections that have failed is completely non-existent physically (all the levee height has been washed away) - which is a worst case scenario, thus these calculations are conservative.
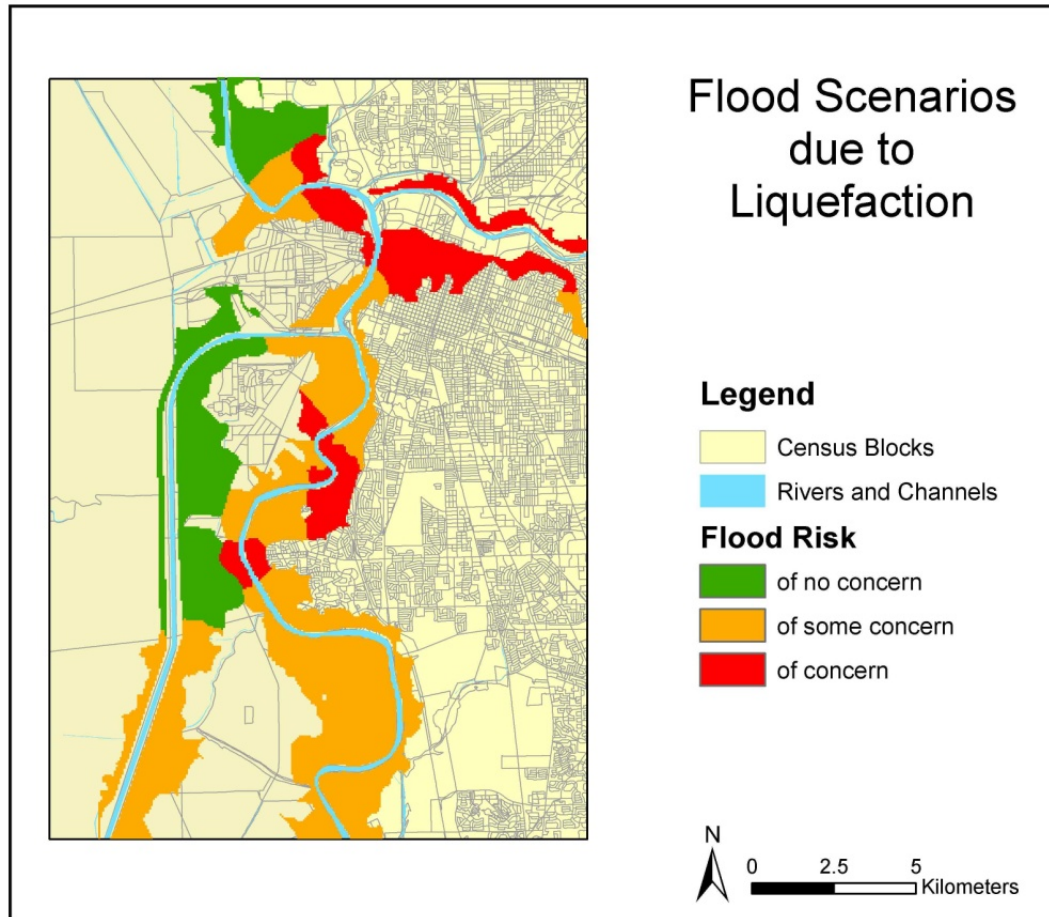
Figure 6.24 Flood scenarios from liquefaction failure for all levee segment (Flood risk levels shown are consistent with the liquefaction failure criteria used).

Flooding from any static or dynamic modes of failure can be simulated using the same approach above. Furthermore, as a check, the ArcScene software can be used to *fly over* and look in perspective at the different resulting flooded areas of different modes of failure, as shown for example in Figures 6.25 and 6.26.
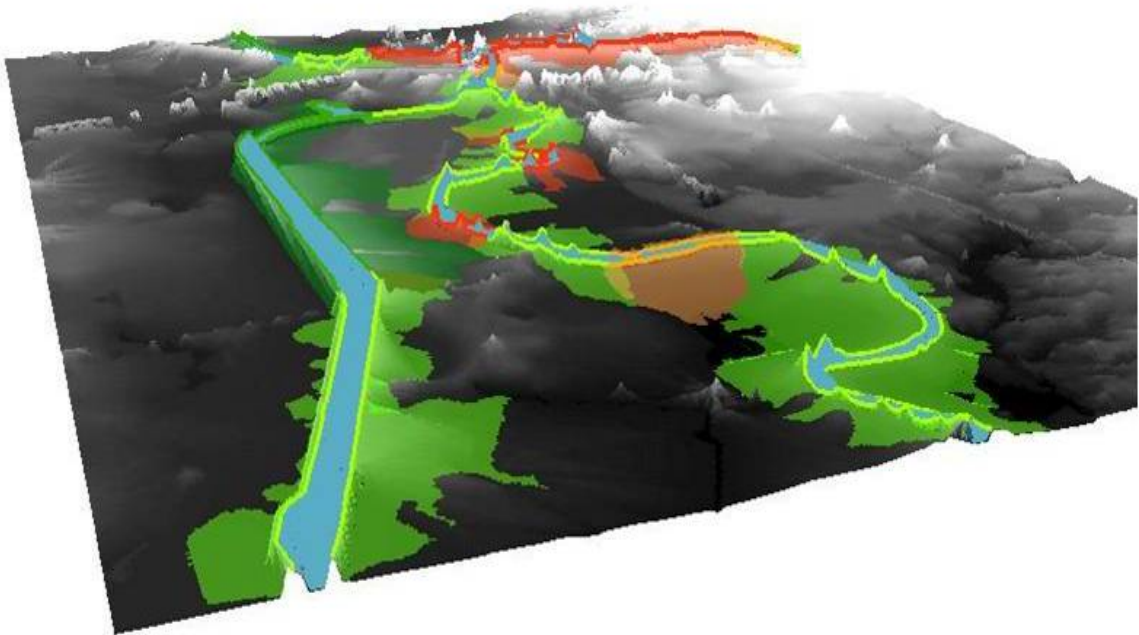
Figure 6.25 Visualization of flood simulation results in Sacramento, for an underseepage failure analysis, in 3D ArcScene environment with exaggerated vertical axis units.
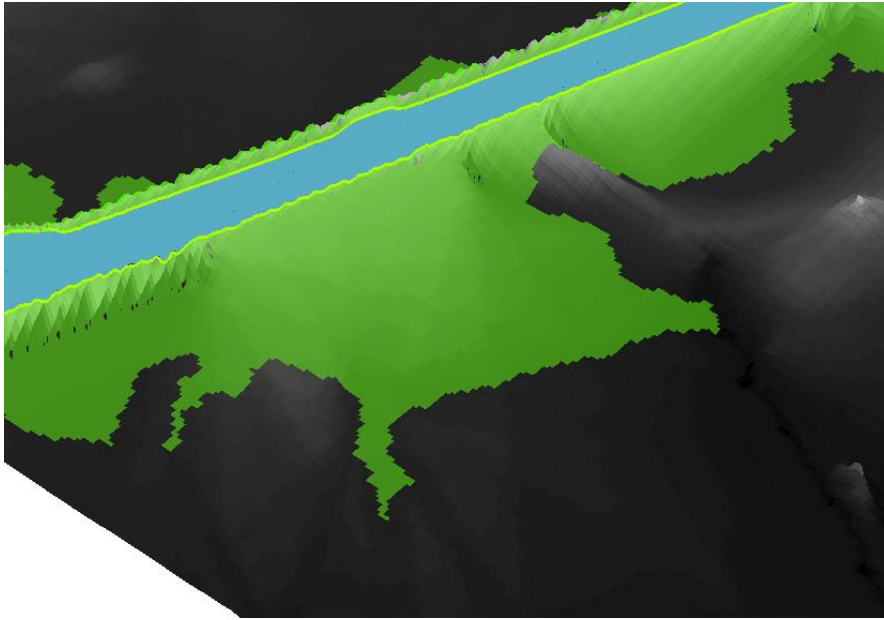
Figure 6.26 Close-up from Figure 6.25 showing the correct simulation of flooding scenario using the ArcScene software, for an underseepage failure analysis in Sacramento (note the hill that was not flooded, next to the levee, in the upper side of the image).

As can be seen in Figure 6.27, the presented sample output of the proposed approach, even though rather simplified, offers an efficient visualization of the results, thus enabling decision makers to quickly identify critical regions.
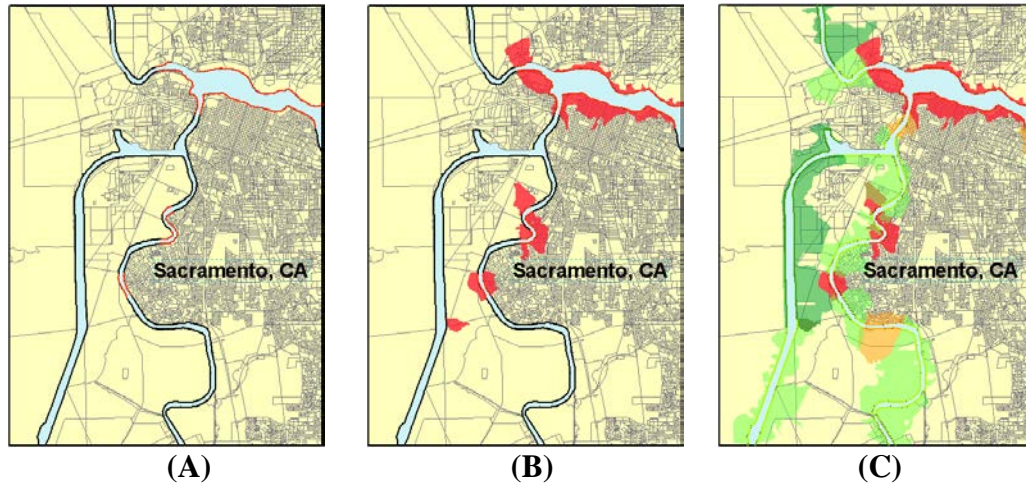
Figure 6.27 Visual representation of results from preliminary underseepage failure analysis in Sacramento: (A) identified critical levee segments, (B) projected flooding scenarios, and (C) aggregation of flooding from multiple failure scenarios.

6.5   Damage Forecasting in Protected Areas

Flooded areas, as determined in the previous step, can be combined with any socio-economic data to reflect potential losses. As an example, flooded areas are overlapped in the GIS platform with population data and then presented in a 3D format using the ArcScene software. Census block population numbers are used in Figure 6.28 , while population density values are shown in Figure 6.29. This step is performed to show the ease of visual representation and usefulness of the proposed work in helping decision makers and engineers to plan maintenance, repair and emergency response operations.

For example, in Figure 6.29, the areas of high population density (higher blocks) that are at highest risk of flooding (red color) can be quickly identified.
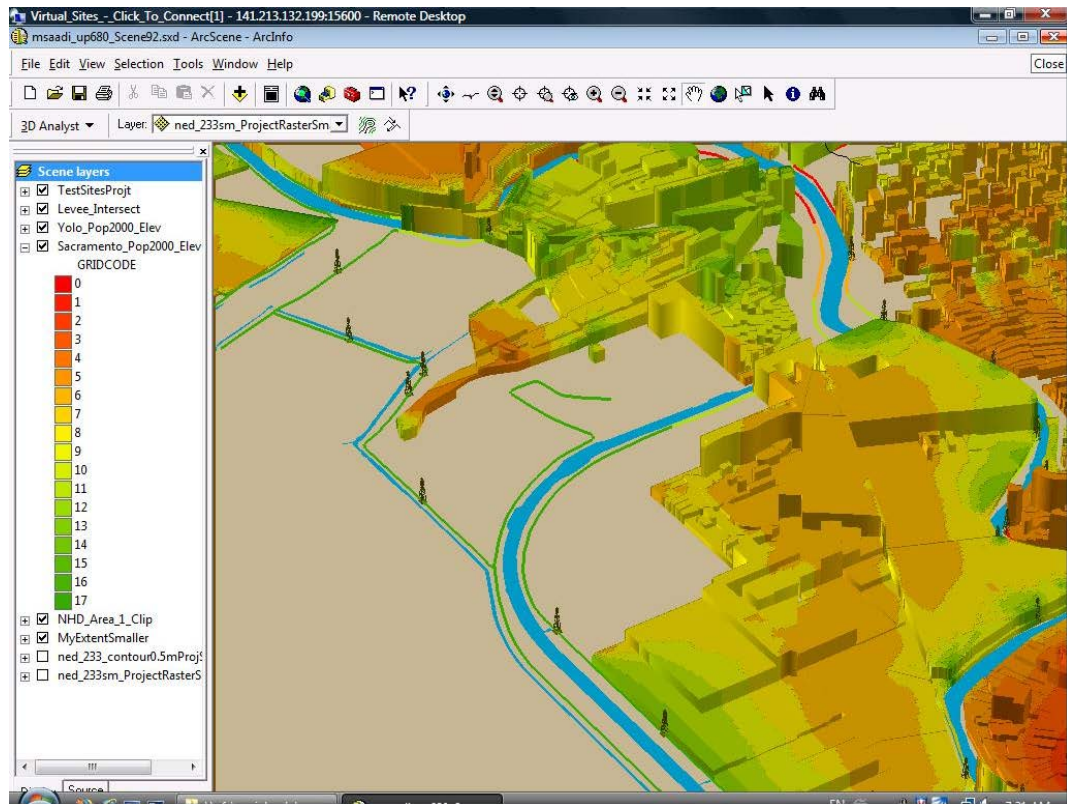
Figure 6.28 A sample screen shot of 3D representation of census block population count (different heights) superimposed on terrain elevation values (different colors, e.g. lowest areas in red, where water would accumulate and not drain).
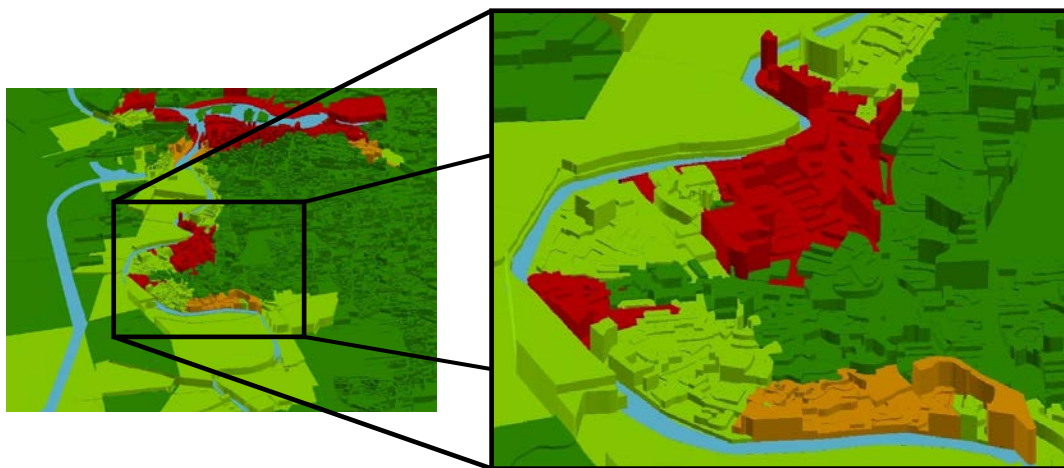
Figure 6.29 A 3D representation of population density (different heights) at the census block level, with flooded scenarios from an underseepage levee failure (different colors).

CHAPTER 7

Conclusions and Future Research

7.1 Summary

A Geographic Information System (GIS)-enabled methodology is proposed to predict soil properties in riverine geologic environments for the seismic risk assessment of earthen flood protection systems. The essential step in the overall approach is the development of a spatial variability model that provides a continuous characterization of soil conditions throughout the system and not solely at locations with known geotechnical investigation data. The model correlates soil strength parameters of identified stratigraphy layers, to preselected regional variables. Layers identified in the chosen pilot case study area in California include sand and clay foundation layers at both shallow and deep levels from the surface.

The spatial parameter variability is modeled using a geostatistical ordinary kriging approach, and correlations are established between strength parameters and regional factors such as classification of geology and river geometry characteristics (distance to nearest river segment and river meandering sinuosity index value).

Finally, the proposed methodology describes further steps for seismic response analysis of levee segments, and flood scenarios in protected areas. An example of a first-

order estimate of the spatial vulnerability of a levee system and an efficient visualization of the results is presented, in order to demonstrate the usefulness of the proposed methodology to decision makers for quick identification of critical regions. Since seismic response of earthen structures is controlled primarily by the input ground motions, a methodology for selecting ground motions for the liquefaction triggering assessment of levees is also developed.

GIS was a crucial component for the completion of this research, and proved to be the appropriate platform for input, manipulation, and output presentation of spatial and non-spatial data components. GIS tools were useful in their capability of referencing geotechnical property information to geographic locations, performing various spatial analysis and correlation functions, geostatistical analysis, and acting as an integrated database management system.

7.2   Conclusions

7.2.1   Spatial Variability of Soil Parameters

As a result of analyzing geotechnical investigation data in the area of study, the concept of "**Effective Correlation Distance**" between the soil parameters and regional factors is introduced. This is a physical representation of the distance beyond which no trend/correlation was observed or deemed physically significant. For **clay** parameters this distance came out to be 600m from either side of the river centerline.   For **sand** parameters the distance was 450m. Possible explanation of why sand distance is less than clay distance may be in the fact that sands settle closer to the levee in times of overtopping flooding due to larger heavier particle size as compared to silts and clays.

Note that in Sacramento, the average river width is 150m, and levees are typically around 100m from the river centerline (i.e. on average 25 meters from river edge). Thus, for example, the limit of this effective correlation distance for clays is still 500m away from the levees, which can be approximated as free-field conditions.

Another concept established is the "**Sinuosity Index Segmentation Level**". This is a reflection of the river meander length period. Based on the available data, the ideal segmentation level was found to be close to 10 times the river channel width. Values imply that the Feather River (1,000m segmentation) has a shorter meander length than the Sacramento River (1,750m segmentation), i.e. the Feather River meanders in shorter meander wave lengths than the Sacramento River.

The main finding of the soil variability model is **the establishment of a number of correlations** between soil strength parameters (Friction Angle, ϕ, for Sands, and Shear Strength, S_u, for Clays) and a number of regional characteristics (underlying geology type, distance to river, and sinuosity of river). The correlations were studied for naturally occurring Clay and Sand typical foundation layers, located at both shallow and deep levels, in both regions of Sacramento and Feather Rivers.

The major findings from the development of the soil parameters estimation model, based on the above mentioned established correlations, are:

- Clay in both shallow and deep, and in both areas of study (Sacramento and Feather River), showed increasing <u>trend of S_u with increasing distance from</u>

river (Figure 4.34). S_u values also increased with depth, which may be attributed to consolidation of the deeper layers over time.

- As for relation of S_u to the different geological formations in the two study areas (Figure 4.35), a general observation is that clay S_u values in the areas of the Qa formation (defined as Alluvium - Unweathered gravel, sand, & silt) tend to have lower values than other areas. The fact that clay is not the main component in this formation might provide an explanation for the lower values of S_u for any clay showing in these areas, as compared to other formations.

- For S_u relation to Sinuosity Index, (Figure 4.36) there is a large scatter, at lower sinuosity levels. The higher number of data points at this low sinuosity level is due to the smaller number of river segments that are highly sinuous. An important observation across all areas of study, and at all depths of layers, is that S_u tends to decrease with increasing sinuosity of the closest river segment. However, more data points are needed to draw meaningful correlations between SI and shear strength or soil type. Furthermore, due to the specific case study area that was used, the limited data used was primarily available for SI values close to 1 (i.e. straight river sections).

- Sand layers in both shallow and deep, as well as in both areas of study, did not show a global trend of friction angle, ϕ, with increasing distance from river

(Figure 4.37). The friction angle values do not seem to be affected by the depth at which the sand layer is present.

- No clear conclusion could be drawn (Figure 4.38) from the <u>plot of friction angle, ϕ, with respect to different geological formations</u> in the two study areas. It is possible however to draw a relation between ϕ and individual geological formation (i.e. typical value and distribution of ϕ within each geological formation).

- For <u>friction angle, ϕ, relation to Sinuosity Index</u> (Figure 4.39) there is no global effect observed. ϕ values in Sacramento area decrease with increased Sinuosity levels, while in Feather River, there is no clear trend. Furthermore, the small number of data points at high sinuosity levels does not allow for further statistical analysis.

Global observations that apply across the larger area of study included the increasing trend of shear strength, S_u, with increasing distance from the river, and decreasing trend of S_u with increasing river Sinuosity Index levels. Only local trends were observed in the relation of friction angle, ϕ, with Sinuosity Index, as well as in the relation of S_u and ϕ with geological formations.

7.2.2 Seismic Response of Levees

In dynamic analyses of earthen structures the single most important input parameter is the seismic ground motion (Bray 2007). For the case of earthen levees, the parameter that best correlates to the Cyclic Stress Ratio, CSR, used in performing liquefaction triggering evaluation was found to be the mean period, T_m, of the ground motion (Athanasopoulos-Zekkos 2010). In this thesis regression analysis was performed to develop equations that quantitatively describe the correlation between CSR and T_m. In performing the analyses several observations were made:

- The correlation between CSR and T_m is best described using a power function.

- The correlation between CSR and T_m becomes less pronounced as PGA increases and this may be due to non-linearity effects that are more pronounced at high accelerations, but are not captured by the equivalent-linear analyses performed herein.

- The trend in CSR increase with mean period values becomes less pronounced with decreasing depth and the scatter of the values increases. This is expected since the ground motion characteristics (e.g. T_m) change as the ground motion propagates through the soil layers and reaches the surface. Therefore T_m of the original ground motion no longer correlates strongly with the cyclic shear stresses produced near shallower soil layers.

- The main parameters that affect the coefficients used in the proposed equations and therefore the final shape of the CSR vs T_m curves are: soil stratigraphy, cross-section location at levee site (i.e. free-field, levee toe and levee crest), depth and shaking intensity (described herein by PGA_{input}). Soil stratigraphy appears to have the smallest effect whereas depth has the largest effect.

- The effect of cross-section location becomes more pronounced for higher PGA_{input} values since the topographic effects become more pronounced as well.

A CSR_{eq} model is proposed to provide ground motions selection criteria in site-specific dynamic analyses of earthen levees for liquefaction triggering assessment. This model can be used for a maximum PGA_{input} of 0.3g and for levee cross-sections that have a similar soil stratigraphy to levees A, B or C. The profiles used in these analyses are representative of a wide range of levees. However, a site-specific analysis should be performed when a levee is very different from the typical levee sections presented.

The advantage of using the proposed model is that since the ground motion selection criteria are based on the properties of the scaled ground motion rather than just selecting time histories based on magnitude, distance, and site, the range of time series typically considered can be significantly broadened, while at the same time still leading to an average response of the levee with regard to liquefaction triggering assessment.

7.3 Recommendations for Future Research

More precise elevation data for the pilot study have also just recently become available with an improved resolution of 1/9 arc second (~ 3 meters). Furthermore, the California Department of Water Resources (DWR 2011c), partnering with FEMA, is assembling critically needed levee information on geometry, landmarks, test locations, history, etc for all the levees in the state. This is an ongoing project and final information was not available to the public at the time of this study. Once this Levee Database project is completed, the database can be used as input material for the proposed approach across the state.

Because of the geostatistical complexity of combining both the estimation of thickness variation of different layer types (qualitative parameter), with the estimation of the soil parameter variability within each layer (quantitative parameter), and because the focus of this research was the study of soil properties variability, simplified assumptions had to be made regarding the depths where layers start and end. This also resulted in the assumption that the typical identified soil layers exist at a constant thickness across the whole area of study. It was not the objective of this research, nor is it physically possible with limited geotechnical data, to identify, at any location in the study area, where a certain soil layer starts and ends. However, the precise delineation of soil layer depth and thickness is an aspect that requires further study.

The regional factors studied are by no means an exhaustive list, and study of other potential factors (such as soil cover type) should be considered. Furthermore, in other

190

potential areas of study, historical data of river migration are to be included if they are available in that case.

The resulting spatial estimation maps of soil parameters can be validated by measurements on site, or through comparison to additional in-situ tests as they become available to the public by the California Department of Water Resources.

Additional seismic vulnerability analysis using non-linear soil models needs to be performed to study the effect of non-linearity on the response of the levee cross-section soil profiles. Furthermore, another possible area of research is the assessment of the sensitivity of the seismic risk output results due to changes in: ground motion parameters (e.g. PGA, T_m, S_a, etc.), and the level of detail in sub-division of levee segments. These sensitivity analyses will help identify potential benefits in computational and data collection efforts when applying the final resulting methodology to large areas. Also, individual segment and overall levee system risk measures assessed as a function of response analysis and resulting damage estimation must be extended to cover a range of ground motion intensities, resulting in a respective set of fragility curves/maps.

Finally, it is recommended that the proposed approach be extended to other large riverine systems such as the Mississippi river system, and that the assessment of risk measures for other modes of failure (storms, hurricanes, settlement, underseepage, etc.) also be addressed, so that an Overall Risk Measure (ORM) can be determined. Similarly, the effect of the presence of penetrations through the earthen levees on the risk measure of various failure modes is a potential extension of the work.
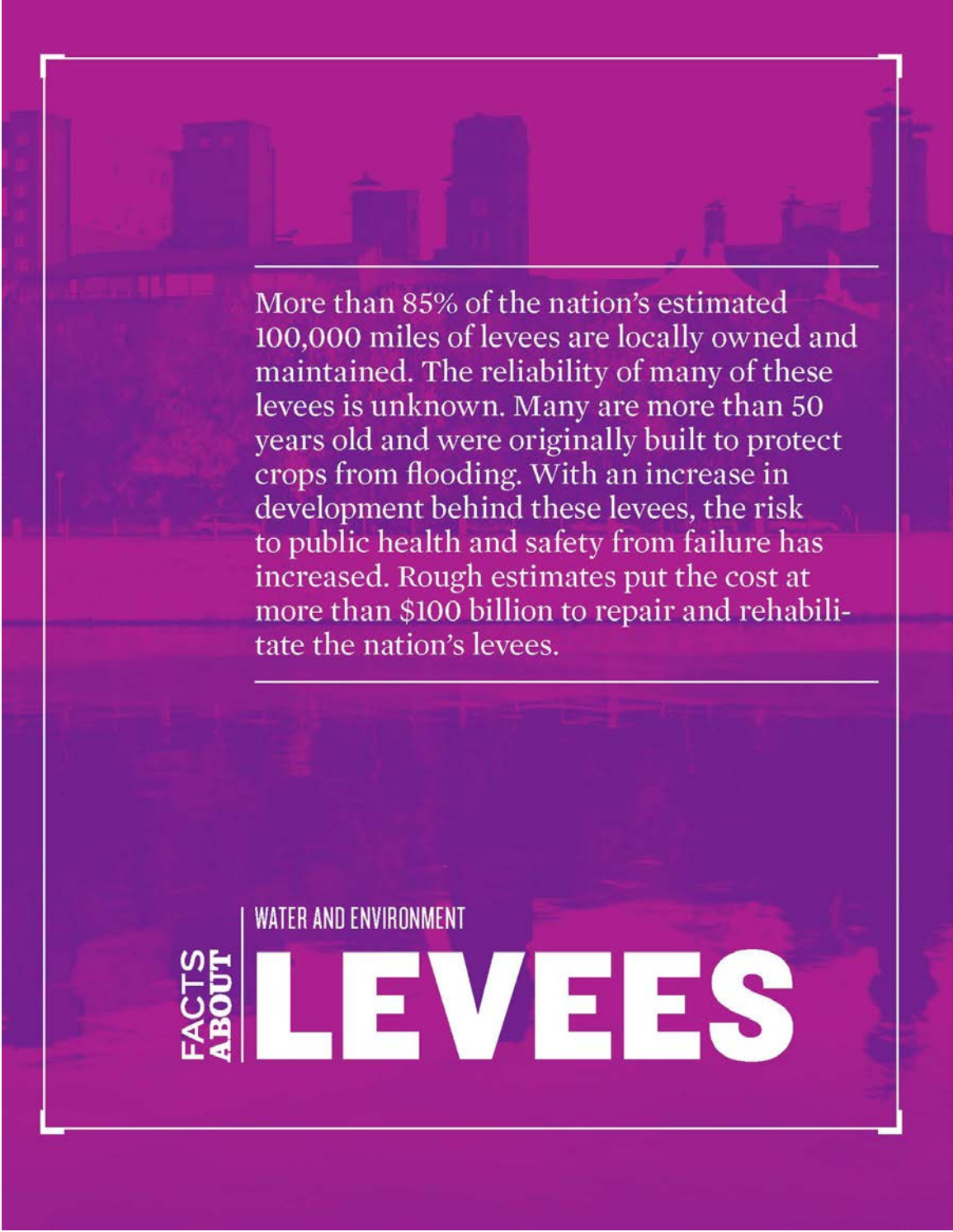
APPENDICES

Appendix A

ASCE (2009) Infrastructure Report Card, Category: Levees

2009 | INFRASTRUCTURE FACT SHEET

ASCE American Society of Civil Engineers

More than 85% of the nation's estimated 100,000 miles of levees are locally owned and maintained. The reliability of many of these levees is unknown. Many are more than 50 years old and were originally built to protect crops from flooding. With an increase in development behind these levees, the risk to public health and safety from failure has increased. Rough estimates put the cost at more than $100 billion to repair and rehabilitate the nation's levees.

WATER AND ENVIRONMENT

FACTS ABOUT **LEVEES**

RAISING THE GRADES
SOLUTIONS
THAT WILL WORK **NOW**

A = Exceptional
B = Good
C = Mediocre
D = Poor
F = Failing

AMERICA'S
INFRASTRUCTURE
G.P.A.

D

ESTIMATED 5-YEAR FUNDING
REQUIREMENTS FOR
LEVEES

Total investment needs
$50 BILLION

Estimated spending
$1.13 BILLION

Projected shortfall
$48.87 BILLION

★ **ADOPT** the following recommendations from the 2009 National Committee on Levee Safety:
ESTABLISH a National Levee Safety Commission;
COMPLETE the National Levee Inventory for both federal and nonfederal levees. The inventory must be regularly updated and maintained;
ADOPT a hazard potential classification system;
CREATE a strong education and outreach program to inform local leaders and residents about the level of protection they can expect from a nearby levee;[5]

★ **PHASE** in mandatory purchase of flood insurance with risk-based premiums for structures in areas protected by levees;

★ **INCREASE** funding at all levels of government to address structural and nonstructural solutions that reduce risk to people and property. Additionally, investments should be targeted to address life-cycle costs and research;

★ **REQUIRE** the development and exercising of emergency action plans for levee-protected areas;

★ **ENSURE** that operation and maintenance plans cover all elements of the system, recognizing that levees are part of complex systems that also include pumps, interior drainage systems, closures, penetrations, and transitions;

★ **ASSESS** levees using updated hydrology and hydraulic analyses that incorporate the impact of urbanization and climate change, particularly for coastal levees.

196

CONDITION

The state of the nation's levees has a significant impact on public safety. Levees are man-made barriers (embankment, floodwall, structure) along a water course constructed for the primary purpose of providing hurricane, storm and flood protection. Levees are often part of complex systems that include not only levees and floodwalls, but also pumps, interior drainage systems, closures, penetrations, and transitions. Many levees are integral to economic development in the protected community.

Federal levee systems currently provide a six-to-one return on flood damages prevented compared to initial building cost.[1] Despite this, baseline information has not been systematically gathered through inspections and post-flood performance observations and measurements to identify the most critical levee safety issues, quantify the true costs of levee safety, prioritize future funding, and provide data for risk-based assessments in an efficient or cost-effective manner.

There is no definitive record of how many levees there are in the U.S., nor is there an assessment of the current condition and performance of those levees. Recent surveys by the Association of State Dam Safety Officials and the Association of State Floodplain Managers found that only 10 states keep any listing of levees within their borders and only 23 states have an agency with some responsibility for levee safety. The Federal Emergency Management Agency (FEMA) estimates that levees are found in approximately 22% of the nation's 3,147 counties. Forty-three percent of the U.S. population lives in counties with levees.[4] Many of those levees were designed decades ago to protect agricultural and rural areas, not the homes and businesses that are now located behind them.[4]

In the aftermath of hurricanes Katrina and Rita in 2005, Congress passed the Water Resources Development Act (WRDA) of 2007. The Act required the establishment and maintenance of an inventory of all federal levees, as well as those non-federal levees for which information is voluntarily provided by state and local government agencies. The inventory is intended to be a comprehensive, geospatial database that is shared between the U.S. Army Corps of Engineers (USACE), FEMA, the Department of Homeland Security (DHS), and the states.

While the USACE has begun the inventory of all federal levees, to date few states or local agencies have provided any formal information, leaving the inventory far from complete. In addition, there is still much to be determined about the condition and performance of the nation's levees, both federal and nonfederal. As of February 2009, initial results from USACE's inventory show that while more than half of all federally inspected levees do not have any deficiencies, 177, or about 9%, are expected to fail in a flood event. The inventory data collection process is ongoing and these preliminary findings are expected to change as the process continues.[1,6]

WRDA 2007 also created a committee to develop for the first time recom-

197

TABLE 4.1 ★ Damages from Flooding in Levee-Related Areas

LOCATION/YEAR	DAMAGES IN DOLLARS
Midwest 1993	$272,872,070
North Dakota/Minnesota 1997	$152,039,604
Hurricane Katrina 2005	$16,467,524,782
Midwest 2008	$583,596,400

SOURCE National Committee on Levee Safety

mendations for a national levee safety program. The National Committee on Levee Safety completed its work in January 2009 and the panel recommended that improvements in levee safety be addressed through comprehensive and consistent national leadership, new and sustained state levee safety programs, and an alignment of existing federal programs.[1]

Often, the risk of living behind levees is not well-known, and the likelihood of flooding is misunderstood. For this reason, little focus is placed on measures that the public can take to mitigate their risks. Though the 1% annual chance flood event ("100-year flood") is believed by many to be an infrequent event, in reality there is at least a 26% chance that it will occur during the life of a 30-year mortgage. The likely impacts of climate change are expected to increase the intensity and frequency of coastal storms and thereby increase the chance of flooding.[6]

In 1968, Congress enacted the National Flood Insurance Program (NIFP). One of the primary purposes of the NFIP was to address the inability of the public to secure privately backed insurance for economic losses from flooding. The NFIP designated the 1% annual chance event ("100-year flood") as a special flood hazard area in which those holding federally backed mortgages would be required to purchase flood insurance.

Never intended to be a safety standard, the 1% annual chance event became the target design level for many levees because it allowed development to con-

> There is no definitive record of how many levees there are in the U.S., nor is there an assessment of the current condition and performance of those levees.

198

FIGURE 4.1 ★ Likelihood of Levee Failure/Flooding Over a 30-Year Residential Mortgage
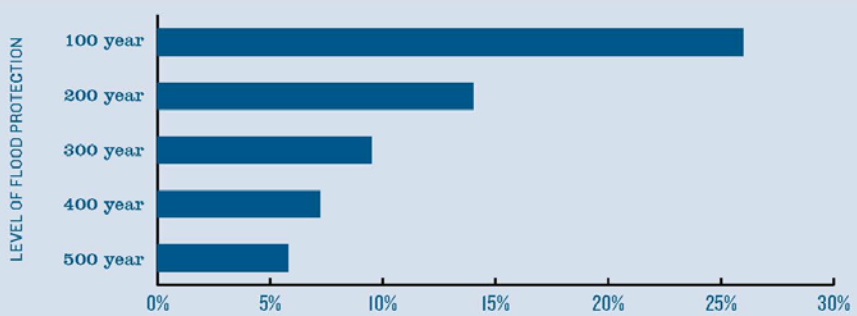
SOURCE National Committee on Levee Safety

tinue while providing relief from mandatory flood insurance purchase for homeowners living behind accredited levees. Allowing levees to simply meet the minimum requirements of the NFIP has created an unintentional—and potentially dangerous—flood insurance standard that is now used as a safety standard.

During the past 50 years there has been tremendous development on lands protected by levees. Coupled with the fact that many levees have not been well maintained, this burgeoning growth has put people and infrastructure at risk—the perceived safety provided by levees has inadvertently increased flood risks by attracting development to the floodplain. Continued population growth and economic development behind levees is considered by many to be the dominant factor in the national flood risk equation, outpacing the effects of increased chance of flood occurrence and the degradation of levee condition. Unfortunately, lands protected by levees have not always been developed in a manner that recognizes the benefits of the rivers and manages the risk of flooding.

Additionally, in the absence of a comprehensive levee inventory, there are many uncertainties regarding location, performance, and condition of levees. There has been a lack of formal government oversight, sufficient technical standards, and effective communication of the risks of living behind a levee, further placing people and property in danger of floods.

Finally, FEMA's Flood Map Modernization Program, which remaps floodplains using modern technologies, is resulting in a reexamination of levees throughout the United States to determine if they can still be accredited. Before accrediting a levee, FEMA is requiring many communities to certify that their levees meet the 1% criteria.

199

UNITED STATES ★ National Levee Safety Commission

After decades of ignoring the safety and condition of the nation's levees, the U.S. Congress in 2007 recognized the dangers that a lack of a federal levee safety program posed to the nation. As part of the Water Resources Development Act, the USACE was charged with developing guidelines for a program and released its report in January 2009. This, in conjunction with the national levee inventory, is an important first step to protecting lives and property behind the nation's levees.

CALIFORNIA ★ Investment in Levees

There are more levees in California than in any other state. The levee systems in California are fragile and subject to the risk of failure. Estimates put the cost of bringing the state's levees and flood control system up to good condition at $42.2 billion. In February 2006, Governor Arnold Schwarzenegger proclaimed a state of emergency for the California levee system to address the problems. Voters in the state agreed with the need for comprehensive repairs and modernization and approved a multibillion-dollar bond issue to begin the funding process in 2006. *Photo courtesy of the California Department of Water Resources, Division of Safety of Dams.*

MISSISSIPPI RIVER ★ Levee Protection

Since 1885, the USACE has been armoring more than 1,000 miles of levees on the Mississippi River to prevent scour and protect the population behind the levee. Over the years, the Corps has developed a process of plating the levees with concrete mats that prevent erosion. To date, about 95% of the levees under the New Orleans District jurisdiction, which reaches as far north as Cairo, Illinois, have been armored and the bulk of work performed today is maintenance on the work completed in the last century.[7] BELOW: USACE mat sinking unit, placing concrete revetment mattresses along the Mississippi in Poydras, Louisiana. *Photo courtesy of Angelle Bergeron, New Orleans Correspondent,* Engineering News-Record.

201

Flood insurance is one of the most effective ways to limit financial damages in the case of flooding and speed recovery of flood damaged communities. Currently, many people who live behind levees do not believe that they need flood insurance, believing that they are protected by a levee structure. Requiring the purchase of mandatory flood insurance is intended to increase the understanding that living behind even well-engineered levees has some risk. This may encourage communities to build levees to exceed the 1% annual-chance protection standard that has mistakenly become a target minimum.

RESILIENCE

Levees serve to protect the public and critical infrastructure and to prevent flooding. With increasing development behind existing levees, the risk to public health and safety from failure has increased. To address the current lack of resilience in the nation's levee system, DHS has included levees within the critical infrastructure protection program in an attempt to identify those levees that present the greatest risk to the nation. DHS has also funded research to increase the robustness of levees—for example, armoring the slopes to resist erosion should floodwaters exceed the design elevation— and technologies are currently under study to rapidly repair any breaches that may occur in a levee. To ensure system integrity, future investments must also focus on life-cycle maintenance, research, development of emergency action plans for levee-protected areas, and security.

CONCLUSION

Much is still unknown about the condition of the nation's tens of thousands of miles of levees. The residual risk to life and property behind such structures cannot be ignored. Due to their impact on life and safety issues, and the significant consequences of failure, as well as the financial burden of falling property values behind levees that are not safe and are being decertified, the nation must not delay addressing levee issues. ★

SOURCES

1 U.S. Army Corps of Engineers, Summary Information from U.S. Levee Inventory.

2 Lee Bowman and Thomas Hargrove, Scripps Howard News Service, "America's Neglected Levees Put Millions in Danger," July, 2008.

3 U.S. Senate Testimony by Gerald Galloway, October 2, 2007.

4 Federal Emergency Management Agency, "The National Levee Challenge: Report of the Interagency Levee Policy Review Committee," September 2006.

5 National Committee on Levee Safety "Recommendations for a National Levee Safety Program," January 2009.

6 Peter Eisler, "Army Corps Cracks Down on Flunking Levees," USA Today, February 24, 2008.

7 Angelle Bergeron "Technique Conquers All as Long-Running Job Nears End," Engineering News-Record, January 19, 2009.

202

Appendix B

Flood Control Act, U.S. Congress (1917)

CHAP. 141.—An Act Granting the consent of Congress to the County of Pearl River, Mississippi, and the fourth ward of the Parish of Washington, Louisiana, to construct a bridge across Pearl River, between Pearl River County, Mississippi, and Washington Parish, Louisiana.

Pearl River.
Pearl River County, Miss., and Washington Parish, La., may bridge.

Be it enacted by the Senate and House of Representatives of the United States of America in Congress assembled, That the consent of Congress is hereby granted to the county of Pearl River, Mississippi, and the fourth ward of the parish of Washington, State of Louisiana, and their successors and assigns, to construct, maintain, and operate a bridge and approaches thereto across the Pearl River at a point suitable to the interests of navigation, at or near the fourth ward of the parish of Washington, State of Louisiana, in accordance with the provisions of the Act entitled "An Act to regulate the construction of bridges over navigable waters," approved March twenty-third, nineteen hundred and six.

Construction.
Vol. 34, p. 84.

Amendment.

SEC. 2. That the right to alter, amend, or repeal this Act is hereby expressly reserved.

Approved, February 27, 1917.

CHAP. 144.—An Act To provide for the control of the floods of the Mississippi River and of the Sacramento River, California, and for other purposes.

Mississippi River.

Plans adopted for flood control, etc., to mouth of the Ohio.

Be it enacted by the Senate and House of Representatives of the United States of America in Congress assembled, That for controlling the floods of the Mississippi River and continuing its improvement from the Head of the Passes to the mouth of the Ohio River the Secretary of War is hereby empowered, authorized, and directed to carry on continuously, by hired labor or otherwise, the plans of the Mississippi River Commission heretofore or hereafter adopted, to be paid for as appropriations may from time to time be made by law, not to exceed in the aggregate $45,000,000: *Provided,* That not more than $10,000,000 shall be expended therefor during any one fiscal year.

Limit of cost.
Proviso.
Annual expenditures.
Scope of improvements.

(a) All money appropriated under authority of this section shall be expended under the direction of the Secretary of War in accordance with the plans, specifications, and recommendations of the Mississippi River Commission as approved by the Chief of Engineers, for controlling the floods and for the general improvement of the Mississippi River, and for surveys, including the survey from the Head of the Passes to the headwaters of the river, and a survey of the Atchafalaya Outlet so far as may be necessary to determine the cost of protecting its basin from the flood waters of the Mississippi River either by its divorcement from the Mississippi River or by other means, and for salaries, clerical, office, traveling, and miscellaneous expenses of the Mississippi River Commission.

Surveys to headwaters.
Atchafalaya Outlet.

Salaries.

Levees.
Amount conditional on local, etc., contribution.

(b) That no money appropriated under authority of this section shall be expended in the construction or repair of any levee unless and until assurances have been given satisfactory to the commission that local interests protected thereby will contribute for such construction and repair a sum which the commission shall determine to be just and equitable but which shall not be less than one-half of such sum as may have been allotted by the commission for such work: *Provided,* That such contributions shall be expended under the direction of the commission, or in such manner as it may require or approve, but no contribution made by any State or levee district shall be expended in any other State or levee district except with the approval of the authorities of the State or district so contributing.

Proviso.
Approval of expenditure.
Use of contributions.

Levee work may be extended to Rock Island, Ill.

(c) Any funds which may hereafter be appropriated under authority of this Act for improving the Mississippi River between the Head of the Passes and the mouth of the Ohio River, and which may be

allotted to levees, may be expended upon any part of said river between the Head of the Passes and Rock Island, Illinois.

(d) No money appropriated under authority of this Act shall be expended in payment for any right of way for any levee which may be constructed in cooperation with any State or levee district under authority of this Act, but all such rights of way shall be provided free of cost to the United States: *Provided,* That no money paid or expense incurred by any State or levee district in securing such rights of way, or in any temporary works of emergency during an impending flood, or for the maintenance of any levee line, shall be computed as a part of the contribution of such State or levee district toward the construction or repair of any levee within the meaning of paragraph (b) of this section. *Rights of way to be provided free of cost.*

Proviso.
Moneys for, not included in contributions to construction, etc.

That the watercourses connected with the Mississippi River to such extent as may be necessary to exclude the flood waters from the upper limits of any delta basin, together with the Ohio River from its mouth to the mouth of the Cache River, may, in the discretion of said commission, receive allotments for improvements now under way or hereafter to be undertaken. *Allotments to connecting watercourses.*

Upon the completion of any levee constructed for flood control under authority of this Act, said levee shall be turned over to the levee district protected thereby for maintenance thereafter; but for all other purposes the United States shall retain such control over the same as it may have the right to exercise upon such completion. *Maintenance of completed levees by local interests.*

SACRAMENTO RIVER, CALIFORNIA.

Sacramento River, Cal.

Sec. 2. That for controlling the floods, removing the débris, and continuing the improvement of the Sacramento River, California, in accordance with the plans of the California Débris Commission, the Secretary of War is hereby authorized and directed to carry on continuously, by hired labor or otherwise, the plan of said commission contained in its report submitted August tenth, nineteen hundred and ten, and printed in House Document Numbered Eighty-one, Sixty-second Congress, first session, as modified by the report of said commission submitted February eighth, nineteen hundred and thirteen, approved by the Chief of Engineers of the United States Army and the Board of Engineers for Rivers and Harbors, and printed in Rivers and Harbors Committee Document Numbered Five, Sixty-third Congress, first session, in so far as said plan provides for the rectification and enlargement of river channels and the construction of weirs, to be paid for as appropriations may from time to time be made by law, not to exceed in the aggregate $5,600,000: *Provided,* That not more than $1,000,000 shall be expended therefor during any one fiscal year. *Plan adopted for flood control, etc.*

Limit of cost.
Proviso.
Annual expenditures.

(a) All money appropriated under authority of this section shall be expended under the direction of the Secretary of War, in accordance with the plans, specifications, and recommendations of the California Débris Commission, as approved by the Chief of Engineers, for the control of floods, removal of débris, and the general improvement of the Sacramento River: *Provided,* That no money shall be expended under authority of this section until assurances have been given satisfactory to the Secretary of War (a) that the State of California will contribute annually for such work a sum equal to such sum as may be expended annually therefor by the United States under authority of this section; (b) that such equal contributions by the State of California will continue annually until the full equal share of the cost of such work shall have been contributed by said State; and (c) that the river levees contemplated in the report of the California Débris Commission, dated August tenth, nineteen hundred and ten, will be constructed to such grade and section and *Scope of improvement, etc.*

Proviso.
Assurance of annual contribution by State.

Continuance, etc.

Levee construction.

State expenditures limited.

within such time as may be required by said commission: *Provided further*, That said State shall not be required to expend for such work, for any one year, a sum larger than that expended thereon by the United States during the same year: *And provided further*, That the total contributions so required of the State of California shall not exceed in the aggregate, $5,600,000.

Total amount.

Expenditure of State contribution.

(b) All money contributed by the State of California, as herein provided, shall be expended under the direction of the California Débris Commission and in such manner as it may require or approve, and no money appropriated under authority of this section shall be expended in the purchase of or payment for any right of way, easement, or land acquired for the purposes of this improvement, but all such rights of way, easements, and lands shall be provided free of cost to the United States: *Provided*, That no money paid or expense incurred therefor shall be computed as a part of the contribution of the State of California toward the work of improvement herein provided for within the meaning of paragraph (a) of this section.

Free rights of way.

Proviso.
Not included in improvement work.

(c) Upon the completion of all works for flood control herein authorized the said works shall be turned over to the State of California for maintenance thereafter; but for all other purposes the United States shall retain such control over the same as it may have the right to exercise upon such completion.

Maintenance by State when completed.

General provisions.

GENERAL PROVISIONS.

Laws applicable.

Sec. 3. That all the provisions of existing law relating to examinations and surveys and to works of improvement of rivers and harbors shall apply, so far as applicable, to examinations and surveys and to works of improvement relating to flood control. And all expenditures of funds hereafter appropriated for works and projects relating to flood control shall be made in accordance with and subject to the law governing the disbursement and expenditure of funds appropriated for the improvement of rivers and harbors.

Disbursements.

Flood-control surveys.

All examinations and surveys of projects relating to flood control shall include a comprehensive study of the watershed or watersheds, and the report thereon in addition to any other matter upon which a report is required shall give such data as it may be practicable to secure in regard to (a) the extent and character of the area to be affected by the proposed improvement; (b) the probable effect upon any navigable water or waterway; (c) the possible economical development and utilization of water power; and (d) such other uses as may be properly related to or coordinated with the project. And the heads of the several departments of the Government may, in their discretion, and shall upon the request of the Secretary of War, detail representatives from their respective departments to assist the Engineers of the Army in the study and examination of such watersheds, to the end that duplication of work may be avoided and the various services of the Government economically coordinated therein: *Provided*, That all reports on preliminary examinations hereafter authorized, together with the report of the Board of Engineers for Rivers and Harbors thereon and the separate report of the representative of any other department, shall be submitted to the Secretary of War by the Chief of Engineers, with his recommendations, and shall be transmitted by the Secretary of War to the House of Representatives, and are hereby ordered to be printed when so made.

Scope of reports.

Area affected.

Navigation.
Water-power utilization.

Assistance of other departments, etc.

Proviso.
Printing, etc., reports.

Board of Engineers for Rivers and Harbors to report on projects.

In the consideration of all works and projects relating to flood control which may be submitted to the Board of Engineers for Rivers and Harbors for consideration and recommendation, said board shall, in addition to any other matters upon which it may be required to report, state its opinion as to (a) what Federal interest, if any, is involved in the proposed improvement; (b) what share of the expense,

if any, should be borne by the United States; and (c) the advisability of adopting the project.

All examinations and reports which may now be made by the Board of Engineers for Rivers and Harbors upon request of the Committee on Rivers and Harbors relating to works or projects of navigation shall in like manner be made upon request of the Committee on Flood Control on all works and projects relating to flood control. *Examinations on request of Flood Control Committee.*

Sec. 4. That the salary of the civilian members of the Mississippi River Commission shall hereafter be $5,000 per annum. *Mississippi River Commission. Pay increased. Vol. 21, p. 37.*

Approved, March 1, 1917.

CHAP. 145.—An Act To provide a civil government for Porto Rico, and for other purposes. *March 2, 1917. [H. R. 9533.] [Public, No. 368.]*

Be it enacted by the Senate and House of Representatives of the United States of America in Congress assembled, That the provisions of this Act shall apply to the island of Porto Rico and to the adjacent islands belonging to the United States, and waters of those islands; and the name Porto Rico as used in this Act shall be held to include not only the island of that name but all the adjacent islands as aforesaid. *Porto Rico civil government. Territory included.*

BILL OF RIGHTS.

Bill of rights.

Sec. 2. That no law shall be enacted in Porto Rico which shall deprive any person of life, liberty, or property without due process of law, or deny to any person therein the equal protection of the laws. *Protection of life, liberty, and property.*

That in all criminal prosecutions the accused shall enjoy the right to have the assistance of counsel for his defense, to be informed of the nature and cause of the accusation, to have a copy thereof, to have a speedy and public trial, to be confronted with the witnesses against him, and to have compulsory process for obtaining witnesses in his favor. *Criminal prosecutions.*

That no person shall be held to answer for a criminal offense without due process of law; and no person for the same offense shall be twice put in jeopardy of punishment, nor shall be compelled in any criminal case to be a witness against himself. *Trials, etc.*

That all persons shall before conviction be bailable by sufficient sureties, except for capital offenses when the proof is evident or the presumption great. *Bail; exception.*

That no law impairing the obligation of contracts shall be enacted. *Contracts.*

That no person shall be imprisoned for debt. *Imprisonment for debt.*

That the privilege of the writ of habeas corpus shall not be suspended, unless when in case of rebellion, insurrection, or invasion the public safety may require it, in either of which events the same may be suspended by the President, or by the governor, whenever during such period the necessity for such suspension shall exist. *Writ of habeas corpus.*

That no ex post facto law or bill of attainder shall be enacted. *Ex post facto laws, etc.*

Private property shall not be taken or damaged for public use except upon payment of just compensation ascertained in the manner provided by law. *Public use of private property.*

Nothing contained in this Act shall be construed to limit the power of the legislature to enact laws for the protection of the lives, health, or safety of employees. *Life, health, etc., of employees.*

That no law granting a title of nobility shall be enacted, and no person holding any office of profit or trust under the government of Porto Rico shall, without the consent of the Congress of the United States, accept any present, emolument, office, or title of any kind whatever from any king, queen, prince, or foreign State, or any officer thereof. *Titles of nobility, etc.*
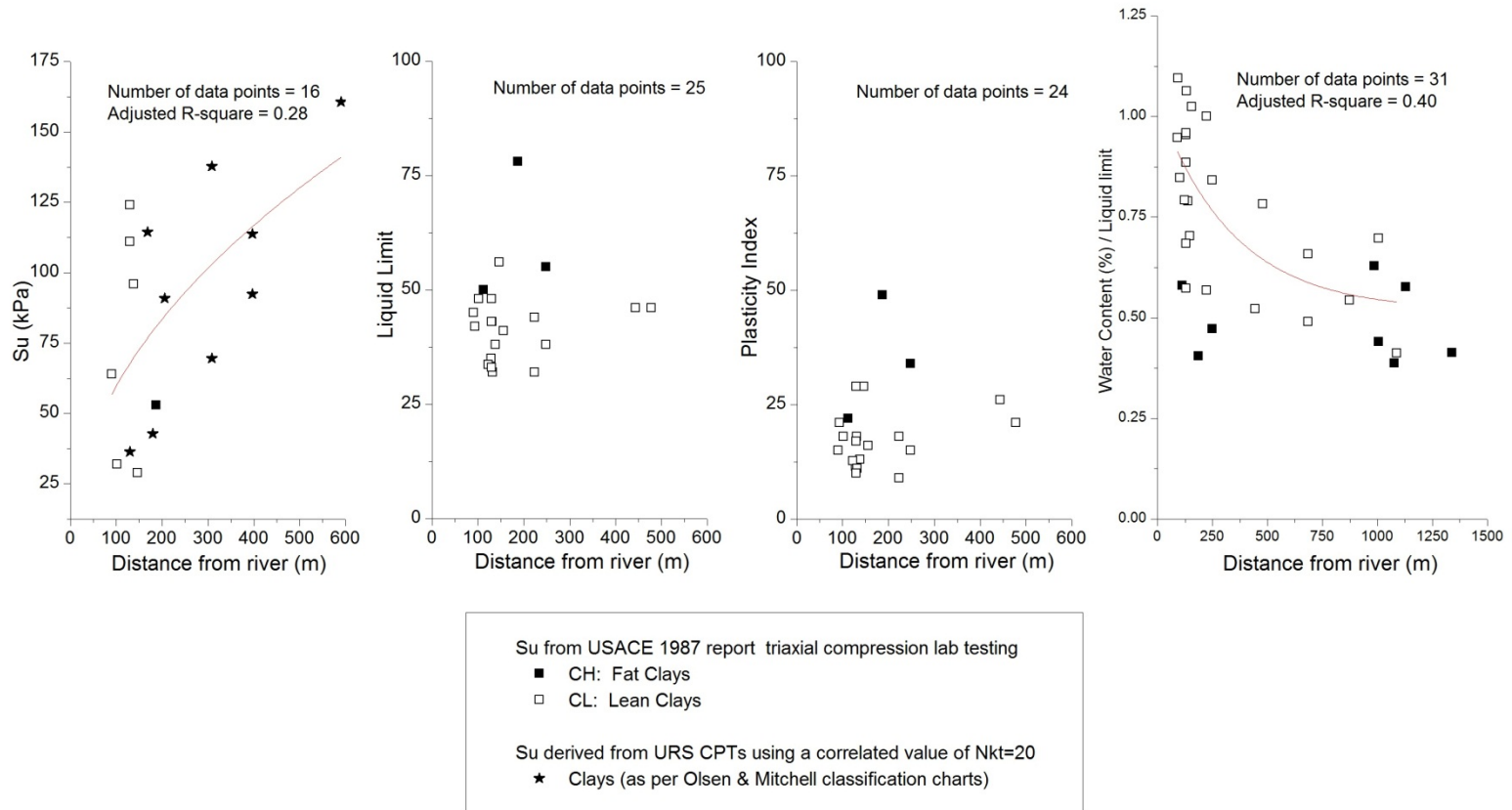
Appendix C

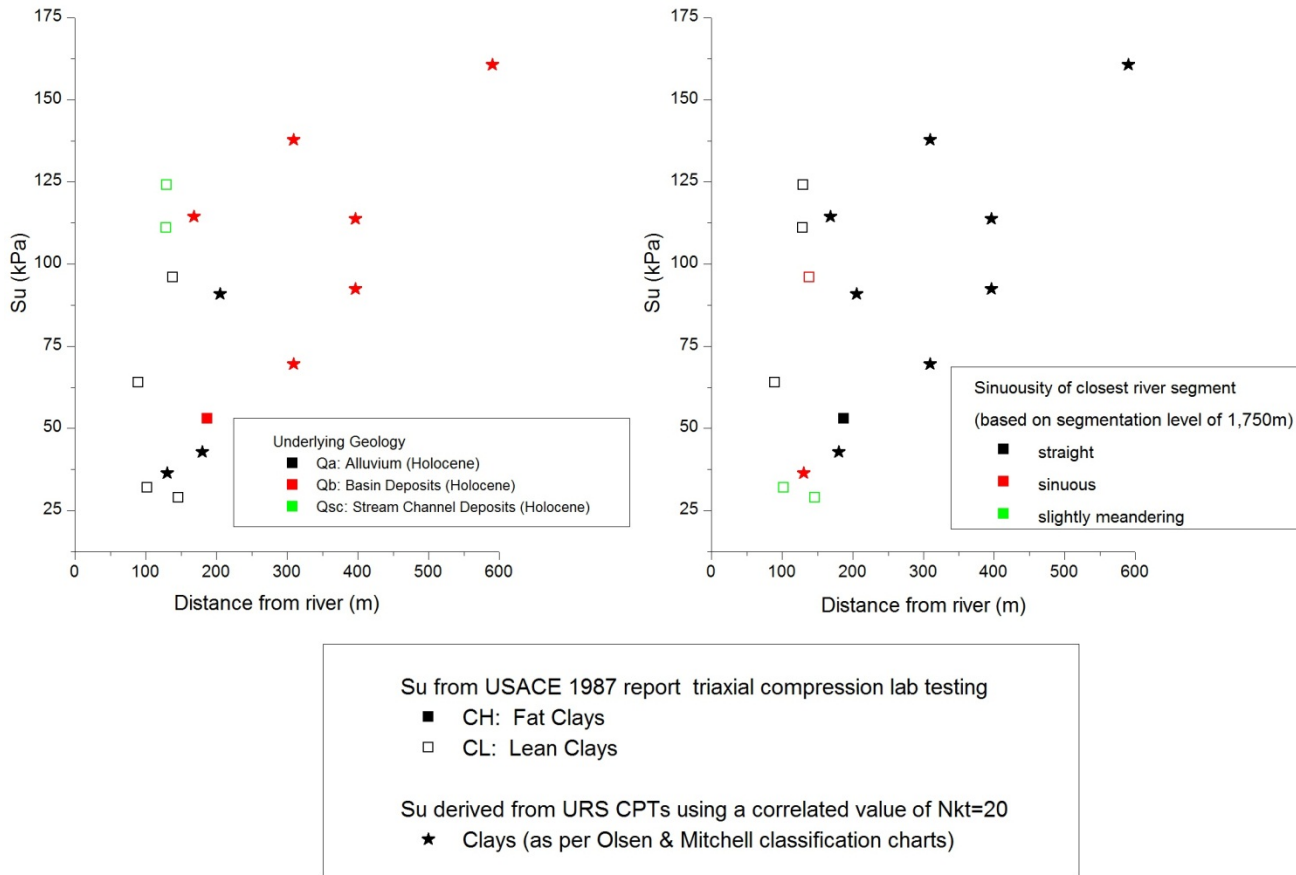**Correlation of Soil Parameters to Regional Factors**

SACRAMENTO

<u>Shallow Clay Layer</u>
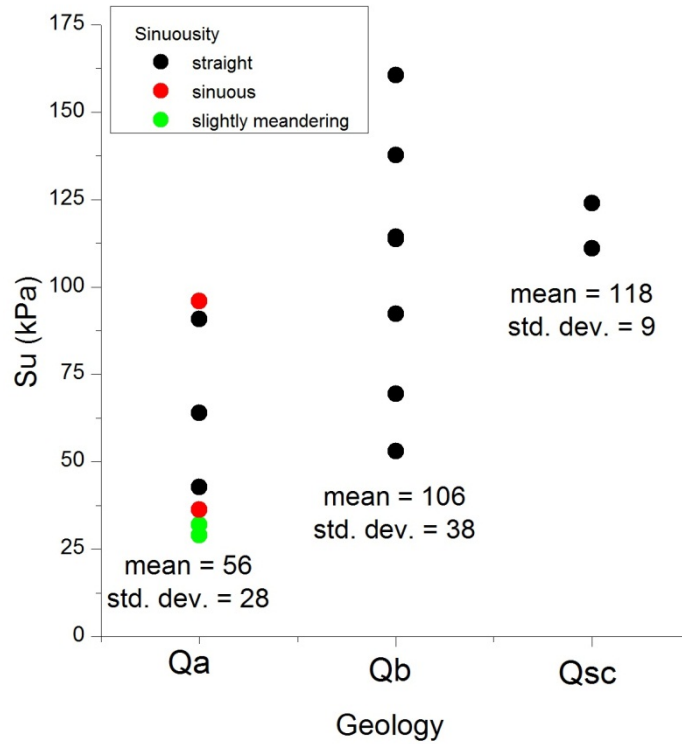
Relation of soil parameters to distance from centerline of closest river segment (m) for shallow clay layer in Sacramento
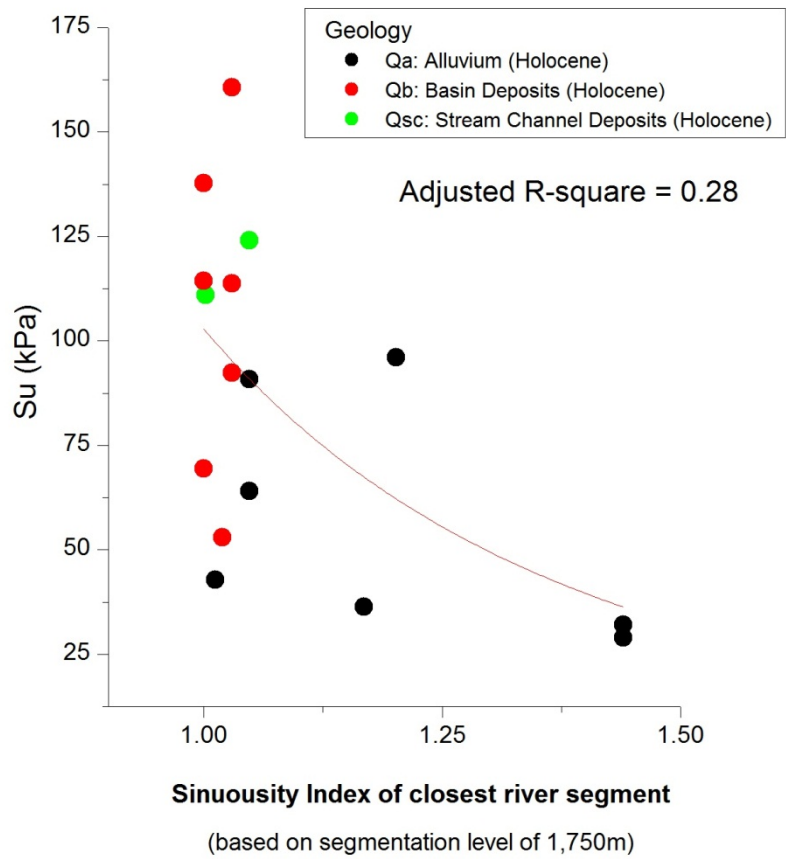
Relation of shear strength S$_u$ (kPa) to distance from centerline of closest river segment (m) for shallow clay layer in Sacramento
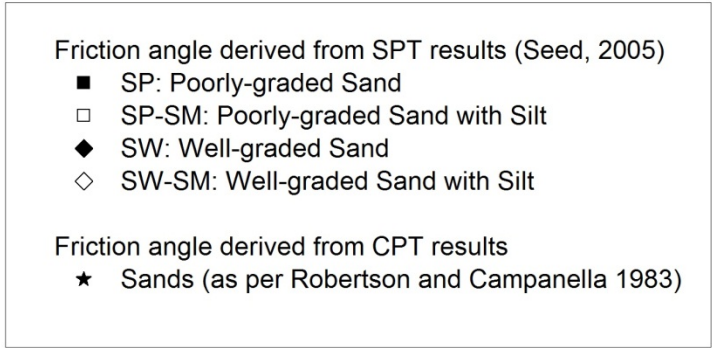
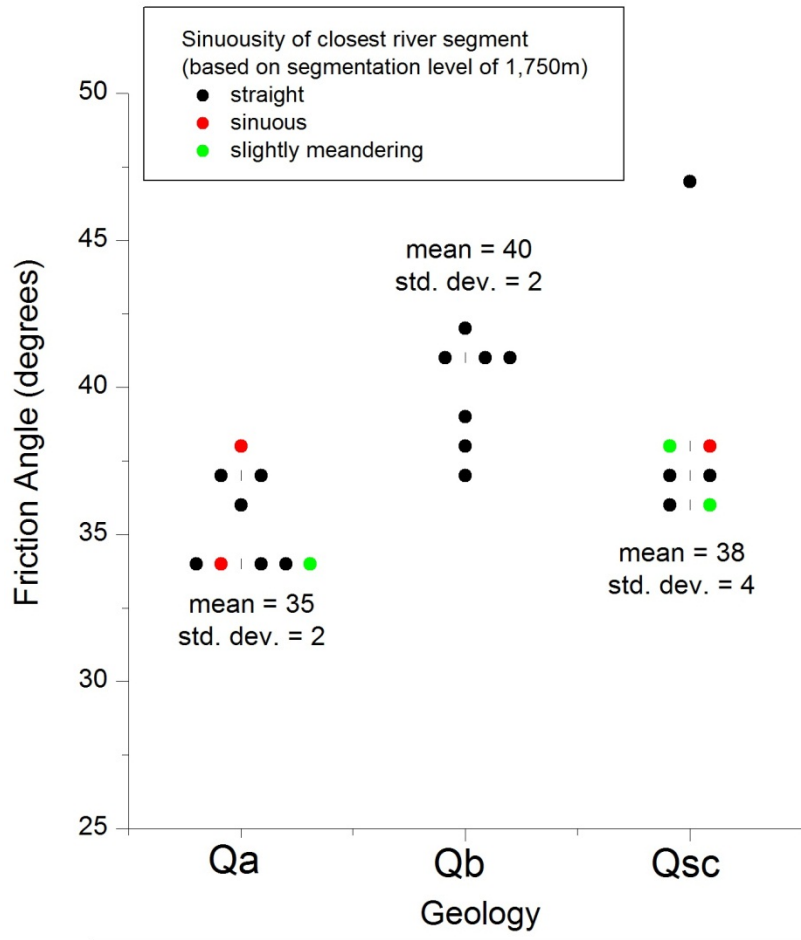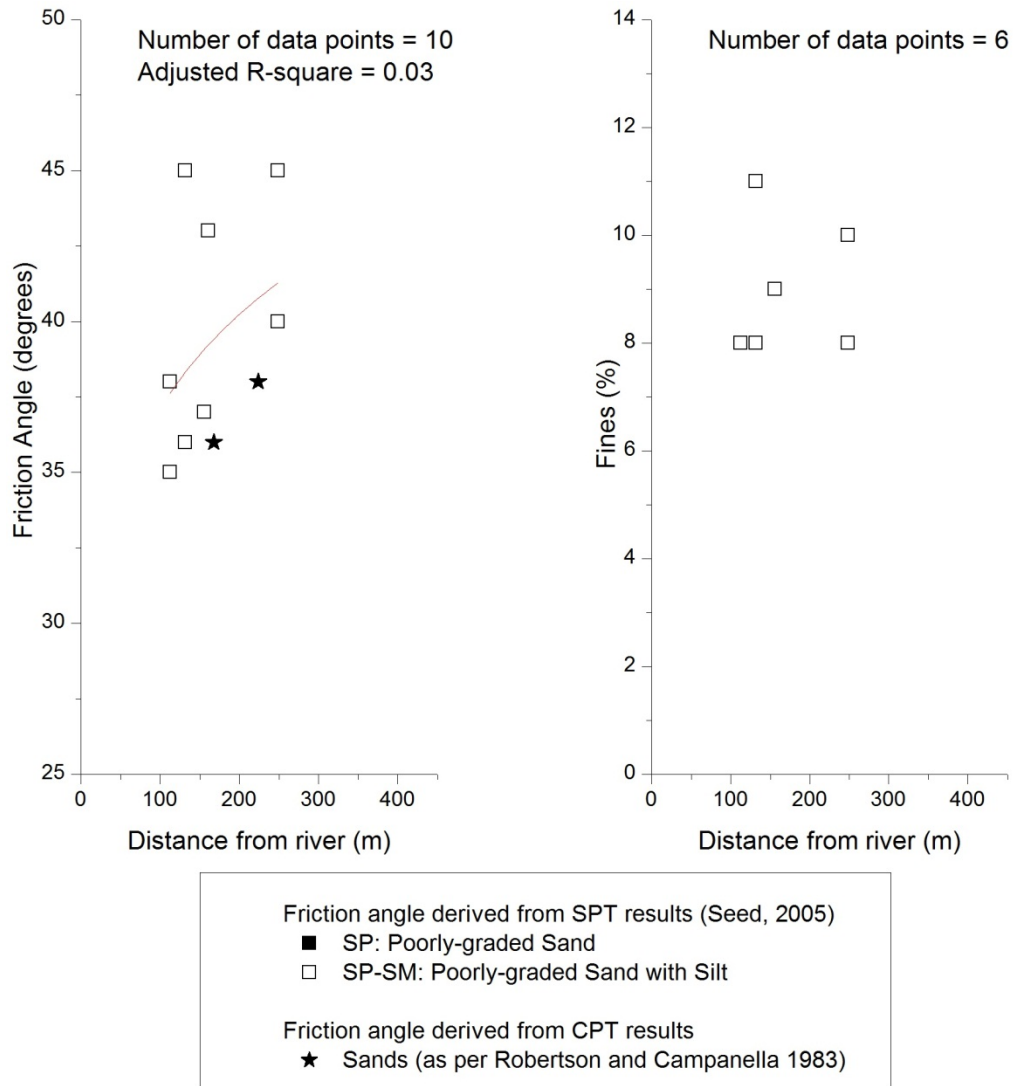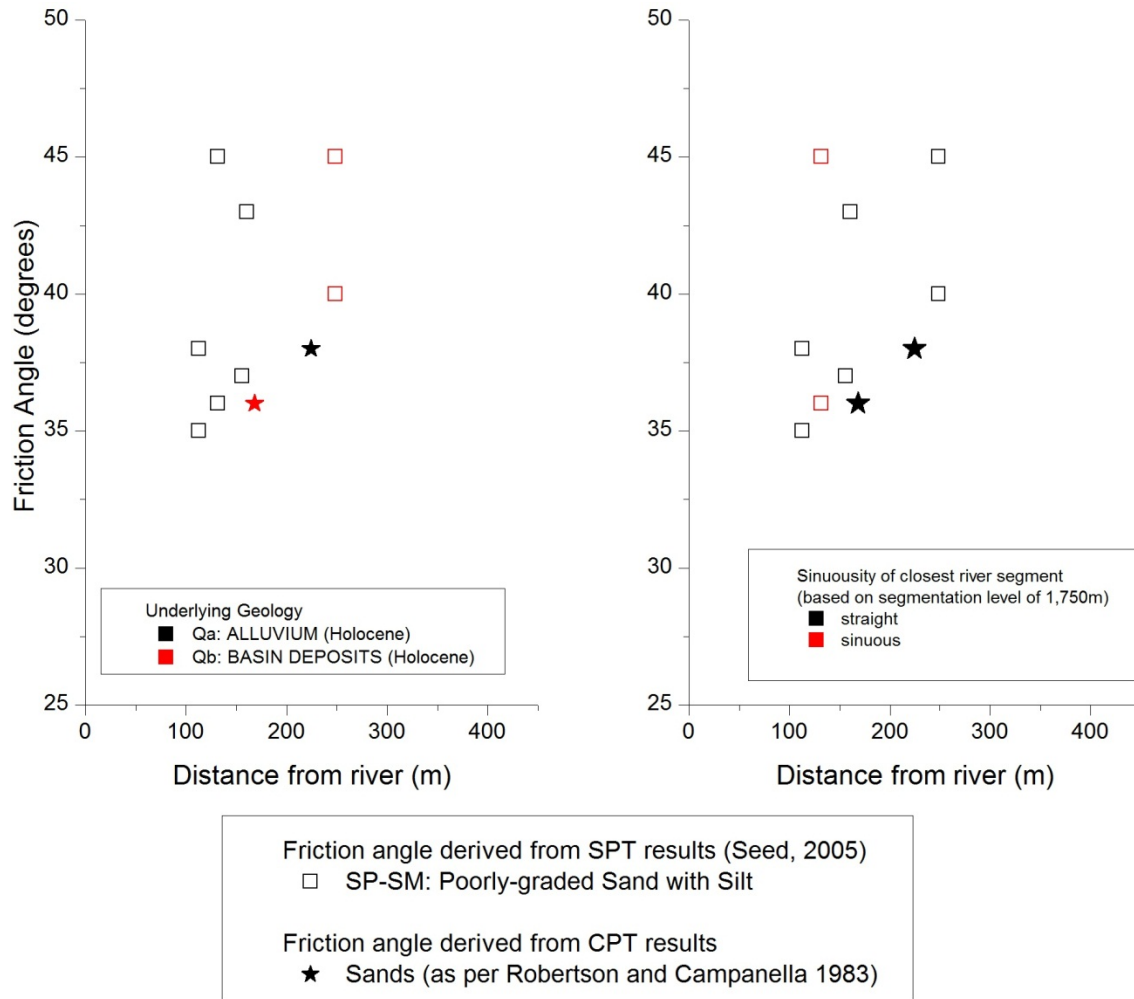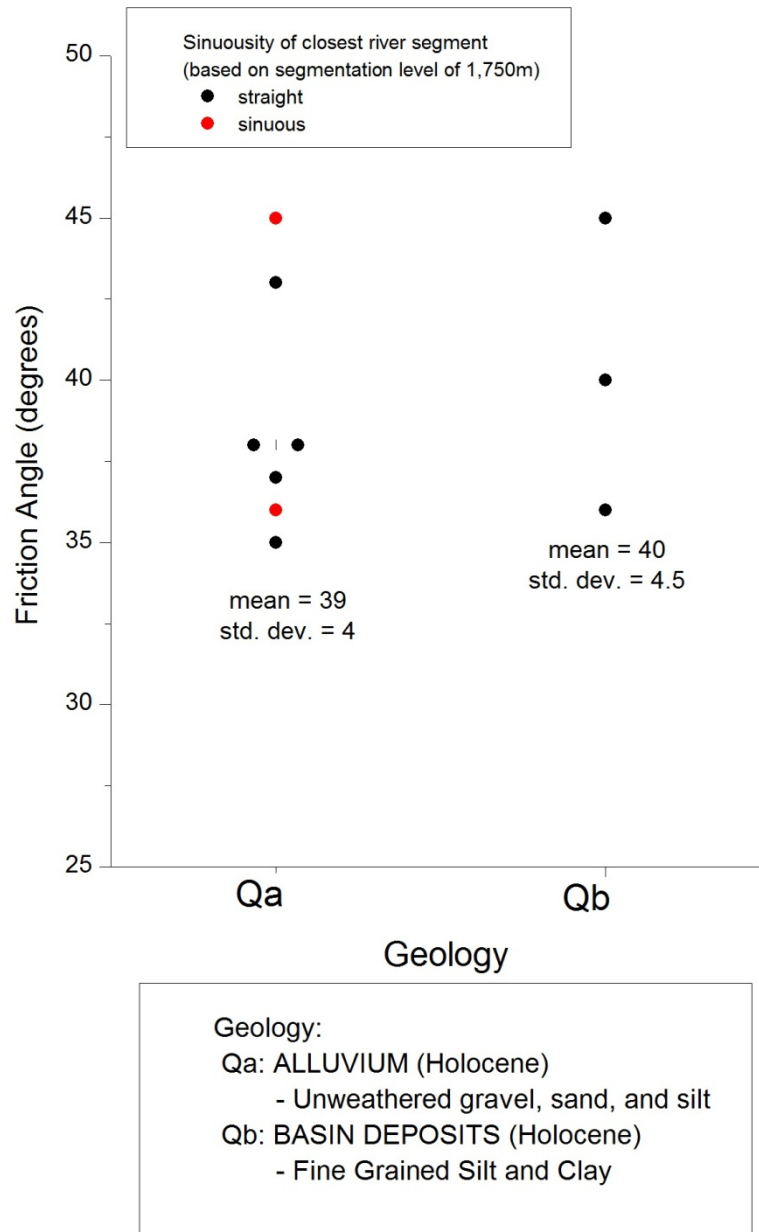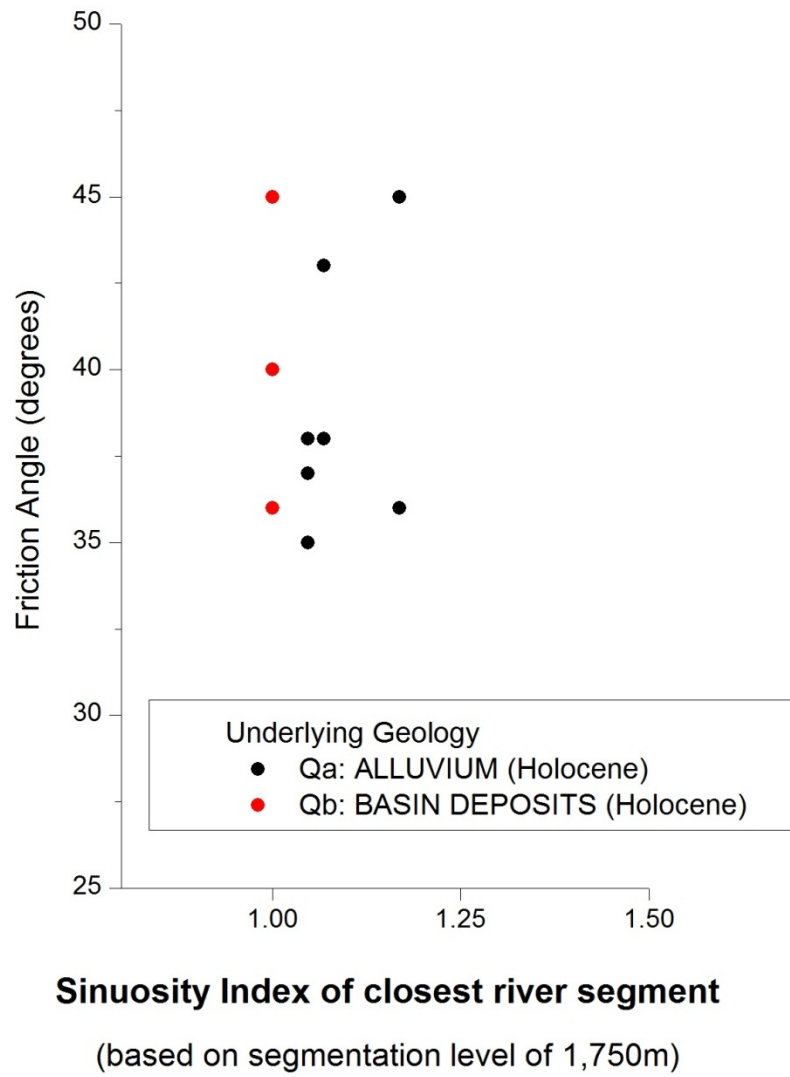**Relation of shear strength S_u (kPa) to geology for shallow clay layer in Sacramento**

Relation of shear strength S$_u$ (kPa) to Sinuosity Index for shallow clay layer in Sacramento

SACRAMENTO

Shallow Sand Layer

Relation of soil parameters to distance from centerline of closest river segment (m) for shallow sand layer in Sacramento

Relation of friction angle ϕ (degrees) to distance from centerline of closest river segment (m) for shallow sand layer in Sacramento

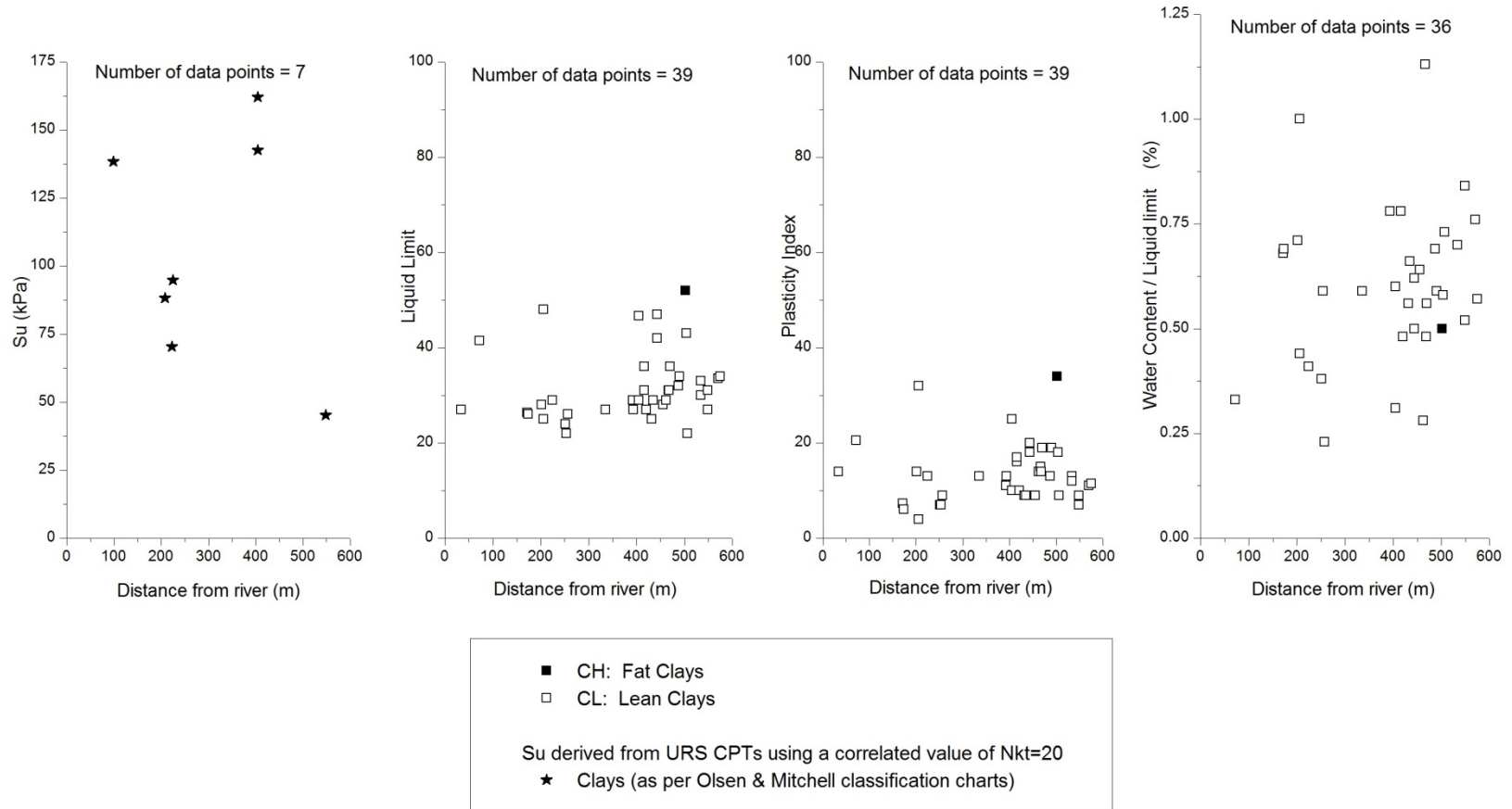**Relation of friction angle φ (degrees) to geology for shallow sand layer in Sacramento**

Sinuosity Index of closest river segment

(based on segmentation level of 1,750m)

Relation of friction angle φ (degrees) to Sinuosity Index for shallow sand layer in Sacramento

SACRAMENTO

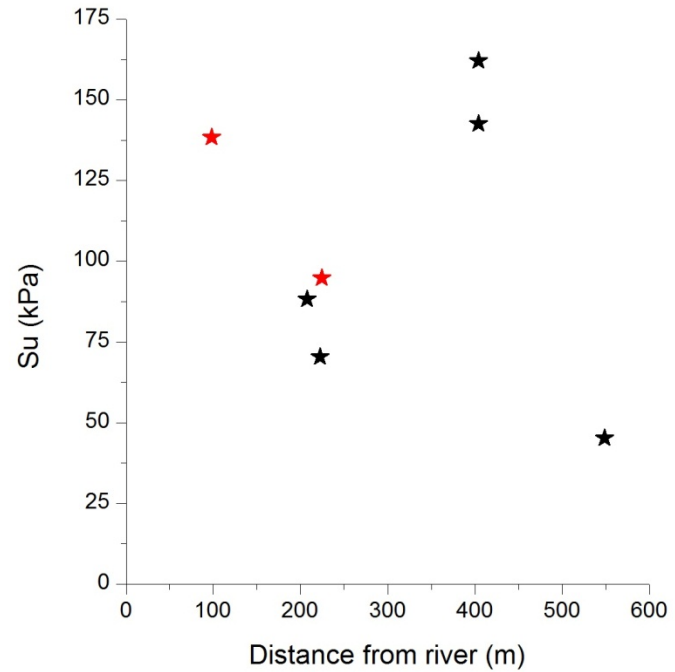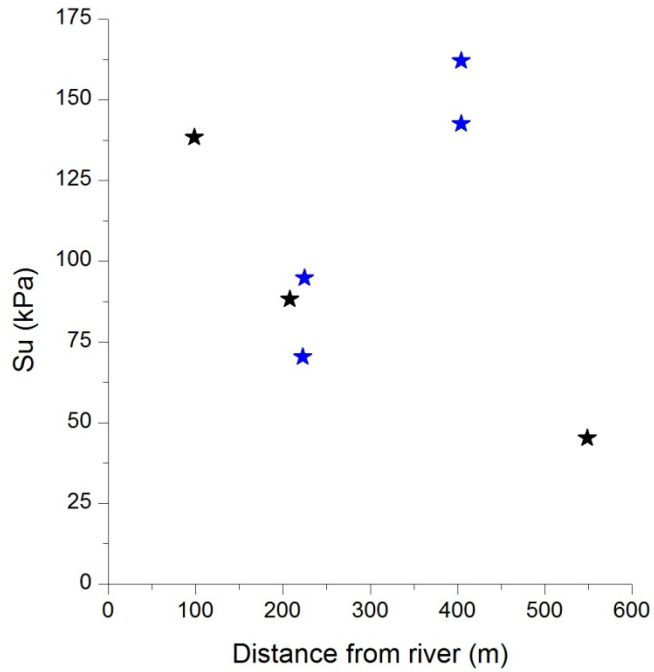## Deep Clay Layer
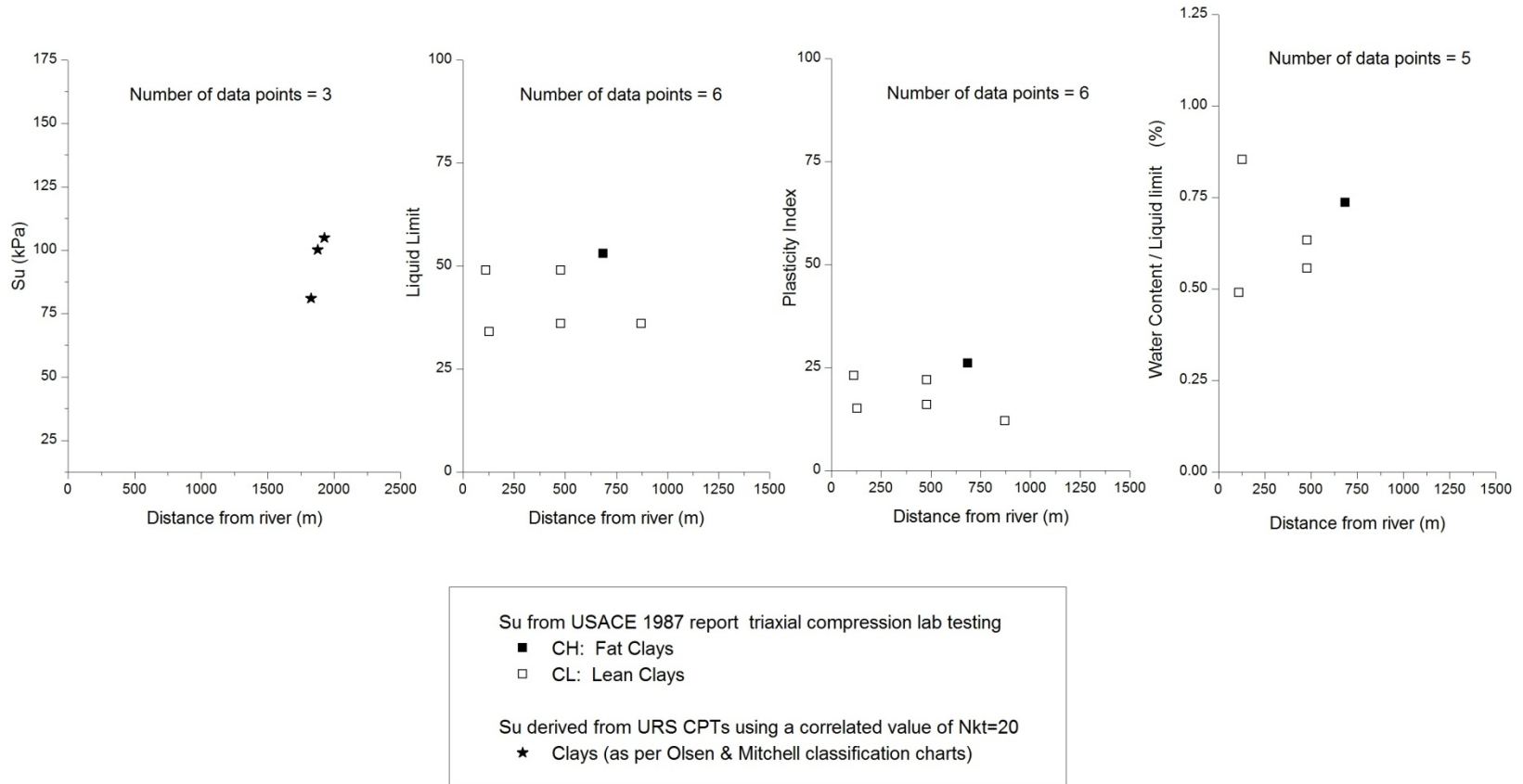
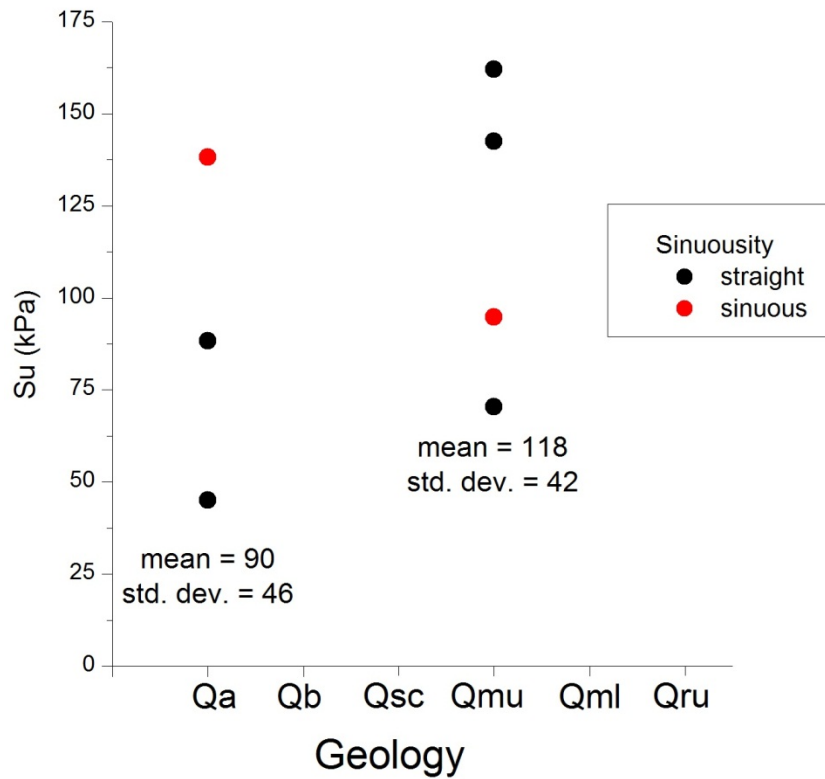**Relation of soil parameters to distance from centerline of closest river segment (m) for deep clay layer in Sacramento**

SACRAMENTO

<u>Deep Sand Layer</u>

Left plot:

Number of data points = 10
Adjusted R-square = 0.03

Friction Angle (degrees) vs Distance from river (m)

Right plot:

Number of data points = 6

Fines (%) vs Distance from river (m)

Friction angle derived from SPT results (Seed, 2005)
■ SP: Poorly-graded Sand
□ SP-SM: Poorly-graded Sand with Silt

Friction angle derived from CPT results
★ Sands (as per Robertson and Campanella 1983)

Relation of soil parameters to distance from centerline of closest river segment (m) for deep sand layer in Sacramento

Relation of friction angle φ (degrees) to distance from centerline of closest river segment (m) for deep sand layer in Sacramento

Legend (in plot):
Sinuousity of closest river segment
(based on segmentation level of 1,750m)
● straight
● sinuous

Qa: mean = 39
std. dev. = 4

Qb: mean = 40
std. dev. = 4.5

Friction Angle (degrees) — y-axis

Geology — x-axis (Qa, Qb)

Geology:
  Qa: ALLUVIUM (Holocene)
      - Unweathered gravel, sand, and silt
  Qb: BASIN DEPOSITS (Holocene)
      - Fine Grained Silt and Clay

Relation of friction angle ϕ (degrees) to geology for shall deep sand layer in Sacramento

Relation of friction angle ϕ (degrees) to Sinuosity Index for deep sand layer in Sacramento

FEATHER RIVER

<u>Shallow Clay Layer</u>

Relation of soil parameters to distance from centerline of closest river segment (m) for shallow clay layer in Feather River

Relation of shear strength S_u (kPa) to distance from centerline of closest river segment (m) for shallow clay layer in Feather River

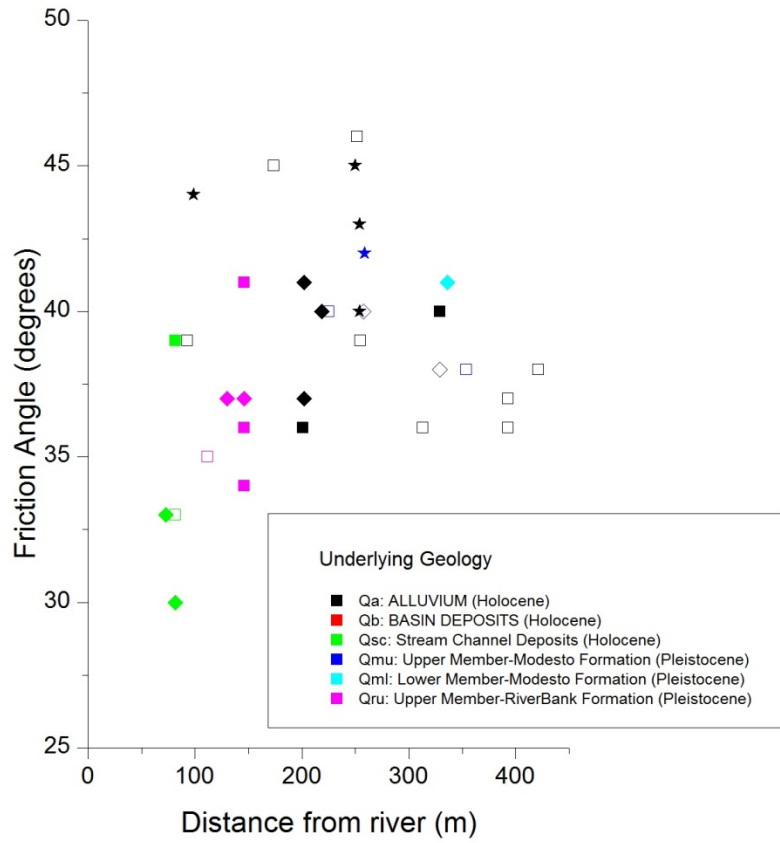**Relation of shear strength S_u (kPa) to geology for shallow clay layer in Feather River**

Relation of shear strength S_u (kPa) to Sinuosity Index for shallow clay layer in Feather River

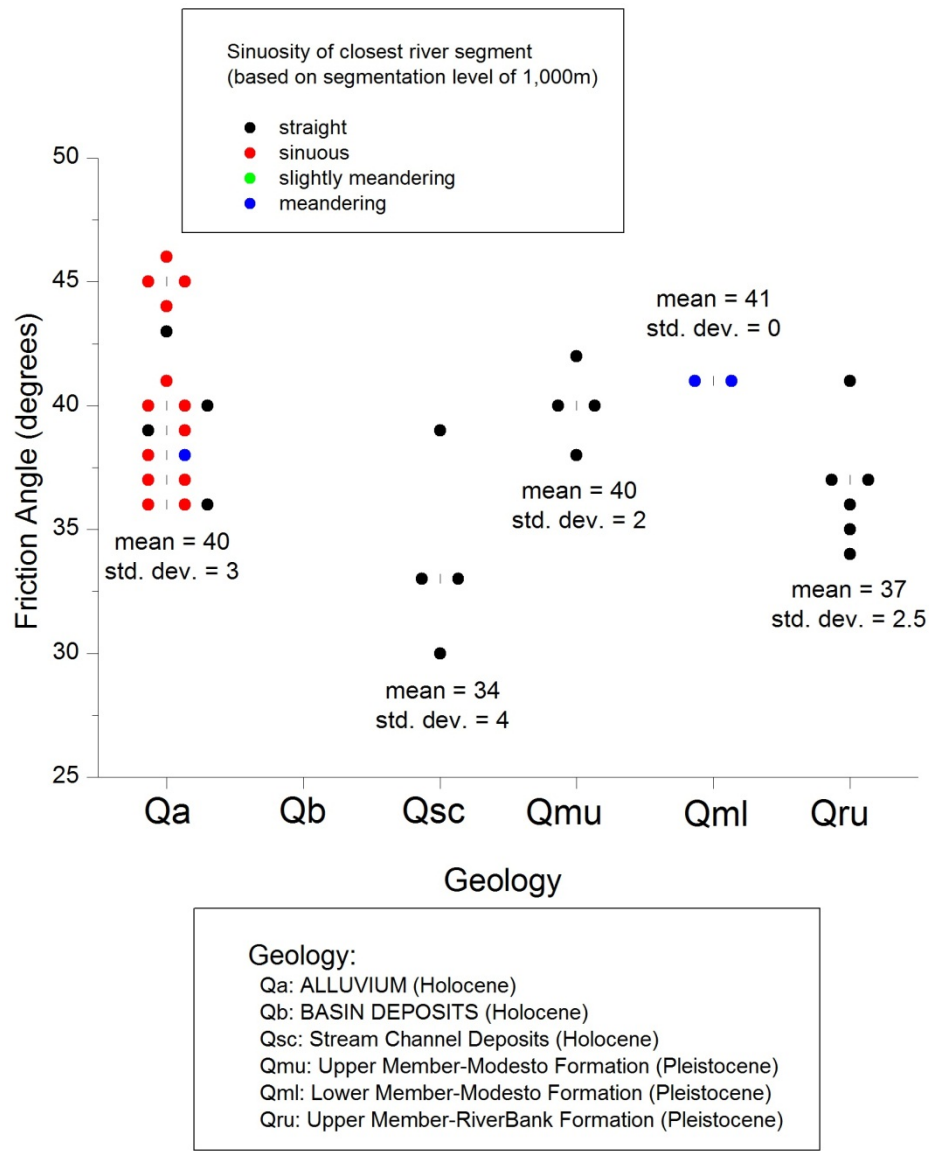# FEATHER RIVER

<u>Shallow Sand Layer</u>

Relation of soil parameters to distance from centerline of closest river segment (m) for shallow sand layer in Feather River
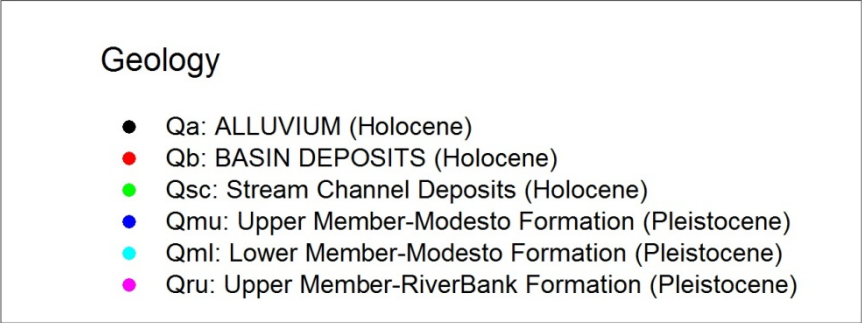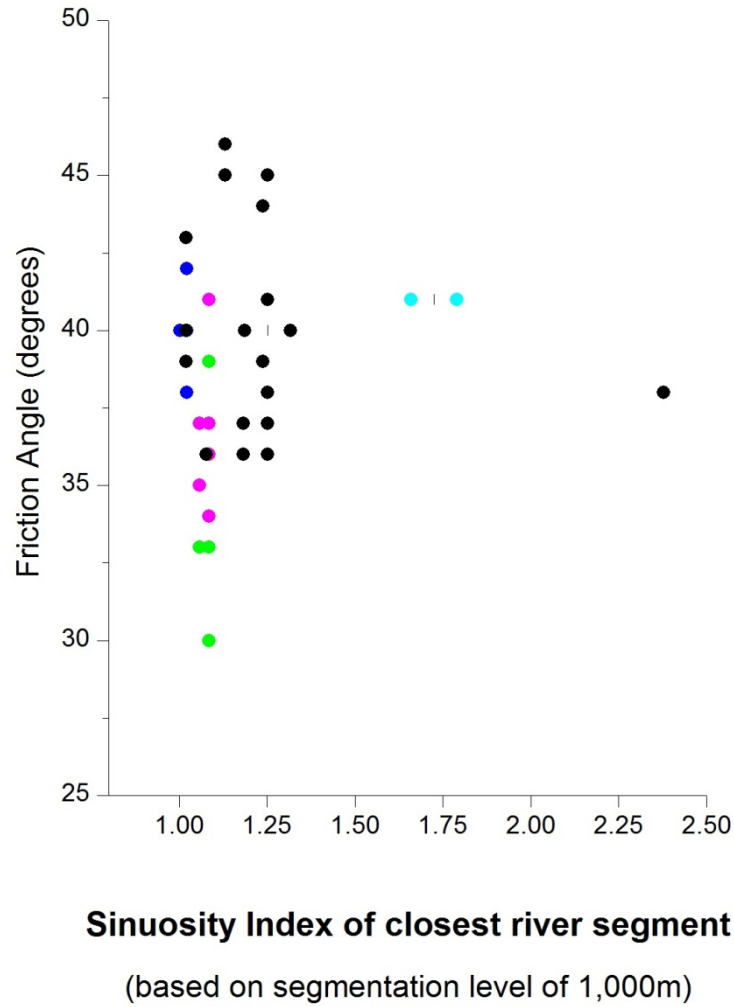
Relation of friction angle φ (degrees) to distance from centerline of closest river segment (m) for shallow sand layer in Feather River
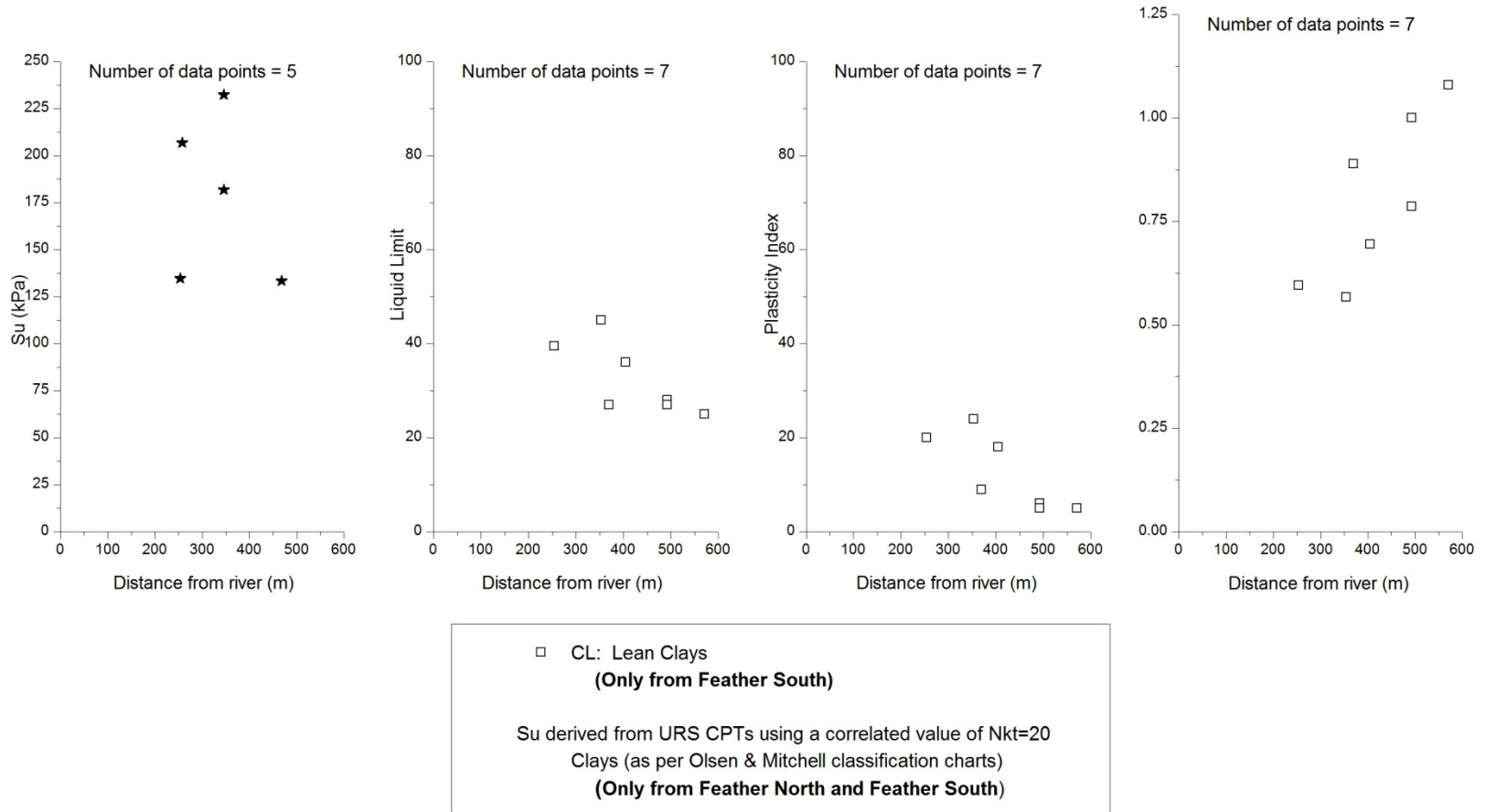
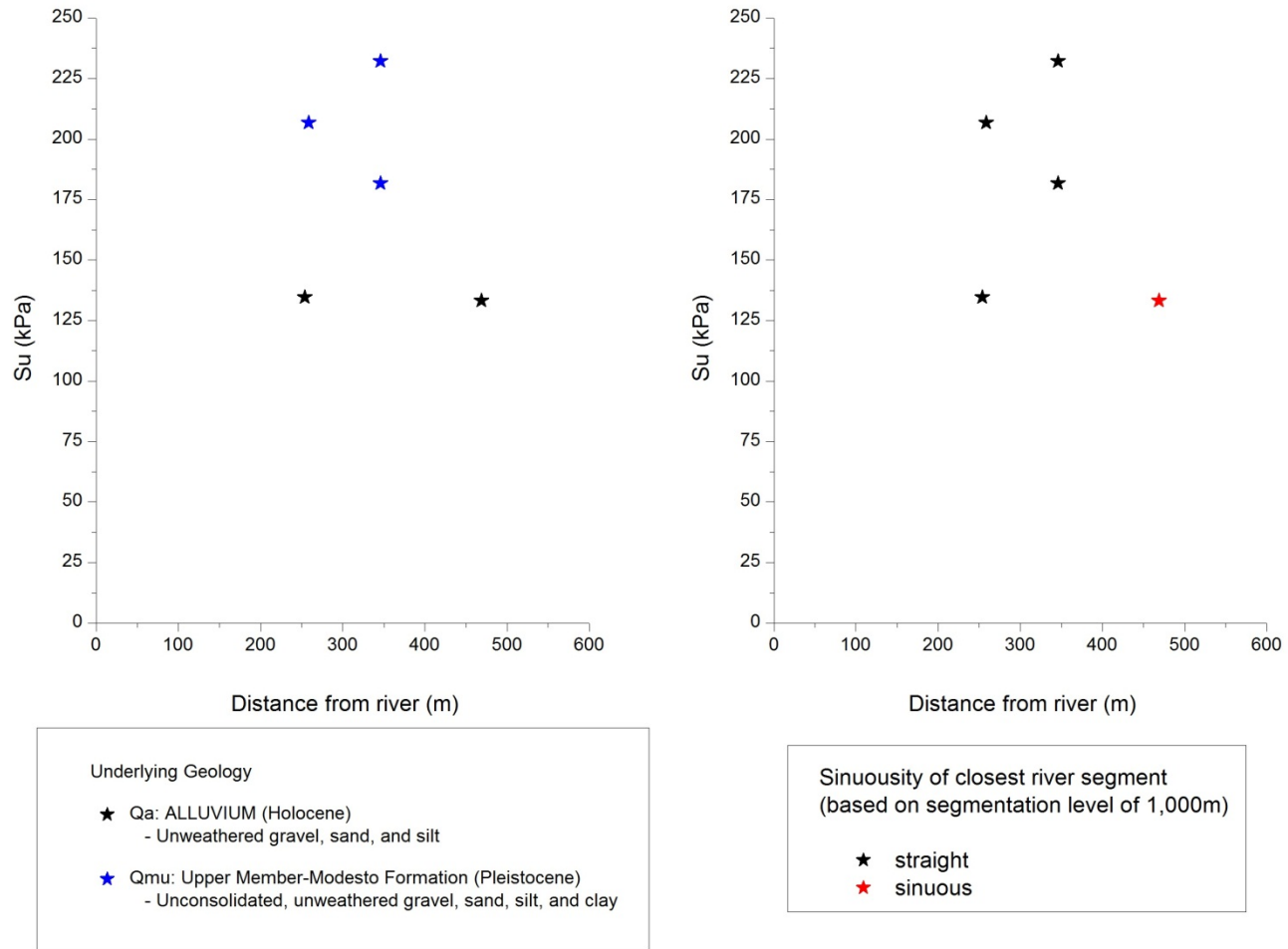**Relation of friction angle ϕ (degrees) to geology for shallow sand layer in Feather River**

Sinuosity Index of closest river segment

(based on segmentation level of 1,000m)

Geology

- Qa: ALLUVIUM (Holocene)
- Qb: BASIN DEPOSITS (Holocene)
- Qsc: Stream Channel Deposits (Holocene)
- Qmu: Upper Member-Modesto Formation (Pleistocene)
- Qml: Lower Member-Modesto Formation (Pleistocene)
- Qru: Upper Member-RiverBank Formation (Pleistocene)

Relation of friction angle ϕ (degrees) to Sinuosity Index for shallow sand layer in Feather River

FEATHER RIVER

Deep Clay Layer

Figure: Plot 1 — Su (kPa) vs Distance from river (m), Number of data points = 5 (star markers). Plot 2 — Liquid Limit vs Distance from river (m), Number of data points = 7 (open squares). Plot 3 — Plasticity Index vs Distance from river (m), Number of data points = 7 (open squares). Plot 4 — (unlabeled y-axis, 0.00–1.25) vs Distance from river (m), Number of data points = 7 (open squares).

Legend:
□ CL: Lean Clays
(Only from Feather South)

Su derived from URS CPTs using a correlated value of Nkt=20
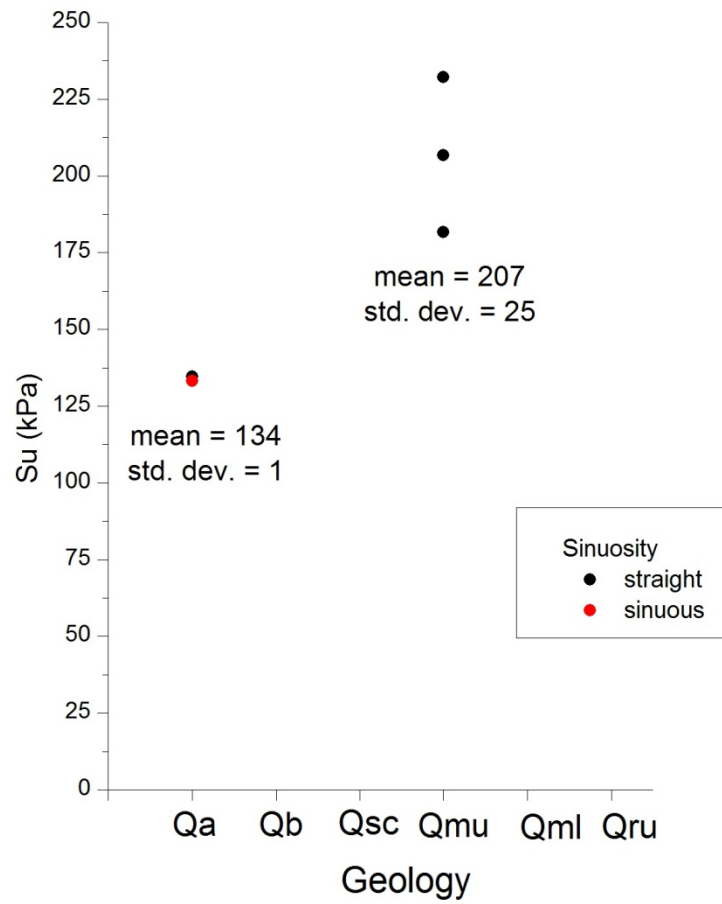Clays (as per Olsen & Mitchell classification charts)
(Only from Feather North and Feather South)

Relation of soil parameters to distance from centerline of closest river segment (m) for deep clay layer in Feather River

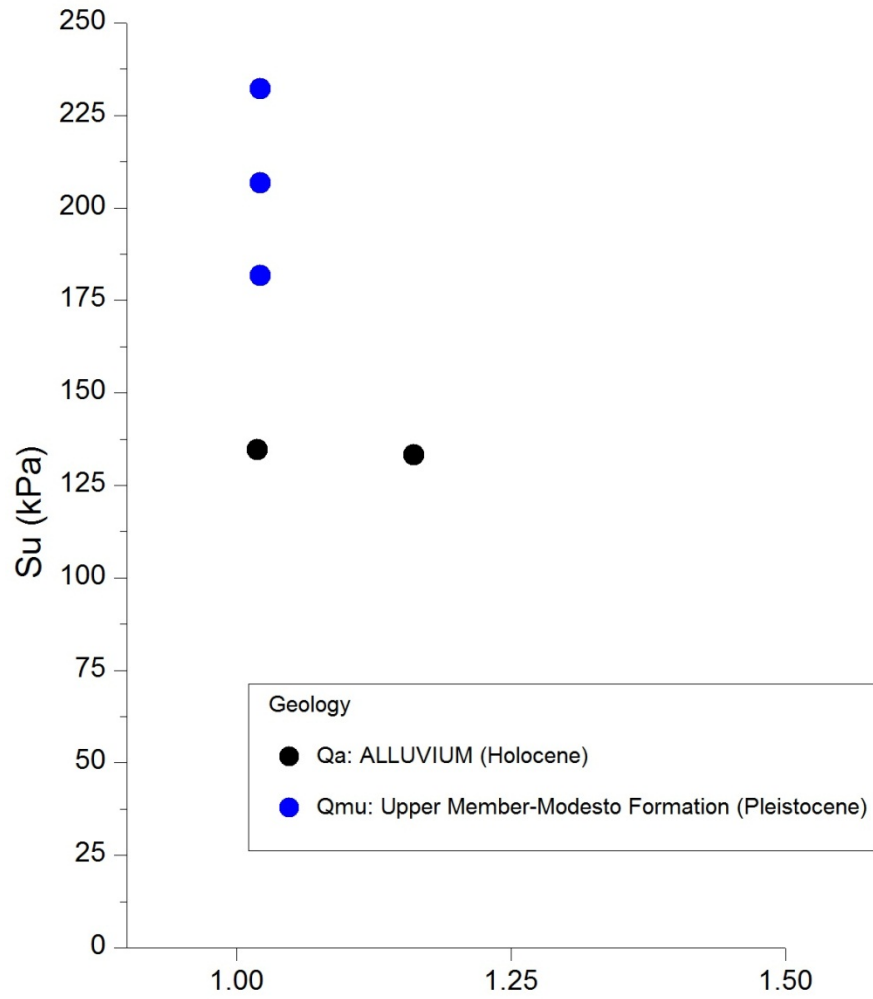**Relation of shear strength S$_u$ (kPa) to distance from centerline of closest river segment (m) for deep clay layer in Feather River**

Relation of shear strength S_u (kPa) to geology for deep clay layer in Feather River
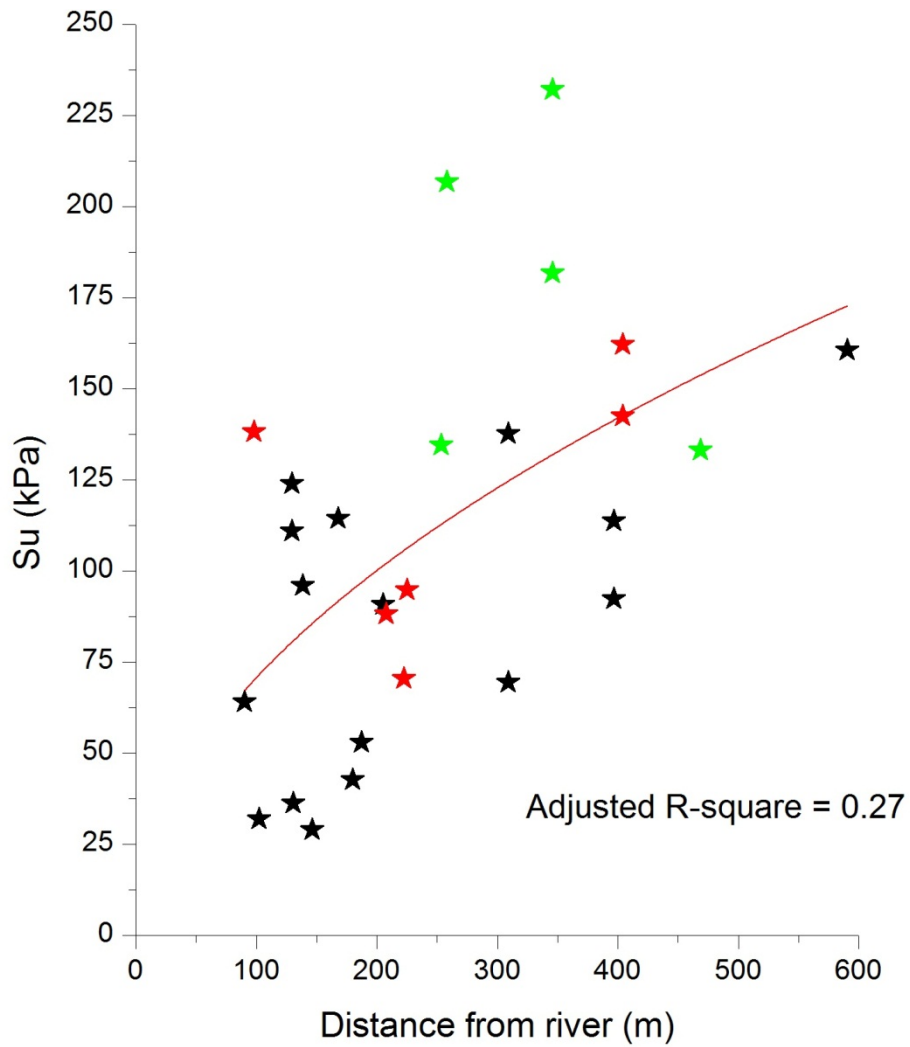
Sinuosity Index of closest river segment

(based on segmentation level of 1,000m)

Relation of shear strength S_u (kPa) to Sinuosity Index for deep clay layer in Feather River
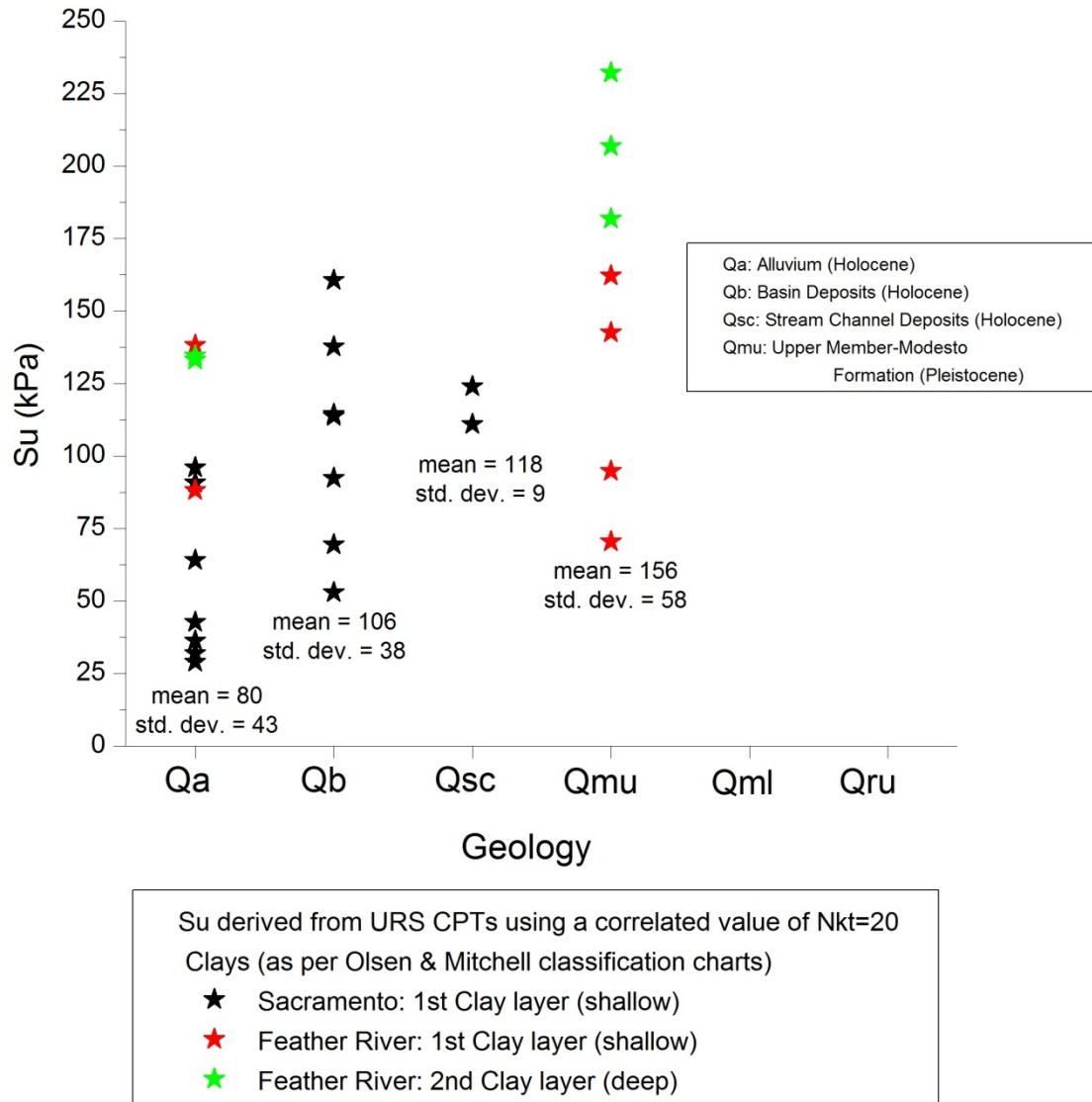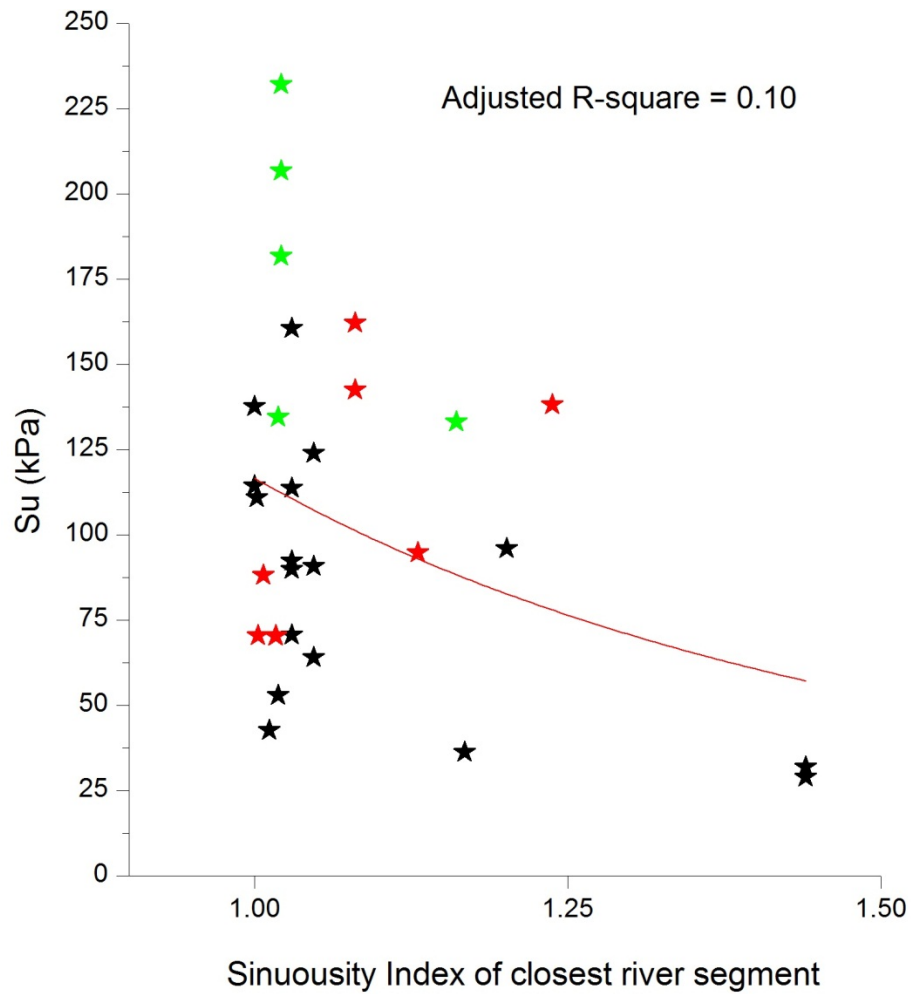
COMBINED AREAS OF STUDY

<u>All Clay Layers</u>

Relation of shear strength Su (kPa) to distance from centerline of closest river segment (m) for all clay layers in both areas of study

Relation of shear strength S_u (kPa) to geology for all clay layers in both areas of study

Relation of shear strength S_u (kPa) to Sinuosity Index for all clay layers in both areas of study

COMBINED AREAS OF STUDY

All Sand Layers

Relation of friction angle φ (degrees) to distance from centerline of closest river segment (m) for all sand layers in both areas of study
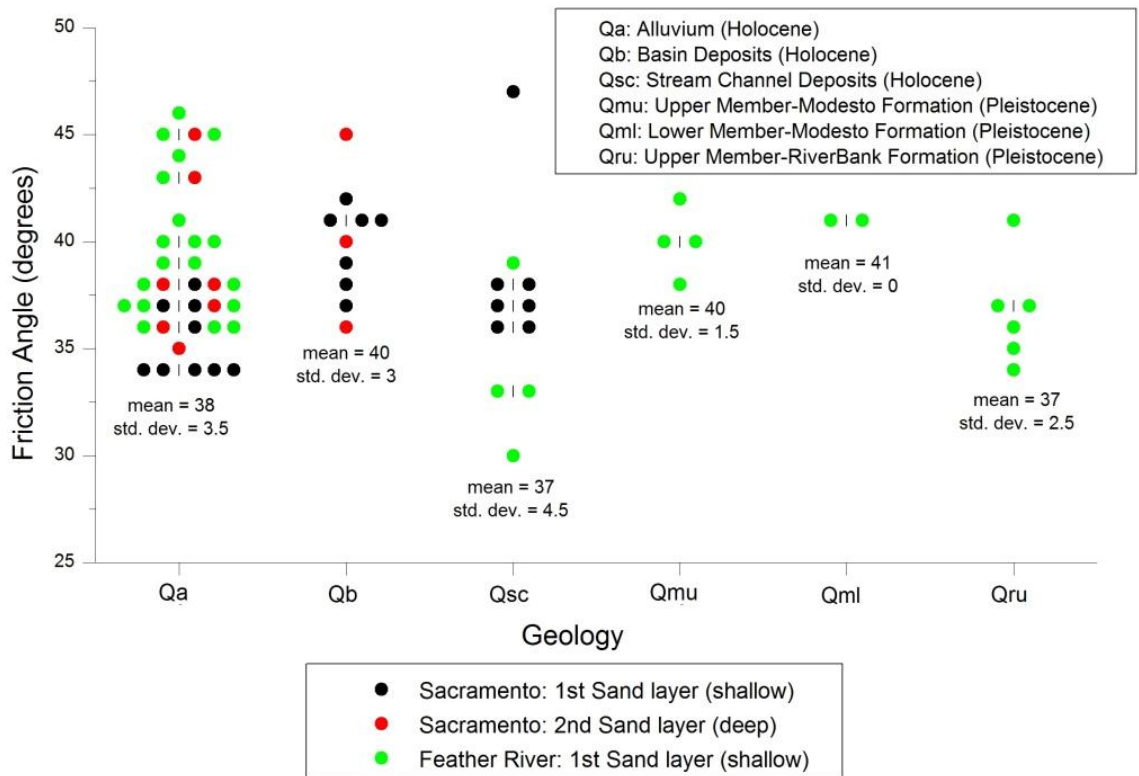
Relation of shear strength S_u (kPa) to geology for all sand layers in both areas of study
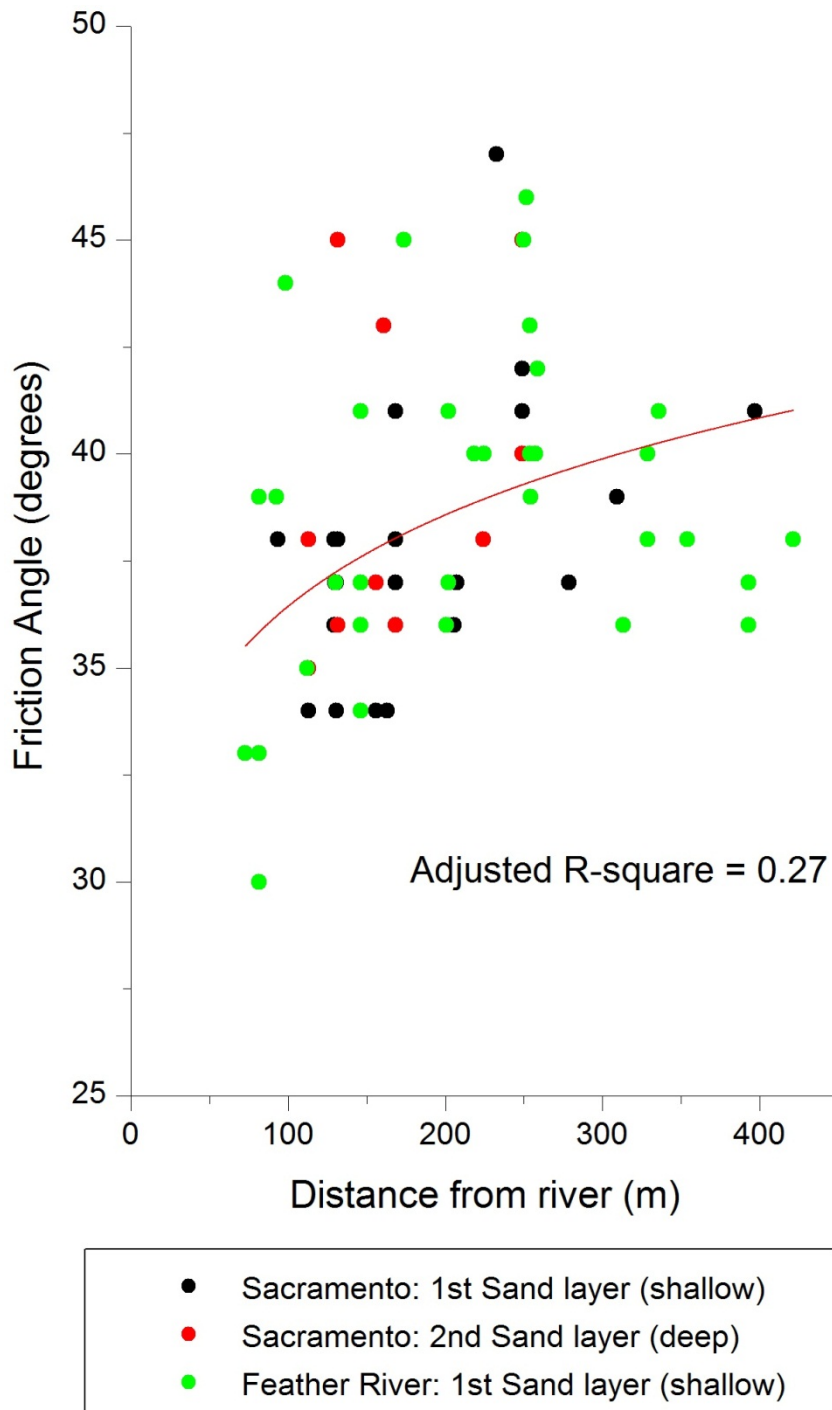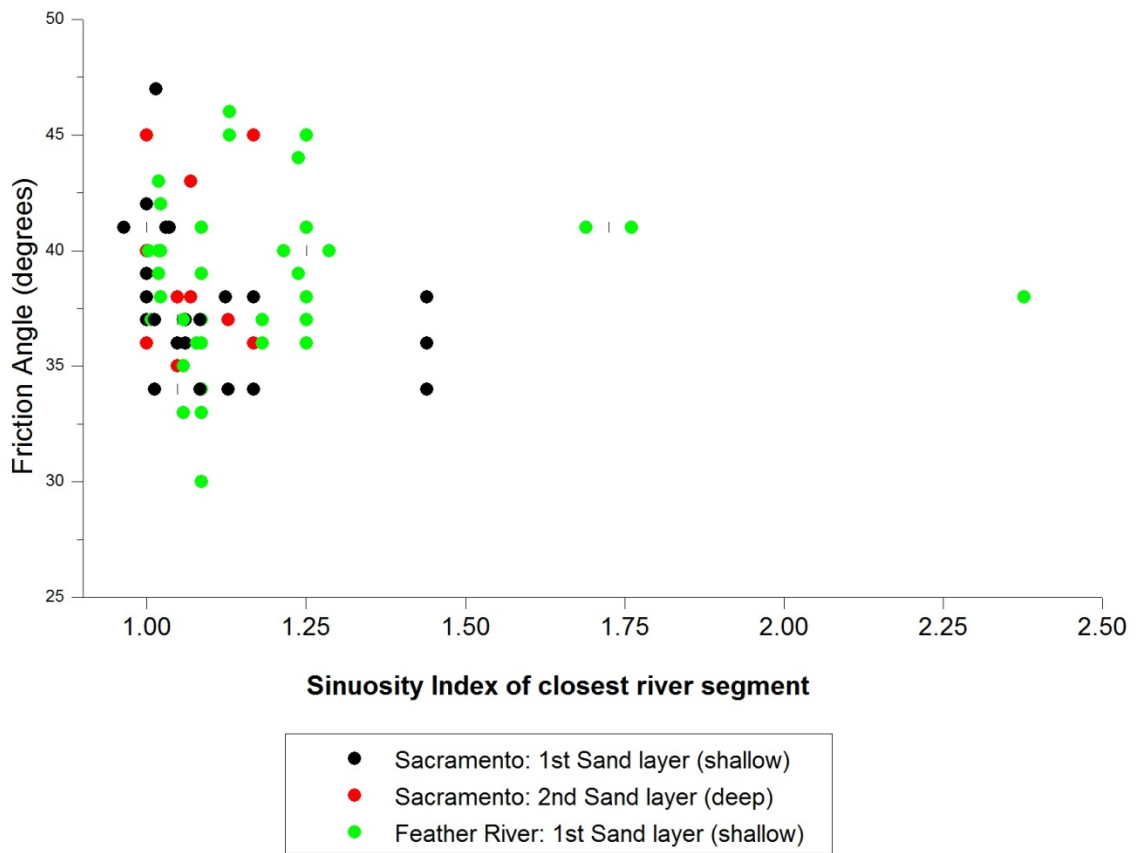
Relation of shear strength S$_u$ (kPa) to Sinuosity Index for all sand layers in both areas of study

Appendix D

Curve Fitting Residuals of Soil Parameter to Regional Factor Plots

CLAY LAYERS
Residuals from fit of shear strength S_u (kPa) to distance from river (m)
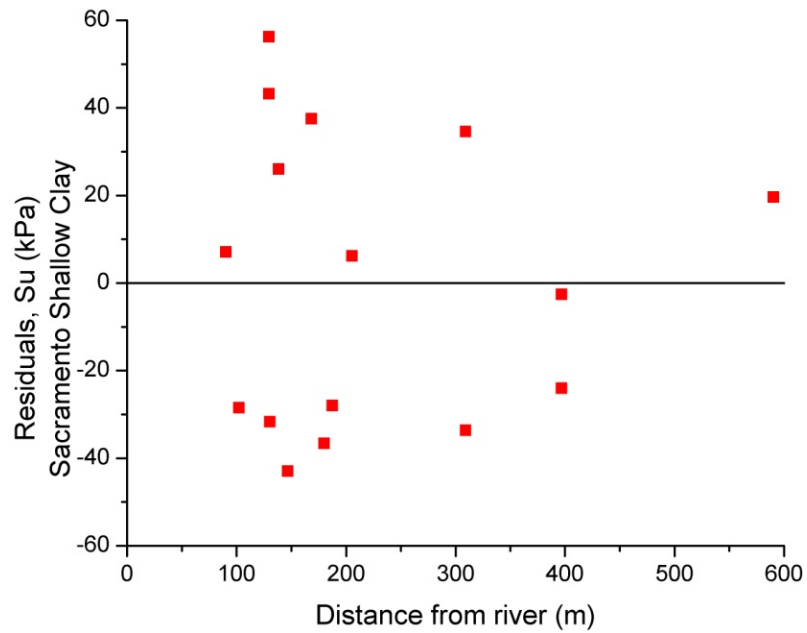
Shallow clay layer in Sacramento
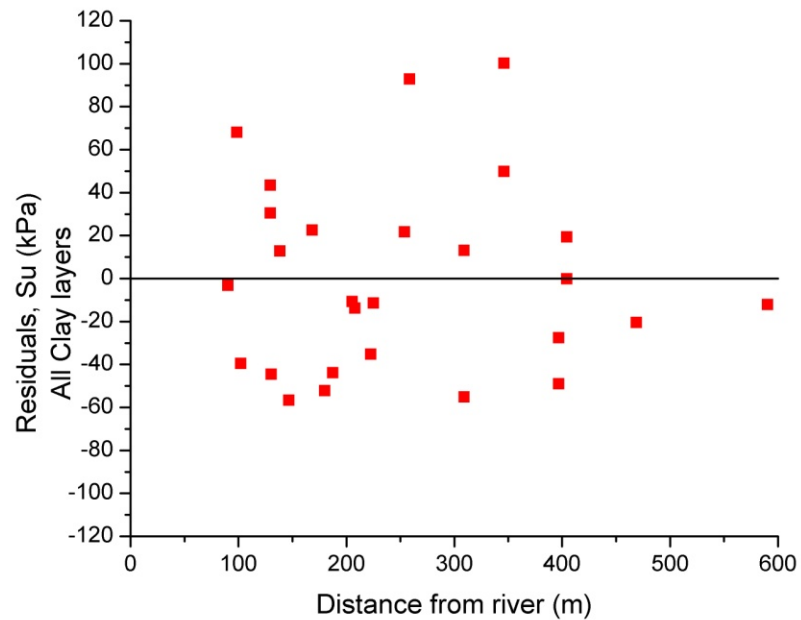
Overall clay layer in all study areas

CLAY LAYERS
Residuals from fit of shear strength S_u (kPa) to Sinuosity Index
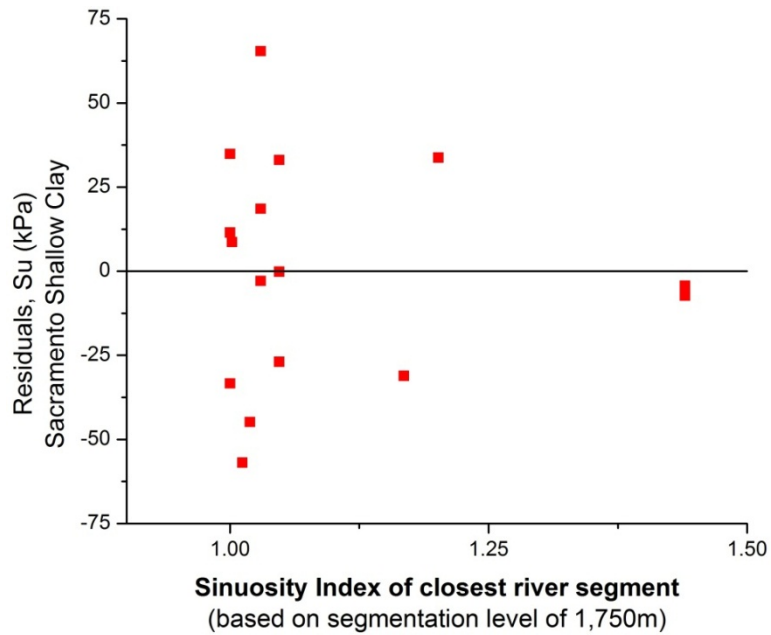
Shallow clay layer in Sacramento
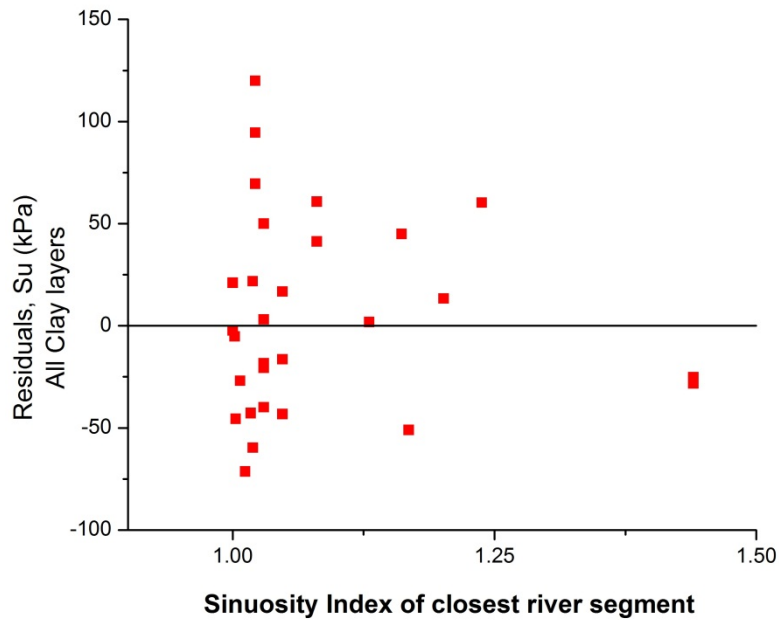
Overall clay layer in all study areas

SAND LAYERS
Residuals from fit of friction angle ϕ (degrees) to distance from river (m)
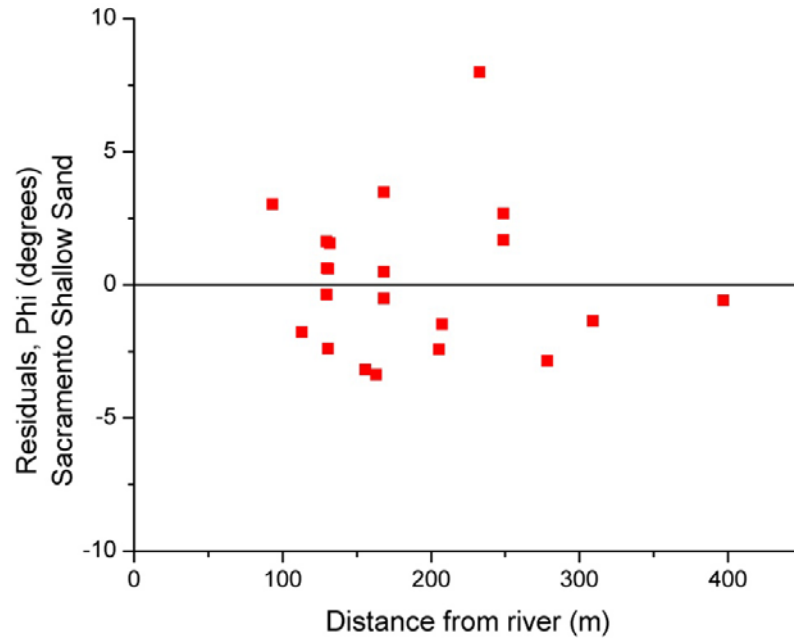
Shallow sand layer in Sacramento
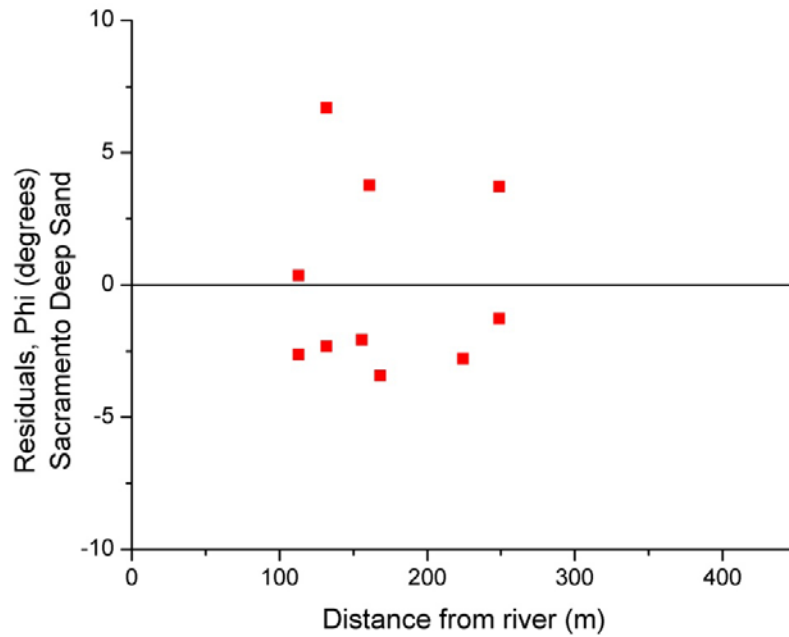
Deep sand layer in Sacramento
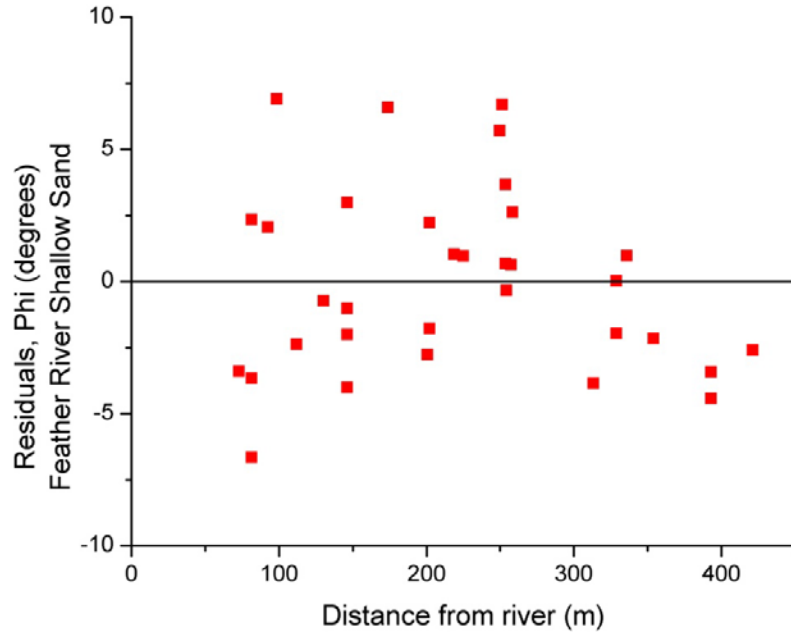
Shallow sand layer in Feather River
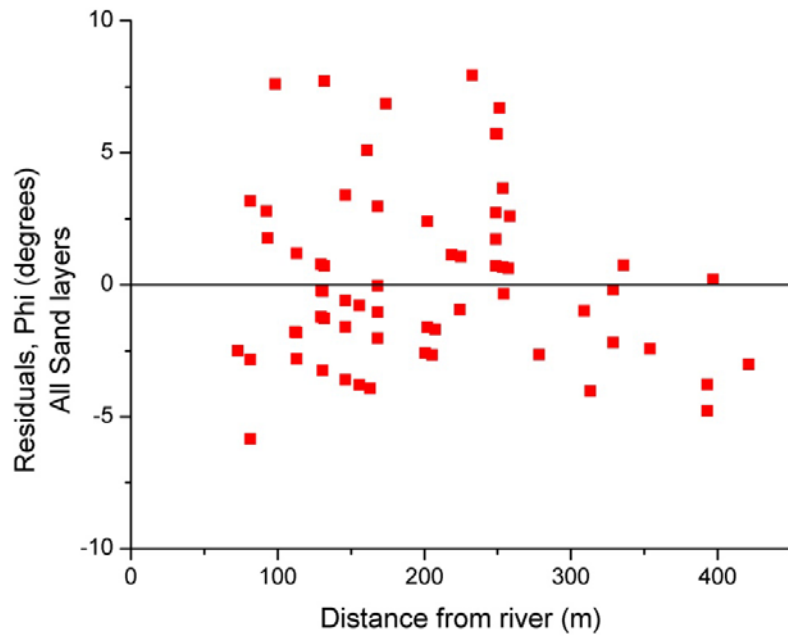
Overall sand layer in all study areas

SAND LAYERS
Residuals from fit of friction angle ϕ (degrees) to Sinuosity Index

Sinuosity of closest river segment

(based on segmentation level of 1,750m)
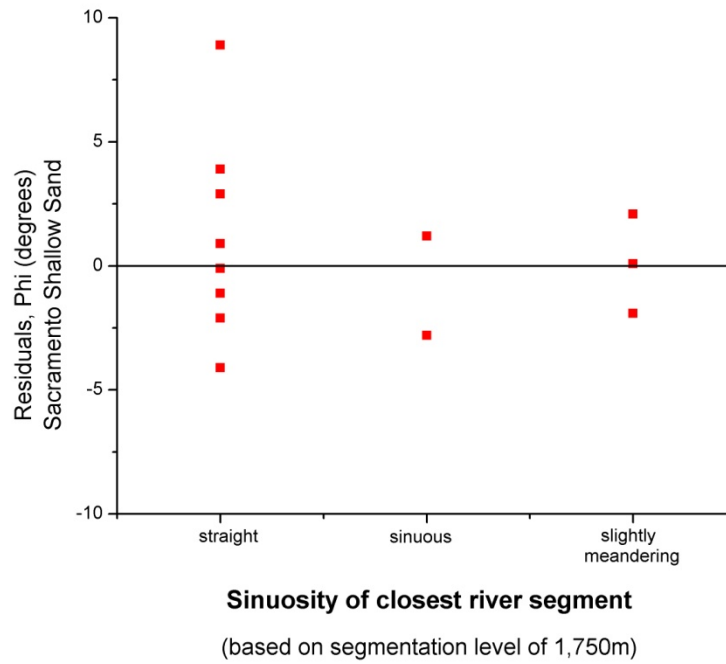
Shallow sand layer in Sacramento

Appendix E

Ordinary Kriging Estimate Maps for Soil Strength Parameters

SACRAMENTO
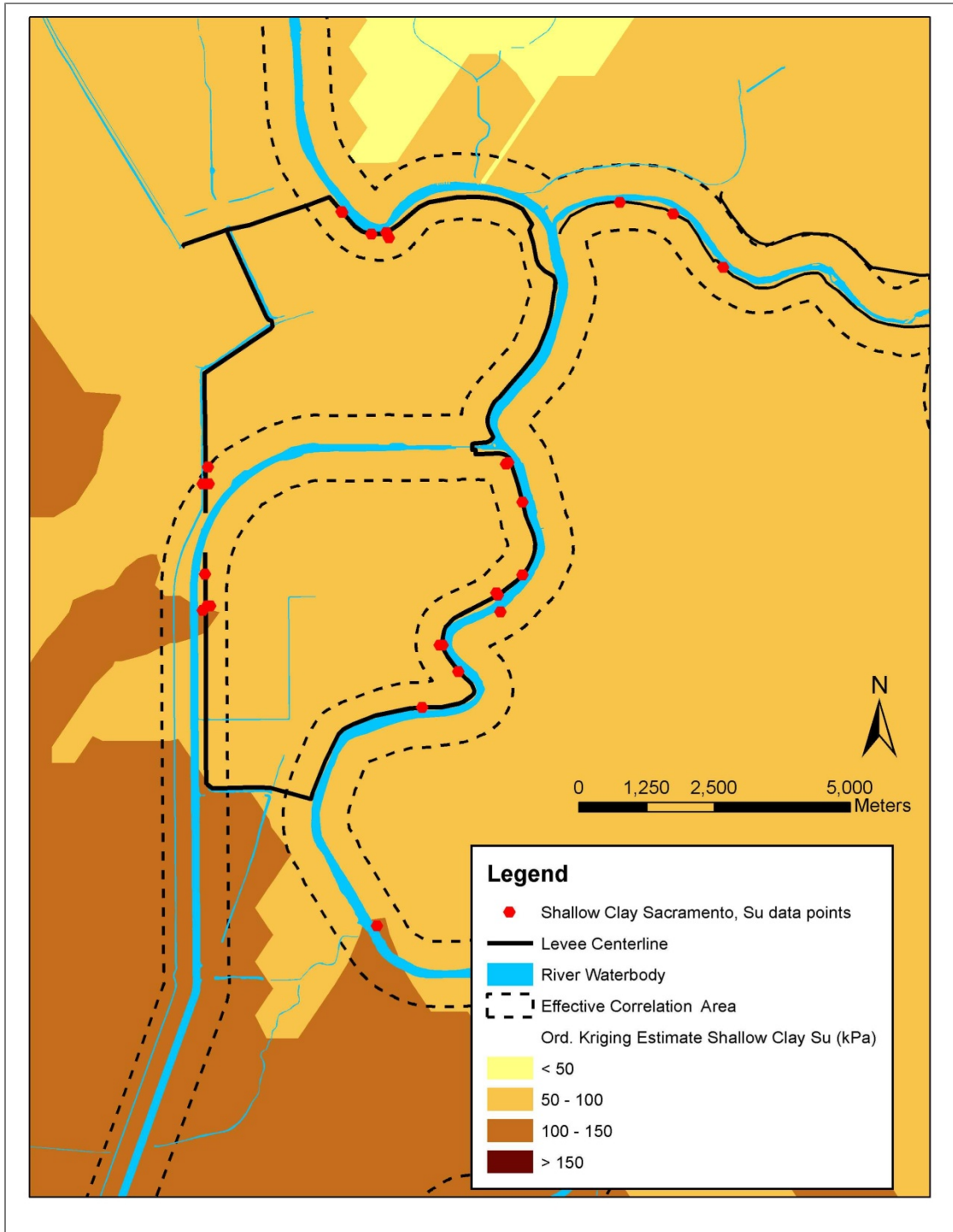
Shallow Clay Layer

Map of the Ordinary Kriging estimate for S_u (kPa)

SACRAMENTO

Shallow Sand Layer
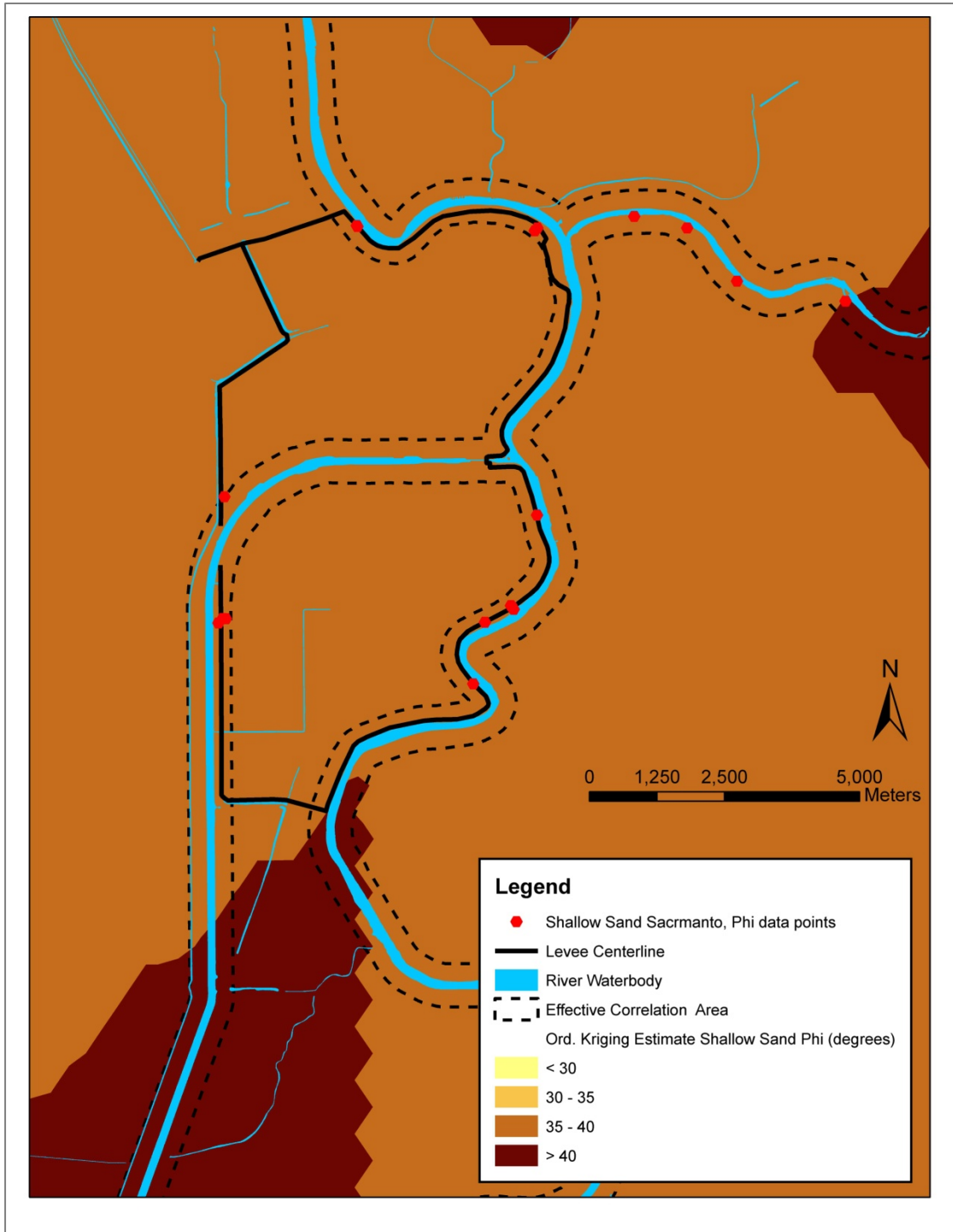
Map of the rdinary kriging estimate for friction angle φ (degrees)

SACRAMENTO

Deep Clay Layer

No Kriging estimate could be done due to limited number of data points available for the S_u (kPa) parameter of this layer

SACRAMENTO

Deep Sand Layer
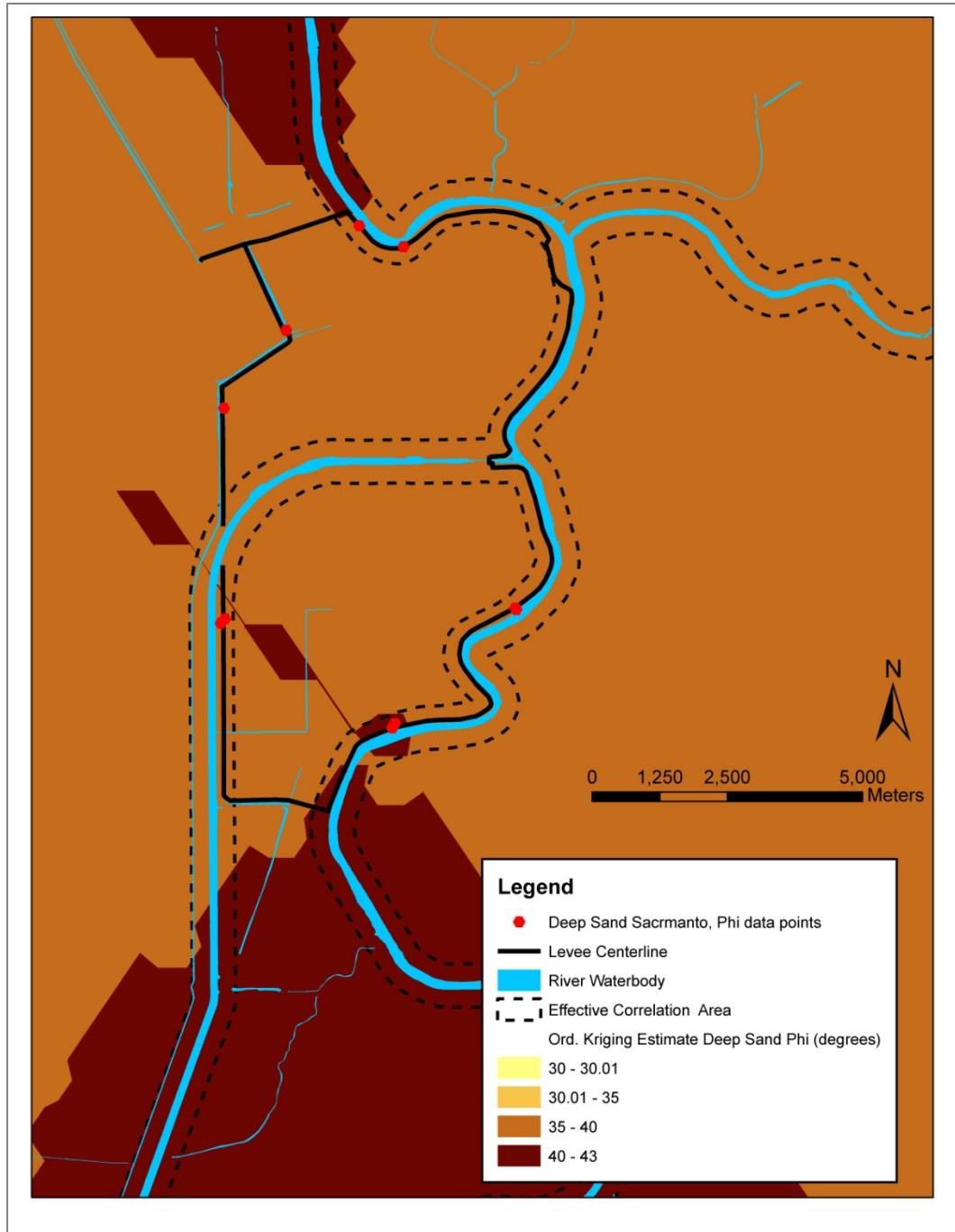
Map of the ordinary kriging estimate for friction angle φ (degrees)

FEATHER RIVER

Shallow Clay Layer

No Kriging estimate could be done due to limited number of data points available for the S_u (kPa) parameter of this layer

FEATHER RIVER

Shallow Sand Layer
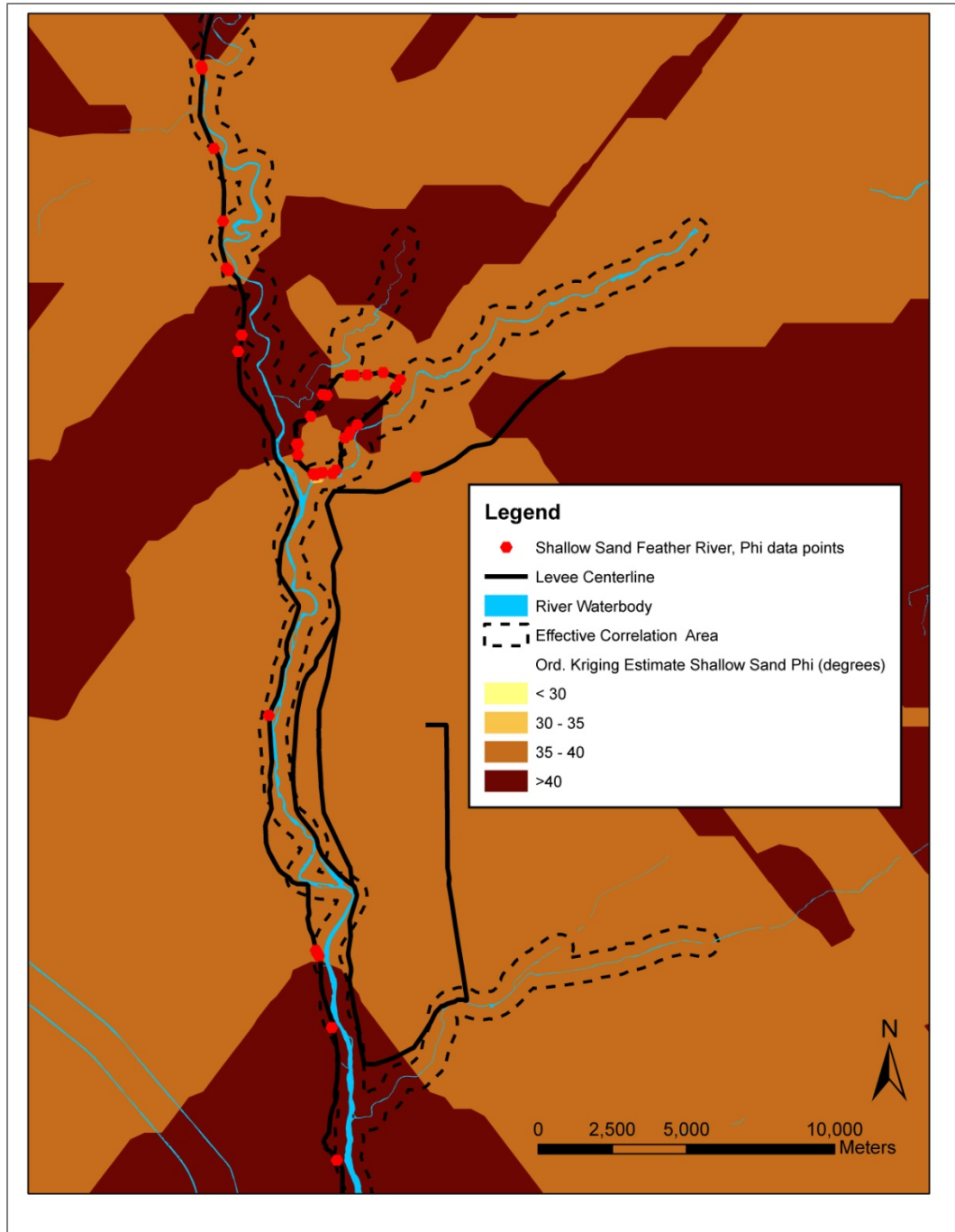
Map of the ordinary kriging estimate for friction angle ϕ (degrees)

FEATHER RIVER

Deep Clay Layer

No Kriging estimate could be done due to limited number of data points available for the S_u (kPa) parameter of this layer

Appendix F

Semi-variograms of the Ordinary Kriging for Soil Strength Parameters
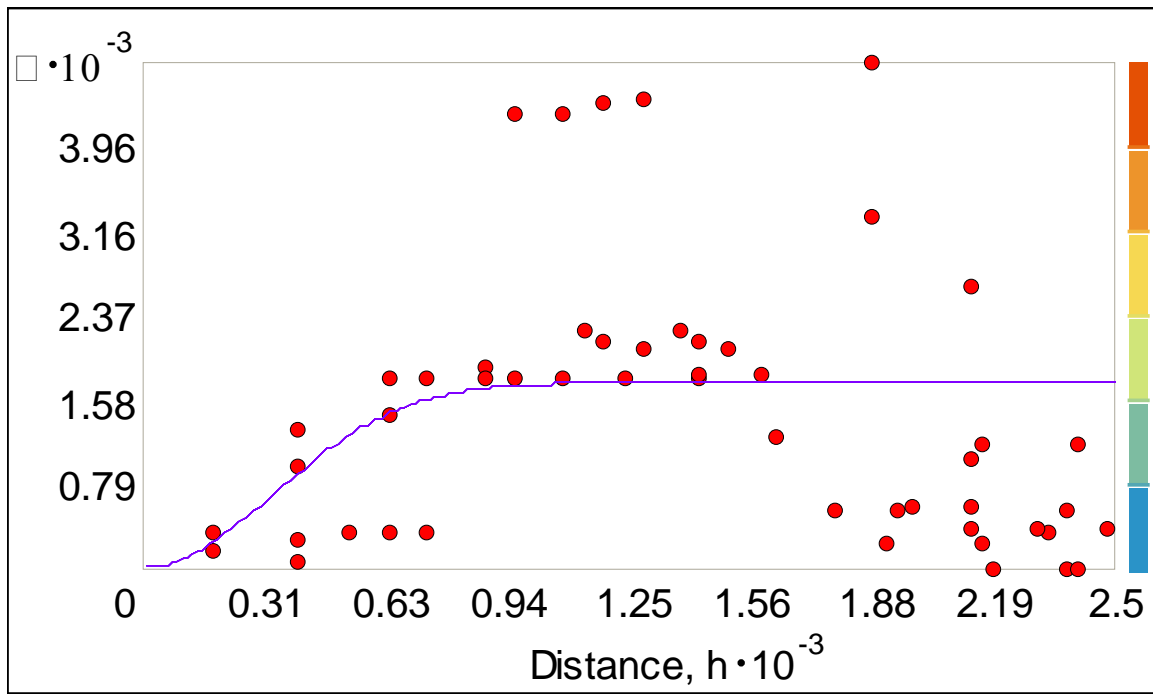
SACRAMENTO

Shallow Clay Layer

parameter: S_u (kPa)

Note: The value of 2.5 on the x-axis is equivalent to Distance$*10^{-3}$, thus the corresponding distance would be 2,500 meters.

Shallow Sand Layer
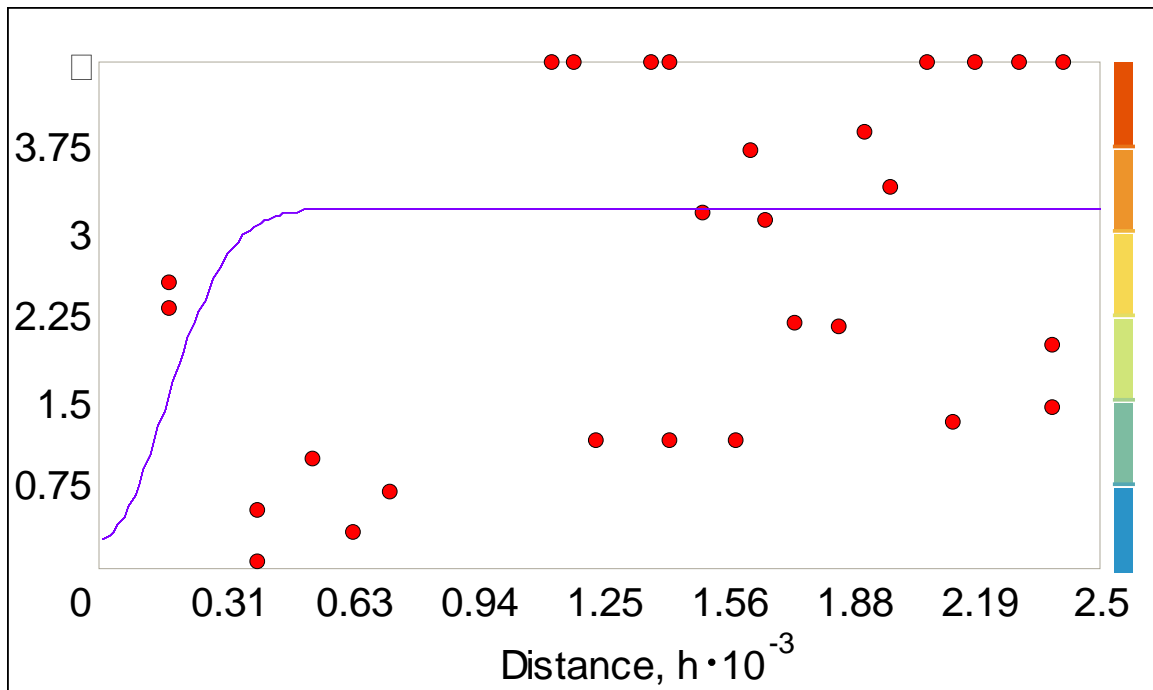
parameter: φ (degrees)

Note: The value of 2.5 on the x-axis is equivalent to Distance*10^{-3}, thus the corresponding distance would be 2,500 meters.

Deep Clay Layer

parameter: S_u (kPa)

Note: No Kriging estimate could be done due to limited number of data points available for the S_u (kPa) parameter of this layer

Deep Sand Layer

parameter: φ (degrees)
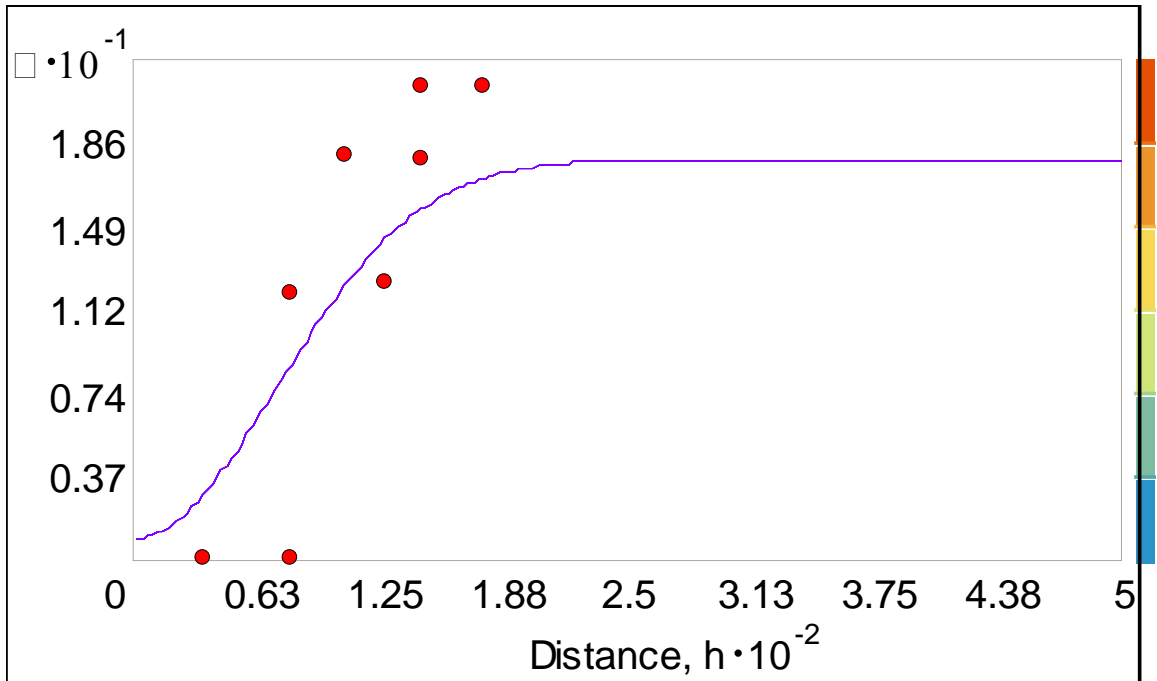
Note: The value of 5 on the x-axis is equivalent to Distance*10^{-3}, thus the corresponding distance would be 5,000 meters.

FEATHER RIVER

Shallow Clay Layer

parameter: S_u (kPa)

Note: No Kriging estimate could be done due to limited number of data points available

for the S_u (kPa) parameter of this layer

Shallow Sand Layer
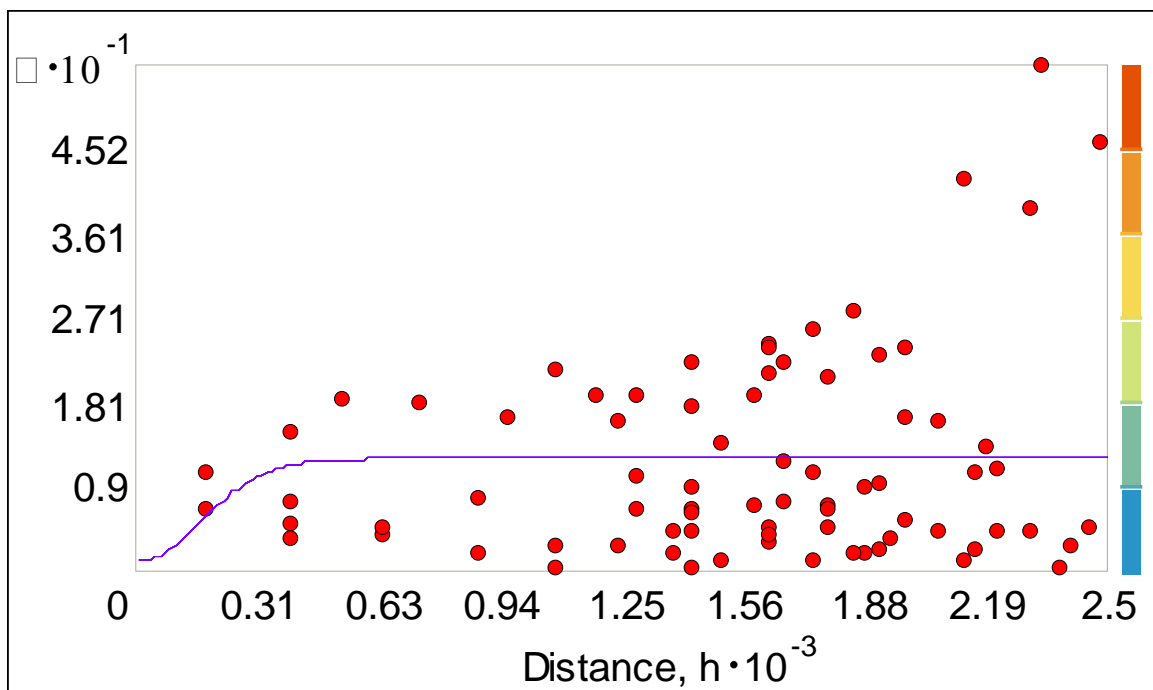
parameter: ϕ (degrees)

Note: The value of 2.5 on the x-axis is equivalent to Distance*10^{-3}, thus the

corresponding distance would be 2,500 meters.

Deep Clay Layer

parameter: S_u (kPa)

Note: No Kriging estimate could be done due to limited number of data points available

for the S_u (kPa) parameter of this layer

REFERENCES

Abbas, S. H. et al. (2009). "GIS-based disaster management; A case study for Allahabad Sadar sub-district (India)." Management of Environmental Quality; Bradford 20(1): 33.

Abrahamson, N. A. and K. M. Shedlock (1997). "Overview." Seismological Research Letters 68(1): 9-23.

Alkhaled, A. A. et al. (2008). "Using CO_2 spatial variability to quantify representation errors of satellite CO_2 retrievals,." Geophysical Research Letters 35(L16813).

Andresen, J. et al. (2000). "A Framework for Measuring IT Innovation Benefits." ITcon 5: 57-72.

Anumba, C. (1998 of Conference). Industry uptake of construction IT innovations - key elements of a proactive strategy. Proceedings of the CIB W78's workshop: The life-cycle of construction IT innovations - Technology transfer from research to practice, Stockholm, Sweden

Arciszewski, T. (2006). "Civil Engineering Crisis." Leadership and Management in Engineering, ASCE 6(1): 26.

ASCE (2006). The Vision for Civil Engineering in 2025, American Society of Civil Engineers.

ASCE. (2009). "Report Card for America's Infrastructure." Retrieved May 6, 2009, from http://www.infrastructurereportcard.org/, American Society of Civil Engineers.

ASCE (2010). So You Live Behind a Levee ? American Society of Civil Engineers.

ASTM Standard D2487-11 (2011). "Standard Practice for Classification of Soils for Engineering Purposes (Unified Soil Classification System)", ASTM International, West Conshohocken, PA, 2003, www.astm.org.

Athanasopoulos-Zekkos, A.-M. (2008). Select Topics on the Static and Dynamic Response and Performance of Earthen Levees. Doctor of Philosophy, Department of Civil and Environmental Engineering, University of California, Berkeley, USA.

Athanasopoulos-Zekkos, A.-M. (2010). Variability in Earthen Levee Seismic Response due to Time-History Selection. Recent Advances in Geotechnical Earthquake Engineering and Soil Dynamics, San Diego, California, May 24-29, 2010.

Athanasopoulos-Zekkos, A.-M. and M. Saadi (2011). "Ground Motion Selection for Liquefaction Evaluation Analysis of Earthen Levees." Earthquake Spectra - EERI. Accepted for Publication 2011.

Austin, C. (2011). Sacramento's flood control system: Under pressure but holding up. 2011.

Baecher, G. B. and J. T. Christian (2008). Spatial Variability and Geotechnical Engineering. <u>Reliability Based Design in Geotechnical Engineering: Computations and Applications</u>. K.-K. Phoon, Taylor & Francis.

Bailey, E. (2008). When drought isn't the problem. <u>Los Angeles Times</u>.

Bray, J. D. (2007). Simplified Seismic Slope Displacement Procedures. <u>4th ICEGE, Thessaloniki, Greece, June 25-28, 2007.</u>

Brice, J. (1977). Lateral Migration of the Middle Sacramento River.

California DWR & DFG (2008). Risks and Options to Reduce Risks to Fishery and Water Supply Uses of the Sacramento/San Joaquin Delta.

Capilleri, P. and M. Maugeri (2008). Geotechnical Seismic Hazard Evaluation At Sellano (Umbria, Italy) Using The GIS Technique. <u>Seismic Engineering Conference Commemorating the 1908 Messina and Reggio Calabria Earthquake</u>. A. Santini and N. Moraci.

Cetin, O. K. et al. (2004). "Standard Penetration Test-Based Probabilistic and Deterministic Assessment of Seismic Soil Liquefaction Potential." <u>Journal of Geotechnical and Geoenvironmental Engineering, ASCE.</u> 130(12): 1314-1340.

Chiles, J.-P. and P. Delfiner (1999). <u>Geostatistics: Modeling Spatial Uncertainty</u>.

271

Christian, J. and G. Baecher (2011). Unresolved Problems in Geotechnical Risk and Reliability. <u>Proceedings of the ASCE GeoRisk2011: Geotechnical Risk Assessment and Management conference, Atlanta, GA.</u>, ASCE. 418: 3.

Chung, J. and J. Rogers (2011). Spatial Prediction of Groundwater Depth to Trigger Liquefaction in St. Louis. <u>Proceedings of the ASCE GeoRisk2011: Geotechnical Risk Assessment and Management conference, Atlanta, GA.</u>, ASCE. 418: 84.

Coppock, J. T. (1995). GIS and natural hazards: an overview from a GIS perspective. <u>Geographical Information Systems in Assessing Natural Hazards</u>. A. Carrara and F. Guzzetti: 21-34.

Davis, T. J. and C. P. Keller (1997). "Modelling uncertainty in natural resource analysis using fuzzy sets and Monte Carlo simulations: slope stability prediction." <u>International Journal of Geographical Information Science</u> 11(5): 409-434.

Deretsky, Z., (National Science Foundation) (2010). Ten Ways a Levee Can Fail.

DKKV (2002). <u>Journalists' Manual on Disaster Management</u>, German Committee for Disaster Reduction.

DRMS (2006a). Delta Risk Management Strategy, Initial Technical Framework Paper: Levee Fragility

DRMS (2006b). Delta Risk Management Strategy, Initial Technical Framework Paper: Sacramento-San Joaquin Delta Risk Analysis (Approach and Basis of Analysis)

Duncan, J. M. and W. N. Houston (1983). "Estimating failure probabilities for California levees." Journal of Geotechnical Engineering, ASCE 109(2).

DWR (2004). Sacramento Valley Groundwater Basin, South American Subbasin, Groundwater Basin Number: 5-21.65, Bulletin 118.

DWR. (2011a). "California Department of Water Resources." Retrieved September 5, 2011, from http://www.water.ca.gov/.

DWR. (2011b). "California Department of Water Resources Publications." Retrieved September 5, 2011, from http://www.water.ca.gov/floodmgmt/pubs/#.

DWR. (2011c). "California Levee Database." Retrieved September 5, 2011, from http://www.water.ca.gov/floodmgmt/lrafmo/fmb/fes/levee_database.cfm.

EERI/GEER (2011). Geotechnical Effects of the M_w 9.0 Tohoku, Japan, Earthquake of March 11, 2011

ESRI. (2009a). "Regression Analysis Basics." Retrieved September 1, 2009, from http://webhelp.esri.com/arcgisdesktop/9.3/index.cfm?TopicName=welcome.

ESRI. (2009b). "What is a z-score and a p-value?" Retrieved September 1, 2009, from http://webhelp.esri.com/arcgisdesktop/9.3/index.cfm?TopicName=welcome.

ESRI. (2011). "ESRI main website." Retrieved September 5, 2011, from http://www.esri.com/.

Faber, M. H. et al. (2007). Principles of risk assessment of engineered systems. Applications of Statistics and Probability in Civil Engineering.

FEMA. (2008). "FEMA-366: HAZUS-MH Estimated Annualized Earthquake Loss for the United States." Retrieved September 1, 2009, from http://www.fema.gov/library/viewRecord.do?id=3265.

FEMA. (2009). "HAZUS-MH, FEMA's Methodology for Estimating Potential Losses from Disasters." Retrieved September 1, 2009, from http://www.fema.gov/plan/prevent/hazus/.

Fenton, G. A. and D. V. Griffiths (2008). Risk Assessment in Geotechnical Engineering.

Fookes, P. G. et al. (2007). Engineering Geomorphology: Theory and Practice, Whittles Publishing - CRC Press.

Frost, J. D. et al. (1992). Geographic Information Systems in Earthquake Hazard Analyses. Proc. of Symp. on Geographic Information Analysis, 8th Conf. on Computing in Civil Engr. Dallas: pp 452-460.

Garrett, J. H. et al. (2004). "Information Technology in Civil Engineering-Future Trends." Journal of Computing in Civil Engineering, ASCE 18: 185-186.

Gilbert, R. et al. (2011). Short course on "Risk and Reliability of Levees and Dams", at the ASCE GeoRisk2011: Geotechnical Risk Assessment and Management conference, Atlanta, GA.

Goovaerts, P. (1998). "Ordinary cokriging revisited." <u>Mathematical Geology</u> 30: 21-42.

Goovaerts, P. (1999). "Geostatistics in soil science: state-of-the-art and perspectives." <u>Geoderma</u> 89: 1–45.

Gordon, N. D. et al. (2004). <u>Stream Hydrology</u>, John Wiley & Sons, Ltd.

Haining, R. P. et al. (2010). "Geography, Spatial Data Analysis, and Geostatistics: An Overview." <u>Geographical Analysis</u> 42(1): 7-31.

Harder, L. (2008). California Levee System, Personal Communication.

Haselton, C. B. (2009). Evaluation of Ground Motion Selection and Modification Methods: Predicting Median Interstory Drift Response of Buildings.

Hatanaka, M. and A. Uchida (1996). "Empirical correlation between penetration resistance and internal friction angle of sandy soils." <u>Soils and Foundations, Japanese Geotechnical Society.</u> 36(4): 1-9.

Hellawell, E. E. et al. (2001). "GIS as a tool in geotechnical engineering " <u>Geotechnical Engineering</u> 149(2): 85-93.

Helley, E. J. and D. S. Harwood (1985). Geologic map of the Late Cenozoic deposits of the Sacramento Valley and Northern Sierran Foothills, California, U.S. Geological Survey: Miscellaneous Field Studies Map MF-1790.

Hess, J. R. et al. (2006). "California's Levees at Risk." <u>Geo-Strata</u> 7(6).

Hudson, M. et al. (1994). QUAD4M - A computer program to evaluate the seismic response of soil structures using the finite element procedures and incorporating a compliant base., Center for Geotechnical Modelling, Department of Civil and Environmental Engineering, University of California, Davis, CA. .

Hutchinson, D. J. et al. (2007). Four dimensional considerations in forensic and predictive simulation of hazardous slope movement Rock Mechanics: Meeting Society's Challenges and Demands

Idriss, I. M. and R. W. Boulanger (2006). "Semi-empirical procedures for evaluating liquefaction potential during earthquakes." Soil Dynamics and Earthquake Engineering. (26),: 115-130.

James, L. A. and M. B. Singer (2008). Development of the Lower Sacramento Valley Flood-Control System: Historical Perspective, ASCE.

Journel, A. G. and C. J. Huijbregts (1978). Mining Geostatistics, Academic Press, New York.

Julien, P. (2002). River Mechanics, Cambridge University Press, Cambridge, UK.

King, S. (1997). Integration of Earthquake Hazards in GIS. Spatial Analysis in Soil Dynamics and Earthquake Engineering (GSP 67): 103-116.

Kondolf, G. M. and H. Piegay, Eds. (2003). Tools in Fluvial Geomorphology, John Wiley & Sons, Ltd, West Sussex, UK.

Krige, D. G. (1951). A statistical approach to some mine valuations and allied problems at the Witwatersrand, The University of Witwatersran. Masters.

Lacasse, S. and F. Nadim (1996). Uncertainties in characteristic soil properties. Uncertainty in the Geologic Environment, ASCE specialty conference.

Lan, H. and C. D. Martin (2007). A digital approach for integrating geotechnical data and stability analyses Rock Mechanics: Meeting Society's Challenges and Demands

Lee, I. K. et al. (1983). Geotechnical Engineering.

Leopold, L. B. et al. (1964). Fluvial Processes in Geomorphology.

Lumb, P. (1966). "The Variability of Natural Soils." Canadian geotechnical journal 3(2): 74-97.

Lumb, P. (1974). Application of statistics in soil mechanics. Soil Mechanics: New Horizons. I. K. Lee.

Lunne, T. et al. (1997). Cone penetration testing in geotechnical practice. London : New York, Blackie Academic & Professional.

Matheron, G. (1962). Traité de géostatistique appliquée.

McGaughey, J. et al. (2007). Integrated, real-time, 3D GIS-based geotechnical hazard assessment. Rock Mechanics: Meeting Society's Challenges and Demands: 21-28.

McGuire, R. K. (2004). <u>Seismic hazard and risk analysis</u>. Oakland, Calif., Earthquake Engineering Research Institute.

Miller, H. J. (2004). "Tobler's First Law and Spatial Analysis." <u>Annals of the Association of American Geographers</u> 94(2): 284-289.

Mount, J. F. (1995). <u>California rivers and streams: the conflict between fluvial process and land use</u>. Berkeley, University of California Press.

Mueller, J. E. (1968). "An Introduction to the Hydraulic and Topographic Sinuosity Indexes 1." <u>Annals of the Association of American Geographers</u> 58(2): 371-385.

National Research Council (2000). <u>Risk Analysis and Uncertainties in Flood Damage Reduction Studies</u>, National Academy Press.

Newkirk, R. T. (1993). Simulation for risk analysis: a challenge for GIS. <u>International Emergency Management and Engineering Conference: 10th Anniversary: Research and Applications</u>: 62-65.

Olsen, R. S. and J. V. Farr (1986 of Conference). <u>Site Characterization Using the Cone Penetration Test</u>. Proceedings, In-situ '86, ASCE Specialty Conference. Blacksburg. VA.

Olsen, R. S. and J. K. Mitchell (1995 of Conference). <u>CPT Stress Normalization and Prediction of Soil Classification</u>. Proceedings of the International Symposium on Cone Penetration Testing, CPT 95, Linkoping, Sweden.

Peck, R. B. et al. (1974). Foundation engineering. New York, Wiley.

Peter, P. (1982). Canal and River Levees, Elsevier Scientific Publishing Company.

Phoon, K.-K. and F. H. Kulhawy (1996). On quantifying inherent soil variability. Uncertainty in the Geologic Environment, ASCE specialty conference.

Player, R. S. V. (2004). "Geotechnical use of GIS in transportation projects." Geotechnical Engineering for Transportion Projects(126): 886-893.

Posamentier, H. W. (2003). "Depositional elements associated with a basin floor channel-levee system: case study from the Gulf of Mexico." Marine and Petroleum Geology 20(6-8): 677-690.

Rathje, E. M. et al. (1998). "Simplified Frequency Content Estimates of Earthquake Ground Motions." Journal of Geotechnical and Geoenvironmental Engineering, ASCE 124(2): 150-159.

Rejeski, D. (1993). GIS and risk: a three culture problem. Environmental Modeling with GIS. M. F. Goodchild, B. O. Parks and L. T. Steyaert: 318-331.

RESIN. (2011). "Resilient and Sustainable Infrastructure Networks project (RESIN) at the University of California, Berkeley."   Retrieved November 11, 2011, from http://ccrm.berkeley.edu/resin/index.shtml.

Robertson, P. K. and R. G. Campanella (1983). "Interpretation of cone penetration tests. Part I: Sand." Canadian geotechnical journal 20(4): 718-733.

Roy, S. (2008). "The Future of Earthquake Disaster Management." GeoWorld October 2008.

Saadi, M. and A.-M. Athanasopoulos-Zekkos (2010 of Conference). A GIS-enabled approach for the risk-assessment of levee systems. 9th U.S. National and 10th Canadian Conference on Earthquake Engineering, July 25-29, 2010, Toronto, Canada

Schmertmann, J. H. (1975 of Conference). Measurement of in-situ shear strength *Proceedings, ASCE Specialty Conference on In Situ Measurement of Soil Properties*, Vol. 2, 57-138.

Seed, R. B. (2005). CE270B-Advanced foundation engineering class notes. University of California, Berkeley, California.

Serre, D. et al. (2006). A Spatial Decision support System to Optimize Inspection, Maintenance and Reparation Operations of River Levees. Joint International Conference on Computing and Decision Making in Civil and Building Engineering.: 173-182.

Snow, J. (1855). On the Mode of Communication of Cholera.

Stewart, M. G. and R. E. Melchers (1997). Probabilistic Risk Assessment of Engineering Systems.

Swiss Re (2008). Natural catastrophes and man-made disasters in 2007: high losses in Europe.

Terzaghi, K. (1936). Presidential Address: Relation between Soil Mechanics and Foundation Engineering. Proceedings of the First International Conference on Soil Mechanics and Foundation Engineering, June 22 to 26, 1936. Cambridge, Massachusetts, USA. .

Thorne, C. R. et al., Eds. (1997). Applied Fluvial Geomorphology for River Engineering and Management, John Wiley & Sons, Ltd.

Tobler, W. R. (1970). "A Computer Movie Simulating Urban Growth in the Detroit Region." Economic Geography 46.

Trangmar, B. B. et al. (1986). Application of Geostatistics to Spatial Studies of Soil Properties. Advances in Agronomy, Academic Press. Volume 38: 45-94.

U.S. Congress (1917). "Flood control act: An act to provide for the control of the floods of the Mississippi River and of the Sacramento River, Calif., and for other purposes.". 64th Congress.

URS (2008). Technical Memorandum - Levee Seismic Vulnerability Assessment Methodology. Urban Levee Geotechnical Evaluations Program.

URS (2010). Geotechnical Investigation data for West Sacramento, American River, Marysville, Sutter, and RD784. Received August 30, 2010. , Personal

Communication with Mr. Richard Millet, Vice President, Program Manager DWR Geo-Levee, URS Corporation. .

USACE (1987). Levee Investigation, Reclamation District's 537 and 900 and Maintenance Areas 4 and 9, Sacramento River, Sacramento Bypass and Yolo Bypass, Yolo and Sacramento Counties, California, Department of the Army, Office of the Chief of Engineers, U.S. Army Corps of Engineers.

USACE (1991). Policy Guidance Letter No. 26: Benefit Determination Involving Existing Levees, Department of the Army, Office of the Chief of Engineers, U.S. Army Corps of Engineers.

USACE (1999). Risk-Based Analysis in Geotechnical Engineering for Support of Planning Studies, Engineering Technical Letter 1110-2-556, Department of the Army, Office of the Chief of Engineers, U.S. Army Corps of Engineers.

USGS. (2008). "United States National Seismic Hazard Maps." from http://earthquake.usgs.gov/hazards/products/conterminous/2008/.

USGS (2009a). Earthquake Hazard in the New Madrid Seismic Zone Remains a Concern

USGS. (2009b). "Major Faults of California."   Retrieved September 3, 2009.

USGS. (2010). "National Map Viewer."   Retrieved multiple dates in 2010., from http://viewer.nationalmap.gov/viewer/.

USGS. (2011). "National Water Information System: Web Interface." Retrieved March 30, 2011, from http://nwis.waterdata.usgs.gov/nwis.

Vanmarcke, E. (1977). "Probabilistic modeling of soil profiles " Journal of the Geotechnical Engineering Division, ASCE 103(11): 1227-1246.

Vanmarcke, E. (2011). Risk of Limit Equilibrium Failure of Long Earth Slopes: How It Depends on Length. Proceedings of the ASCE GeoRisk2011: Geotechnical Risk Assessment and Management conference, Atlanta, GA. 418: 1-1.

Vazquez, E. (2005). Example of Kriging.

Venigalla, M. and M. Casey (2006). "Innovations in Geographic Information Systems Applications for Civil Engineering." Journal of Computing in Civil Engineering 20(6): 375-376.

Vieira, S. R. et al. (1983). "Geostatistical theory and application to variability of some agronomical properties." Hilgardia 51: 1-75.

Voortmann, H. G. (2003). Risk-based dsign of flood defense systems, Delft Technical University. PhD thesis.

Vorster, M. and G. Lucko (2002). Construction Technology Needs Assessment Update, Report RR173-11, Construction Technology Needs Assessment Update Research Team, Construction Industry Institute.

Vrouwenvelder, A. C. W. M. (1987). Probabilistic Design of Flood Defenses, Report No. B-87-404, Institute for Building Materials and Structures of the Netherlands Organization for Applied Scientific Research.

Wackernagel, H. (1994). "Cokriging versus kriging in regionalized multivariate data analysis." <u>Geoderma</u> 62: pp 83–92.

Warrick, A. W. et al. (1986). Geostatistical methods applied to soil science. <u>Methods of soil analysis. Part 1, Physical and mineralogical methods</u>. A. Klute and G. S. Campbell. Madison, Wis., Soil Science Society of America.

Watson-Lamprey, J. and N. Abrahamson (2006). "Selection of ground motion time series and limits on scaling." <u>Soil Dynamics and Earthquake Engineering.</u>(2): 477-482.

Webster, R. and M. A. Oliver (1993). How large a sample is needed to estimate the regional variogram adequately? <u>Geostatistics Tro´ia '92</u>. A. Soares: pp. 155–166.

Wilding, A. J. (2008). Development of a GIS-based Seismic Hazard Screening Tool, Missouri University of Science and Technology. Masters.

Wolff, T. F. (1994). Evaluating the Reliability of Existing Levees, U.S. Army Engineer Waterways Experiment Station, Geotechnical Laboratory.

Wolff, T. F. (2008). Reliability of levee systems. <u>Reliability Based Design in Geotechnical Engineering: Computations and Applications</u>. K.-K. Phoon, Taylor & Francis.

Yamaguchi, S. et al. (2007). Development of a GIS-Based Flood-Simulation Software and Application to Flood-Risk Assessment. <u>Second IMA International Conference on Flood Risk Assessment.</u>

Zhou, Y. (2009). Figures from presentation titled "Estimation of Dissolved Oxygen Distribution Using Geostatistical Methods and Remote Sensing Data", Personal Communication.